

**EVALUATION OF THE HAZARD OF STATIC  
ELECTRICITY IN NONMETALLIC POL  
SYSTEMS--STATIC EFFECTS IN HANDLING  
JET FUEL IN FIBERGLASS  
REINFORCED PLASTIC PIPE**

Kenneth C. Bachman

J. C. Munday

Esso Research and Engineering Company

TECHNICAL REPORT NO. AFWL-TR-72-90

June 1973

DTIC QUALITY INSPECTED 4

**AIR FORCE WEAPONS LABORATORY**  
Air Force Systems Command  
Kirtland Air Force Base  
New Mexico

19960328 130

Approved for public release; distribution unlimited.

FILED 19661

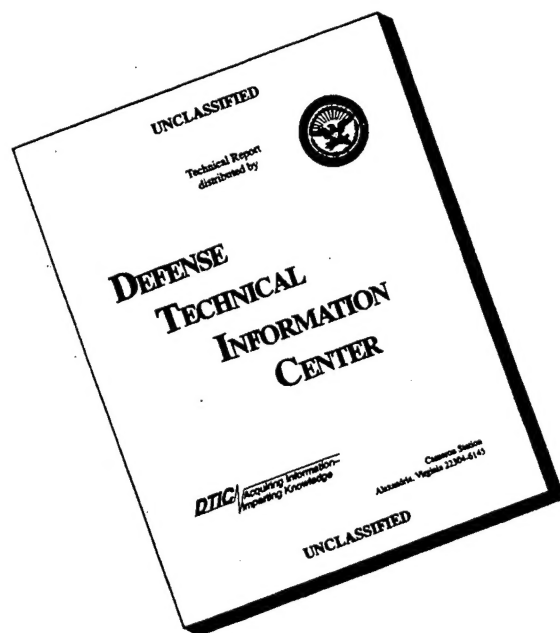
AFWL-TR-72-90

AIR FORCE WEAPONS LABORATORY  
Air Force Systems Command  
Kirtland Air Force Base  
New Mexico 87117

When US Government drawings, specifications, or other data are used for any purpose other than a definitely related Government procurement operation, the Government thereby incurs no responsibility nor any obligation whatsoever, and the fact that the Government may have formulated, furnished, or in any way supplied the said drawings, specifications, or other data, is not to be regarded by implication or otherwise, as in any manner licensing the holder or any other person or corporation, or conveying any rights or permission to manufacture, use, or sell any patented invention that may in any way be related thereto.

DO NOT RETURN THIS COPY. RETAIN OR DESTROY.

# DISCLAIMER NOTICE



**THIS DOCUMENT IS BEST QUALITY AVAILABLE. THE COPY FURNISHED TO DTIC CONTAINED A SIGNIFICANT NUMBER OF PAGES WHICH DO NOT REPRODUCE LEGIBLY.**

AFWL-TR-72-90

EVALUATION OF THE HAZARD OF STATIC ELECTRICITY IN NONMETALLIC  
POL SYSTEMS--STATIC EFFECTS IN HANDLING JET FUEL  
IN FIBERGLASS REINFORCED PLASTIC PIPE

Kenneth C. Bachman

J. C. Munday

Esso Research and Engineering Company

TECHNICAL REPORT NO. AFWL-TR-72-90

Approved for public release; distribution unlimited.





FOREWORD


This report was prepared by the Esso Research and Engineering Company, Linden, New Jersey under Contract F29601-71-C-0071. The research was performed under Program Element 63723F, Project 683 M, Task 2.

Inclusive dates of research were June 1971 through June 1972. The report was submitted 8 May 1973 by the Air Force Weapons Laboratory Project Officer, Mr. Frederick H. Peterson (DEZ).

This technical report has been reviewed and is approved.

  
FREDERICK H. PETERSON  
Project Officer

  
OREN G. STROM  
Lt Colonel, USAF  
Chief, Aerospace Facilities Branch

  
WILLIAM B. LIDDICOET  
Colonel, USAF  
Chief, Civil Engineering Research  
Division

## ABSTRACT

### (Distribution Limitation Statement A)

There is increasing interest in fiberglass reinforced plastic (FRP) pipe for minimizing contamination in ground handling of aviation fuels. This report presents the results of a literature search and experimental study conducted to determine if static electricity hazards would be increased by substituting FRP for metal pipe in such systems. Experiments were conducted in 6 inch diameter, matched volume, carbon steel and Bondstrand 2000 pipes at four fuel conductivities between 0.2 and 5.5 CU and at flow rates between 200 and 1500 GPM at controlled temperatures.

Charge generation in the pipes was low ( $2.5 \mu\text{C}/\text{m}^3$  maximum with 0.9 CU fuel at 1200 GPM in steel); generation in FRP was generally less than in steel.

Relaxation in FRP pipe depended on fuel polarity; on the average, relaxation was 8 percent faster, with negatively-charged fuel and 30 percent slower with positively-charged fuel than in steel. The slower relaxation should not prevent the use of FRP in Air Force hydrant systems handling JP-4 where a minimum of 2 minutes residence time is available downstream of filter-separators.

Voltages up to 55 kv were measured on the FRP pipe and sparks up to 1/2 inch long could be discharged from ungrounded metal components on the FRP pipe. These effects should be of no concern in underground installations; methods for eliminating them in above-ground installations are recommended.

An evaluation of the A. O. Smith Static Charge Reducer (SCR) showed that it was more efficient with positively- than negatively-charged fuel and that deposit-buildup could reduce its efficiency. Available data suggest that static electricity hazards might exist downstream of an SCR although the average charge level is below  $30 \mu\text{C}/\text{m}^3$ .

An annotated bibliography covering 71 recent, relevant literature articles is included.

## CONTENTS

<u>Section</u>	<u>Page</u>
I INTRODUCTION	1
II LITERATURE REVIEW AND ANALYSIS OF AVAILABLE DATA	5
III EXPERIMENTAL STUDY	7
1. Outline of Test Program	7
2. Description of Test Facility	8
a. Base Facility	8
b. The Test Section	11
3. Test Procedure	24
a. Cleanup and Maintenance of Test Facility	24
b. Test Sequence; Temperature Control	24
c. Zero Correction for Charge Density Measurements	26
d. Surface Voltage Measurements	26
e. Other Measurements	26
4. Test Fuel(s)	26
IV TEST RESULTS	28
1. Fuel Conductivity vs. Temperature Data	28
2. Charge Generation - FRP vs. Steel Pipe	31
3. Charge Relaxation - FRP vs. Steel Pipe	36
4. Surface Voltage Measurements and Spark Generation	61
5. Evaluation of the Static Charge Reducer	77
V CONCLUSIONS	88
VI RECOMMENDATIONS	96
APPENDIX I REVIEW OF AVAILABLE DATA ON STATIC ELECTRIFICATION IN METALLIC AND NON-METALLIC SYSTEMS	97
A. Review of The Data	97
1. Scope of The Review	97
2. Charge Generation	98

## CONTENTS (CONT'D.)

	<u>Page</u>
3. Charge Relaxation	104
4. Grounding and Bonding	113
5. Methods for Minimizing the Static Hazard	115
6. Field Contacts	117
B. ANNOTATED BIBLIOGRAPHY	118
APPENDIX II      TABLES	146
APPENDIX III     A COMPARISON OF OHMIC AND HYPERBOLIC CHARGE RELAXATION	192
REFERENCES	201
DISTRIBUTION	202

## ILLUSTRATIONS

<u>Figure</u>	<u>Page</u>
1 Key Features of Basic Fueling Facility	9
2 View of Base Facility (Fuel Storage Tanks at Right, Cleanup Filters in Left Foreground and Pumps in Right Foreground)	10
3 Schematic of The Test Section	12
4 View of Filter/Filter Bypass Array (Bendix GO-NO-GO Gages at Left, Fram Filter/Separator at Right and Filter Bypass Line Between Them)	13
5 Schematic of Carbon Steel and FRP Test Pipe Installation	15
6 View of Charge Density Meter Installation Installed on Long FRP Pipe Section (Fuel Inlet at Lower Left, Outlet at Upper Center, Jumper Connecting Two Pipe Sections at Upper Left)	16
7 Overall View of Test Section (Steel Pipe Sections at Right, FRP Sections in Center, Filter/Filter Bypass Array at Upper Left)	18
8 View of Electrostatic Field Meter As Used to Measure Surface Voltage on FRP Pipe	22
9 Comparison of Charge Generating Characteristics of FRP and Steel Pipe at 600 GPM as a Function of Fuel Rest Conductivity	34
10 Charge Generated by Fram Filter/Separator and Bendix Gages as a Function of Fuel Conductivity, Flow Rate and Temperature	38
11 Relaxation Times for Short Pipe Sections with Negatively-Charged Fuel as a Function of CU and Flow Rate	45
12 Relaxation Times for Long Pipe Sections with Negatively-Charged Fuel as a Function of CU and Flow Rate	46
13 Relaxation Times for Short Pipe Sections with Positively-Charged Fuel as a Function of CU and Flow Rate	47
14 Relaxation Times for Long Pipe Sections with Positively-Charged Fuel as a Function of CU and Flow Rate	48
15 Ratio of $k_e/k_o$ Versus $k_o$ Obtained with Steel Pipe	54
16 Ratio of $k_e/k_o$ Versus $k_o$ Obtained with FRP Pipe	56
17 Location of Positions Where Surface Voltage Was Measured on FRP Pipe Relative to Distance from Pipe Inlet and Stanchions	62

## ILLUSTRATIONS (CONT'D.)

<u>Figure</u>		<u>Page</u>
18	Surface Voltage Versus Distance from Pipe Inlet - Using Gages (Positively Charged Fuel) at 5.5 CU and 600 GPM	66
19	Surface Voltage Versus Distance from Pipe Inlet - Using Filter-Separator (Negatively-Charged Fuel) at 5.5 CU	67
20	SCR Efficiency with Positive and Negative Fuel, Before and After Cleaning	78
21	SCR Startup Time Versus Flow Rate	83
22	Predicted Charge Density vs. Residence Time By Hyperbolic and Ohmic Relaxation Theories	198

# TABLES

<u>Table</u>		<u>Page</u>
1	Residence Times for FRP and Steel Test Pipe Sections as a Function of Flow Rate	19
2	Regression Analysis of Measured Rest Conductivity Against Temperature at CU Levels Tested	29
3	Charge Generation in FRP and Carbon Steel Pipe	32
4	Average Charge Densities Generated by Fram Filter/Separator and Bendix Gages as a Function of CU and Flow Rate	37
5	Relaxation Times for FRP and Steel Pipe Obtained with Negatively-Charged Fuel (Generated by Filter/Separator)	41
6	Relaxation Times for FRP and Steel Pipe Obtained with Positively-Charged Fuel (Generated by Bendix Gages)	42
7	Percent Change in Relaxation Rate in Substituting FRP for Steel Pipe as a Function of Fuel Polarity	50
8	Residence Times Required to Reduce Charge Density to $30 \mu\text{C}/\text{m}^3$ in Steel and FRP Pipe	57
9	Maximum Surface Voltages Measured on FRP Pipe Using Bypass, Filter/Separator and Gages	63
10	Static Effects and Spark Generation Observed with Short FRP Test Pipe Section and 0.9 CU Fuel	69
11	Observations on Spark Production Using Bypass	71
12	Observations on Spark Production Using Fram Filter/Separator	72
13	Observations on Spark Production Using Bendix Gages	73
14	Evaluation of SCR Startup Time with 0.2 CU Fuel	82
15	Maximum Surface Voltages Measured on FRP Pipe in SCR Evaluation	85

# TABLES (CONT'D)

<u>Table</u>		<u>Page</u>
16	Dimensions and Electrical Properties of FRP (Bondstrand 2000) Pipe	146
17	Inspection Data for Test Fuel	147
18	Measured Rest Conductivities for 0.2 CU Fuel	148
19	Measured Rest Conductivities for 0.9 CU Fuel	149
20	Measured Rest Conductivities for 3 CU Fuel	150
21	Measured Rest Conductivities for 5.5 CU Fuel	151
22	Evaluation of Charge Generation Using Filter Bypass with 0.2 CU Fuel	152
23	Evaluation of Charge Generation Using Filter Bypass with 0.9 CU Fuel	153
24	Evaluation of Charge Generation Using Filter Bypass with 3 CU Fuel	154
25	Evaluation of Charge Generation Using Filter Bypass with 5.5 CU Fuel	155
26	Evaluation of Charge Relaxation Using Fram Filter/Separator as Charge Generator with 0.2 CU Fuel	156
27	Evaluation of Charge Relaxation Using Fram Filter/Separator as Charge Generator with 0.9 CU Fuel	157
28	Evaluation of Charge Relaxation Using Fram Filter/Separator as Charge Generator with 3 CU Fuel	158
29	Evaluation of Charge Relaxation Using Fram Filter/Separator as Charge Generator with 5.5 CU Fuel	159
30	Evaluation of Charge Relaxation Using Bendix Gages as Charge Generator with 0.2 CU Fuel	160
31	Evaluation of Charge Relaxation Using Bendix Gages as Charge Generator with 0.9 CU Fuel	161
32	Evaluation of Charge Relaxation Using Bendix Gages as Charge Generator with 3 CU Fuel	162



## TABLES (CONT'D)

<u>Table</u>		<u>Page</u>
33	Evaluation of Charge Relaxation Using Bendix Gages as Charge Generator with 5.5 CU Fuel	163
34	Surface Voltage Data - Using Bypass with 0.2 CU Fuel	164
35	Surface Voltage Data - Using Bypass with 0.9 CU Fuel	165
36	Surface Voltage Data - Using Bypass with 3 CU Fuel	166
37	Surface Voltage Data - Using Bypass with 5.5 CU Fuel	167
38	Surface Voltage Data - Using Filter/Separator with 0.2 CU Fuel	168
39	Surface Voltage Data - Using Filter/Separator with 0.9 CU Fuel	169
40	Surface Voltage Data - Using Filter/Separator with 3 CU Fuel	170
41	Surface Voltage Data - Using Filter/Separator with 5.5 CU Fuel	171
42	Surface Voltage Data - Using Gages with 0.2 CU Fuel	172
43	Surface Voltage Data - Using Gages with 0.9 CU Fuel	173
44	Surface Voltage Data - Using Gages with 3 CU Fuel	174
45	Surface Voltage Data - Using Gages with 5.5 CU Fuel	175
46	Tests with SCR in Combination with Fram Filter/Separator at 0.2 CU	176
47	SCR Tests in Combination with the Fram Filter/Separator at 0.9 CU	177
48	Tests with SCR in Combination with Fram Filter/Separator at 3 CU	178
49	Tests with SCR in Combination with Fram Filter/Separator at 5.5 CU	179
50	Tests with SCR in Combination with Bendix Gages at 0.9 CU	180
51	Tests with SCR in Combination with Bendix Gages at 3 CU	181
52	Tests with SCR in Combination with the Bendix Gages at 5.5 CU	182
53	Surface Voltage Data - Using SCR with Fram Filter/Separator at 0.2 CU	183

# TABLES (CONT'D)

<u>Table</u>		<u>Page</u>
54	Surface Voltage Data - Using SCR with Fram Filter/ Separator at 0.9 CU	184
55	Surface Voltage Data - Using SCR with Fram Filter/Separator at 3 CU	185
56	Surface Voltage Data - Using SCR with Fram Filter/Separator at 5.5 CU	186
57	Surface Voltage Data - Using SCR with Bendix Gages at 0.9 CU	187
58	Surface Voltage Data - Using SCR with Bendix Gages at 3 CU	188
59	Surface Voltage Data - Using SCR with Bendix Gages at 5.5 CU	189
60	Observations on Spark Production Using SCR with Filter/ Separator	190
61	Observations on Spark Production Using SCR with Bendix Gages	191
62	Ion Mobility Based on Tests Carried Out with Negatively Charged 0.2 CU Fuel	194
63	Predicted Charge Densities for 0.2 CU Fuel Based on Hyperbolic Charge Relaxation	196

# ABBREVIATIONS, SYMBOLS AND TERMINOLOGY

CD	Charge Density per unit volume of fuel, usually expressed as micro-coulombs/cubic meter, $\mu\text{C}/\text{m}^3$ (See Q below)
CU	Conductivity Unit, a means of expressing fuel conductivity; $1 \text{ CU} = 10^{12}$ Siemens/meter = 1 Picosiemen/meter; the term Siemen has recently been adopted in place of mho (reciprocal ohm or $\Omega^{-1}$ )
GPM	Flow rate, U.S. Gallons/minute
Q	Charge Density, $\mu\text{C}/\text{m}^3$
$Q_0$	Initial Charge; Charge at Pipe Inlet, $\mu\text{C}/\text{m}^3$
$Q_t$	Charge after time t; Charge at Pipe Outlet, $\mu\text{C}/\text{m}^3$
T	Temperature, $^{\circ}\text{F}$
c	Rest conductivity, $k_0$ , at $0^{\circ}\text{F}$
e	Base of the Natural System of Logarithms, 2.7183
i	Streaming Current, usually expressed as microamperes, $\mu\text{A}$ , ie. micro-coulombs/second, $\mu\text{C}/\text{sec}$ .
k	Fuel Conductivity (See CU)
$k_e$	Effective fuel conductivity, conductivity of charged fuel, CU
$k_0$	Rest conductivity, conductivity of uncharged fuel, CU
kv	Surface Voltage, Kilovolts
m	Temperature coefficient for rest conductivity, $dk_0/dT$
t	Elapsed time, residence time, seconds
v	Volumetric flow rate, cubic meters/sec.
$\epsilon$	Dielectric constant of fuel relative to a vacuum, a dimensionless quantity equal to about 2 for hydrocarbons
$\epsilon_0$	Absolute dielectric constant of a vacuum, $8.854 \times 10^{12}$ ampere seconds/volt meter
T	Relaxation Time equal to $\epsilon\epsilon_0/k$ , expressed in seconds.

## SECTION I

### INTRODUCTION

Corrosion is a major source of contamination in ground handling systems for aviation fuels. Not only does corrosion introduce particulates into the fuel, but it may also introduce metal ions into the fuel which can degrade the thermal stability of the fuel -- a property which becomes increasingly important as flight speeds of aircraft are increased. There is increasing interest in minimizing or eliminating the problem of contamination with so-called "sanitary" systems (i.e. systems which provide full span quality control) by utilizing FRP (fiberglass reinforced plastic) aluminum, stainless steel or plastic coated steel for piping and vessels. While all of these materials would essentially eliminate the problem of corrosion, FRP offers some additional advantages which make it attractive, particularly for piping. It is less expensive than aluminum or stainless steel, it needs no external corrosion protection (of particular concern in underground installations), it promises easier and faster installation and its physical and mechanical properties are such that smaller pipe diameters and/or lower pumping investment are required than for metal systems of equivalent flow rates (Ref. 1).

At present, FRP pipe is authorized for use in Air Force POL systems under AFM 88-15.(Chapter 14, paragraph 7b[2]) if it conforms to specification MIL-P-22245. The selection of the pipe is made on the basis of pressure rating and on compatibility with fuel with special consideration given to the combination of pipe and fittings to insure adequacy and to accomodate surge pressures. The use of FRP pipe in the Air Force has been extremely limited; only a few specialized installations have been built. These include a prototype C-5A fueling facility at Edwards AFB, an underwater POL line at Eniwetok and a 100 foot test section at Patrick AFB (Ref. 2).

Since FRP pipe could find wide-spread use in high-speed, large-volume fuel handling systems in the future, questions have been raised regarding the possible electrostatic hazards that might result by using FRP

in place of metal in such systems. To understand this concern, it is necessary to understand some of the factors affecting static charge generation and charge dissipation or relaxation.

Static charge is generated when two dissimilar materials are brought together and separated. In a fuel system, this occurs whenever the fuel flows; the static charge is produced by a process called charge separation. Charge separation takes place at surfaces where an electrical double-layer can form due to ionic impurities in the fuel. Under flow conditions, charged ions of one polarity are swept along with the fuel leaving those of the other polarity to be discharged through contact with ground. The amount of charge generated is a function of the flow rate, the surface area and the fuel charging tendency, which depends on the characteristics of the fuel/surface interface. In general, charging tendency is an unpredictable factor since it depends on the type and quantity of ionizable materials in the fuel as well as the properties of the surface presented in the fuel. As a result, while filter-separators, which present very large surface areas to fuel, are generally the major source of static charge in aviation fuel systems, the amount of charge generated by a particular type of filter can vary, and even the polarity of the charge can change, depending on the fuel to which it is exposed.

When charge has been generated in a fuel, the charge creates an electrical field which causes the charge carriers to migrate to the grounded walls and to recombine with charge of opposite polarity. In a flowing system, however, both charge generation and relaxation occur simultaneously so that in a long length of pipe, for example, an equilibrium is obtained. Since the charge that can be generated by flowing fuel in a pipe is generally several orders of magnitude less than that generated in a filter-separator, the equilibrium charge level obtained in a pipe is usually very small relative to the charge leaving a filter.

The rate at which charge relaxes or decays is usually determined by the conductivity of the fuel (the reciprocal of resistivity). It is independent of the size, shape or geometry of the pipe, hose, filter case or tank. However, since size controls the time available for charge to

relax (eg. pipe dimensions determine residence time of the flowing fuel), highly charged fuel leaving a filter separator will relax to a low equilibrium value if the residence time in the downstream piping is sufficiently long. (A more detailed discussion of charge generation and charge relaxation is provided in Appendix I.)

The concerns regarding the use of FRP pipe in aviation fueling systems result primarily from the fact that FRP is an excellent insulator compared to metal. Metal pipe with its high conductivity, allows charge carriers which migrate to the walls during charge relaxation to recombine with charge of opposite polarity through ground. There is some concern that charge recombination might be reduced or limited by the high resistance between the fuel and ground provided by FRP pipe, whether the exterior of the pipe is grounded, as in an underground installation, or not. Thus a higher, more hazardous charge level might occur at the outlet end of an FRP pipe than from a metal pipe, all other conditions being identical. There is also concern that the resistivity of FRP could lead to the accumulation of charge and a buildup of voltage sufficient to produce discharges from the fuel or from pipe to ground. Such discharges could puncture the pipe wall and produce leaks or act as an ignition source if a flammable vapor were present. If the resistivity of the pipe is not uniform, charges might be expected to flow to ground at points where the resistivity is low and the method of grounding, particularly if the pipe is used in above-ground installations, could become important because of the possible production of high localized potentials. And finally; there is some concern that charge generation in FRP might be greater than in metal pipe where charge generation is known to be low.

This report describes the program that was carried out to determine whether or not the concerns expressed regarding the use of FRP in place of metal pipe have any validity. The overall objective was to provide guidelines for the safe use of FRP pipe in the event that such pipe appeared to present more of a hazard from static-related phenomenon than metal pipe. To this end, the program was designed to answer the following questions on charge generation, charge relaxation and other static-related characteristics

of fueling systems which were of specific concern to the Air Force.

1. Does FRP pipe generate a significantly higher charge than metallic systems of a given pipe length and fuel velocity?
2. Does the charge generated in FRP pipe relax or dissipate at substantially the same rate as in metallic systems of equivalent size?
3. Is the bonding and/or grounding now prescribed for metallic systems of any value in systems fabricated of FRP pipe?
4. Are the velocity restrictions and the prescribed tank filling techniques, now mandatory on metallic systems, still required on FRP systems?
5. Are there any special techniques necessary for the safe transfer of aviation fuels from FRP systems to metallic system (aircraft, trucks and storage) or from metallic systems to FRP systems?
6. In a typical metallic aviation fuel system (bulk storage to receiving aircraft), which components are the major contributions to the static electricity hazard problem? Does this list change when major portions of the system are converted to FRP material?
7. Is there presently available, or potentially available with a modest development program, a device or technique for minimizing the present hazard from static charge? If available, would this device or technique allow lifting the present restrictions on flow rate or at least raise the maximum flow allowed?

The program was carried out in two phases: The first phase involved a literature search and direct contact with selected individuals to establish the state of current knowledge regarding the questions posed. The second phase was an experimental program in which tests were conducted which were to be directed at trying to answer those questions in the above list which remained unanswered after the available data on the subject had been evaluated.

The results of these investigations are described in the following sections of this report.

## SECTION II

### LITERATURE REVIEW AND ANALYSIS OF AVAILABLE DATA

The first phase of the program involved a literature review to establish if any of the questions listed in Section I, had been resolved by previous investigations. Particular emphasis was placed on establishing whether there was any difference between metal and non-metal systems in their effect on static charge generation and relaxation in flowing hydrocarbons. Operating practices that have been recommended to minimize or eliminate the static problem and provide for safe fuel transfer operations were also covered.

In general, the search covered literature published during the last ten years, although some earlier references were included where they appeared to be relevant. The review covered a total of 71 references; an analysis of the data is provided in Appendix I along with abstracts of the references.

In addition to the literature review, a canvass of some workers in this field was made to insure that no recent or unpublished data that might be of value were overlooked.

The available data indicated that charge generation in FRP pipe would be small and that there would probably be little difference between FRP and metal in charge generating characteristics. The available data on charge relaxation indicated that the rate of relaxation might be less in plastic pipe than in comparable metal systems. The resistivity of the pipe appeared to be a major factor in determining whether or not a hazardous situation could develop. Thus clearly visible electrical discharges and voltages which were high enough to puncture the pipe wall have been observed in studies in Teflon, which has a very high resistivity (eg.  $10^{18}$  ohm-cm) while these phenomena were not observed with Teflon pipe coated on the inside with a more conductive material or with commercially available FRP pipe which has a lower resistivity ( $10^{13}$  -  $10^{14}$  ohm cm). In the only



documented study with FRP pipe, low level sparking was produced when a grounding device was brought near the pipe but this was not considered to be a problem since plastic pipe is only approved for underground installations at present.

While there have been numerous studies on charge generation and relaxation in systems covering a wide variety of materials, there has only been one study carried out in a full-scale system using commercially available pipe. The study was carried out at CLA-VAL Corporation, Newport Beach, California in early 1969 using 8-inch diameter Bondstrand 2000 pipe. However, as indicated in Appendix I, these tests were limited and the fuel properties, particularly the fuel conductivity, were not clearly defined. It was concluded that a side-by-side comparison of FRP and metal pipe over a wide range of closely controlled conditions was necessary before any recommendations could be made regarding the use of FRP in place of metal piping in fuel handling systems. The program is described in Section III and the results that were obtained are presented in Section IV of this report. Answers to the questions listed in Section I incorporating the experimental results and information developed in the literature search, are given in Section V.

As indicated in Appendix I, a canvass of individuals who have been active in or whose interests would make them aware of research in this field was made prior to initiating the experimental work to insure that there was no duplication of previous or current effort. None of the individuals contacted were aware of any information that had not been turned up in the literature search.

During this period, we learned that Shell was carrying out studies on charge generation and relaxation in FRP pipe. In response to our inquiry, we were informed in July, 1971, that the work was not complete or published for distribution. Except for the Shell program, the background information is considered to be complete.

### SECTION III

#### EXPERIMENTAL STUDY

##### 1. OUTLINE OF TEST PROGRAM

Charge generation and charge relaxation were determined in two different lengths of nominal 6-inch diameter FRP and carbon steel pipe. The holdup volumes of the short and long sections of steel pipe were matched as closely as possible to those of the corresponding FRP sections so that direct and unambiguous comparisons could be made. The test sections were installed above ground to allow for detection and evaluation of any electrical phenomenon that might occur with the FRP pipe and for possible installation and evaluation of grounding on the FRP pipe. Data were obtained at four conductivity levels ranging from  $\sim 0.2$  to 5.5 CU (Conductivity Units) using Jet A as the base fuel and at flow rates generally ranging from 300 to 1500 GPM (eg. linear velocity 3.1 to 15.6 feet/sec). This range of conductivities was intended to include those typical of JP-4's at the high end and highly refined, thermally stable fuels such as JP-7, as well as typical JP-5, at the low end. The range of flow rates included the Air Force criteria of approximately 7 feet/second for fuel products (Ref. 3).

Charge generation and relaxation were based on continuous measurement of the charge density in the fuel at the inlet and outlet of the test pipe section. To evaluate charge relaxation, charge was generated in the fuel by either an 1100 GPM Fram filter-separator or by a pair of 600 GPM Bendix GO-NO-GO Gages mounted in parallel. To evaluate charge generation, a low charge level was maintained at the inlet of the test section by bypassing these filter units. An A. O. Smith Static Charge Reducer (SCR) was available as a backup for generating a low charge level in evaluation of charge generation. Because of the wide range of conditions which were to be covered in this program, and the fact that the SCR is the only commercially available device for reducing static charge in flowing fuel, an evaluation of the device was included as an integral part of the program.

## 2. DESCRIPTION OF THE TEST FACILITY

The test facility used in this program consists of two separate, but integrated, systems. One system, designated the base facility, contains the storage tanks, cleanup filters, refrigeration equipment, flow meter and pumps which are used to establish and maintain the test fuel at the desired conductivity levels, temperatures and flow rates required for the test program. The other system is the test section. It consists of the matched-volume, FRP and carbon steel test pipe sections which were fabricated for this program, as well as the means used for providing either charged or essentially uncharged fuel for testing and the instrumentation used for monitoring the charge levels on the fuel. Details on the two systems follow:

### a. The Base Facility

A schematic of the base facility is shown in Figure 1. The important features of this part of the facility include two 20,000 gallon storage tanks, three 600 GPM Gilbarco (6 x 4 series) centrifugal pumps and three different types of Filters, Incorporated filters, including an 1800 GPM vertical filter-separator (Model V-4256), a vertical clay filter (Model VC-4854B) and a 600 GPM vertical filter-separator (Model VV-2238B). During clay treatment, the clay treater effluent is always passed through the 600 GPM filter-separator to remove any clay that might migrate out of the clay filter and insure that the cleanliness of the fuel and the system are maintained.

The refrigeration system consists of two York, Model PS15-45A, compressor units, with a total overall capacity of 40 tons. The heat exchanger is a U-tube, bundle-type having stainless steel tubes; it was made by Precision Heat Exchanger Co., Inc., Montvale, N. J.

The flowmeter was a Model 6X5-5555X, Pottermeter, a turbine flow meter made by Potter Aeronautical Corp., Union, N. J.

As shown all piping is of stainless steel and all vessels (storage tanks, heat exchanger, filters) are epoxy lined to minimize uncontrolled contamination of the test fuel. A photograph of this section of the facility is provided in Figure 2.

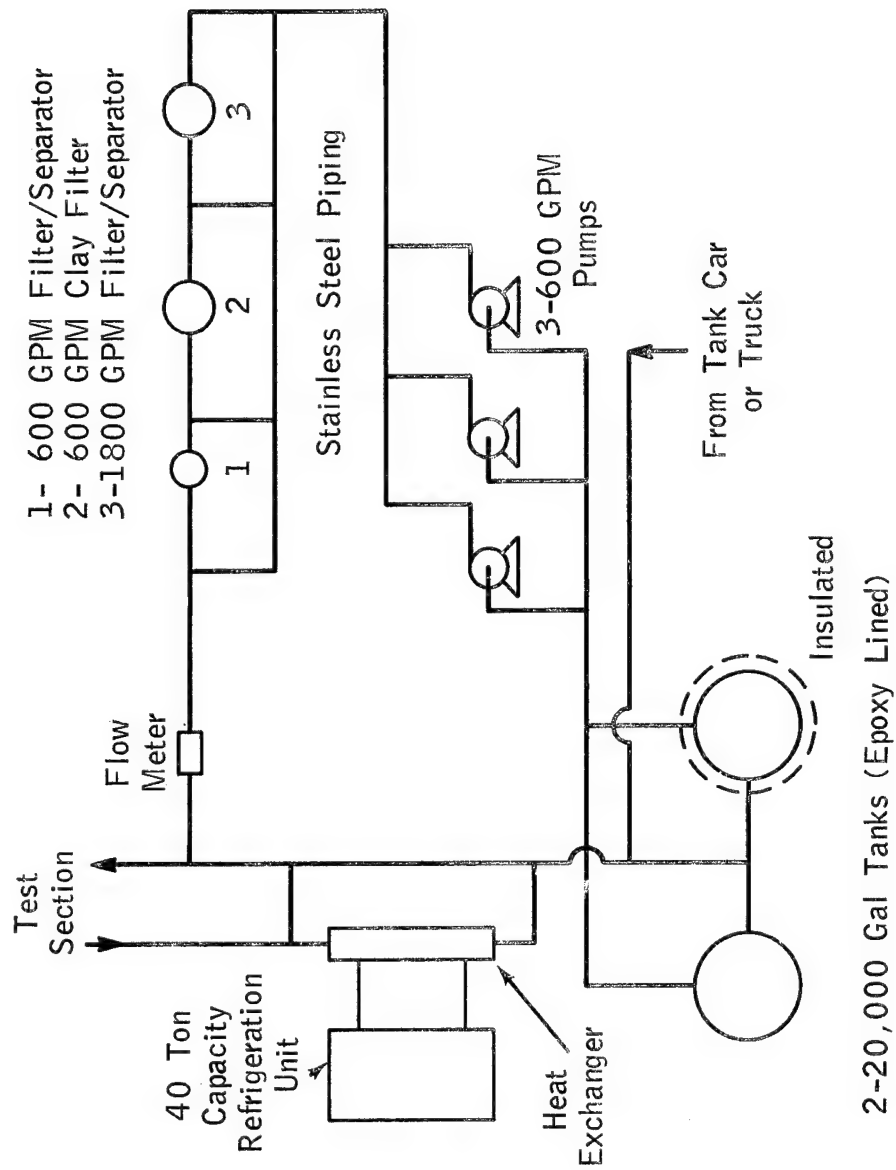


Figure 1. Key Features of Basic Fueling Facility

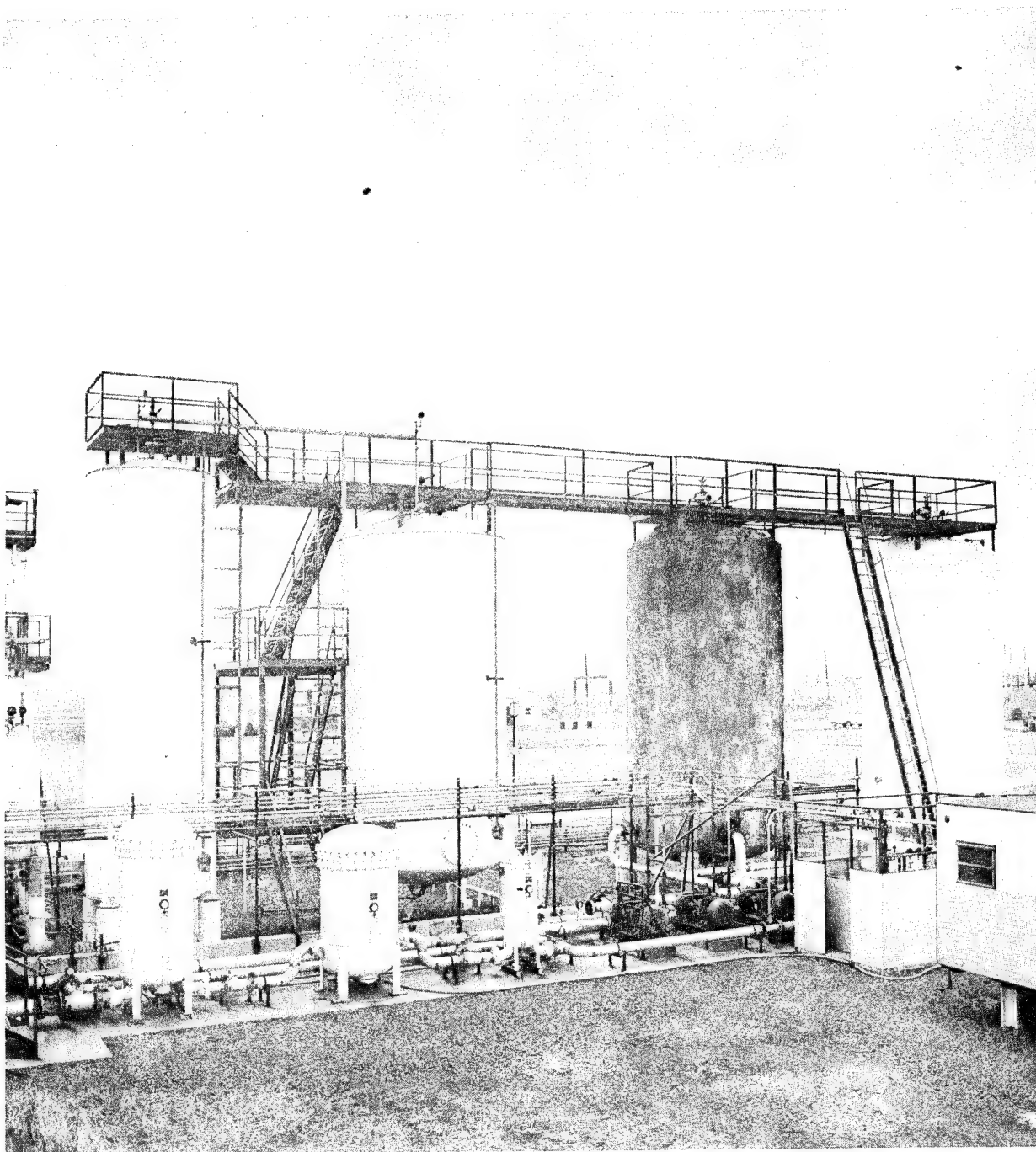


Figure 2. View of Base Facility (Fuel Storage Tanks at Right, Cleanup Filters in Left Foreground and Pumps in Right Foreground)

#### b. The Test Section

A schematic of the test section is shown in Figure 3.

Two different systems were available to deliver charged fuel to the test pipe for comparing charge relaxation characteristics of the two types of pipe. One system consisted of a pair of 600 GPM Bendix GO-NO-GO Gages, Part No. 04600-23, mounted in parallel; the other was an 1100 GPM Horizontal Fram Filter/Separator, Model SO-FCS-3263-36N11. (Each Gage contained 20-30 GPM fuses, Part No. 041630-S, each of which contains hundreds of thin, specially treated cellulose washers as the filtering medium. The Fram filter/separator contained 36-CCN11 coalescer cartridges and 32-CS63 separator cartridges. The coalescer cartridges are fabricated with resin impregnated cellulose paper interpleated with glass fibers; the separator cartridges are fabricated of resin impregnated cellulose). A line was installed which bypassed these devices so that essentially uncharged fuel could be delivered to the test pipe sections for comparing their charge generating characteristics. A picture of this part of the facility is shown in Figure 4. While this part of the facility was normally grounded, it was mounted on Teflon pads and insulated from the rest of the system by Teflon gaskets, as indicated in Figure 3. This made it possible to determine the charge generated in either of the filter devices by direct measurement of current flow to ground when desired.

An A. O. Smith Static Charge Reducer, Model SCR-6-36, was also available in the facility. It offered a second means of providing fuel with low charge for evaluation of charge generation in the test pipe sections as well as an opportunity to evaluate the performance of the device itself over a wide range of conditions.

##### (1) Experimental Pipe Test Sections

Two types of nominal 6-inch diameter pipe were used in the test section, a standard, Schedule 40, commercial grade carbon steel pipe and Bondstrand 2000, a fiberglass reinforced epoxy pipe manufactured by Ameron (formerly Amercoat) Corporation. Since electrical resistivity was considered to be a critical factor in dissipation of charge from plastic pipe,

# THE TEST FACILITY

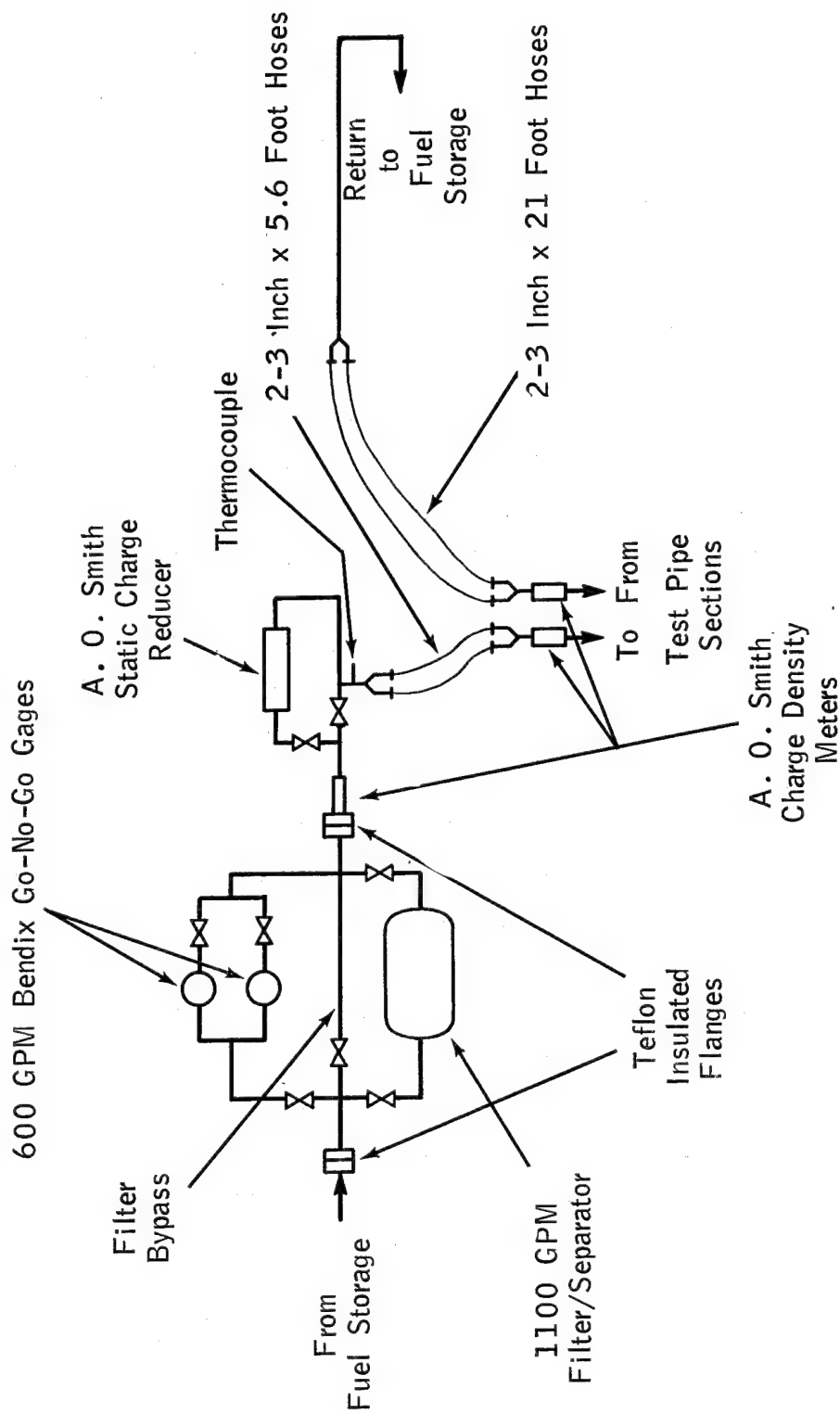


Figure 3. Schematic of The Test Section

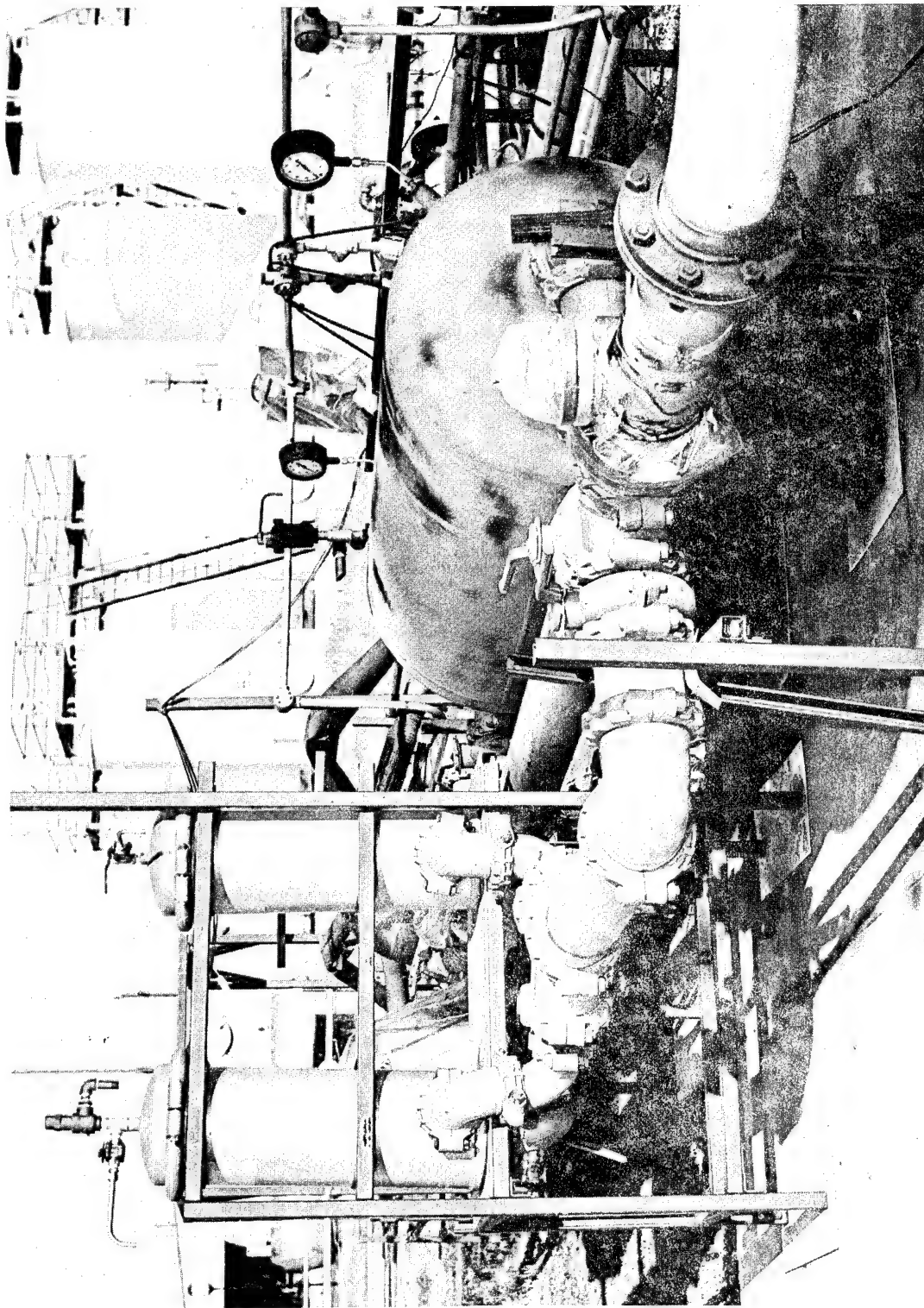


Figure 4. View of Filter/Filter Bypass Array (Bendix GO-NO-GO Gages at Left, Fram Filter/Separator at Right and Filter Bypass Line Between Them)



the highest resistivity that might be encountered in this type of pipe was desired for this installation. Bondstrand 2000 was selected because it showed the highest volume resistivity (eg.  $1.1$  to  $8.8 \times 10^{14}$  ohm cm [Ref. 4]) of the commercially available plastic pipes which meet Air Force specifications and for which typical measured resistivity data were available. Other electrical properties and dimensions of Bondstrand 2000 are shown in Table 16.

Each pipe type was installed in two lengths, a U approximately 80 feet long and a W approximately 160 feet long, as shown in Figure 5. Jumpers, made of corresponding materials, were provided, so that the two pipe lengths could be joined together to give a total run length of approximately 240 feet. (For this program, tests were only conducted in the 80 and 240 foot lengths.) The steel pipe runs were welded and the open ends were provided with Victaulic connections. The FRP sections were fabricated from nominal 20 foot pipe lengths and fitted with FRP flanges at the open ends; all joints were made using the approved epoxy adhesive. Carbon steel stubs (8-1/2 inches long) were used to convert the flanged ends of the plastic pipe to Victaulic connections.

Although FRP pipe is only approved for underground use at present, the installation was constructed above ground to allow for detection and observation of electrical discharges from the surface of the FRP pipe, the measurement of surface voltages and possible application and evaluation of grounding techniques. Each type of pipe was supported on four stanchions (12-to-13 feet apart) which were carefully grounded.

An A. O. Smith Charge Density Sensor Housing, Model H-66 (containing a sensor head, Model SH-1, and a Sensor Drive Head, Model SD-1) was installed at the outlet of the filter/filter bypass array to measure the charge density in the fuel at this point. Two more housings, with sensor heads and drives, were mounted on a rack in front of the test pipe array, as shown in Figure 6, to measure the charge densities on the fuel at the inlet and outlet of the pipe section under test. The ends of the

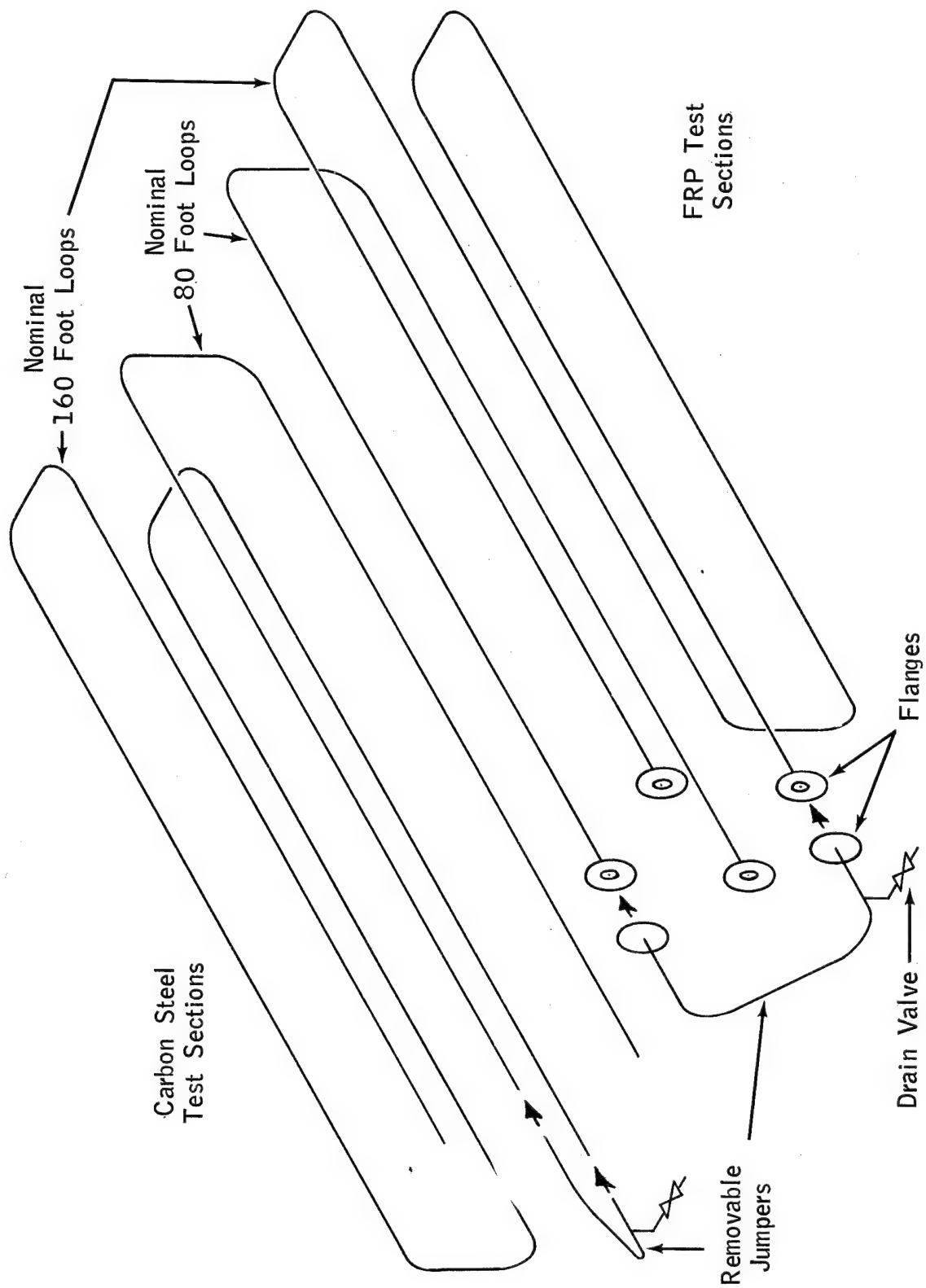


Figure 5. Schematic of Carbon Steel and FRP Test Pipe Installation

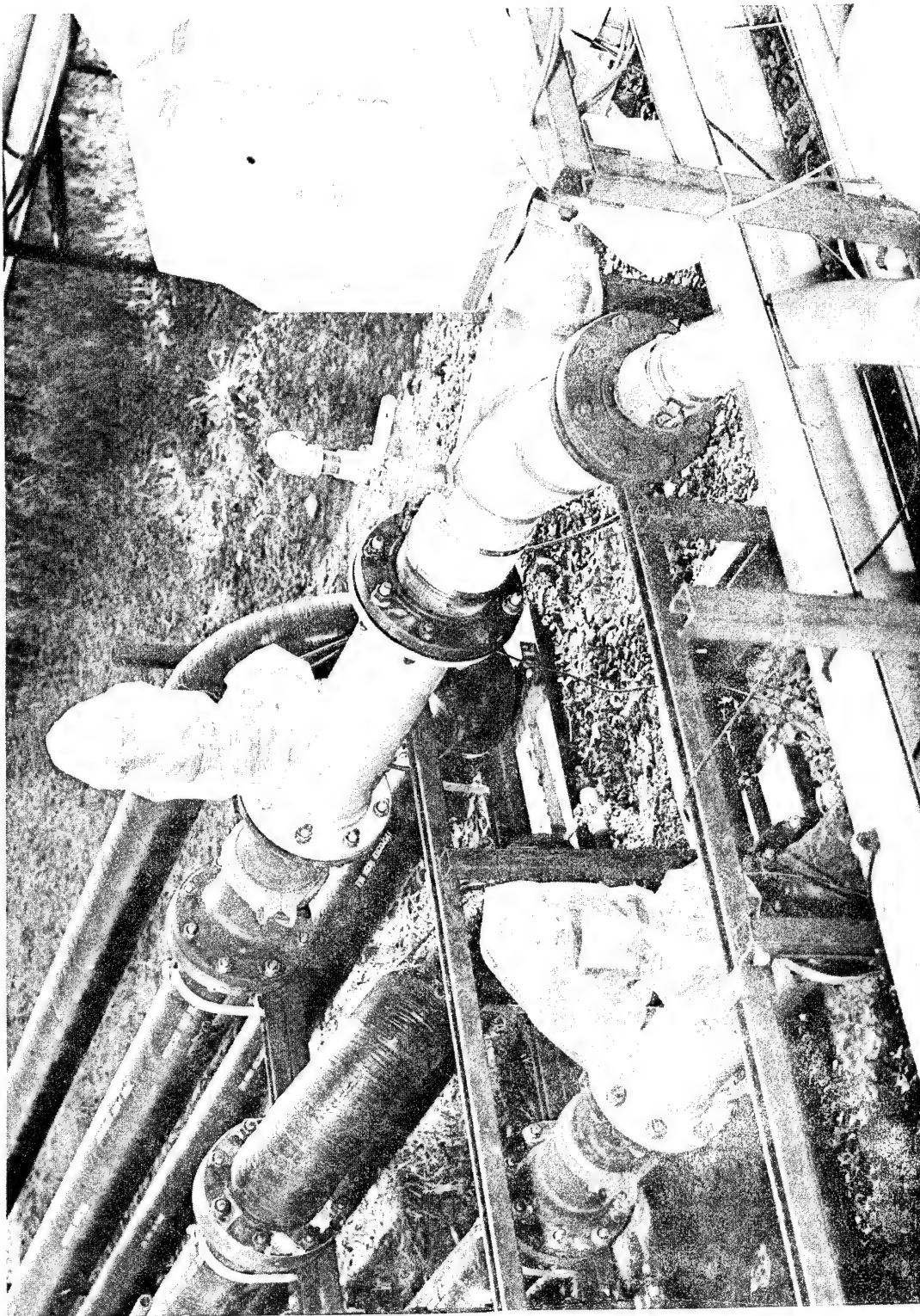


Figure 6. View of Charge Density Meters Installed on Long FRP Pipe Section (Fuel Inlet at Lower Left, Outlet at Upper Center, Jumper Connecting Two Pipe Sections at Upper Left)

sensor housings facing the pipe array were fitted with Victaulic connections for easy coupling with a given test pipe section, as also shown in Figure 6.

Parallel 3 inch hoses, 5.6 feet long, and a pair of reducing Y's connected the filter/filter-bypass/SCR array to the charge density meter at the pipe inlet. The meter at the pipe outlet was connected to the line which returned the fuel to storage through a similar system using a pair of 3 inch hoses, 21 feet long. The hoses made it possible to move the charge density meters from one pipe section to another with relatively little difficulty.

To allow for a direct and unambiguous comparison of the charge generation and relaxation characteristics of the two pipe types, a special effort was made to match the holdup volumes between the inlet and outlet charge density meter sensors for both short and both long sections of the two pipe types, so that the residence times would be the same for equivalent test pipe lengths at a given flow rate. The I.D.'s of the steel and FRP pipes were 6.065 and 6.265 inches, respectively. As a result, the steel runs were somewhat longer than the FRP runs as shown in the overall view of the facility in Figure 7. The calculated volumes of the test sections were almost identical, as shown below:

<u>Pipe Length</u>	<u>Volume of Test Pipe Section, Gals.</u>	
	<u>FRP</u>	<u>Carbon Steel</u>
Short	136.0	135.7
Long	401.3	402.5

The corresponding residence times for the four test sections at the various flow rates used in this program are given in Table 1.

While it was desirable to have the inlet to the test pipe array as close to the outlet of the filter/filter bypass array as possible to maximize the charge level at the test pipe inlet, the location of the pipe

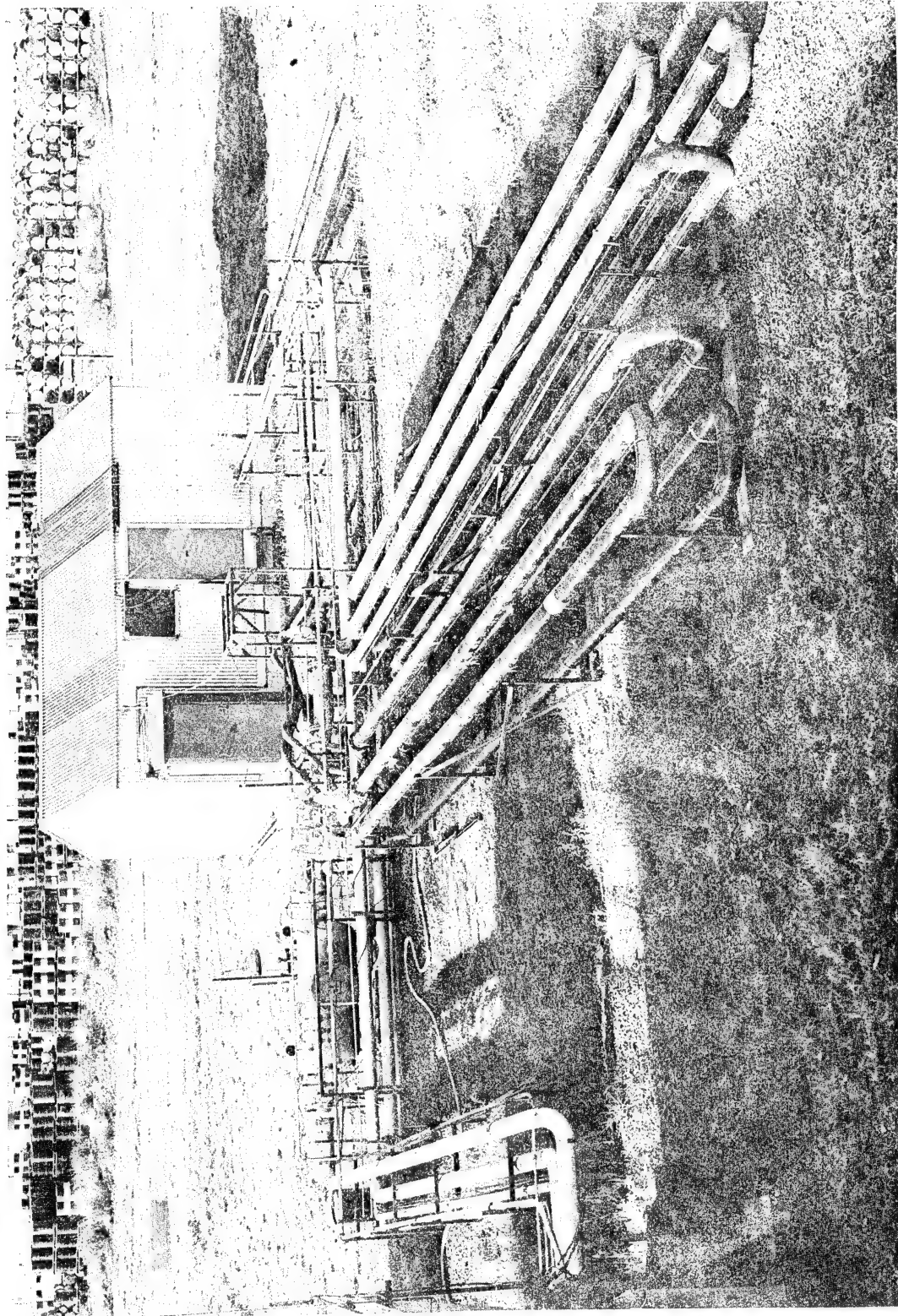


Figure 7. Overall View of Test Section (Steel Pipe Sections at Right, FRP Sections in Center, Filter/Filter Bypass Array at Upper Left)

TABLE 1

RESIDENCE TIMES FOR FRP AND STEEL TEST  
PIPE SECTIONS AS A FUNCTION OF FLOW RATE

	Residence Time, Seconds				
Pipe Type	FRP		Carbon Steel		Inlet
Pipe Length	Short	Long	Short	Long	To Test
Holdup Volume, Gals.	136.0 (a)	401.3(a)	135.7 (a)	402.5(a)	Pipe
Residence Time, Seconds					
at 200 GPM	40.8	120.4	40.7	120.8	7.42
300	27.2	80.3	27.2	80.5	4.94
600	13.6	40.1	13.6	40.2	2.47
900	9.06	26.8	9.06	26.8	1.65
910	8.94	26.4	8.94	26.4	1.62
1200	6.80	20.1	6.80	20.1	1.24
1500	5.43	16.1	5.43	16.1	0.99

- (a) Between charge density meter sensors at inlet and outlet of test section.
- (b) Between charge density meter sensors at outlet of filter/by-pass array and inlet to test pipe section.

array was limited because it was added to an existing system which had been used for other investigations (Appendix I [1]). The calculated volume hold up between the charge density sensor at the outlet of the filter/filter bypass array and the sensor at the test pipe inlet was 24.7 gallons. Residence times between these two locations at the various flow rates used in this study are included in Table 1.

## (2) Measurements and Instrumentation

### (a) Charge Density

Charge density was measured continuously at the outlet of the filter/filter bypass array, and at the inlet and outlet of the test pipe section during each test, using A. O. Smith Charge Density Measuring Systems as described above. These are basically rotating vane field strength meters which measure the charge density of a given volume of fuel. The Keithley, Model 600-B, electrometer which is normally used to readout charge density meter output was replaced by an amplifier which was designed and built by Esso Research. The amplified signal was transmitted back to a trailer, where it passed through an attenuator, which allowed for range changes, before the signal was recorded. The attenuator covered the following ranges:  $\pm 2.75$ ,  $\pm 7.5$ ,  $\pm 27.5$ ,  $\pm 77.5$ ,  $\pm 275$  and  $\pm 775 \mu\text{C}/\text{m}^3$ . Prior to the start of the program, each attenuator switch was calibrated against known inputs. In addition, each A. O. Smith Sensor Head and Drive was installed at the outlet of the filter-separator array and the gain of its respective amplifier was set so that the recorder readout agreed with charge density determined by current flow between the filter-separator and ground at two different flow rates.

### (b) Flow Rate

Flow rate was measured using a Model 6X5-5555X, Pottermeter, a turbine flow meter. A full scale range of 1000 GPM was used for tests below 1000 GPM; a full scale range of 2000 GPM was used for higher flow rates. The meter has an accuracy of 1% at full scale.



### (c) Temperature

A calibrated bimetallic thermometer, TEL-TRU Model GT 200, Type 304, TEL-TRU Manufacturing Co., Rochester, N. Y., which could be read to 0.5°F was used for the first two series of tests (eg. with the fuel at 0.9 and 3 CU). It was mounted in the base facility ahead of the valve controlling flow to the test section. In the last two series, temperature was recorded continuously using an iron-constantan thermocouple mounted in the reducing Y at the outlet of the filter/bypass array. Temperatures could be read to 0.1°F.

### (d) Rest Conductivity

Rest conductivity (eg. conductivity of the uncharged fuel) was measured on grab samples which were collected at random times during each pipe type/pipe length test series using a new precision technique developed as part of an ASTM program (Appendix I [57]). Samples were collected in the base loop ahead of the flow control valve; samples of ~0.9 CU and higher were allowed to relax for 5 minutes before a measurement was made; those below 0.9 CU were allowed 10 minutes to relax. In many cases, a second reading was taken on the same sample after it had warmed up to establish the effect of temperature on conductivity for the fuels used.

### (e) Surface Voltage

A rotating-vane, Electrostatic Field Meter, Model 12009-1, made by Comstock and Wescott, Inc., Cambridge, Mass. was used for the majority of surface voltage measurements made on the FRP pipe. A fitting was designed for the meter which utilized a pair of Nylon bolts to hold it at a fixed distance from the pipe, as shown in Figure 8. The meter was calibrated up to 30 kv by impressing known voltages on aluminum foil which had been wrapped around a 3 foot length of the FRP pipe. The meter had an accuracy of about  $\pm 4\%$  at voltages up to 15 kv, increasing to about  $\pm 7\%$  at voltages up to 30 kv. The meter output was recorded.

A Sweeney Static Meter, Model SWE 1127, was used occasionally when the surface voltage on the pipe exceeded 30 kv or some other difficulty was encountered with the field meter. The static meter depends on



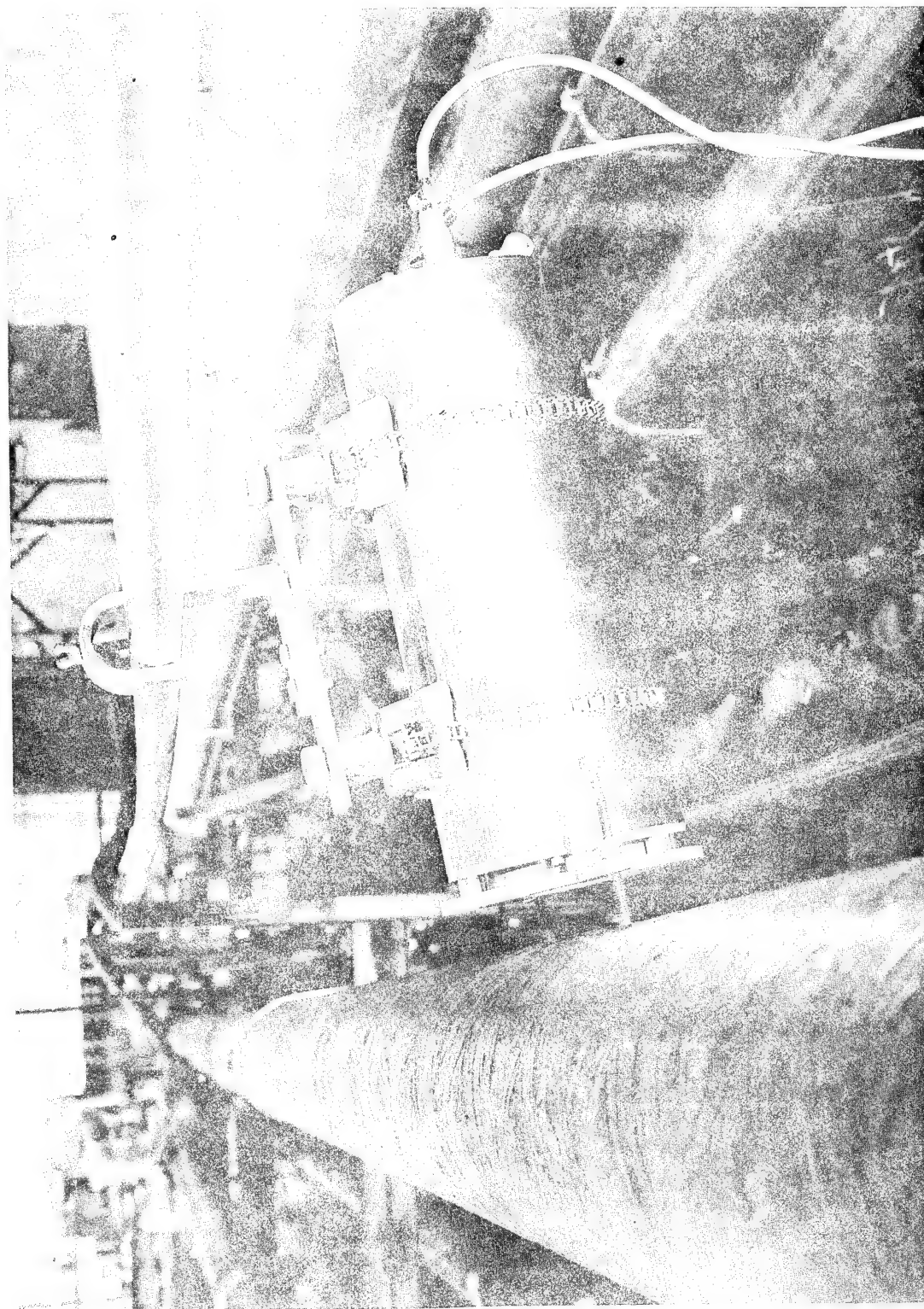


Figure 8. View of Electrostatic Field Meter as Used to Measure Surface Voltage on FRP Pipe

low level radioactivity to ionize the air between the meter and the surface being measured which allows electric charges to flow and develop the correct readout. The results from this device appeared to be much more erratic than those from the field meter and it was used as little as possible.

(f) Spark Discharges

Evidence of spark discharges during tests with the FRP pipe sections was based on either visual or aural observation; a CB walkie-talkie radio was used to detect low level discharges. No actual measurements of spark energies were made.

(g) Humidity

Humidity measurements during the first series of runs were based on readings obtained from a local weather station. During the last three series of runs, humidity was measured at the test installation using a Bendix Psychron, Model 566, Bendix Corporation, Environmental Science Division, Baltimore, Maryland.

### 3. TEST PROCEDURE

#### a. Cleanup and Maintenance of Test Facility

Prior to assembly, the FRP pipe sections were swabbed out with hexane-soaked cloths. Following assembly, the interior of the carbon steel pipe was sandblasted down to a clean metal surface and blown out with an air jet. Following this, the test sections were maintained under a dry atmosphere whenever they were not in use by placing cannisters of desiccant at the open ends and sealing them with polyethylene bags or blind flanges.

Prior to actual testing, the entire system was flushed with 5000 gallons of production Jet A turbo fuel, the FRP and steel pipe sections were each flushed for 2 hours at about 1000 GPM. During this cleanup, the fuel was filtered using the 1800 GPM filter/separator in the base facility; no elements were installed in either the filter/separator or the Gages in the test section. The cleanup fuel was slopped, new elements, which were used throughout the subsequent tests, were installed in both the filter/separator and Gages in the test section and 20,000 gallons of fresh production Jet A were charged to the system.

The charge density meters were then calibrated as discussed on page 20.

#### b. Test Sequence; Temperature Control

The first series of tests was carried out using the production Jet A; it had a fuel conductivity of about 0.9 CU. The next two series of tests were carried out after the fuel conductivity had been increased to about 3 and then 5.5 CU by incremental additions of oxidized asphalt; the final series was carried out with the fuel at about 0.2 CU following clay treatment of the test fuel supply.

In the first test series at 0.9 CU, the long FRP pipe section was tested first, followed by the long steel, the short steel and finally the short FRP. In the three subsequent series, the pipe sections were equilibrated with the fuel supply prior to actual testing by recirculation of the fuel at about 1000 GPM through the long steel and then long FRP pipes until the conductivity of the fuel stabilized. During recirculation, the test fuel was directed for about equal lengths of time through the Gages

and the filter/separator in the test section to assure that they were also in equilibrium with the fuel supply. The long pipe lengths were always tested first, following the equilibration, to insure that there would be as little change as possible in the fuel properties during each test series covering the four pipe type/pipe length combinations.

Temperature was a critical variable in comparing charge relaxation in the two types of pipe and its control was complicated by the fact that the test facility was out-of-doors, where the ambient temperature and cloud cover were important factors. As a result, it was not possible to run all tests at the same temperature. However, it was found that the temperatures for a given flow rate and pretreatment (eg. using the filter/separator, Gages or bypass) could be matched to within about  $\pm 0.5^{\circ}\text{F}$  over the four pipe type/pipe length combinations by running the tests in each pipe section in the same sequence and controlling the rate of temperature rise due to pump heat and ambient conditions by judicious use of refrigeration.

The sequence for each series of tests in a given pipe was generally started with the use of the filter bypass, then the filter/separator, filter/separator plus SCR, Gages and finally Gages plus SCR. The runs using the bypass were made first, because the charge density levels measured during this part of the test were small, and the effect of temperature was also considered to be small. It was possible therefore to obtain data while the fuel temperature was being adjusted for subsequent tests, where temperature was critical.

Tests using either the filter/separator or the Gages to generate charge on the fuel were generally started at the highest flow rate to be tested, since the charge generated stabilized more rapidly at this flow rate and at subsequent lower flow rates than if the tests were started at the lowest rate and then increased.

Data were collected at each flow rate tested for a minimum of 6 minutes or until the charge density readings stabilized or the fuel temperature reached the desired level.

#### c. Zero Correction for Charge Density Measurements

Charge density meter readings at zero flow were not always zero. Zero corrections were established at the start of each pipe test by pumping at about 1000 GPM through the filter bypass and the test pipe section for 5 minutes to equilibrate the temperatures at the three charge density meter locations. Flow was then stopped; and the charge was allowed to relax until the charge density leveled off. The readings obtained after the charge relaxed were used as the zero corrections. Zero corrections were also generally obtained following each set of runs with a given fuel pretreatment (eg. following each series using the bypass, the filter/separator, etc.) by stopping flow and allowing charge to relax. The corrections were small, generally ranging between  $\pm 1.5 \mu\text{C}/\text{m}^3$ , however, they were felt to be critical in the development of the data on charge generation in pipe flow as obtained in this program.

#### d. Surface Voltage Measurements

During tests carried out with the FRP pipe sections, surface voltage measurements were made during selected runs at several positions along the pipe. The field meter was left at each location long enough to get a stabilized reading before it was moved to the next location.

#### e. Other Measurements

Details on measurement of conductivity and observation of spark discharges are provided elsewhere in this report.

### 4. TEST FUEL(S)

As indicated in Appendix I, charge generation is controlled to a large extent by ionic impurities in fuel. Charge relaxation is controlled in large measure by fuel conductivity, which is also strongly influenced by impurities. Since the type and amount of impurity can vary widely for a particular fuel type, a wide range of fuel conductivity (and impurity) levels were investigated.

The test fuel was a production Jet A turbo fuel which met JP-8 specifications as shown in Table 17. The first series of tests was carried out with the fuel as received; it had a conductivity of about 0.9 CU at test temperatures. The fuel conductivity was increased to about 3 CU and then 5.5 CU to simulate JP-4 conductivity levels for the second and third series of tests by incremental addition of oxidized asphalt. For the final series of tests, the fuel was cleaned up by repeated passes through the clay filter at 200 GPM by flowing the fuel from one storage tank to the other. Effluent from the clay treater was flowed alternately through the Fram filter/separator and the Gages as well as both test pipe sections in their long configuration until no further reduction in conductivity could be obtained. This fuel was used for the final series of tests. It had a conductivity slightly above 0.2 CU at the test temperatures and represented a highly refined, thermally stable fuel.

The volume of test fuel maintained in the test section and storage tank was about 16,650 gallons (113,090 lbs.). The sensitivity of conductivity to impurities is demonstrated by the fact that the increase in CU from 0.9 to 3 only required 0.27 ppm (14.0 grams) of asphalt; while the 5.5 CU blend only required a total addition of 0.48 ppm (24.4 grams) to this volume of fuel.

# SECTION IV

## TEST RESULTS

### 1. FUEL CONDUCTIVITY VS. TEMPERATURE DATA

The rest conductivities measured (as described on page 20) on grab samples collected during tests carried out at each of the four fuel conductivity levels are shown in Tables 18 through 21. Since the initial measurement was made five to ten minutes after the sample was taken, the temperature at which the conductivity was measured was always higher than that which prevailed at the time of sampling. As the program progressed, it became the rule to make a second measurement on each sample after it had warmed up further so that a better estimate of the change in CU with temperature could be obtained. The conductivities measured at each of the four levels evaluated in this program were used to find the best least squares fit to the equation:

$$\log CU = mT + c \quad (1)$$

which expresses the relationship between CU and temperature, T. The results are summarized in Table 2. As indicated the standard error of estimate was about the same for all four CU levels, but the standard error on the slope was greatest for the 0.9 CU fuel where the fewest number of repeat measurements were made. As shown in the last column of the table, CU doubles with increase of about 40°F in temperature for all fuels except the 0.9 CU fuel. This is in good agreement with previous data (Appendix I [67]).

The rest conductivities,  $k_o$ , expressed as CU, at the test temperature as provided in this report were calculated using these relationships. The range over which CU varied at each level because of temperature variation is shown below:

<u>Nominal <math>k_o</math>, CU</u>	<u>Range Over Which CU Varied</u>
0.2	0.22 - 0.25
0.9	0.66 - 1.01
3	2.7 - 3.3
5.5	5.3 - 5.8

TABLE 2

REGRESSION ANALYSIS OF MEASURED REST  
CONDUCTIVITY AGAINST TEMPERATURE  
AT CU LEVELS TESTED

Nominal CU Level	Coefficients		Standard Error of		$\Delta T$ , °F, For CU to Double
	m	c	m	Estimate	
0.2	$.8361 \times 10^{-2}$	-0.9545	$.089 \times 10^{-2}$	.040	36.5
0.9	$.9309 \times 10^{-2}$	-0.6122	$.20 \times 10^{-2}$	.038	32.0
3.0	$.7852 \times 10^{-2}$	0.1645	$.15 \times 10^{-2}$	.040	38.5
5.5	$.7252 \times 10^{-2}$	0.4606	$.062 \times 10^{-2}$	.029	41.5



As shown, the CU's were maintained within a narrow range at each level, except for 0.9 CU. The latter included the first experimental runs where the temperature control was somewhat poorer than was achieved in subsequent runs as a result of experience.

The nominal rest conductivity of the test fuel, eg. 0.2 CU, 0.9 CU, etc., is used in discussing the data throughout most of this report. Rest conductivity is measured on the uncharged fuel. A second conductivity, which is measured when the fuel is charged, is also referred to; it is known as "effective" conductivity.

## 2. CHARGE GENERATION - FRP VS. STEEL PIPE

The charge generating characteristics of FRP and metal pipe were determined at each of the four conductivity levels at four flow rates, 300, 600, 1200 and 1500 GPM. Tests were conducted in both the short and long lengths of pipe; the fuel was flowed through the bypass line in the filter array to keep the charge at the pipe inlet as low as possible. Charge densities measured at the outlet of the bypass and at the inlet and outlet of the test pipe section are given in Tables 22 through 25, along with the fuel temperature and corresponding calculated rest conductivity,  $k_o$ , expressed in conductivity units, CU, for each run.

In general, the charge density at the pipe inlet increased with increasing flow rate, but the objective of providing a low charge level at the test pipe inlet was met. The fuel was charged negatively at the pipe inlet in all runs. Charge level at the pipe inlet ranged from minimum of  $-0.5 \mu\text{C}/\text{m}^3$  at 300 GPM with the 3 CU fuel (Table 24) to  $-4.4$  at 1500 GPM with the 0.9 (Table 23) and 5.5 CU fuels (Table 25). During each of these test runs, the charge level generally stabilized at all three locations within one to two minutes after a change in flow rate. The tabulated values are considered to be good to  $\pm 0.1 \mu\text{C}/\text{m}^3$ .

The difference in charge density between the pipe inlet and pipe outlet represents the charging tendency. These differences are summarized in Table 3. A positive value in this table indicates that charge was being generated, a negative value generally indicates that charge was relaxing (although it might also mean that charge of opposite polarity was being generated).

Table 3

## CHARGE GENERATION IN FRP AND CARBON STEEL PIPE

(A positive value indicates charge was being generated,  
a negative value indicates charge was relaxing.)

Nominal Fuel CU	Pipe Length Pipe Type Flow Rate, GPM	Change in Charge Density Between Pipe Inlet and Pipe Outlet, $\mu\text{C}/\text{m}^3$			
		Short		Long	
		Steel	FRP	Steel	FRP
0.2	300	0.1	0.0	0.2	0.2
	600	0.2	0.1	0.9	0.5
	1200	0.2	0.2	1.3	0.5
	1500	0.4	0.2	1.3	0.4
0.9	300	0.0	-0.5	-0.3	-0.6
	600	0.4	-0.3	0.4	-0.5
	1200	0.8	-0.3	2.5	-0.3
	1500	0.9	0.0	2.5	-0.7
3.	300	-0.8	-0.7(a)	-0.5	-0.6(a)
	600	-0.6	-1.5	-0.5	-1.1(a)
	1200	-0.1	-1.2	-0.6	-2.2(a)
	1500	-0.2	-1.1	-0.2	-2.7
5.5	300	-0.5	-1.3	-0.8	-1.0
	600	-1.2	-1.9	-1.7	-2.5
	1200	-0.3	-1.7	-1.1	-3.7(a)
	1500	0.0	-1.9	-0.4	-4.2

(a) Polarity reversed.

The results show that there was relatively little charge generated in either FRP or steel pipe; the greatest increase in charge was only  $2.5 \mu\text{C}/\text{m}^3$  which was obtained at 1200 and 1500 GPM in the long steel pipe with the 0.9 CU fuel. And on a relative basis, the steel pipe consistently generated more charge than the FRP pipe under all conditions. With the 0.2 CU fuel, all pipe length/pipe type combinations gave a net increase in charge, but the increase with the steel was almost always greater than that observed with the FRP. With the 0.9 CU fuel, both lengths of steel pipe generally gave a net increase in charge with increasing flow rate while charge relaxation generally took place in the FRP pipe. With the 3 and 5.5 CU fuels, charge relaxation was the rule with both pipe type/pipe length combinations, but there was generally a greater reduction in charge in the FRP pipe than in the steel, which indicates that the latter was tending to generate some charge. This can be seen in Figure 9, where the change in charge density obtained at 600 GPM for each pipe length/pipe type combination is plotted against rest conductivity. As shown, charge tends to relax in FRP pipe at all CU's but 0.2; somewhat more relaxation occurs in the long test section than in the short. With the steel pipe, there is some charge generation at CU's below 1.5 and relaxation at CU's above this level. The amount of relaxation in the steel pipe is less than is obtained in the FRP pipe under comparable conditions.

As shown in Table 3, the polarity of the fuel reversed during transit through the long FRP pipe in four runs involving 3 and 5.5 CU fuel. This might indicate that some charging was taking place under these test conditions. However, since the highest charge level reached at the pipe outlet in these runs was only  $0.3 \mu\text{C}/\text{m}^3$ , the effect is probably not significant.

In those runs where charge generation occurred (eg. both pipe type/pipe length combinations with 0.2 CU fuel and the steel pipe at 0.9 CU), charge generation increased with pipe length. However, since there

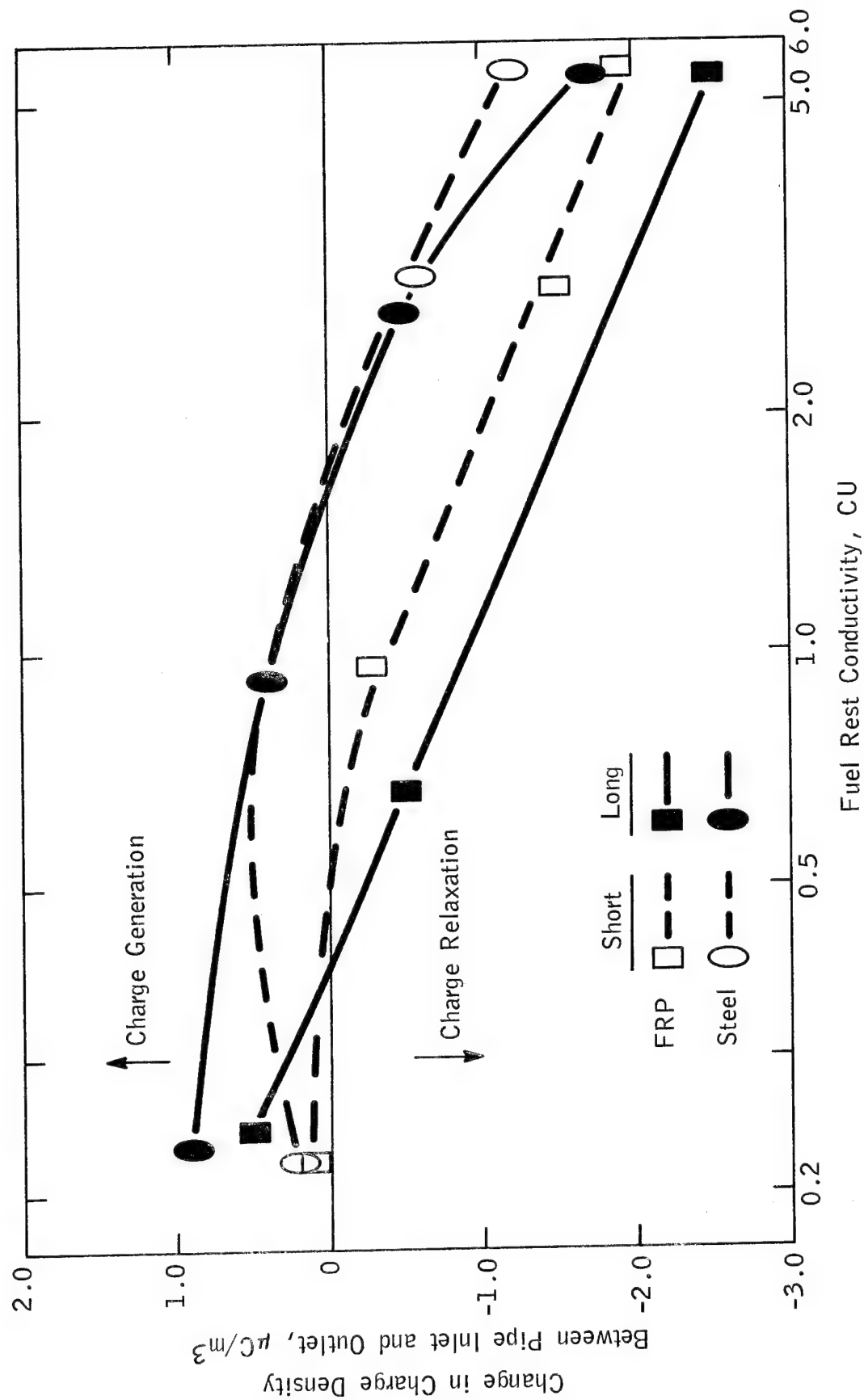


Figure 9. Comparison of Charge Generating Characteristics of FRP and Steel Pipe at 600 GPM as a Function of Fuel Rest Conductivity

was no increase in charge when flow rate was increased from 1200 to 1500 GPM in these runs, it suggests that the charge levels reached in these runs represent equilibrium levels and that little additional increase in charge would occur if the pipes were longer. This effect is not apparent with the 3 and 5.5 CU fuels where there is generally a net charge relaxation due to the shorter relaxation times resulting from the higher conductivities. The small effect of temperature on charge generated in pipe (or hoses) flow is shown by the data obtained with the 0.9 CU fuel (Table 23). Runs carried out with the long FRP test section were carried out at temperatures between 12.5 and 15.5°F colder than those in the long steel pipe. The maximum difference in charge level between these two runs was 1.0 to 1.1  $\mu\text{C}/\text{m}^3$  observed at 1200 and 1500 GPM at both the bypass outlet and pipe inlet. The data indicate that there would be less than a 0.1  $\mu\text{C}/\text{m}^3$  increase in charge level for each degree of temperature rise.

It must be concluded from these data that charge generation in FRP pipe is no greater than in a metal system under comparable fuel velocities and pipe lengths and actually would appear to be less. The observed difference between the two pipe types may be due to the fact that the internal surface of the carbon steel pipe is rough compared to the FRP pipe which is relatively smooth. The differences between the two pipes are much too small to be of practical significance in the field.

### 3. CHARGE RELAXATION

Charge relaxation in FRP pipe was compared to that in steel pipe by charging the fuel prior to introduction to the test pipe sections and then comparing the rates at which the charge relaxed in each pipe type under essentially identical conditions. Charge was generated with either an 1100 GPM Fram filter/separator or with a pair of 600 GPM Bendix GO-NO-GO Gages. Tests were conducted in all four pipe length/pipe type combinations at 300, 600 and 1200 GPM; some additional tests were also made at 200 and 900 to augment the data collected at the other flow rates. Charge densities measured at the outlet of the filter/separator and at the inlet and outlet of the test pipe section for each run are given in Tables 26 through 29. The relaxation time,  $T$ , the fuel temperature, the rest,  $k_o$ , and effective,  $k_e$ , conductivities, both expressed in CU, and the ratio of effective to rest conductivity for each run are also listed. Similar data obtained when the Bendix Gages were used to charge the fuel are shown in Tables 30 through 33.

The use of both the Fram filter/separator and the Bendix Gages to generate charge on the fuel provided a wide range of charge levels of both positive and negative polarity. The average charge densities obtained at the outlet of both the filter/separator and the Gages as a function of CU and flow rate are listed in Table 4 and shown graphically in Figure 10. All averages were based on four comparable runs; duplicate runs, which might bias the average, were not included. Numbers in parentheses are the average temperatures at which the charge densities were measured. As shown in Figure 10, there was a striking difference between the filter/separator and the Gages in their response to CU (or impurity level) and flow rate. The filter/separator generally gave an increase in charge density with increasing flow rate and a decrease in charge level with increasing CU. The filter charged the fuel negatively, except for a reversal in polarity that was obtained at 300 GPM with the fuel at 5.5 CU. The Gages performed almost diametrically opposite to this. The Gages charged the fuel positively, the charge

Table 4

AVERAGE CHARGE DENSITIES GENERATED BY  
FRAM FILTER/SEPARATOR AND BENDIX GAGES  
AS A FUNCTION OF CU AND FLOW RATE

Charge Generator	Fuel CU	Charge Density, $\mu\text{C}/\text{m}^3$ , @ GPM(a)			
		300	600	900	1200
(Average Temperatures Shown in Parentheses)					
Fram Filter/ Separator	0.2	-74(39)	-126(38)	150(37)	-166(38)
	0.9	-51(60)	-102(59)	-	-148(58)
	3.	-4(41)	-18(40)	-	-62(40)
	5.5	5(41)	-2(39)	-22(39)	-44(40)
Bendix Gages	0.2	12(40)	9(39)	-	6(38)
	0.9	24(57)	20(56)	-	16(55)
	3.	132(44)	118(43)	-	97(42)
	5.5	178(40)	174(39)	159(38)	150(39)
Fram Filter/ Separator	0.9	-36(38)	-68(36)	-	-96(40)
Bendix Gages	0.9	20(37)	16(36)	-	-

(a) Based on the average of four comparable runs, no repeat runs were included; values in parentheses show average temperature for the four runs.



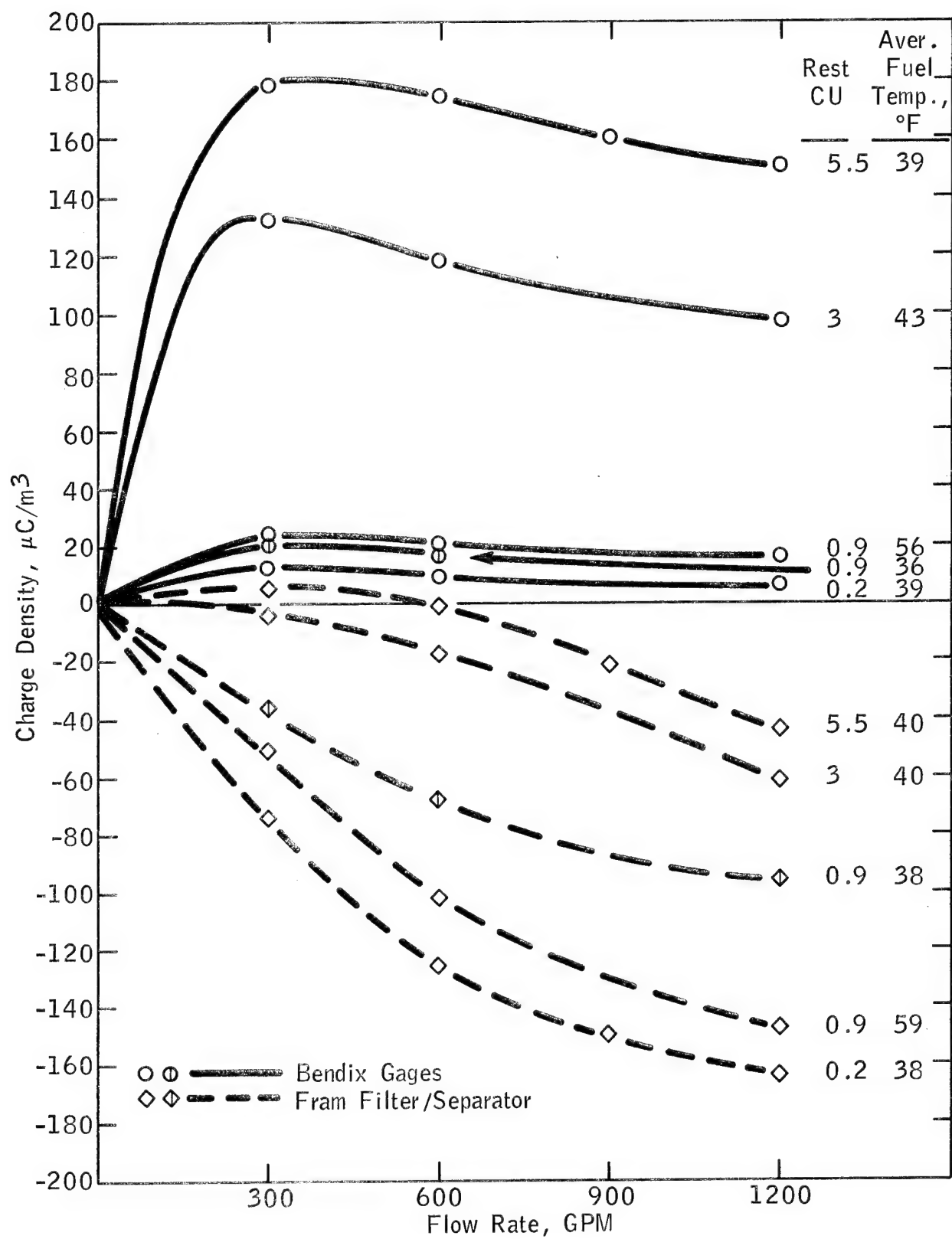


Figure 10. Charge Generated by Fram Filter/Separator and Bendix Gages as a Function of Fuel Conductivity, Flow Rate and Temperature

level increased with increasing CU and the charge level tended to rise to maximum at a low flow rate and then decrease with increasing flow rate. These data clearly demonstrate how sensitive charging tendency is to impurities in the fuel and why it is impossible to predict what charge a given fuel/filter combination will produce.

The differences in charging tendency between the filter/separator and the Gage can be explained in part by the geometry of the vessels which hold the filter elements and by the design of the elements themselves. The filter/separator case holds about 275 gallons of fuel the Gage cases only about 18 gallons each. At equivalent flow rates, fuel charged by the filter elements gets much more opportunity to relax charge within the filter/separator vessel than in the Gage.

The two filter media are also entirely different. The filter/separator contains two elements, a fiberglass depth filter at the inlet that has a very large holding capacity for contaminants and a treated paper separator at the outlet which provides a very large surface area for charge separation. The Bendix Gages on the other hand are composed of hundreds of paper wafers which provide for edge filtration. Holding capacity for contaminants is very low but the surface area for charge separation is very large. These differences in filter element design can explain why a filter/separator charges to a different level than a Gage while the differences between filter media doubtless influence the polarity of the charge separated.

It should also be noted that temperature can have a very pronounced affect on charge level. This program was initiated in late fall with the 0.9 CU fuel when the weather was still relatively warm. As indicated in Table 4, these runs were made at temperatures between 55 and 60°F compared to the runs at the other CU levels which were conducted at temperatures between 37 and 44°F. In the week following the initial series of tests there was a sharp drop in temperature and a limited amount of data was collected to show how temperature can affect charge generation; the results are provided in the bottom two lines of Table 4 and are included in Figure 10. The charge generated by the

Gages showed a decrease of only  $4 \mu\text{C}/\text{m}^3$  as a result of the temperature drop; the filter/separator showed a larger effect which increased with flow rate. At 1200 GPM, the data indicate that there was a decrease of  $52 \mu\text{C}/\text{m}^3$  with a decrease of  $18^\circ\text{F}$  or about  $3 \mu\text{C}/\text{m}^3/^\circ\text{F}$ . This large temperature coefficient indicates much higher charge levels would have been reached if the program had been carried out in warm weather.

Relaxation time,  $T$ , was used as the criteria for comparing the relaxation characteristics of FRP with metal pipe. As discussed in Appendix I,  $T$  is defined as the time required for a charge to decay to 36.8% of its original value; it can be calculated from the test data by the relation:

$$T = t / \log_e (Q_0 / Q_t) \quad (2)$$

where:

$Q_0$  = Charge density at test pipe inlet

$Q_t$  = Charge density at test pipe outlet and

$t$  = Residence time between pipe inlet and outlet at the flow rate tested. (Values used for each pipe type/pipe length and flow rate combination are shown in Table 1.)

The  $T$  obtained under each test condition is listed in Tables 26 through 33.  $T$  values obtained using the filter/separator, which generally charged the fuel negatively, are summarized in Table 5;  $T$  values obtained with the Gages which charged the fuel positively are summarized in Table 6.

In general, charge densities are good to  $\pm 0.2$  up to  $27.5 \mu\text{C}/\text{m}^3$ ,  $\pm 0.3$  to  $\pm 0.5$  up to  $77.5 \mu\text{C}/\text{m}^3$  and  $\pm 1$  above  $77.5 \mu\text{C}/\text{m}^3$ ; the standard deviations are considered to be smaller than the indicated  $\pm$  deviations. In general, no  $T$  value is shown for runs in which the charge density at the pipe outlet was less than  $1.0 \mu\text{C}/\text{m}^3$ . While the readings were considered accurate, the effect of small changes in outlet charge density, which is strongly influenced by charging characteristics of the pipe at these low levels, would have relatively large effects on  $T$ , making it of little value in any comparison. For this reason, as indicated in Table 5,

TABLE 5

RELAXATION TIMES FOR FRP AND STEEL  
PIPE OBTAINED WITH NEGATIVELY-CHARGED FUEL  
(GENERATED BY FILTER/SEPARATOR)

Nominal CU of Fuel	Flow Rate, GPM	Range of Charge Densities at Pipe Inlet, $\mu\text{C}/\text{m}^3$	Relaxation Time, $\tau$ , Seconds			
			FRP Pipe		Steel Pipe	
			Short	Long	Short	Long
0.2	300	-66/-70	56	74	61	77
	600	-115/-120	39	53	41	54
	900	-138/-147	34	44; 45	37	44
	1200	-151/-167	31	40	32; 33	41
0.9	300	-42/-49	32	36	36	40; 40
	600	-86/-97	26	30	29	34
	910	-126/-137	--	24	--	27; 28
	1200	-135/-142	20	23	21	26
3.0	300	0/4	(a)	(a)	(a)	(a)
	600	-6/-20	10.1	(a)	10.4	(a)
	900	-46	--	--	10.0	--
	910	-24/-37	--	10.3	--	12
	1200	-36/-68	8.9	9.9	9.4	11
5.5	300	0.2/0.6	(a)	(a)	(a)	(a)
	600	-1/-7	(a)	(a)	(a)	(a)
	900	-12/-30	5.9	(a)	7.2	9.1; 9.2
	1200	-27/-56	5.8	5.4(b)	6.5	7.5

(a) Charge density at pipe outlet was  $< 1.0 \mu\text{C}/\text{m}^3$ .

(b) Charge density at pipe outlet was  $0.8 \mu\text{C}/\text{m}^3$ .

TABLE 6

RELAXATION TIMES FOR FRP AND STEEL  
PIPE OBTAINED WITH POSITIVELY-CHARGED FUEL  
(GENERATED BY BENDIX GAGES)

Nominal CU of Fuel	Flow Rate, GPM	Range of Charge Densities at Pipe Inlet, $\mu\text{C}/\text{m}^3$	Relaxation Time, $\tau$ , Seconds			
			FRP Pipe		Steel Pipe	
			Short	Long	Short	Long
0.2	200	10/17	55	--	45	--
	300	8/19	56; 57	68	44	52
	600	6/16	60; 58	73	50	48
	1200	4/14	67; 56	60	26	28
0.9	300	14/23	28	31	26	(a)
	600	13/23	26	40	24	24
	910	12/20	---	48	--	24
	1200	11/20	39	52	24	23
3.0	300	68/91	6.7	(a)	5.3(b)	(a)
	600	82/106	12	14	9.7	11
	900	80	--	--	11	--
	910	94/104	--	18	--	14
	1200	76/101	16	21	13	16
5.5	300	63/100	(a)	(a)	(a)	(a)
	600	104/136	7.8	9.4	4.4	(a)
	900	114/137	8.5	9.8	6.2	7.7
	1200	119/134	9.4	10.7	7.5	9.6

(a) Charge density at pipe outlet was  $< 1.0 \mu\text{C}/\text{m}^3$ .

(b) Charge density at pipe outlet was  $0.4 \mu\text{C}/\text{m}^3$ .

no comparison between the FRP and metal pipe was possible with negatively charged fuel in either pipe length at 300 GPM when the fuel conductivity was 3 or 5.5 CU or at 600 GPM when the fuel conductivity was 5.5. And it was not possible to compare relaxation in the long pipe lengths at 600 GPM with the 3 CU fuel or at 900 GPM with the 5.5 CU fuel. The low charge densities obtained at the pipe outlet in these runs were due both to the low charge level delivered by the filter/separator under these conditions and the relatively high rate of relaxation obtained at these CU levels.

With the Gages, as shown in Table 6, the high rate of relaxation prevented a direct comparison in both pipe lengths at 300 GPM with the 5.5 CU fuel and in the long pipe lengths with the 5.5 CU fuel at 600 GPM and with the 3 CU fuel at 300 GPM.

As shown in Tables 5 and 6, the T values on repeat runs were generally within 1 second of each other. The difference of 11 seconds shown in Table 6 for the 0.2 CU fuel with the short FRP pipe at 1200 GPM was due to the fact that these particular T values are based on differences of only 1.0 and 1.6  $\mu\text{C}/\text{m}^3$  between the inlet and outlet of the pipe at charge density levels at the pipe inlet of 10.3 and 13.9  $\mu\text{C}/\text{m}^3$  (as shown in Table 30). Under these conditions, an increase in the inlet charge and a decrease in the outlet charge of 0.2  $\mu\text{C}/\text{m}^3$  would decrease the T from 67 to 48; if the inlet charge were decreased and the outlet charge were increased by 0.2  $\mu\text{C}/\text{m}^3$ , the relaxation time would increase to 111 from 67.

T values obtained using the filter/separator, which generally charged the fuel negatively, are shown graphically as a function of flow rate and CU in Figures 11 and 12 for the short and long test sections, respectively. As shown, T decreased with increasing CU and with increasing flow rate. There is good agreement between the T values obtained with FRP and metal pipe at all flow rates and CU levels. However, the relaxation time in the FRP pipe was almost always less than that in the steel pipe under the same test conditions, indicating that the fuel was relaxing somewhat faster in the FRP than the metal pipe. While not readily apparent in the figures, relaxation time was generally shorter in the short pipe lengths than in the long pipe lengths, when all other conditions were equal.

Results obtained using the Bendix Gages, which charged the fuel positively, are shown graphically in Figures 13 and 14 for the short and long test sections, respectively. In this case, T, again decreased with increasing CU. However, there tended to be an increase in T with increasing flow rate in all pipe type/pipe length combinations at 3 and 5.5 CU levels and with the short pipe sections at the 0.2 level. At the 0.9 CU level and with the long pipe sections at 0.2 CU, relaxation time tended to

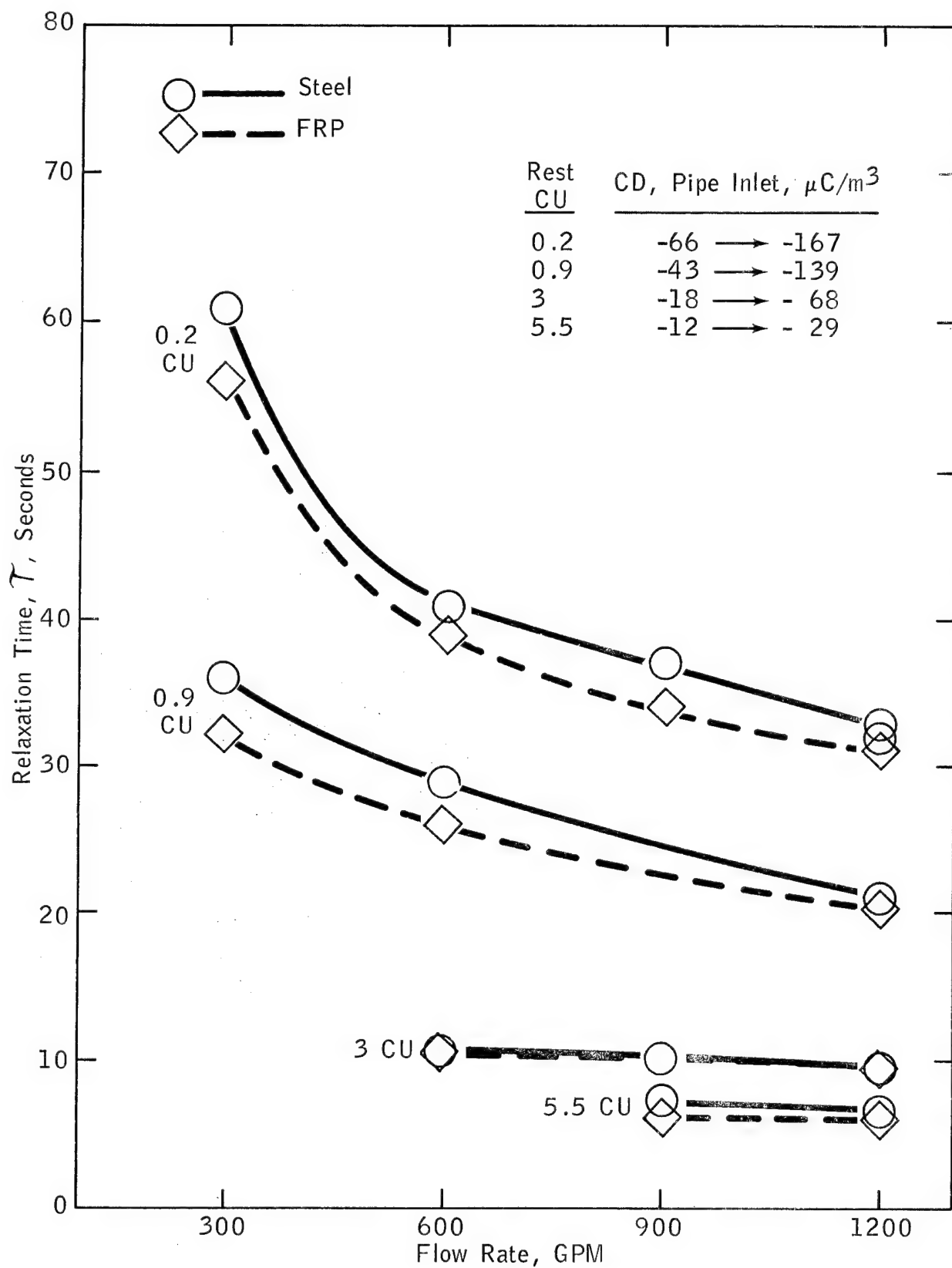


Figure 11. Relaxation Times for Short Pipe Sections With Negatively-Charged Fuel as a Function of CU and Flow Rate



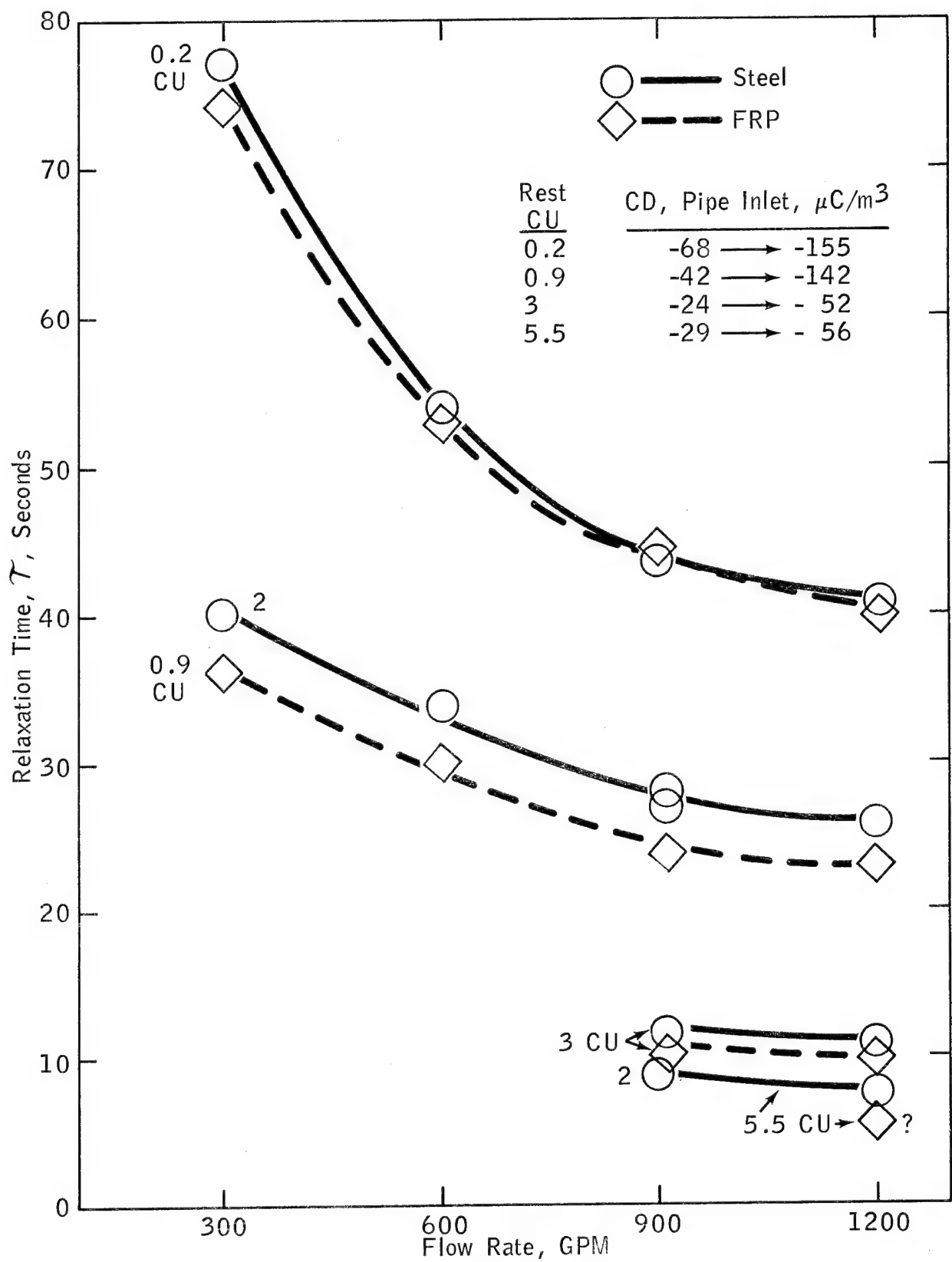


Figure 12. Relaxation Times for Long Pipe Sections With Negatively-Charged Fuel as a Function of CU and Flow Rate

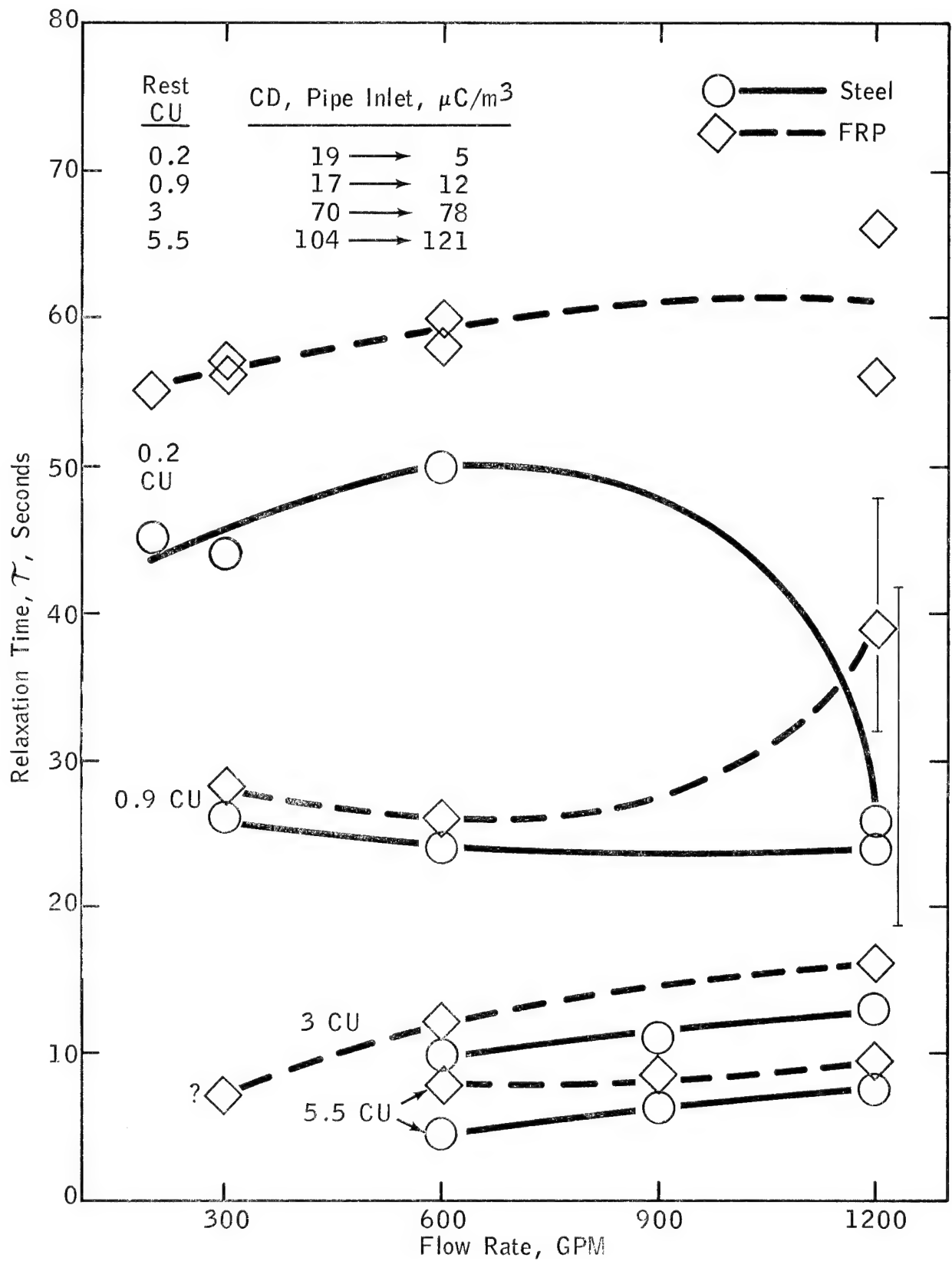


Figure 13. Relaxation Times for Short Pipe Sections with Positively-Charged Fuel as a Function of CU and Flow Rate

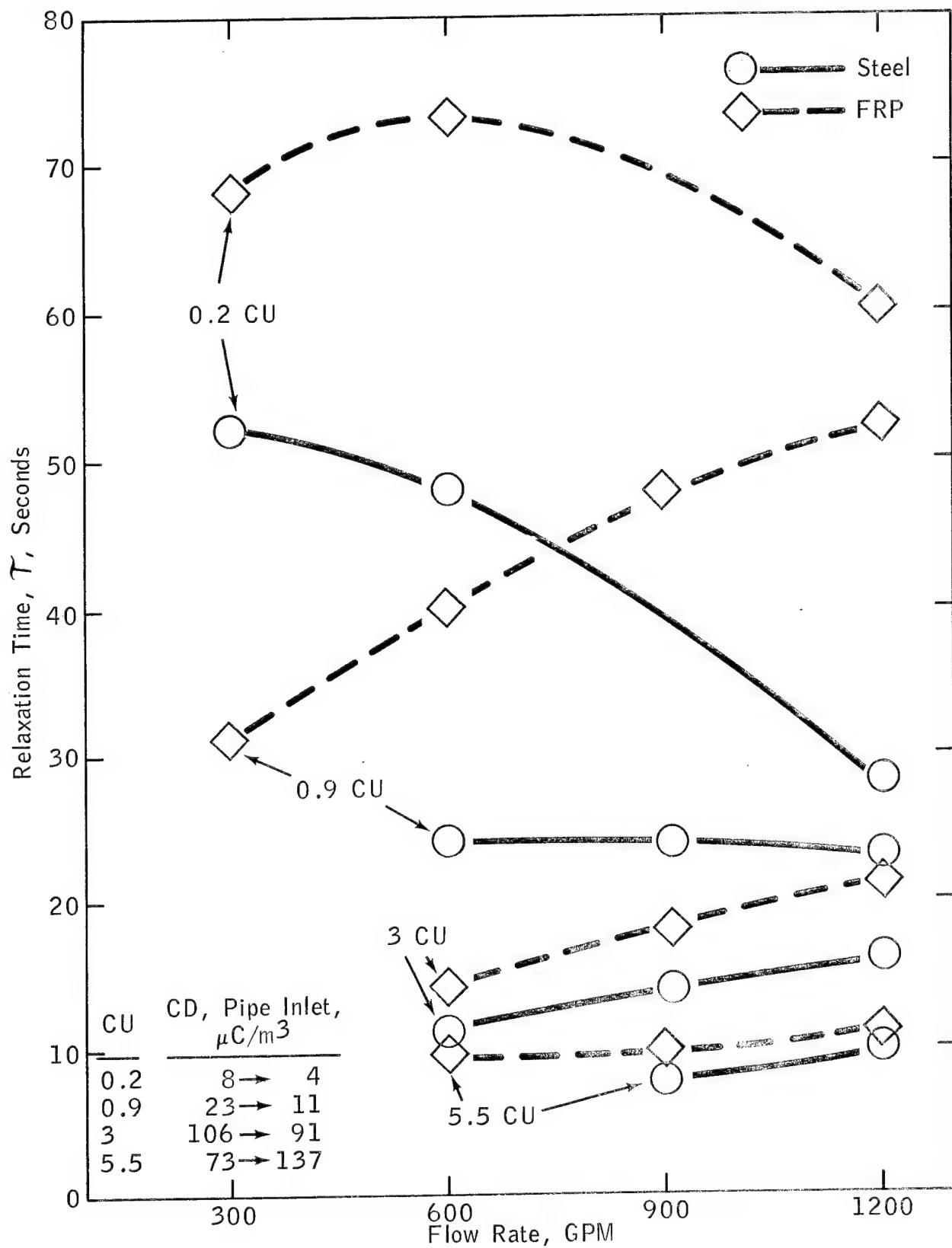


Figure 14. Relaxation Times for Long Pipe Sections with Positively-Charged Fuel as a Function of CU and Flow Rate

increase with flow rate with the FRP pipe and decrease or remain relatively constant with the steel pipe. There is relatively good agreement between the T values obtained with the FRP and metal pipe at all flow rates with the fuel at 3.3 and 5 CU and in the short pipe sections with the 0.9 CU fuel at 300 and 600 GPM. There are fairly large differences between the T values at all other conditions with the 0.9 and 0.2 CU fuels. Where large differences are observed, the T values were generally based on charge densities at the pipe outlet which were below  $5 \mu\text{C}/\text{m}^3$ . At these levels an increase in inlet charge and a decrease in outlet charge of  $0.2 \mu\text{C}/\text{m}^3$  (or vice-versa) can have large affects on T as shown in Figure 13 by the limits on the T values obtained at 1200 GPM with the 0.9 CU fuel.

Again the relaxation time was generally shorter in the short pipe lengths than the long under comparable conditions. It should be noted, however, that in all of these runs, relaxation time was greater in the FRP than in the steel pipe under matched conditions.

Thus, the data obtained indicate that there is a difference in charge relaxation between FRP and steel pipe which is due to the polarity of the charge on the fuel. Charge relaxation proceeds faster in FRP than steel pipe when the fuel is charged negatively and slower in FRP than in steel when the fuel is charged positively.

The increase or decrease in relaxation rate obtained in FRP pipe from that obtained in the steel pipe, expressed as a percentage change, at each flow rate and CU tested is shown in Table 7. In this table, a faster relaxation rate in the FRP pipe (which would be equivalent to a smaller T) is indicated by a positive value; a slower rate by a negative value. As shown, with negatively charged fuel, the increase in relaxation rate was fairly uniform, ranging from 0 to 18 percent over the conditions tested. The average increase was 8 percent overall, and 8 percent in both short and long test sections. On the other hand, the percent decrease in relaxation rate with the positively charged fuel was quite variable, ranging from a low of 8 percent to a high of 154 percent, with an overall

Table 7

PERCENT CHANGE IN RELAXATION RATE IN SUBSTITUTING FRP  
FOR STEEL PIPE AS A FUNCTION OF FUEL POLARITY

Negatively-Charged Fuel (Charge Generated with Fram Filter/Separator)  
Percent Change in Relaxation Rate @ GPM (a)

Nominal CO	200				300				600				900				1200			
	S	L	S	L	S	L	S	L	S	L	S	L	S	L	S	L	S	L	S	L
0.2	--	--	8	4	8	10	5	2	5	10	3	2	8	0; 2	3; 6	2				
0.9	--	--	11	10	11	10	10	12	10	10	3	12	--	11; 14	5	12				
3	--	--	--	--	--	--	3	--	--	--	--	--	--	14	5	10				
5.5	--	--	--	--	--	--	--	--	--	--	--	--	18	--	11	28(b)				

Averages: S (Short) Pipe = 8; L (Long) Pipe = 8; Overall = 8

Positively-Charged Fuel (Charge Generated With Bendix Gages)

0.2	-22	--	-27; -30	-31	-20, -16	-52	--	--	--	-154; -115	-114
0.9	--	--	-8	--	-8	-67	--	--	-100	-62	-126
3	--	--	-26(b)	--	-24	-27	--	--	-29	-23	-31
5.5	--	--	--	--	-75	--	-37	-29	-29	-25	-11

Averages: S (Short) Pipe = -44; L (Long) Pipe = -56; Overall = -49  
-30(c)

$$(a) \text{ Percent Change in Relaxation Rate} = \left[ \left( \frac{T_{\text{Steel}} - T_{\text{FRP}}}{T_{\text{Steel}}} \right) \times 100 \right]$$

(b) Value not used in averages; charge density at pipe outlet < 1.0.

(c) Average calculated excluding underlined values.

average decrease of 46 percent. However, there are several factors which indicate that some of these values can be omitted from consideration. For example, the values in both the short and long pipe sections with the 0.2 CU fuel at 1200 GPM were based on small differences between charge densities which never exceeded  $13.9 \mu\text{C}/\text{m}^3$  at the pipe inlet. (See Table 30) As indicated previously, the T values obtained under these conditions are subject to large deviations and this is reflected in the two widely different values of -154 and -115 for the percent change in relaxation rate observed for tests in the short pipe. In addition, as shown in Table 31, runs carried out in the long FRP pipe with the 0.9 CU fuel were conducted at temperatures which were 2.5 to 4°F lower than those in the long steel pipe and at charge levels at the pipe inlet which averaged about  $22 \mu\text{C}/\text{m}^3$  for the FRP versus about  $13 \mu\text{C}/\text{m}^3$  for the steel pipe. The relatively large differences in charge density at these low levels along with the differences in temperature, which are much larger than in any other runs carried out in this program, make the percentage changes in relaxation rate, which ranged from -67 to -126 percent in these runs, suspect. If these runs are excluded from the overall analysis, the decrease in relaxation rate would be 30 percent for tests in both short and long pipe and thus overall. The decrease in relaxation times would range from 8 to 75 percent.

The primary question then is this: Would reductions in the relaxation rate of these magnitudes limit or rule out the use of FRP pipe in fuel handling facilities?

To answer this, it is desirable to define the maximum charge level that would be considered safe at the point of delivery. For this study, a charge level of  $30 \mu\text{C}/\text{m}^3$  will be used as the criterion for "safe" fueling. The value was originally proposed by American Oil (Appendix I [28]) and has been generally accepted by others in the industry as a reasonable guide. Esso Research studies on superjet fueling (Appendix I [1]) showed that a minimum charge density of  $70 \mu\text{C}/\text{m}^3$  was required to generate

incendiary sparks during fueling if a "charge collector" was present in the receiving tank. Since it is desirable to provide for safe fueling in the most hazardous situations, the use of a maximum of  $30 \mu\text{C}/\text{m}^3$  as a "safe" charge level is considered reasonable.

Now let us assume that FRP pipe decreases the relaxation rate by either 30 or 90 percent. The first value is equal to the average decrease of 30 percent obtained in these studies; the second is somewhat greater than the maximum of 75 percent, which was obtained with the 5.5 CU fuel at 600 GPM after eliminating suspect values and those subject to large deviations. The following table shows how these changes in relaxation rate would theoretically affect the charge delivered by a system designed to deliver fuel at  $30 \mu\text{C}/\text{m}^3$ , assuming different charge levels at the inlet to the system.

Charge Density, $\mu\text{C}/\text{m}^3$			
At System Inlet	Design	At System Outlet	
		With Decrease In Relaxation Rate Of	
		30%	90%
100	30	40	53
300	30	51	89
500	30	58	114
1000	30	68	158

As shown, the increase in amount of charge delivered should essentially double with a 90 percent decrease in relaxation rate with a system sized to decrease charge from 100 to  $30 \mu\text{C}/\text{m}^3$ ; it should double with a 30 percent decrease in rate with a system designed to reduce charge from 500 to  $30 \mu\text{C}/\text{m}^3$ . The data indicate that outlet charge could increase markedly with higher inlet charge levels as relaxation rate decreased.

Theoretically, a 30 percent decrease in relaxation rate would be equivalent to an increase of 30 percent in the amount of time that would have to be provided to allow fuel to dissipate a given quantity of charge,

a decrease of 90 percent in rate would require that the time provided be almost doubled. However, the conductivity of charged fuel is not necessarily the same as the rest conductivity, used in developing the data tabulated above. As indicated in Appendix I, the conductivity under charged conditions is referred to as "effective" conductivity,  $k_e$ , to differentiate it from "rest" conductivity,  $k_0$ , which is measured on the uncharged fuel, and referred to in these studies as the nominal fuel conductivity. The following relationship, based on equation 12 (in Appendix I) has been used to calculate  $k_e$  for the runs carried out in evaluating charge relaxation:

$$k_e = 18 \log_e (Q_0/Q_t)/t = 18/T \quad (3)$$

where  $Q_0$ ,  $Q_t$ ,  $t$  and  $T$  are the same as defined previously.

Values for  $k_e$  and  $k_e/k_0$  are included in Tables 26 through 29 for fuels charged negatively with the filter-separator and in Tables 30 through 33 for the positively-charged fuels obtained with the Gages. Figure 15 shows  $k_e/k_0$  as a function of  $k_0$ , expressed in CU, for both negatively- and positively-charged fuels with the steel pipe. As indicated, the  $k_e/k_0$  values obtained with the positively-charged fuel (filled-in circles) have about the same average value as those obtained with the negatively-charged fuel (open circles) at all levels of  $k_0$ . The dashed lines in this figure represent the average values obtained for two different types of filters in previous studies (Appendix I [33]). As shown, the relationship between  $k_e/k_0$  and  $k_0$  obtained in this study follows much the same pattern as that obtained in previous work. Fuels having a  $k_0$  below about 0.5 CU tended to behave as if they had a higher CU; those above 0.5 tended to behave as if they had a lower CU.



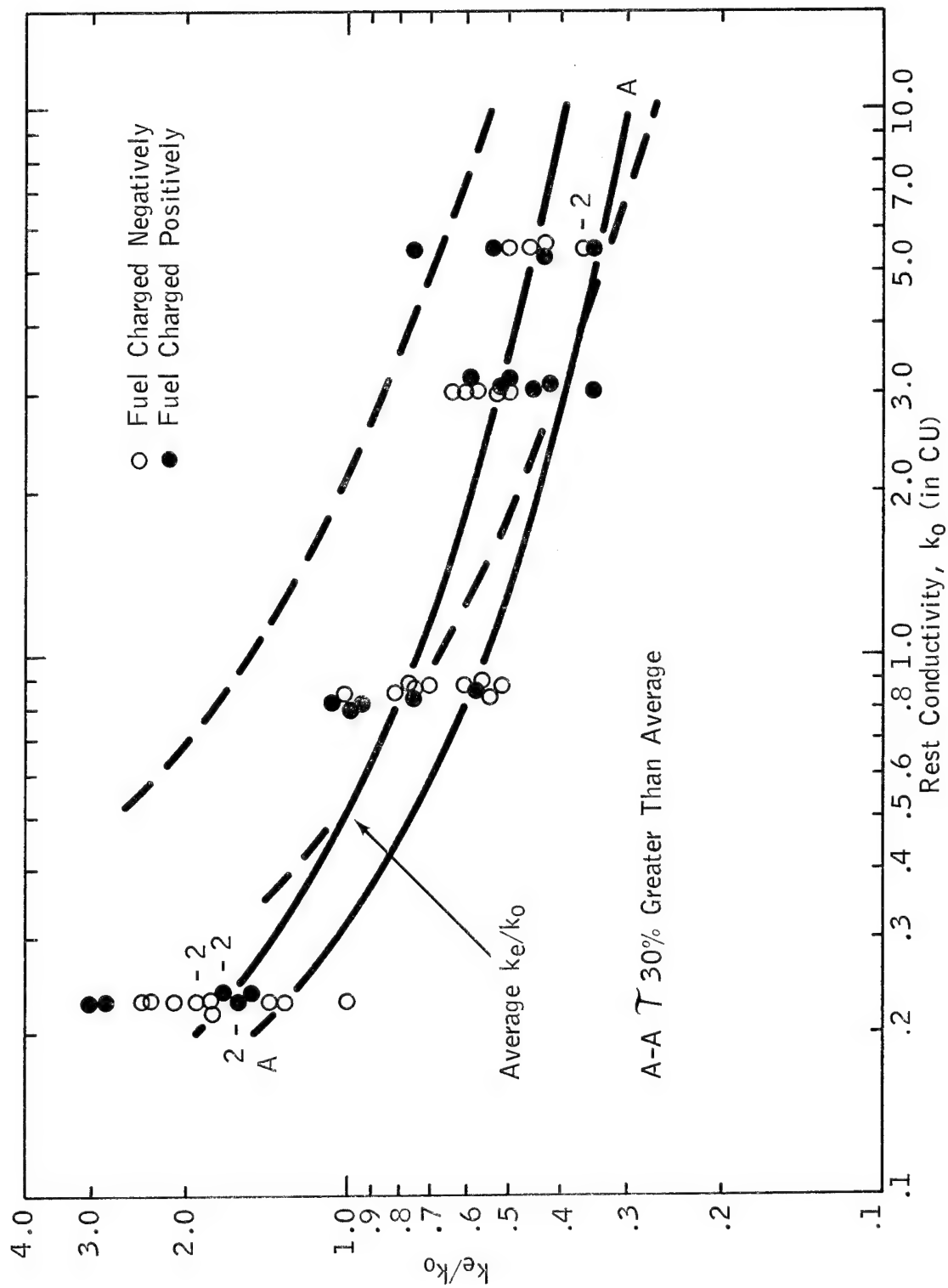


Figure 15. Ratio of  $k_e/k_o$  Versus  $k_o$  Obtained With Steel Pipe

The  $k_e/k_o$  versus  $k_o$  data obtained with the FRP pipe are shown in Figure 16. Again the open circles represent data obtained with negatively-charged fuel; the filled circles, positively-charged fuel. Runs with the negatively-charged fuel tend to exhibit a higher  $k_e$  than those made with the positively-charged fuel, which reflects the fact that relaxation in plastic pipe is faster than in steel with negatively-charged fuel and slower with positively-charged fuel.

Bustin et al (Appendix I [9]) have shown that fuels having  $k_o$ 's below 1.0 CU relax at a rate which depends on charge density and ion mobility, not  $k_o$ , and charge relaxation is hyperbolic rather than exponential, as in the ohmic theory of relaxation. A comparison of the hyperbolic and ohmic theories based on the data obtained in this study with the 0.2 CU fuel when it was charged negatively is provided in Appendix III.

It is obvious from these data that any recommendation regarding the use of FRP pipe must take into account the fact that positively-charged fuel has a slower rate of relaxation in FRP than in steel pipe and the fact that the charge may relax faster or slower than would be expected based on the rest conductivity.

The residence times that would be required to reduce the charge from initial levels between 100 and 1000  $\mu\text{C}/\text{m}^3$  at the inlet to 30  $\mu\text{C}/\text{m}^3$  at the outlet are shown for steel and FRP pipe in Table 8. Data for the latter are shown, assuming increases in relaxation time of 30 and 90 percent over the average for steel pipe.

Relaxation times listed in the table for the steel pipe at the rest conductivity levels of 1,3,5 and 10 CU were developed using the relation:

$$T = (18/k_o)(k_o/k_e) \quad (4)$$

The value of  $k_o/k_e$  was obtained from the curve representing the average  $k_e/k_o$  over the range of  $k_o$ 's evaluated in this program, as described by the solid line in Figure 15. Values for  $k_o$ ,  $k_e/k_o$  and  $T$  used in the calculations are shown in Table 8. The  $T$  values for steel pipe were in-

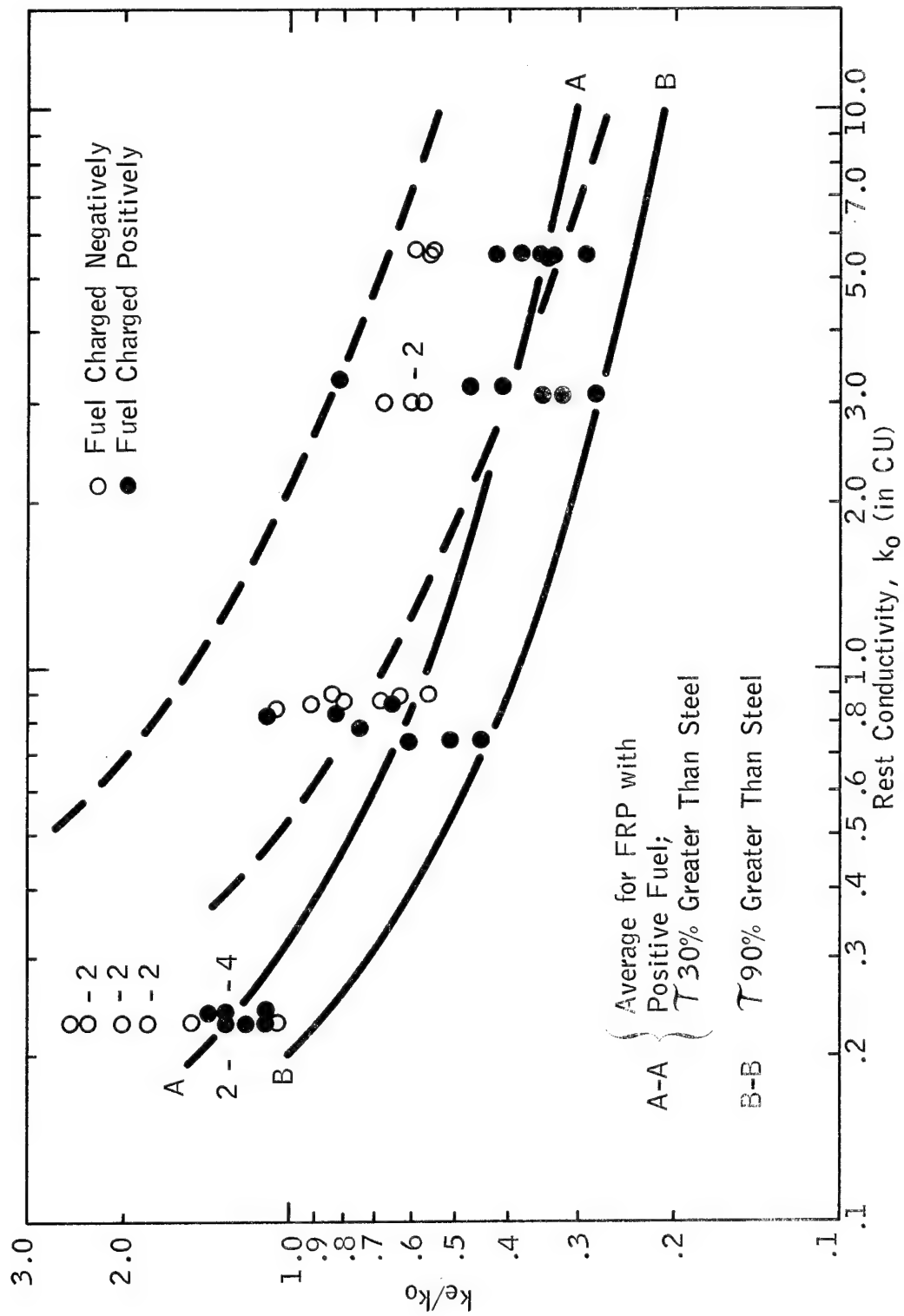


Figure 16. Ratio of  $k_e/k_o$  Versus  $k_o$  Obtained With FRP Pipe

TABLE 8

RESIDENCE TIMES REQUIRED TO REDUCE  
CHARGE DENSITY TO  $30 \mu\text{C}/\text{m}^3$  IN STEEL AND FRP PIPE\*

Steel Pipe

$k_o$ , CU	$k_e/k_o$	$k_e$ , CU	$\tau$ , Secs	Residence Time, Seconds, to Reach $30 \mu\text{C}/\text{m}^3$ from $\mu\text{C}/\text{m}^3$ of:			
				100	300	500	1000
0.2	--	--	--	111	143	149	154
1.	.74	.74	24 (18)	28 (22)	55 (41)	68 (51)	84 (63)
3.	.52	1.56	11.5 (6)	14 (7)	26 (14)	32 (17)	40 (21)
5.	.46	2.30	7.8 (3.6)	9.4 (4.3)	18 (8)	22 (10)	27 (13)
10.	.39	3.9	4.6 (1.8)	5.5 (2.2)	10.6 (4.1)	13 (5.1)	16 (6.3)

FRP Pipe (Assuming Relaxation Time 30% Greater Than Steel)

0.2	--	--	--	144	186	194	200
1.	.58	.58	31	37	71	87	109
3.	.40	1.20	15	18	35	42	53
5.	.36	1.78	10.1	12	23	28	35
10.	.30	3.0	6.0	7.2	14	17	21

FRP Pipe (Assuming Relaxation Time 90% Greater Than Steel)

0.2	--	--	--	211	272	283	293
1.	.39	.39	46	55	106	129	161
3.	.27	.82	22	26	51	62	77
5.	.24	1.20	15	18	34	42	53
10.	.21	2.1	8.7	10.4	20	24	31

\* $30 \mu\text{C}/\text{m}^3$  was assumed to be a safe charge level at the point of delivery.

creased by 30 and 90 percent to provide the values for  $T$  and  $k_e/k_o$  used in developing the data shown for the FRP pipe at these CU levels. The residence times were calculated using the expression:

$$t = T \log_e (Q_o/Q_t) \quad (5)$$

where  $Q_o = 100, 300$ , etc. and  $Q_t = 30$ .

The residence times shown in Table 8 for the steel pipe at 0.2 CU were calculated using equation 17 (Appendix III) assuming a mobility,  $\mu$ , of  $0.38 \times 10^{-8} \text{ m}^2/\text{volt sec}$ . This is the average mobility obtained for runs carried out in the steel pipe at the two highest flow rates tested. This value was selected because it was based on the highest inlet charge levels attained in this study and provides the most conservative estimate of the time required for charge relaxation. The residence times were simply increased by 30 and 90 percent to provide the values shown for the FRP pipe.

The dashed line running through each set of data in Table 8 separates the conditions for which 30 seconds of residence time would be adequate for reducing the charge level to  $30 \text{ } \mu\text{C}/\text{m}^3$  from those conditions which would not be adequate.

As shown, more than 30 seconds of relaxation would be required to reach  $30 \text{ } \mu\text{C}/\text{m}^3$  in the effluent from the steel pipe with the 0.2 CU fuel at all inlet charge densities. Residence times of more than 30 seconds would also be required with the 1 CU fuel for inlet charge densities above  $100 \text{ } \mu\text{C}/\text{m}^3$  and with the 3 CU fuel at inlet charge densities of  $500 \text{ } \mu\text{C}/\text{m}^3$  and higher. Since  $k_e/k_o$  falls below 1 for  $k_o$  greater than about 0.5 CU, the actual time required to reach  $30 \text{ } \mu\text{C}/\text{m}^3$  is greater than what would be predicted based on  $k_o$ . (Residence times based on  $k_o$  for CU's of 1,3,5 and 10 are shown in parentheses in Table 8.)

Data for the FRP pipe based on a relaxation time 30 percent greater than for steel represents the average performance observed for FRP pipe in this program, as shown by line A-A in Figure 16. In this case, residence times greater than 30 seconds would be required for the

effluent to drop to  $30 \mu\text{C}/\text{m}^3$  for fuels of 1 CU and lower at all inlet charge densities listed in Table 8. More than 30 seconds would be required with 3 CU fuel at inlet charge densities of about  $300 \mu\text{C}/\text{m}^3$  and higher and with 5 CU fuel above  $500 \mu\text{C}/\text{m}^3$  at the inlet. A line representing a 30 percent decrease in relaxation rate is also included in Figure 15 with the data obtained using the steel pipe. As indicated, there were several runs with both negatively and positively charged fuel in which  $k_e/k_o$  fell below the curve (A-A). The runs which provided the low  $k_e/k_o$  values at rest conductivities of 1 and 3 CU were based on maximum inlet charge densities of only  $45 \mu\text{C}/\text{m}^3$ , and would not be indicative of any problem in the field.

Data for FRP pipe based on a relaxation time 90 percent greater than the average for steel includes the lowest  $k_e/k_o$  ratios observed in FRP pipe with positively charged fuel as shown by line B-B in Figure 16. Under these conditions, residence times of greater than 30 seconds are required for 3 and 5 CU fuels at inlet charge densities above  $100 \mu\text{C}/\text{m}^3$  and with 10 CU fuel at inlet charge densities above  $500 \mu\text{C}/\text{m}^3$ .

These data indicate that it would not be advisable to use FRP pipe in place of steel pipe where only 30 seconds of relaxation time are available. However, this is not a restriction where the pipe is used in Air Force (AF) Type III Hydrant system where AF experience indicates that the minimum length of pipe between the final filter and the first fueling station in typical installations would be 900 to 1000 feet (Ref. 5). At the design flow rate of 4 feet/second, the residence time would be 225 to 250 seconds. At 7 feet/second, the maximum flow velocity which such systems could handle in the future, if required, the residence time would be 130 to 140 seconds. These parameters would not apply to an AF Type II Hydrant system, since a hose cart with a filter/separator is immediately adjacent to discharge point; minimal relaxation time is available for the charged fuel.

Conditions for which more than 130 seconds of residence time would be required to provide a maximum of  $30 \mu\text{C}/\text{m}^3$  at the point of delivery fall above the solid line shown in each set of data in Table 8. As shown,  $30 \mu\text{C}/\text{m}^3$  would be exceeded with 130 seconds of relaxation available in FRP pipe, assuming relaxation is 90 percent slower than in metal pipe, with fuels of 0.2 CU starting at inlet charge levels below  $100 \mu\text{C}/\text{m}^3$  and at inlet charge levels above  $500 \mu\text{C}/\text{m}^3$  with fuels of 1 CU. With 225 seconds of relaxation available,  $30 \mu\text{C}/\text{m}^3$  would only be exceeded with fuels of 0.2 CU at inlet charge levels above  $100 \mu\text{C}/\text{m}^3$ .

The data indicate that FRP pipe can be used in new or redesigned AF hydrant systems handling JP-4 fuel if 130 seconds of residence time are available between the final filter/separator and the first fuel station. This must be qualified since no hard data are available on either conductivity of JP-4 fuel from various suppliers or to what extent the fuel is charged through MIL-F-8901 filter/separator elements in AF systems. Obviously, the residence time required to deliver a "safe" charge is dependent on both fuel conductivity and charge generation, an unpredictable factor which depends on both type and quantity of impurities in the fuel and their interaction with the properties of the filter surface. This suggests that a field survey be conducted to determine the range and potential minimum conductivity, and range and potential maximum charge level that can be obtained in Air Force fueling systems.

#### 4. SURFACE VOLTAGE MEASUREMENTS AND SPARK GENERATION

The voltage on the surface of the FRP pipe was measured during a majority of the runs. No measurements were made on the steel pipe since the conductivity of steel prevents buildup of significant voltages. Measurements were made after the charge densities measured at the pipe inlet and outlet had stabilized; the measurements were generally made at 10 foot intervals on the short pipe and at ten-to-twenty foot intervals with the pipe in the long configuration. The points at which measurements were made are indicated in Figure 17, relative to the location of the stanchions which support the pipe. The location of a metal drain valve which was only in the long pipe configuration, and three aluminum foil wrappings that were used in observing the sparking tendency are also indicated. The surface voltage data that were obtained are provided in Tables 34 through 45; the ambient temperature and humidity at the time the measurements were made are also provided. The amount of data obtained was quite extensive and only the most pertinent information will be discussed in this report.

The maximum surface voltages measured on the straight pipe sections during the runs carried out using the filter bypass, the filter/separator or the Gages, are summarized in Table 9. The distance from the pipe inlet at which the maxima were observed are indicated in parentheses. Actually, the highest voltages were often measured at the first bend, eg. at 40 feet from the inlet, sometimes accompanied by a reversal in polarity, as indicated in Table 34. The effect of a bend on surface voltage was less obvious at 120 and 200 feet, although relatively large changes were observed at these locations in some runs, as indicated in Table 41. Similar effects have been noted at constrictions in tubes by previous investigators (Appendix I [52]). These maxima were disregarded in the analysis of the data since they did not give a consistent basis for comparison.



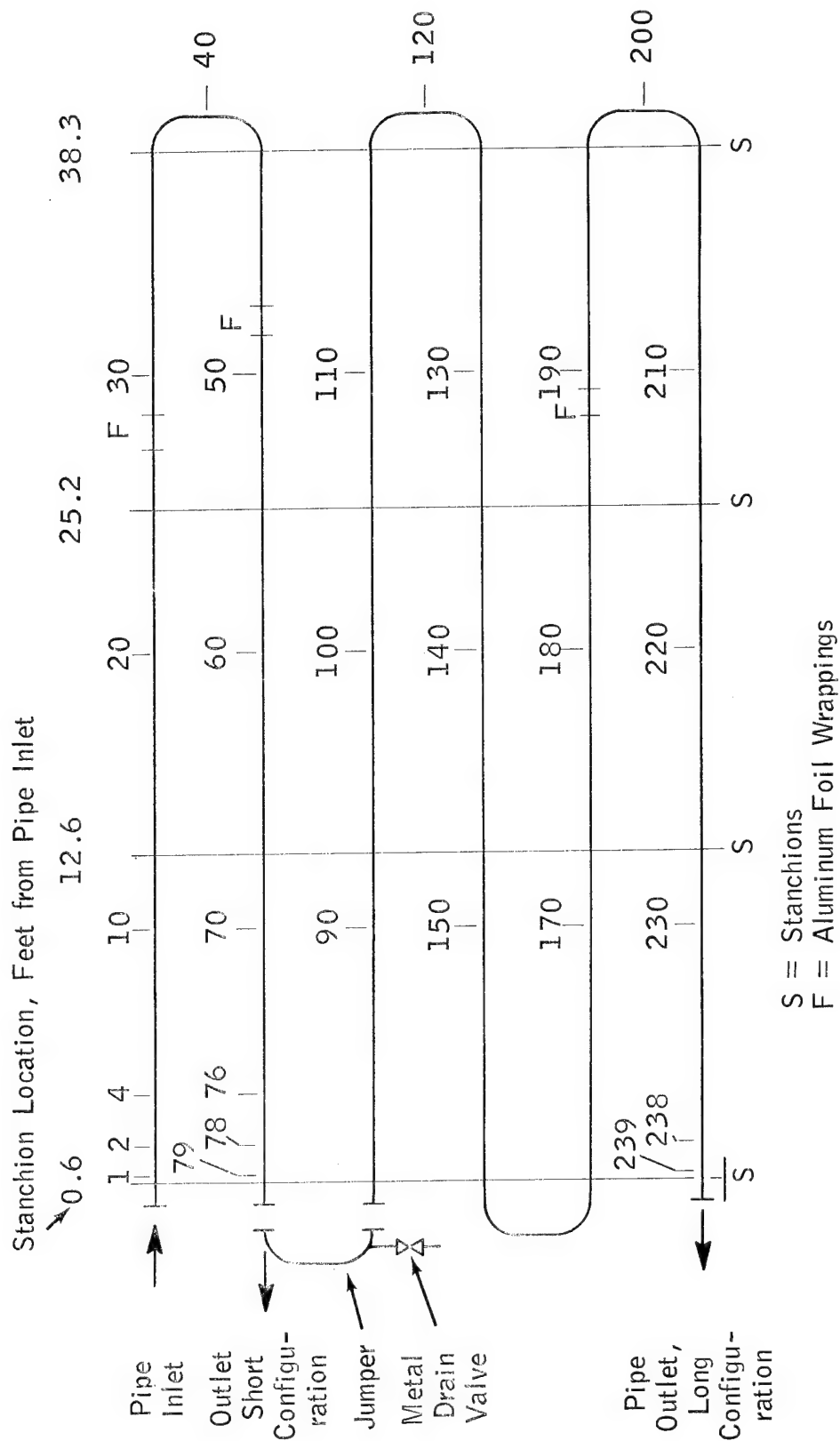


Figure 17. Location of Positions Where Surface Voltage Was Measured on FRP Pipe Relative to Distance From Pipe Inlet and Stanchions

Table 9

MAXIMUM SURFACE VOLTAGES MEASURED ON FRP PIPE USING  
BYPASS, FILTER/SEPARATOR AND GAGES

## Using Filter Bypass

		Maximum Surface Voltage, kv, at Flow Rate, GPM, and Feet From Inlet Indicated(a)					
		300		600		1200	
Rest	Pipe Inlet CU	Short	Long	Short	Long	Short	Long
0.2	-0.7 → -1.3	3.0(50)	-4.8(170)	-	-2.7(150)	-	-
0.9	1.5 → 3.4	4.3(20)	-	4.6(20)	-	4.6(20)	-
	-1.2 → -2.8	-	-0.24(b)	-	-0.026(150)	-	-0.039(170)
3.	-0.9 → -3.8	7.1(30)	.23(50)	6.9(30)	-0.018(c)	6.6(30)	-
5.5	-1.3 → -4.2	-1.29(30)	-1.53(60)	-1.75(30)	-	-2.4(30)	-7.7(150)
						2.6(50)	2.2(20)
						4.1(30)	-
						-	-
						6.0(d)	-0.108(170)
						-2.4(30)	-0.018(e)

## Using Fram Filter/Separator

		300		600		900		1200	
Rest	Pipe Inlet CU	Short	Long	Short	Long	Short	Long	Short	Long
0.2	-66 → -161	-11.7(30)	-30(f)	-23(30)	-48(50)	-28(30)	-	-23(60)	-52(60)
0.9	-44 → -139	-1.26(37)	-21(78)	-5.8(30)	-34(78)	-	-	-7.1(20)	-38(78)
3.	0 → -68	2.9(20)	-	0.2(10)	.054(50)	-	-	0.2(10)	-0.080(50)
5.5	0.3 → -32	-1.29(30)	-	-1.53(30)	4.3(20)	-5.5(30)	-17.7(10)	-12.4(30)	-34(20)

## Using Bendix Gages

		300		600		900		1200	
Rest	Pipe Inlet CU	Short	Long	Short	Long	Short	Long	Short	Long
0.2	7.8 → 4.2	-	14.5(20)	-	-	-	-	-	20.5(20)
0.9	17 → 22	.51(30)	4.3(60)	.25(30)	3.8(60)	-	-	.122(78)	3.55(130)
3.	70 → 91	6.0(50)	2.9(60)	5.1(50)	5.5(60)	-	-	6.0(20)	4.3(60)
5.5	(g)	-13.1(30)	16.5(60)	38(20)	55(20)	42(20)	36(10)	42(20)	30(10)

(a) Values in parentheses indicate distance from pipe inlet in feet at which maximum voltage was measured.  
 (b) 50, 60 and 150 feet (c) 1, 79, 239 (d) 20, 30 feet (e) 79, 170, 190, 230, 239 feet (f) 60, 70 feet  
 (g) Inlet charge densities on long pipe were 73, 131, 129, 125 for each respective flow rate.

As shown in Table 9, the surface voltage generally increased with increasing charge level at the pipe inlet, and higher surface voltages were generally measured on the long pipe configuration at a given condition. Thus maxima of -30 to -52 kv were measured with inlet charge levels ranging from -66 to -161 as obtained using the filter/separator with the 0.2 CU fuel and a maximum of 55 kv at an inlet charge of  $131 \mu\text{C}/\text{m}^3$  using the Gages with the 5.5 CU fuel. It should also be noted that substantial voltages were generated on the pipe surface even when the fuel was entering the test section through the filter-bypass where the maximum charge level measured at the inlet was  $-4.2 \mu\text{C}/\text{m}^3$ . The highest surface voltage was 7.1 kv obtained in the short pipe with the 3 CU fuel at 300 GPM.

The maximum voltage was reached nearer to the inlet end of the pipe than the outlet. For the short test section the maximum was generally reached between 20 and 30 feet from the inlet; for the long test section, the maximum generally occurred between 20 and 80 feet of the inlet.

The low surface voltage readings obtained with the long pipe section and the 0.9 CU fuel using the bypass were due to early morning fog and high humidity (eg. 90-94 percent) which tended to wet the pipe surface. Surface voltage readings increased with this fuel CU and pipe length combination in the tests carried out using the Gages and the filter/separator, during which time the humidity levels dropped (eg. from 83 to 62 percent). Similarly, the low readings obtained with the short pipe section and the 0.9 CU fuel using the filter/separator and Gages was probably due to the fact that the humidity levels exceeded 80 percent during these determinations. The low readings obtained on the long pipe section with the 3 CU fuel using the bypass and filter/separator are directly attributable to a very light drizzle, which did not produce very high humidity levels, but was sufficient to wet the outer surface of the pipe sufficiently to increase its conductivity, preventing a buildup in the surface voltage.

While making the outside of the pipe conductive will eliminate buildup of surface potential, it does not affect the rate at which charge relaxes inside the pipe. This shown by the following data which were collected with the short FRP pipe on a bright clear day before and after wetting the entire length of pipe:

	<u>Charge Density, <math>\mu\text{C}/\text{m}^3</math>, @ (a)</u>		<u>Fuel</u>
	<u>Pipe Inlet</u>	<u>Pipe Outlet</u>	<u>Temp., °F</u>
Before Wetting	146.5	112.5	36.2
After Wetting	146.0	112.0	36.2

(a) Obtained at 900 GPM with 0.2 CU Fuel.

It should be noted that the relaxation times obtained with the 3 CU fuel using the filter/separator (Figure 12), when outer surface of the pipe was wet, as mentioned above, lined up very well with the steel pipe data. The agreement was similar to that obtained between the long FRP and long steel pipe at the other CU's tested with negatively-charged fuel. These observations, along with the results described above, show that the conductivity of the outer surface of the pipe does not affect the rate of charge relaxation within the pipe and any deviations between FRP and steel pipe mentioned previously, are not attributable to humidity or moisture on the outer surface or the pipe.

The change in surface voltage with distance from the pipe inlet for tests conducted at 600 GPM in both long and short pipe sections at 5.5 CU using the Bendix Gages which charged the fuel positively is shown in Figure 18. The inlet charge level was  $114 \mu\text{C}/\text{m}^3$  for the short and 131 for the long pipe section. As shown, the surface voltages on the long pipe were higher than on the short. The increase in voltage at the inlet end is in each case rapid; the drop at the outlet is also rapid, but more gradual. There are pronounced increases in the surface voltage on the bends at 40 and 120 feet from the inlet. Similar data are provided in Figure 19 for tests conducted using the filter/separator with the 5.5 CU fuel. Here the fuel was charged negatively and the surface voltage was negative. Data are shown for both pipe lengths at 900 and 1200 GPM; at

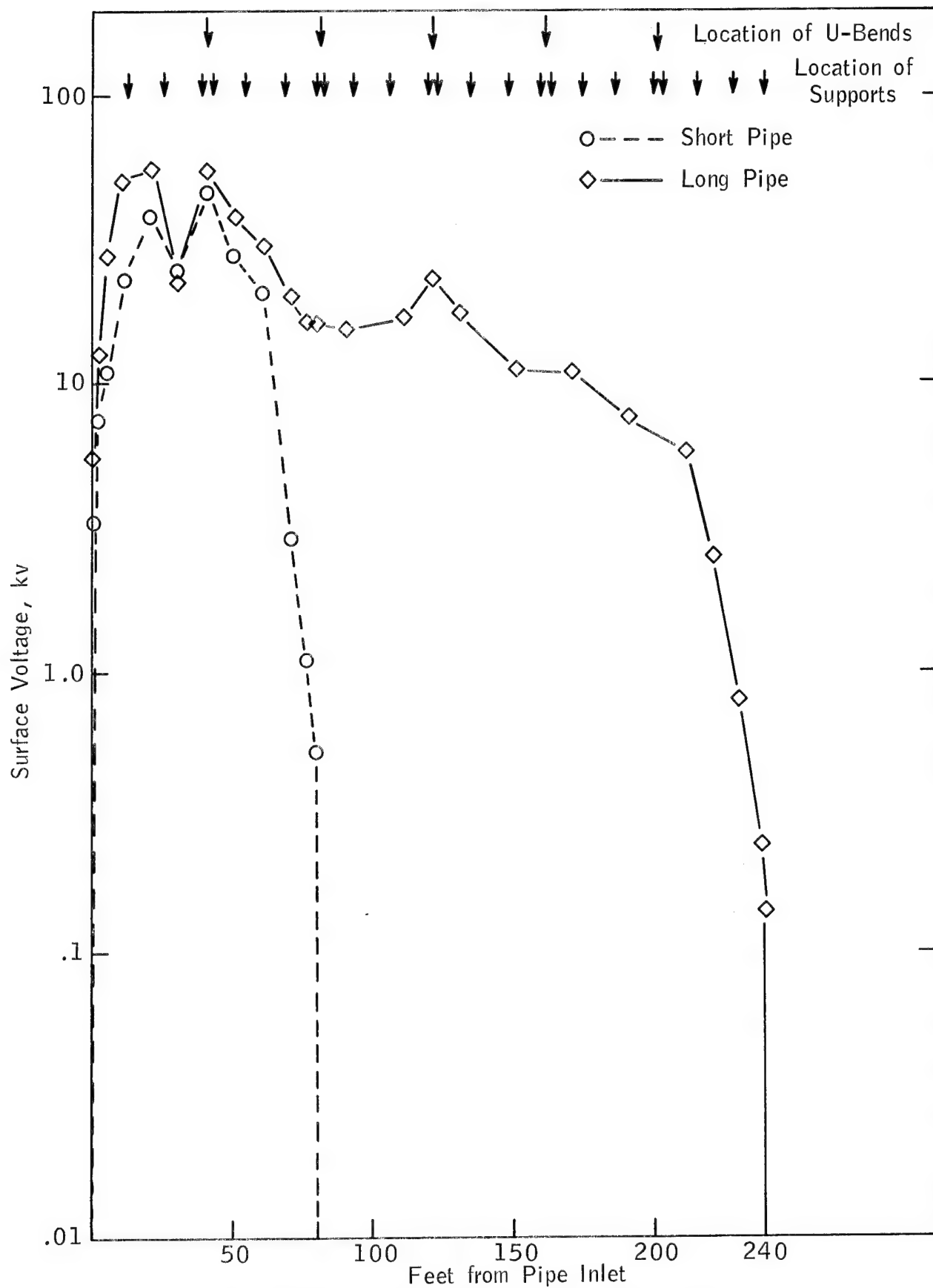


Figure 18. Surface Voltage Versus Distance From Pipe Inlet -  
Using Gages (Positively Charged Fuel) at 5.5 CU  
and 600 GPM

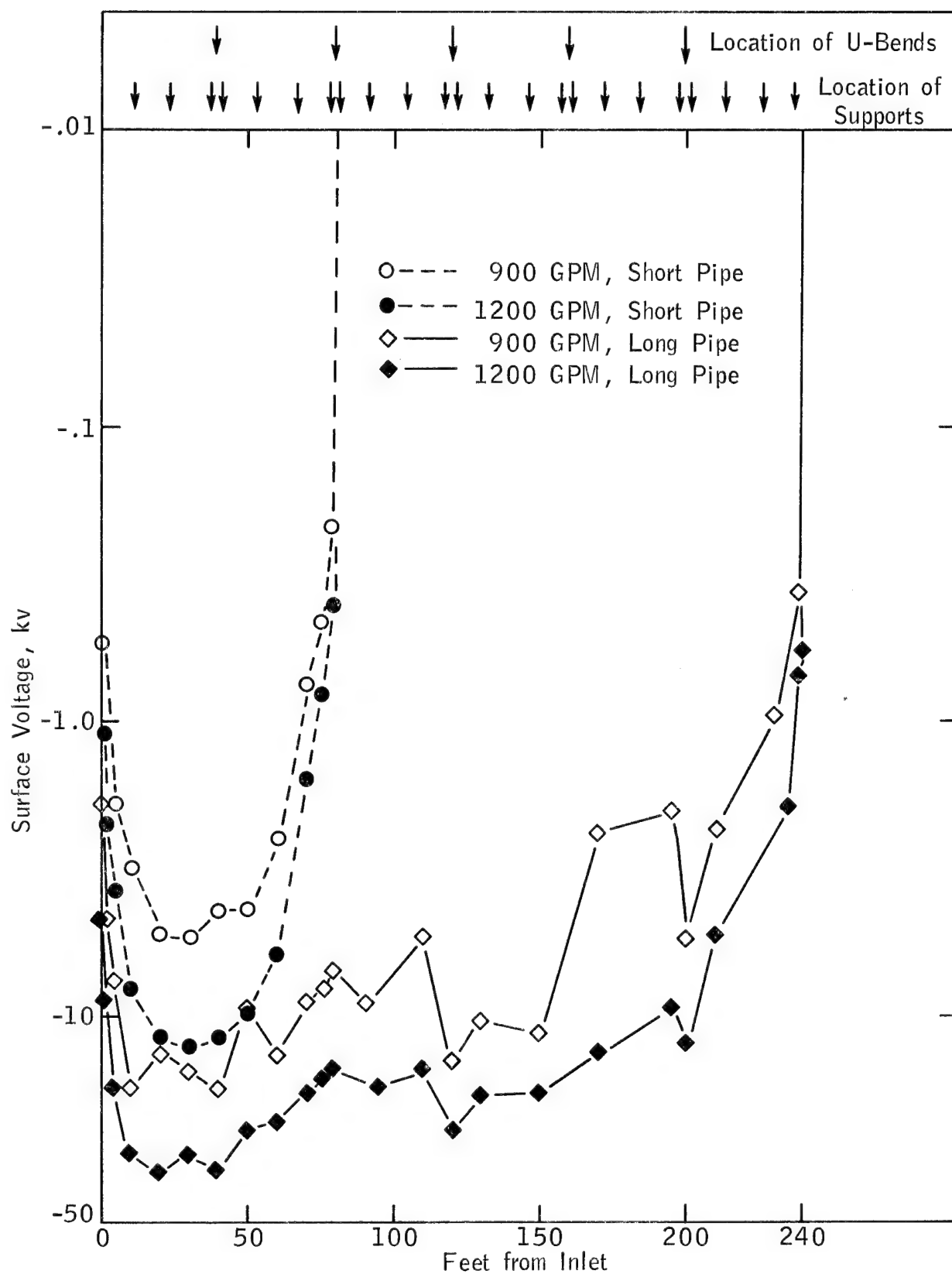


Figure 19. Surface Voltage Versus Distance From Pipe Inlet - Using Filter/ Separator (Negatively Charged Fuel) at 5.5 CU

these flow rates the inlet charge levels were  $-13$  and  $-30 \mu\text{C}/\text{m}^3$ , respectively. Here the increase in surface voltage with increasing charge density is apparent in both pipe lengths, again the long pipe exhibits the higher surface voltage for a given inlet charge level. In these runs the increase in surface voltage is more apparent at the 120 and 200 foot bends than in Figure 18.

In these runs, there was little evidence to indicate there is any pronounced decrease in surface voltage near the stanchions. The shape of these curves and the fact that wetting the pipe surface does not affect the charge level at the pipe outlet suggests that most, if not all, of the charge recombination that occurs in FRP pipe results from electron flow along the inner wall of the pipe either to or from the grounded metal pipe connections at the pipe ends.

The first observations on spark generation were carried out during tests on the short FRP pipe section with 0.9 CU fuel. During startup, when temperatures were being equilibrated, it was noticed that moisture had condensed on the pipe during the night and that numerous water droplets were hanging along the bottom of the pipe. While the water was being wiped off, it was noted that a drop could be attracted if a finger was placed alongside the drop, and it could actually be distorted into a conical shape with a pointed tip if a finger were placed within about  $3/8$  inches beneath the drop. The pipe was wiped dry except for the section between 45 and 55 feet from the inlet; the observations that were made on the water drops that remained are summarized in Table 10.

As indicated, the drops could easily be distorted into a conical shape at a surface voltage on the pipe between 2.5 and 5.3 kv, and sparks were clearly audible on the walkie-talkie radio. This was observed when the filter/seperator was being used to charge the fuel. As indicated before, the surface voltages were relatively low due to the high humidities that prevailed during these tests although the charge densities were high. Only slight deflections of the drops were observed at surface voltages between 0.85 and 2.5 kv and spark discharges could barely be detected

Table 10

STATIC EFFECTS AND SPARK GENERATION OBSERVED  
WITH SHORT FRP TEST PIPE SECTION AND 0.9 CU FUEL

Using	Flow Rate, GPM	Charge Density, $\mu\text{C}/\text{m}^3$ , @ Pipe Inlet	Rel Hum, %	Surface Voltage @ 50 ft, kv	Distortion of Water Drops on Pipe Into Conical Shape	Sparks Detected With CB Walkie-Talkie When Water Drop Grounded
Bypass	300	1.5	81	1.62	Very Slight	No
	600	2.3	81	1.53	Slight	No
	1200	3.1	82	1.5	Slight	Barely
	1500	3.4	82	1.31	(a)	(a)
Filter/ Separator	300	-48.8	84	.85	Very Slight	(a)
	600	-97.	89	-2.5	Slight	(a)
	1200	-139.	91	-5.3	Obvious	Clearly
Gages	300	17.1	94	.053	No	No
	600	15.5	93	.045	No	No
	1200	13.1	93	-.039	No	No

(a) No observations made.



on the radio at a surface voltage of about 1.5 kv. No deflection or radio detection of sparks was observed at surface voltages at or below 53 volts. Under conditions where spark discharges were detected with the radio, no sparks could be detected when the pipe was touched (either with a finger or a grounded wire) at a point other than where a water drop was located.

In subsequent tests, spark production was based on radio, aural or visual observation of sparks produced when a grounded wire or finger was brought near to aluminum foil wrappings or the metal drain valve that was present in the long pipe configuration. When sparks were detected, the size and the number that were generated per second were noted; these data are summarized for runs carried out using the bypass, filter/separator and Gages in Tables 11, 12 and 13, respectively.

As shown in Table 11, sparks were produced under all conditions when fuel was flowed through the bypass prior to introduction into the test pipe. These were generally very small discharges which could only be detected by radio. There was some evidence that the largest sparks were obtained from the drain valve with the 5.5 CU fuel, since sparks could be detected on the radio (but not seen visually) when the grounding wire was held about 1/8 inch away from the valve. In all other tests, the grounding wire had to be almost touching the valve or foil for sparks to be detected.

Sparks were also obtained under all conditions for which observations were made using the filter/separator or the Gages to generate charge on the fuel, as shown in Tables 12 and 13. With the filter/separator, charge density at the pipe inlet had to reach about  $15 \mu\text{C}/\text{m}^3$ , with an ambient relative humidity of 50 percent or less before sparks could be observed visually. Sparks up to 1/4 inch in length could be obtained from both the aluminum foil and the drain valve when the charge densities ranged from -68 to  $-155 \mu\text{C}/\text{m}^3$  at an ambient humidity of 56 percent. Under these conditions sparks were also obtained from the bolts which held the jumper in place in this pipe configuration, although they were smaller and less frequent than those generated by the valve. As indicated, the sparks obtained from the valve were the most energetic since they had the greatest

Table 11

## OBSERVATIONS ON SPARK PRODUCTION USING BYPASS

Nom. Fuel CU	Pipe Lgth.	Flow Rate, GPM	CD, $\mu\text{C}/\text{m}^3$ At Pipe In	Rel. Hum., %	Spark Characteristics Generated By									
					Foil Wrapping @ Feet From Inlet				Valve, @ 81 Feet					
					27		48		189					
					Lgth., Ins.	No./ Sec.	Lgth., Ins.	No./ Sec.	Lgth., Ins.	No./ Sec.	Lgth., Ins.	No./ Sec.	Lgth., Ins.	No./ Sec.
0.2	Short	300	-0.7	74	( a )	( a )	( a )	( a )	( a )	( a )	( a )	( a )	( a )	( a )
		600	-1.0	73	( a )	( a )	( a )	( a )	( a )	( a )	( a )	( a )	( a )	( a )
		1200	-1.2	72	( a )	( a )	( a )	( a )	( a )	( a )	( a )	( a )	( a )	( a )
		1500	-1.3	70	( a )	( a )	( a )	( a )	( a )	( a )	( a )	( a )	( a )	( a )
0.2	Long	300	-0.6	62	( a )	( a )	( a )	( a )	( a )	( a )	( a )	( a )	( a )	( a )
		600	-0.7	63	( a )	( a )	( a )	( a )	( a )	( a )	( a )	( a )	( a )	( a )
		1200	-1.1	62	( a )	( a )	( a )	( a )	( a )	( a )	( a )	( a )	( a )	( a )
		1500	-1.3	60	( a )	( a )	( a )	( a )	( a )	( a )	( a )	( a )	( a )	( a )
5.5	Short	300	-1.3	55	( a )	( a )	( a )	( a )	( a )	( a )	( a )	( a )	( a )	( a )
		600	-2.1	51	( a )	( a )	( a )	( a )	( a )	( a )	( a )	( a )	( a )	( a )
		1200	-3.4	59	( a )	( a )	( a )	( a )	( a )	( a )	( a )	( a )	( a )	( a )
		1500	-4.2	59	( a )	( a )	( a )	( a )	( a )	( a )	( a )	( a )	( a )	( a )
5.5	Long	300	-1.4	58	No Audible Sparks (Radio Not Working)									
		600	-2.5	56(b)	-	( a )	( a )	( a )	( a )	( a )	( a )	( a )	( a )	$\sim 1/8(a)$
		1200	-3.8	54	-	( a )	( a )	( a )	( a )	( a )	( a )	( a )	( a )	$\sim 1/8(a)$
		1500	-4.3	54(b)	-	( a )	( a )	( a )	( a )	( a )	1/32	1-2	( a )	$\sim 1/8(a)$

(a) Audible on radio only

(b) Estimated.

Table 12

## OBSERVATIONS ON SPARK PRODUCTION USING FRAM FILTER/SEPARATOR

Nom. Fuel CU	Pipe Lgth.	Flow Rate, GPM	CD, $\mu\text{C}/\text{m}^3$ At Pipe In	Rel. Hum., %	Spark Characteristics Generated By									
					Foil Wrapping @ Feet From Inlet					Valve, @ 81 Feet				
					27	48	189							
					Lgth., Ins.	No./ Sec.	Lgth., Ins.	No./ Sec.	Lgth., Ins.	No./ Sec.	Lgth., Ins.	No./ Sec.	Lgth., Ins.	No./ Sec.
0.2	Short	300	-66.1	65	Audible on Radio Only									
		600	-119	68	1/16	2-3	1/8	2-3	-	-	-	-	-	-
		900	-141	69	1/8	2-3	1/8	2-3	-	-	-	-	-	-
		1200	-161	68	3/16	2-3	1/4	2-3	-	-	-	-	-	-
	Long	300	-68.4	57	-	-	1/4	3-4	-	-	1/4	-	1/4	>4
		600	-116	56(a)	-	-	1/4	3-4	-	-	1/4	-	1/4	>4
		900	-140	56	-	-	1/4	3-4	-	-	1/4	-	1/4	>4
		1200	-155	56(a)	-	-	1/4	3-4	-	-	1/4	-	1/4	>4
5.5	Short	300	0.3	47	Barely Audible on Radio									
		600	-1.2	49(a)	"	"	"	"	-	-	-	-	-	-
		900	-12.4	49(a)	"	"	"	"	-	-	-	-	-	-
		1200	-27.3	51	-	-	1/32	2-3	-	-	-	-	-	-
5.5	Long	300	+0.6	-	No Observations Made									
		600	-1.7	46	No Observations Made									
		900	-14.8	46	-	-	1/16	1	1/16	<1	1/16	1	1/16	2
		1200	-32.2	47	-	-	3/16	1	1/16	1	1/16	1	1/4	2

(a) Estimated value.

Table 13

## OBSERVATIONS ON SPARK PRODUCTION USING BENDIX GAGES

Nom. Fuel CU	Pipe Lgth.	Flow Rate, GPM	CD, $\mu\text{C}/\text{m}^3$ At Pipe In	Rel. Hum., %	Spark Characteristics Generated By									
					Foil Wrapping @ Feet From Inlet					Valve, @ 81 Feet				
					27	48		189		Lgth., Ins.	No./ Sec.	Lgth., Ins.	No./ Sec.	Lgth., Ins.
0.2	Short	300	15.9	-	(a)	2-3	<1/16	1	-	-	-	-	-	-
		600	14.4	-	(a)	2-3	1/16	1	-	-	-	-	-	-
		1200	10.3	-	1/16	2-3	1/16	2-3	-	-	-	-	-	-
5.5	Long	300	7.8	39										
		600	5.9	40(c)										
		1200	4.2	41										
5.5	Short	300	68.9	63	-	-	1/16	2-3	-	-	-	-	-	-
		600	114	60	-	-	1/16	2-3	-	-	-	-	-	-
		900	119	58	-	-	1/8	2	-	-	-	-	-	-
		1200	121	59	-	-	1/4	2-3	-	-	-	-	-	-
5.5	Long	300	73	47	-	-	1/8	3	(a)	1/16	2	1/4	2-3	2-3
		600	131	40	-	-	<1/16	3-4		1/16	2	1/4	3-4	3-4
		900	129	44(c)	-	-	<1/16	3-4		3/16	2	1/4	3-4	3-4
		1200	125	47	-	-	<1/16	3-4		3/16	2	1/4	3-4	3-4

(a) Audible on radio only.

(b) 1/4" to finger @ 1/sec.

(c) Estimated.

length and/or were most frequent. It was impossible to prevent one's hand from jerking, if a finger was placed near the valve under these conditions, indicating that the discharges had more than sufficient energy to be incendiary (Ref. 6). Data provided in Tables 38 and 41 indicate that the surface voltage had to reach about 2.5 to 5 kv for visible sparks to be produced from the foil wrappings.

With the Gages, visible sparking was obtained with inlet charge levels as low as  $4.2 \mu\text{C}/\text{m}^3$ ; here the relative humidity was only 41 percent. Sparks up to 1/4 inch long were obtained off the drain valve with the charge density at the pipe inlet as low as  $7.8 \mu\text{C}/\text{m}^3$ . It was not possible to detect sparks between the pipe surface alone and a grounded wire, even using a radio, under any of the conditions tested. However, it was possible to feel and hear sparks being discharged from the pipe surface if one's hand were placed near the pipe. It is estimated that a surface voltage of about 7 to 10 kv was required before such discharges could be sensed.

Since FRP pipe has only been approved for below ground installations, the high surface voltages observed in these tests would not be a deterrent to its use. It is quite obvious, however, that if any part of the plastic piping extends above ground or if it should be approved for above ground installations, that it could be a safety hazard. Careful grounding of all metal components in contact with the pipe would be required to eliminate the possibility of incendiary spark discharges and to prevent any involuntary reaction which could result in injury to an individual who might accidentally contact such components. While the tests indicate that spark generation from the pipe surface itself is too small to produce discharges of sufficient energy to be incendiary, it is conceivable that someone coming in contact with the pipe could be startled or that an ungrounded wet area on the pipe could enhance both effects. For absolute safety, it is recommended that FRP pipe be coated with a non-peeling, non-flaking electrically conductive material (eg. paint or wrapping) and electrically grounded at any location where it is above ground level.

There was no evidence that sparks discharged along the inner surface of the pipe, as has been observed with Teflon (Appendix I, Section 3), nor were any sparks observed discharging from any part of the FRP pipe to the grounded metal fittings to which the test sections are connected, as has been observed with polypropylene pipe (Appendix I, Section 4). Conditions under which the latter were observed were not defined. However, as indicated in Appendix I, the tests in the Teflon were conducted at an inlet charge density of about  $1500 \mu\text{C}/\text{m}^3$  with a fuel of 165 CU. At this CU, most of the charge would relax in a few tenths of a second and it can be estimated that the voltage drop in the first foot or so of pipe could be in excess of  $10^6$  kv. Such voltage drops, which could only result from the combination of high charge level and fast relaxation, could be prevented in a full-scale system if as little as 10 feet of metal pipe are provided between the filter/separator outlet and the inlet to the FRP pipe.

The data obtained in this study strongly suggest that charge recombination in FRP pipe occurs by electron flow along the inner wall of the pipe either to or from the metal pipe connections at either end of the FRP section. This is based on the fact that there is no measurable change in charge density observed at the pipe outlet when the outer surface of the FRP pipe is made conductive, as indicated in Section IV, 3. This theory is reinforced by the surface voltage measurements which show a rapid increase at the inlet end and somewhat slower but still rapid decrease at the outlet, and the fact that the surface voltages measured on the long pipe section were always higher than in the short section under comparable conditions. These results strongly suggest that the rate of relaxation in FRP pipe could be brought closer to that of steel pipe if the volume resistivity of FRP pipe were reduced, or if the inner wall of the pipe were grounded at short intervals so that the charge would not have to travel up to half the length of the pipe run to recombine. An increase in the conductivity along the inner wall of FRP pipe would probably occur in the field, even in "sanitary" systems, due to normal deposition of particulates and other impurities with time. However, it

is suggested that plastic pipe manufacturers be informed that it would be advantageous to formulate plastic pipe for this type of service with as low a volume resistivity as possible without compromising other properties. In lieu of this, it is recommended that a high conductivity adhesive be used and/or an aluminum foil strip be incorporated into each joint between each pipe section during assembly.

## 5. EVALUATION OF THE STATIC CHARGE REDUCER

The Static Charge Reducer (SCR) is marketed by the A. O. Smith Company, Erie, Penna.; it is claimed that the SCR will reduce charge densities of up to  $300 \mu\text{C}/\text{m}^3$  to  $30 \mu\text{C}/\text{m}^3$  or less at flow rates up to 1200 GPM (Ref. 7). A description of the SCR is included in Appendix I, Section 5. An evaluation of the SCR was included in this program because it is the only commercially available device for reducing electrostatic charge in flowing fuel, and the program offered an excellent opportunity to evaluate it over a wide range of conditions. It also offered the opportunity for determining the magnitude, if any, of charge generation downstream of the device.

As shown in Figure 3, the SCR was located between the outlet of the filter array and inlet to the test pipe section; it could be cut in or out of the system by simple manipulation of two valves. In evaluating the SCR, both the filter/separator and the Gages were used to generate charge on the fuel.

The efficiency of the SCR was determined as a percentage using the following relationship:

$$\text{Efficiency, \%} = \frac{|\text{CD, SCR In}| - |\text{CD, SCR Out}|}{|\text{CD, SCR In}|} \times 100 \quad (6)$$

CD, SCR In is the charge at the inlet to the SCR, which is equivalent to the charge density at the outlet of either the filter or the Gages, and CD, SCR Out is the charge density at the outlet of SCR, which is equivalent to the charge density at the test pipe inlet. Absolute values were used, since the magnitude of the charge delivered by the SCR represents the potential hazard regardless of the polarity.

The initial tests were carried out with the 0.9 CU fuel. The results that were obtained using the filter/separator as the charge generator are given in Table 47; those obtained with the Gages are given in Table 50. The dashed curves in Figure 20 show the percent efficiency obtained in these initial tests as a function of charge density at the SCR inlet.



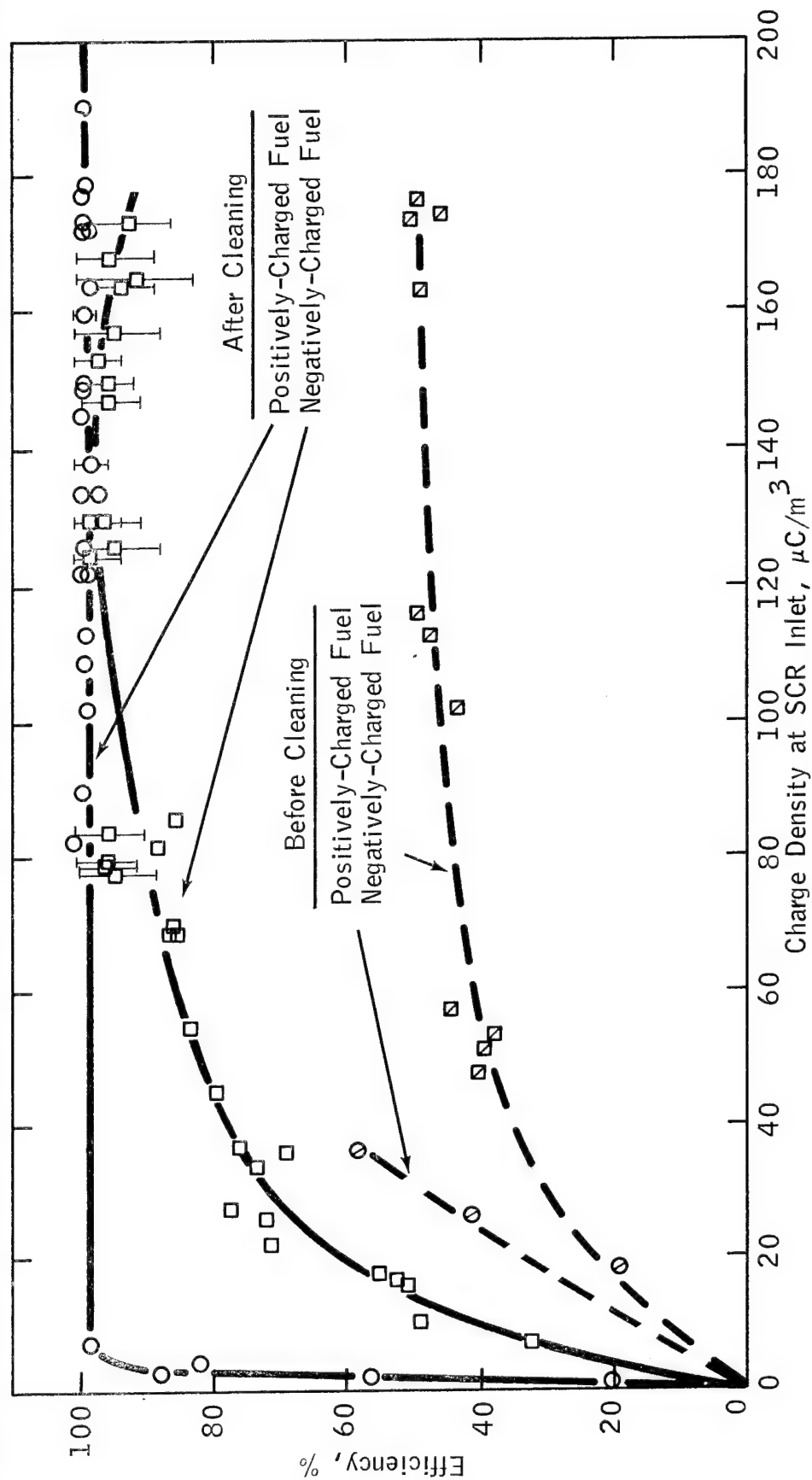


Figure 20. SCR Efficiency with Positive and Negative Fuel, Before and After Cleaning

As indicated, the efficiency of the SCR in the initial tests was low and appeared to depend on the polarity of the fuel entering the SCR. With negatively charged fuel, the efficiency rose from about 40 to 50 percent as charge density at the SCR inlet increased from 50 to  $180 \mu\text{C}/\text{m}^3$ . Based on limited data, the efficiency reached about 60 percent at a charge density of  $40 \mu\text{C}/\text{m}^3$  when the fuel was charged positively.

The charge densities at the SCR outlet reached  $60 \mu\text{C}/\text{m}^3$  at 600 GPM and  $95 \mu\text{C}/\text{m}^3$  at 1200 GPM with the negatively charged fuel at these efficiency levels, as shown in Table 47. These charge levels were considerably higher than the maximum of the  $30 \mu\text{C}/\text{m}^3$  claimed by the manufacturer. It was surprising, since in some preliminary tests carried out about a month earlier, the unit had delivered fuel at charge levels ranging from 13 to  $36 \mu\text{C}/\text{m}^3$  with charge at the inlet ranging from 98 to  $165 \mu\text{C}/\text{m}^3$ , with positively charged fuel.

Following the first series of tests, the unit was opened up and inspected. This indicated that deposits on the polyethylene liner of the SCR were responsible for its decreased efficiency. The deposits showed up as a very faint gray-to-dark brown discoloration on the white polyethylene liner which could go undetected by a less-than-careful inspection. Close inspection also revealed numerous small spots (eg.  $<0.25$  inch diameter) which on culturing showed the presence of fungi and the possibility of some bacterial growth. While the liner appeared clean after wiping with Kimwipes (a disposable paper wiper), it was only after subsequent wipings, first with a hexane-wetted cloth, and then with several chloroform-wetted cloths, that the wiping cloth finally remained unstained, indicating that all the deposits had been removed. All of the pins which protrude through the polyethylene liner were sharp and intact.

Additional evaluation runs on the SCR were continued with the 3, 5.5 and 0.2 CU fuels after the SCR liner was cleaned. Data obtained

using the filter/separator as the charge generator appear in Tables 46, 48 and 49; those obtained using the Bendix Gages are given in Tables 51 and 52. No data were obtained using the Gages with the fuel at 0.2 CU since the maximum charge generated at the SCR inlet was only  $23 \mu\text{C}/\text{m}^3$  under these conditions. The solid curves in Figure 20 show the efficiency of the SCR after cleaning.

The clean SCR showed a marked improvement in efficiency over any previous results. With positively charged fuel, the efficiency was 98 to 100 percent at charge levels from 10 up to  $205 \mu\text{C}/\text{m}^3$  at the SCR inlet; this corresponds to an outlet charge level of 0 to  $4 \mu\text{C}/\text{m}^3$  compared to the 20 to  $30 \mu\text{C}/\text{m}^3$  generally observed previously in this laboratory and by others (Appendix I [53]). The efficiency of the SCR was lower with negatively-charged fuel, rising to about 80 percent at an input charge level of about  $45 \mu\text{C}/\text{m}^3$ , reaching a maximum of about 97 percent at a charge level of  $130 \mu\text{C}/\text{m}^3$  and then decreasing at higher charge levels. The SCR probably functions by allowing electrons to flow into the fuel if it is charged positively, and by extracting electrons when the fuel is charged negatively. The difference in efficiency due to polarity is reasonable since it can be visualized that it would be easier for electrons to flow off the probes in the SCR into the fuel than for the electrons to flow onto the probes from negatively charged fuel flowing at high velocity.

The loss in efficiency noted in this program has recently been experienced by others in field installations and A. O. Smith has issued a bulletin (Ref. 8) which recommends that the SCR performance be checked "not less often than every six months" to see that it reduces charge to a level no greater than  $30 \mu\text{C}/\text{m}^3$  with an inlet charge no greater than  $300 \mu\text{C}/\text{m}^3$  at 1200 GPM. The results of this program indicate that the efficiency can degrade in less than a month and that continuous monitoring of the SCR output would be required to insure that it was operating properly.

The charge level in the fuel leaving the SCR is not smooth but tends to oscillate irregularly at about 30 cycles/minute on a short range basis

and the average overall level also tends to move up and down in irregular fashion over the longer range. An attempt was made to reflect this in presenting the data in Tables 46 through 52 by indicating the overall swing in SCR output (pipe inlet readings) by  $\pm$  deviations (as in Table 47 ) or by actually showing the limits (as in Tables 46 and 51). It is interesting to note that the largest swings were observed with highly charged negative fuel at 0.2 CU (Table 46); the range in efficiency that results from these swings is indicated by the elongated data points in Figure 20.

It was also observed during the runs carried out with the 0.2 CU fuel, that the charge level at the SCR outlet took considerably longer to reach a low level after a change in flow rate than with the higher conductivity fuels. A number of runs were carried out to determine how long it would take for the SCR output to decrease to  $30 \mu\text{C}/\text{m}^3$  at different flow rates and inlet charge levels. In these runs the charge was generated using the Fram filter/separator; the charge was allowed to stabilize through the system at a fixed flow rate and the SCR was then put on stream and the flow rate was quickly readjusted to the desired value, when necessary. In general, the charge at the SCR outlet showed a sharp decrease, due to the uncharged fuel held up in the SCR loop, it rose to a maximum and then decreased to a "stabilized" level. The results of these tests are provided in Table 14 which show the charge density at the SCR inlet, the maximum charge developed at the SCR outlet and the time that was required for the charge at the SCR outlet to decrease to  $30 \mu\text{C}/\text{m}^3$  at the flow rates tested.

The time required for the SCR output to reach  $30 \mu\text{C}/\text{m}^3$  is shown as a function of flow rate in Figure 21. As indicated, 2 to 2.5 minutes were generally required for the charge to decrease to  $30 \mu\text{C}/\text{m}^3$  at flow rates between 600 and 1200 GPM. The shortest time required was slightly less than 2 minutes at 900 GPM. At 300 GPM, about 4 minutes were required

Table 14

EVALUATION OF SCR STARTUP TIME WITH 0.2 CU FUEL

Flow Rate, GPM	Date of Test	Test Temp., °F	Charge Density, $\mu\text{C}/\text{m}^3$			Time for SCR Out to Reach $30 \mu\text{C}/\text{m}^3$ , Seconds
			At SCR Inlet	At SCR Outlet Max.	Max. As % of SCR In	
300	2/16/72	38.1	-70	-56	80	245
	2/17/72	38.2	-75	-60	80	241
	2/24/72	39.3	-75	-55	73	138
	2/24/72(a)	38.6	-78	-63	81	221
	2/28/72	39.2	-75	-62	83	238
600	2/16/72	37.3	-131	-100	76	163
	2/17/72	37.0	-133	-100	75	125
	2/24/72	38.9	-128	-100	78	122
	2/28/72	37.5	-136	-107	79	145
900	2/16/72	37.3	-153	-123	81	150
	2/17/72	36.7	-150	-118	79	115
	2/24/72	37.9	-152	-132	87	151
	2/28/72	37.9	-158	-128	81	150
1200	2/16/72	37.6	-165	-132	80	126
	2/17/72	38.1	-163	-132	81	149
	2/24/72	38.2	-168	-140	83	130
	2/28/72	38.1	-173	-142	82	150

(a) Repeat run.

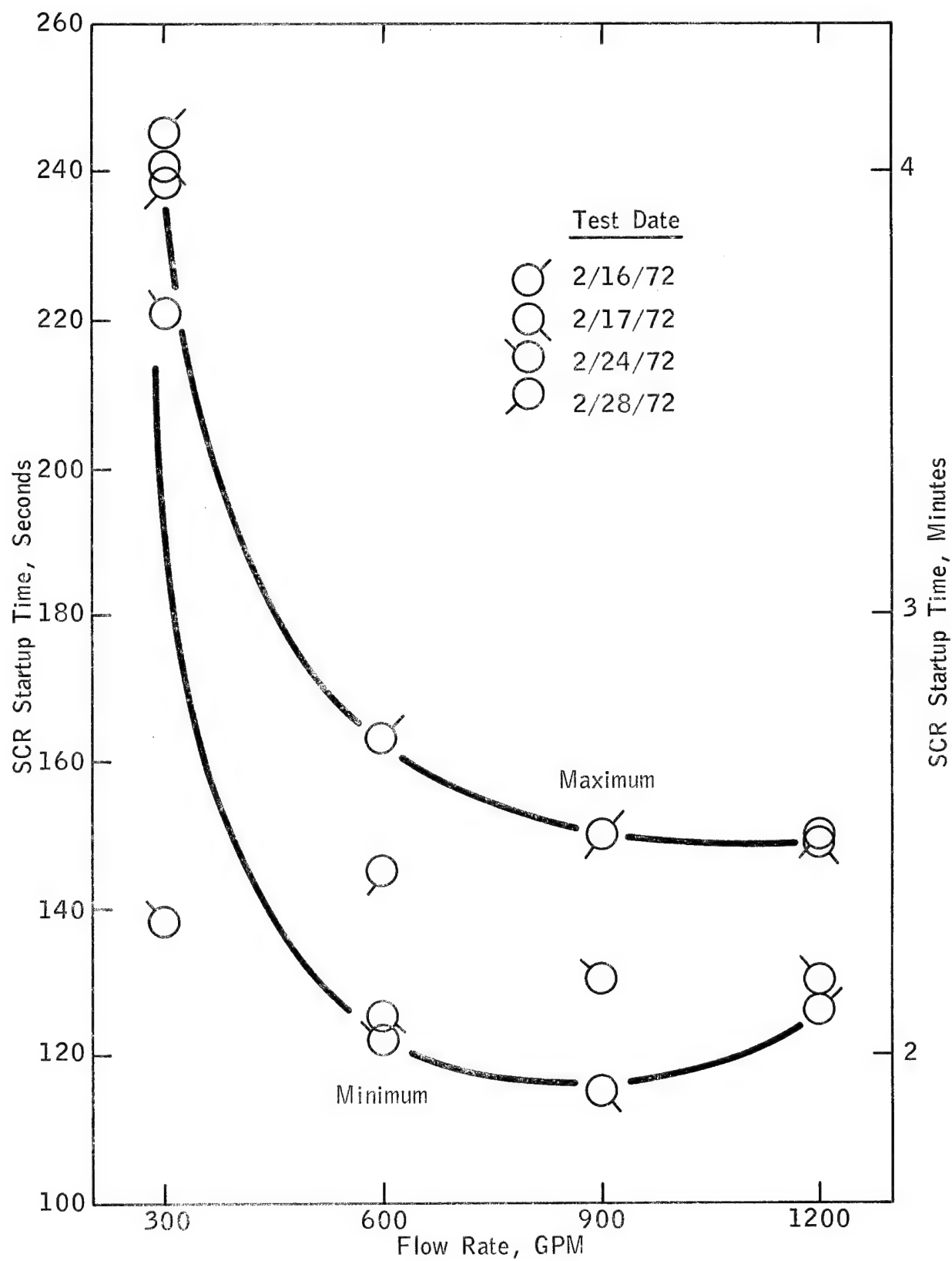


Figure 21. SCR Startup Time Versus Flow Rate

for the charge to drop to  $30 \mu\text{C}/\text{m}^3$  (this would be equivalent to 2 minutes at 600 GPM). It is quite apparent that charge levels above  $30 \mu\text{C}/\text{m}^3$ , a level which has been suggested as a safe level (Appendix I [28]), can be obtained for extended periods of time before the SCR "starts up". And as indicated in Table 14, charge levels as high as  $140 \mu\text{C}/\text{m}^3$  were obtained at the SCR outlet right after startup at 1200 GPM, with charge densities at the SCR inlet of about  $170 \mu\text{C}/\text{m}^3$ . As shown in this table, the maximum charge level measured at the SCR outlet in these tests immediately after the SCR was put on stream was about 80 percent of the charge level at the inlet at all flow rates tested. It must be assumed that at  $300 \mu\text{C}/\text{m}^3$ , the maximum inlet charge level specified for the SCR, that SCR outlet levels of as much as  $240 \mu\text{C}/\text{m}^3$  could be obtained.

Surface voltage measurements as well as some observations on spark generation were carried out during several of the SCR evaluation runs. Surface voltage data obtained using the SCR in combination with the filter/separator are presented in Tables 53 through 56; those obtained using the Gages appear in Tables 57 through 59. The maximum surface voltages obtained for each flow rate and fuel conductivity combination tested are summarized in Table 15. As indicated, surface voltages as high as -38 kv were obtained on the long test section in a run carried out using the filter/separator with the 0.9 CU fuel when the SCR was operating at less than 50 percent efficiency. However, maximum voltages ranging from -21.5 to -26 kv were obtained on the long pipe using the filter/separator with the 0.2 CU fuel. Under these conditions the SCR was operating at efficiencies ranging from 82 to 91 percent and the charge density at the inlet to the pipe section ranged between 2 and  $-30 \mu\text{C}/\text{m}^3$ , as shown in Table 53. More important, maximum voltages between -18.3 and -23 kv were measured on the short pipe section using the Gages with the 5.5 CU fuel. In these runs, SCR efficiencies ranged be-

Table 15

## MAXIMUM SURFACE VOLTAGES MEASURED ON FRP PIPE IN SCR EVALUATION

## Using Fram Filter/Separator As Charge Generator

Nom. Rest CU	Maximum Surface Voltage, kv at Flow Rate, GPM, and Feet From Inlet Indicated(a)					
	300		600		900	
	Short	Long	Short	Long	Short	Long
0.2	8.1(10)	-21.5(90)	7.1(50)	-21.5(70)	5.3(b)	-5.5(30)
0.9	-1.45(30)	-20(78)	-6.6(30)	-34(78)	--	-8.4(20)
3.	4.3(20)	--	2.6(20)	--	--	0.9(20)
5.5	--	--	--	--	-3.6(20)	-4.6(30)
						26(70)
						-38(78)
						.25(50)
						--

## Using Bendix Gages As Charge Generator

0.2	--	--	--	--	--	--
0.9	--	--	--	5.0(c)	--	5.5(50)
3.	-6.0(30)	--	-8.(30)	--	-5.0(30)	-11.3(30)
5.5	-23(30)	-24.5(30)	-21.5(30)	--	-18.3(30)	--

(a) Values in parentheses indicate distance from pipe inlet in feet at which maximum voltage was measured.

(b) 10, 30 feet.

(c) 50, 60, 70 feet.



tween 96 and 100 percent. The latter data were obtained when the SCR was operating so well that it was reversing the polarity on the fuel; the charge density at the pipe inlet ranged between +3 and  $-6 \mu\text{C}/\text{m}^3$  as shown in Table 52. Of particular interest is the run carried out at 300 GPM where a maximum surface voltage of -23 kv was obtained when the charge density at the pipe inlet oscillated between the very low values of -1 and  $-2 \mu\text{C}/\text{m}^3$  and the charge at the pipe outlet was 0.0. For comparison, runs carried out at this CU using the bypass showed a maximum surface voltage of only 2.4 kv in runs carried out at flow rates ranging between 300 and 1500 GPM and at inlet charge densities ranging from -1.3 to  $-4.2 \mu\text{C}/\text{m}^3$ . Thus while the SCR appears to be capable of reducing the charge on a fuel to very low levels, it did not result in low voltages on the FRP pipe.

The observations made on spark production, which are summarized in Tables 60 and 61 for runs made in conjunction with the filter-separator and Gages respectively, back this up. As shown in Table 60, sparks up to 1/2 inch long could be drawn from the drain valve in runs carried out with the 0.2 CU fuel using the filter separator. And sparks up to 1/4 inch in length could be drawn off the aluminum foil wrapping in the runs carried out in the short pipe with the 5.5 CU fuel using the Gages, shown in Table 61. It appears that the high surface voltages and spark energies obtained when the SCR is operating may be due in some way to the oscillations in the charge being delivered by the SCR since this is the only obvious difference between operation with the SCR and with the bypass.

In two recent reports prepared by Air Force personnel (Appendix I [53,70]) concern was expressed regarding the possible magnitude of charge generation downstream of the SCR. In all runs carried out in this program, there was generally a decrease in charge level downstream of the SCR regardless of the flow rate or the pipe type/pipe length combination following the SCR. Where there was an increase in charge, it was too small to be considered significant, especially since the charge levels

were generally varying. Thus, while the results indicate that the SCR can be an extremely efficient device for reducing charge level on flowing hydrocarbons, the high surface voltages measured on the FRP pipe surface in this program suggest that the oscillations in charge density in the fuel delivered by the SCR may in some way be producing a hazardous situation which is not reflected by the average charge density, which is low. These observations strongly imply that charge densities below  $30 \mu\text{C}/\text{m}^3$ , when produced by an SCR, may not actually be safe.

In addition, the SCR has other disadvantages including a loss in efficiency due to deposit buildup and the problem of startup time. Since the loss in efficiency can occur relatively fast, it would be mandatory to continuously monitor the SCR output to assure that it was operating properly. The problem of startup time is not a major disadvantage since it could probably be overcome by recycling fuel through the SCR until the output charge density reached a safe level or by starting at a low flow rate and bringing it up to full flow while the SCR output was monitored.

Of these disadvantages, the most important is the suggestion that a hazardous situation may exist downstream of an SCR although the average charge delivered by the device is below the level of  $30 \mu\text{C}/\text{m}^3$ , which is considered to be safe. Further testing is necessary to establish the significance of this phenomenon, and if valid, to determine if the problem can be eliminated.

## V. CONCLUSIONS

These conclusions are based on both the information obtained in the literature search and the experimental work that was carried out in this program. The conclusions are presented in form of answers to the questions posed by the Air Force in regard to the use of FRP material in aviation fuel systems.

1. Does FRP pipe generate a significantly higher charge than metallic systems of a given pipe length and fuel velocity?

Data obtained in previous studies in small scale equipment and a limited amount of data in full scale equipment indicated that charge generation in FRP pipe would be small and that there would be little difference between FRP and metal pipe. Results obtained in this program not only confirm the conclusions reached in previous studies but extend the observations over a wide range of full-scale conditions and provide quantitative comparisons between FRP and metal pipe.

The experimental data obtained in this program show that charge generation in both steel and FRP pipe is very low at flow rates up to 1500 GPM; a maximum charge of about  $2.5 \mu\text{C}/\text{m}^3$  was observed. Charge generation in FRP pipe is no greater and is generally less than that obtained in metal pipe under comparable fuel velocities and pipe lengths. Any differences in charge generation observed between FRP and metal pipe would be of no significance in the field.

2. Does the charge generated in FRP pipe relax or dissipate at substantially the same rate as in metallic systems of equivalent size?

The results of this study show that there is a difference in charge relaxation between FRP and metal pipe which depends on the polarity of the fuel. Over the range of fuel conductivities and flow

rates tested, charge relaxation with negatively charged fuel was about 8 percent faster in FRP pipe, on the average, than in steel pipe. With positively charged fuel, the relaxation rate in FRP pipe was slower than in steel pipe by 30 percent, on the average. Since the polarity of charged fuel is unpredictable, the data indicate that FRP pipe could only be used in place of metal if the FRP system was designed to incorporate additional residence time to assure that the charge level at the point of delivery would be as low as that expected in a metal system.

For Type III AF hydrant systems, the minimum residence time that would be expected between the final filter and the first fueling station would be 225 seconds at the design flow velocity of 4 feet/second. At 7 feet/second, the maximum flow velocity which such systems could be called on to handle in the future, the minimum residence time would be expected to be 130 seconds. Data obtained in this program indicate that a "safe" charge level, i.e.  $30 \mu\text{C}/\text{m}^3$ , would only be exceeded at the point of delivery in an FRP system having 225 seconds of relaxation with fuels of 0.2 CU at inlet charge levels above  $100 \mu\text{C}/\text{m}^3$ . With 130 seconds of relaxation,  $30 \mu\text{C}/\text{m}^3$  would be exceeded with 0.2 CU fuel at inlet charge levels as low as  $100 \mu\text{C}/\text{m}^3$  and with 1 CU fuel at inlet charge levels above  $500 \mu\text{C}/\text{m}^3$ . These data indicate that FRP pipe can be used in new or redesigned AF hydrant systems handling JP-4 if 130 seconds of residence time are available. However, this conclusion must be qualified since no hard data are available on the range or possible minimum CU of JP-4's in the field or on the maximum charge levels normally obtained with AF filtration equipment. This suggests that a field survey be conducted to determine the range and maximum conductivity and the range and potential maximum charge level that can obtain in Air Force fueling systems.

Data obtained in this program indicate that charge recombination in FRP pipe is due to electron flow either into or out of the fuel along the inner wall of the pipe through the grounded metal fittings on each end of the pipe, since the resistivity of the pipe is too high to allow for much current flow through the pipe wall. If so, this might be expected to reduce rate of relaxation as pipe length increases. It is recommended, therefore, that a conductive path be provided between the inner wall and exterior of the pipe (i.e. electrical ground) at each pipe joint by using a highly conductive adhesive and/or by incorporating aluminum foil or other noncorrosive conductor into each joint during construction. From a long range point of view, this could also be accomplished with FRP pipe of low volume resistivity. It is suggested that plastic pipe manufacturers be informed that it would be advantageous to formulate plastic pipe with as low a volume resistivity as possible without compromising other properties desired for this type of service. Recommendations, similar to those made here, have been made by others in regard to fueling hoses and in filling plastic tanks and vessels (Appendix I, Section 4).

3. Is the bonding and/or grounding now prescribed for metallic systems of any value in systems fabricated of FRP pipe?

Surface voltages as high as 55 kv were measured on the surface of the FRP pipe and loud, visible spark discharges up to 1/2 inch in length, which were considered to be incendiary, were observed between ground and ungrounded aluminum foil wrappings and a metal drain valve on the FRP pipe in this program. Since FRP pipe is only approved for underground installations at present, the high voltages would not prevent its use. For absolute safety, it is recommended that all metal components in contact with the pipe be grounded and that FRP pipe be coated with a non-flaking, non-peeling conductive material (eg. graphite, paint or metal foil or mesh wrapping), which is electrically

grounded, at any location where the FRP pipe extends above ground level (eg. in hydrant pits). This would eliminate any possibility of incendiary spark discharges from isolated metal components on the pipe and would prevent injury to an individual who might be startled by coming into contact with the pipe.

Bonding and/or grounding would be required for any conductive coating on or any isolated metal component in contact with FRP pipe in above-ground installations. However, because of the high resistivity of FRP pipe, bonding and/or grounding would be of little value in above-ground installations if the pipe were not covered with a conductive layer or the formulation changed to increase conductivity.

4. Are the velocity restrictions and the prescribed tank filling techniques, now mandatory on metallic systems, still required on FRP systems?

The answer to this question is yes. While this study showed that charge relaxation may proceed somewhat faster in FRP pipe than in steel when the fuel is charged negatively, it also showed that relaxation may proceed slower in FRP than in steel pipe if the fuel is charged positively. As indicated in the answer to Question 2, normal flow rates could be used if sufficient residence time was provided to reduce charge to a safe level at the point of delivery. On the other hand, if the dimensions of an FRP system were the same as those of a metal system, which was designed to deliver a maximum of  $30 \mu\text{C}/\text{m}^3$  at a given inlet charge level and flow rate, the FRP system could deliver a hazardous charge level (eg.  $>30 \mu\text{C}/\text{m}^3$ ). In this situation, it would be necessary to reduce the flow rate in the FRP system to assure a safe charge level at the point of delivery.

5. Are there any special techniques necessary for the safe transfer of aviation fuels from FRP systems to metallic system (aircraft, trucks and storage) or from metallic systems to FRP systems?

There was no evidence that sparks discharged along the inner surface of the FRP pipe or that sparks discharged from any part of the FRP pipe to grounded metal fittings in contact with the pipe. The available literature data suggest that such effects occur with highly charged fuel of high CU (Appendix I, Section 3). Under these conditions, flowing fuel would relax almost all of its charge in less than 1 second and it has been estimated that this could result in a voltage drop in excess of  $10^6$  kv in the first foot or so of plastic pipe. It should be recognized that such combinations of high charge level and high CU are in all probability not typical of Air Force systems handling JP-4. However, such voltage drops could be prevented in a full-scale system if as little as 10 feet (eg.  $\sim 1.5$  seconds of relaxation at 7 feet/second) of metal pipe are provided between the filter/separator outlet and the inlet to the FRP pipe, since the metal would provide a more than adequate path for charge recombination under such conditions.

There would be no special techniques required at the FRP-metal pipe interfaces if the outer surface of the FRP pipe were coated with a conductor as suggested in the answer to Question 3. Such interfaces must be made outside of any tank or vessel which is receiving fuel through an FRP line and it is recommended that no FRP piping be used inside of storage tanks or in the loading arm for trucks or aircraft.

6. In a typical metallic aviation fuel system (bulk storage to receiving aircraft), which components are the major contributions to the static electricity hazard problem? Does this list change when major portions of the system are converted to FRP material?

There is a considerable body of data available in the literature (Appendix I, Section 1) which show that filter/separators are the major producers of static charge, and thus the major contributors

to the static electricity hazard, in typical metallic aviation fueling systems. The amount of charge generation by a filter is dependent on both the type and quantity of impurities in the fuel and the properties of the surface of the filter elements. Temperature can also have a pronounced affect on charge level. As a result, it is impossible to predict what charge a given fuel/filter combination will produce. However, the charge generated by a filter can be quite low under certain conditions as shown in this study. Nevertheless, the filter must be considered to be the primary contributor to the static hazard in fuel transfer operations and this would still be true if FRP pipe were used extensively in such systems. On the other hand, since charge relaxation can proceed slower in FRP than in metal pipe and sparks can be generated from isolated metal components on the pipe, the use of FRP introduces a potential hazard which must be considered in the design of fuel handling systems.

7. Is there presently available, or potentially available with a modest development program, a device or technique for minimizing the present hazard from static charge? If available, would this device or technique allow lifting the present restrictions on flow rate or at least raise the maximum flow allowed?

The Static Charge Reducer (SCR) is the only commercially available device for decreasing the charge level on flowing fuel. It is manufactured by A. O. Smith, Erie, Penna. and it is claimed that the device will reduce charge densities of up to  $300 \mu\text{C}/\text{m}^3$  down to  $30 \mu\text{C}/\text{m}^3$  or less at flow rates up to 1200 GPM. An evaluation of the SCR carried out in this program indicates that it can be an extremely efficient device for reducing the charge in fuel to a low level but that the efficiency is dependent on the polarity of the fuel. A clean SCR can have an efficiency of 98 to 100 percent with positively-charged fuel and an efficiency between 80 and 97 percent with negatively-charged fuel.



However, the SCR has several disadvantages. The most important of these is a suggestion, based on data obtained in this program, that oscillations of the charge level in the fuel delivered by the SCR, as noted in this program, may be producing a hazardous situation although the average charge in the SCR effluent is below  $30 \mu\text{C}/\text{m}^3$ , the charge which is used to define a safe level in this report. Thus, while the SCR appears to be capable of reducing charge to low levels when maintained properly, which would suggest that maximum flow rates might be increased, the above observations suggest that charge levels below  $30 \mu\text{C}/\text{m}^3$ , when delivered by an SCR, may not be safe regardless of flow rate.

In addition, the SCR can loose efficiency relatively quickly due to deposit buildup and it would be mandatory to monitor the SCR output continuously to assure that it was operating at full efficiency. The SCR also has a startup time. Under certain conditions the SCR may require from 2 to 4 minutes for the charge level in the SCR effluent to drop to  $30 \mu\text{C}/\text{m}^3$ . This is not a major disadvantage since it could probably be overcome by recycling fuel through the SCR until the charge level in the output reached a safe level or by starting at a low flow rate and slowly increasing it to the full rate while the output charge level was monitored.

Further testing is required to determine if the suggestion that fuel of low average charge level delivered by an SCR can still result in an unsafe condition. If valid, further work would be required, to determine if this problem, as well as the other disadvantages, can be corrected or eliminated before it could be recommended for use.

During the course of this program, a patent was issued on an in-line device which releases electric charge into the fuel due to the potential difference between ground and the fuel (Ref. 9). It was also learned that McDonnell-Douglas had tested a prototype device using radiation from  $\text{SR}^{90}$  which reduced charge by 80 to 95 percent at flow rates between 400 and 1200 GPM (Appendix I, Section 5). Both devices would probably require extensive development and/or testing before they could be commercialized.

## VI. RECOMMENDATIONS

No hard data are available on either the conductivities or charging tendencies of Air Force fuels. Since both can influence the residence time required to deliver a "safe" charge level, it is recommended that a survey be conducted to establish the conductivity of a broad spectrum of typical JP-4's as used by the Air Force and that a survey of the charging tendencies of Air Force filter/separators be conducted to establish the range and maximum charge levels generated under typical operating conditions in the field. This might involve monitoring charge density continuously at the outlet of one or more filter/separators at at least two Air Force bases for several months, so that the effect of fuel, filter changes and filter aging can be assessed. Similar programs involving commercial turbo fuels are currently being conducted by the Coordinating Research Council - Aviation Fuel, Lubricant and Equipment Research Committee.

It is recommended that the charge level be monitored continuously at the outlet of the filter/separator(s) and at the first fueling station downstream of the filter/separator(s) for at least six months in the first two or three installations which are fabricated with FRP pipe to determine if the systems are delivering fuel at a "safe" charge level as expected.

Since the data obtained in this program indicate that charge recombination in FRP pipe proceeds by electron flow along the inner wall of the pipe, it is recommended that a limited study be conducted to determine if this is so and if grounding the interior of the pipe at the pipe joints as suggested in this report affects relaxation in the pipe or surface voltage on the pipe.

A further evaluation of the SCR should be carried out to determine if the real and suspected disadvantages of the device brought to light in this program can be corrected or eliminated. This could be done in conjunction with an evaluation of other, recently developed devices, to provide a realistic comparison for use in selecting the best one for minimizing the hazards of static electricity. Such an evaluation should include measurements on the electrical effects produced in a tank being fueled through each device.

## APPENDIX I

### REVIEW OF AVAILABLE DATA ON STATIC ELECTRIFICATION IN METALLIC AND NON-METALLIC SYSTEMS

#### A. REVIEW OF THE DATA

##### 1. SCOPE OF THE REVIEW

The background on this program is discussed in Section I of this report. As indicated, FRP offers several advantages over aluminum, stainless steel or plastic-coated steel for "sanitary" aviation fuel handling systems. However, the use of FRP in place of metal depends to a large extent on whether or not FRP introduces any new or unusual electrostatic hazards into aircraft fuel handling and refueling operations.

This section of the report provides the results of a literature search which was carried out to determine if any of the questions posed by the Air Force (Section I) regarding the use of FRP pipe had been resolved by previous investigations. It also includes the results of a canvass of some workers in the field to insure that no recent or unpublished data were overlooked.

The search covered the period of the last ten years; a few earlier references were included where they appeared to be especially interesting or related to the problem. The source material included the following:

- American Petroleum Institute Index
- Chemical Abstracts
- Electrical Engineering (Science Abstracts)
- Engineering Index
- Petroleum Abstracts (U. Of Tulsa)
- Physics (Science Abstracts)
- Scientific and Technical Aerospace Reports
- Technical Abstracts Bulletin
- U.S. Gov. Research and Development Reports

A total of 71 references was reviewed; the abstracts have been included in this section of the report. The more pertinent references are discussed below under the headings Charge Generation, Charge Relaxation, Grounding and Bonding, and Static Control Techniques. The contacts that were made to insure that no data or related test programs were overlooked are shown under Field Contacts.

## 2. CHARGE GENERATION

Electrostatic charging of a liquid hydrocarbon fuel takes place at surfaces where an electrical double layer can form due to ionic materials in the fuel (or on the surface). The flowing fuel sweeps away charged ions of one polarity, leaving the opposite charges to be discharged by contact with ground. The charge carried in the flowing fuel is known as the streaming current. It is defined as the product of charge density (charge per unit volume of fuel) and the flow rate, i.e.,

$$i = Q \times v, \quad (7)$$

where  $i$  = Streaming current (microamperes,  $\mu A$ )

$Q$  = Charge Density (microcoulombs/meter<sup>3</sup>,  $\mu C/m^3 = \mu A \text{ seconds}/m^3$ )

$v$  = Volumetric Flow Rate (meter<sup>3</sup>/second,  $m^3/sec$ )

The excess of ions of a particular polarity in the fuel causes it to be at a different potential from that of the charge separating surface, and of the pipe or tank into which the fuel flows. This difference in potential causes the charge carriers in the fuel to migrate to the container walls where the charge leaks off, by a process which is known as charge decay, or charge relaxation.

The charge density is a function of flow rate ( $v$ ), the area ( $A$ ), and the characteristics ( $X$ ) of the fuel/surface interface, i.e.,

$$Q = f(v, A, X) \quad (8)$$

The factor,  $X$ , represents the charging tendency. It is an unpredictable factor since it depends on both the type of ionizable materials in the fuel and the properties of the surface presented to the fuel.

Electrostatic charging occurs in the presence of all solids, from those of very high conductivity such as metals, to those of very high resistivity such as certain types of plastics. Most of the early electrostatic studies were made on aqueous solutions flowing through glass capillaries, while recent studies have been made on hydrocarbons flowing past metal, as well as glass surfaces. For example , the Shell Charging Tendency Test uses a metal capillary (40), and the Esso Charging Tendency Test used glass wool (55), for the charge separating surface. A wide variety of materials have been shown to charge a hydrocarbon stream as listed below:

---

Non-Metals

---

Aluminum Oxide (47)  
Cellulose acetate (23)  
Cotton (7)  
Dacron (50)  
Fiberglass, Glasswool (2,6,16,48,49)  
Glass tubing (20,46,52,61)  
KEL-F (38,50)  
Nylon (50)  
Paper (6)  
Platinized Alumina (47)  
Polyethylene (38)  
Polyvinyl Chloride (38)  
Resin bonded fiberglass (48,50)  
Teflon (47,52)  
Zeolite (47)

---

Metals

---

Brass (52)  
Copper (17,52)  
Gold (20,46)  
Silver (20,46)  
Stainless Steel (20,25,26,31,32,35,36,46,52)  
Platinum (20,46)  
Palladium (20,46)

It has been suggested that a solid having electrical properties (e.g. conductivity) similar to those of a hydrocarbon liquid would not cause static charging of the liquid. Klinkenberg states that that is not the case (41), and other investigators agree (5, p.137) that fuel gets charged whenever it flows past any solid. However, there is also some evidence that pure hydrocarbons (eg. with essentially no ionic impurities) will not electrify (19,38). There is a considerable body of data which show that filter/separators, which present very large surface areas to fuel, create much higher charge densities than pipe surfaces or pumps (2,3,7,8,10,33,37). For example, in one of these studies (33), the filter produced 10 to 200 times more charge than was produced with the filters removed. That filter/separators are the major source of charge is further evidenced by the fact that numerous studies, in addition to those cited above, have been carried out to evaluate the static hazard in aircraft fueling (1,5,6,10,60,67) and tank filling (37) in which filter/separators were used to generate charge.

Bruinzeel states (5, p. 139, and 33) that in the Coordinating Research Council's Phase II studies, glass wool filters gave half as much charging as paper filters while Gardner (18) reports that tests of fiberglass and pleated paper filter/separators failed to show any gross differences in electrical behavior. However, since studies by John (37) showed 17-fold current variations with three different filters of the same make and made to the same specifications, the above comparisons are probably not conclusive. Leonard and Carhart (50) studied the charging of JP-4 and JP-5 fuels containing Shell's anti-static additive ASA-3, and found that the streaming current was generally positive with filters whose surfaces were organic materials (phenol-formaldehyde resin-bonded fiberglass, Nylon, Dacron and Kel-F), but was negative with inorganic filters (glass wool, and the resin-bonded fiber glass which had been baked to remove the resin). This is not a general rule, however, as was shown by the experiments of Lauer and Antal (47) on the charging of xylene in the presence of filters made of compacted alumina, platinized alumina, and zeolite.

Good comparisons of the streaming currents produced by various filter materials are often not possible because of differences in porosity, fiber diameter, surface roughness, etc. Leonard and Carhart (50) may have avoided some of these variables in their experiments with baked and unbaked resin-bonded fiberglass filters; here, the maximum levels of charging obtained with the two materials were quite similar, though opposite in polarity.

Several mathematical relationships have been developed to explain and/or predict charge generation in pipe line flow (8,10,19,20,21, 25,26,30,35,36,44,45). These relationships were all based on experimental work conducted in capillary or small bore tubing, except for the one of Gibson and Lloyd (26), which was based on data from stainless steel pipes ranging from 0.64 to 4.4 inches I.D. The latter authors state that these relationships will require "further development before they can accurately predict electrification in large-scale systems". For one thing Gibson and Lloyd found that charge generation decreased with a rougher pipe wall, while others (8,36,46) have found that charge generation increases with increased surface roughness, with a five-fold increase being observed in one case (46).

According to Gavis and Kozman (19), charge generation is comparatively small in laminar flow, and larger for turbulent flow. They also indicate that metals give the highest rate of generation, with comparatively small differences between metals although electrification in glass, plastic and rubber tubes also occurs. They cite earlier references which demonstrate that there is a change in tube surface and in liquid composition associated with charge generation with plastic tubes. Like the information discussed previously for filter/separators, the sign of the charge generated in tubes may be positive or negative depending on the nature of the impurities in the liquid and the nature of the surface.

Gavis and Hoelscher (20) and Koszman and Gavis (46) found no significant difference between charging in glass tubes and in gold,



silver, palladium, and stainless steel tubes; a platinum tube gave higher charging but this was attributed to greater surface roughness. Keller and Hoelscher (38) examined charging in polyvinyl chloride, polyethylene, and Kel-F tubes and found it to be not radically different from that observed in steel pipes.

Fridrikhsberg and coworkers (17,71) studied the charging of petroleum ether containing Nekal (sodium dibutyl-naphthalene sulfonate) in stainless steel, copper and Teflon tubes. In copper, the streaming current was initially positive, indicating adsorption of negative anions on the copper. Later, on continued pumping, the streaming current became negative, indicating adsorption of positive sodium ions on the copper-anion surface. In Teflon the current remained positive throughout the experiment.

Rutgers, deSmet, and Rigole (61) have compared the theory for charging in a glass capillary with the theory for charging in a metal capillary, as developed by Klinkenberg and van der Minne (40). A number of other papers on the theory of charging will be found in the attached abstracts.

Leonard and Carhart (51) measured the potentials developed on the fuel surface when bottom loading refuelers with JP-5 at 300 and 500 GPM through 2-1/2, 3 and 4 inch diameter hoses utilizing a 30 second relaxation chamber with the 2-1/2 inch hose at 500 GPM, a maximum potential of 32 kv was measured in the refueler; with 3 and 4 inch hoses the maximum values ranged from 2 to 12 kv. With the 2-1/2 inch hose at 300 GPM, the maximum voltage was only 1.3 kv. They recommended that 2-1/2 inch hose should not be used for refueler loading at 500 GPM (33 feet/second). They suggested that similar surface potentials could be obtained in a refueler if it was fueled at the same flow velocity with 3 or 4 inch hoses and recommended that the flow velocity in hoses of this diameter be kept below 30 feet/second while 2-1/2 inch hoses be limited to a maximum flow rate of 300 GPM.

The search uncovered only one study (70) which was directed at evaluating charge generation in FRP pipe, such as is proposed for

use in "sanitary" aviation refueling systems. The tests were carried out at the CLA-VAL Corporation, Newport Beach, California in early 1969. Tests were carried out with JP-5 and a water white solvent using a 200 foot run of 8 inch diameter Bondstrand 2000 FRP pipe. An A. O. Smith Static Charge Reducer was used as a means of producing a low charge at the pipe inlet; some typical results are shown below:

<u>Fuel</u>	<u>Flow Rate, GPM</u>	<u>T, °F</u>	<u>Charge Density, <math>\mu\text{C}/\text{m}^3</math>, @</u>	
			<u>Pipe Inlet</u>	<u>Pipe Outlet</u>
JP-5	1200	62	8	2
WWS(a)	300	76	6	4
	600	76	6	3
	1200	76	14	6
	1200	82	6	6

(a) WWS = Water White Solvent

Except for the last run shown, the charge at the pipe outlet was always lower than that at the pipe inlet, indicating that charge was relaxing rather than being generated. No data were provided on the conductivity of the fuels used.

Although no comparable data were obtained on charge generation in metal pipe in this study, the results that were obtained along with the data obtained in small scale studies, indicate that charge generation in FRP pipe would be small and that there would be little difference between FRP and metal pipe in charge generating characteristics. However, because of the limited number of tests in the full scale study and the fact that the fuel properties were not clearly defined, a side-by-side evaluation of FRP and metal pipe would be necessary to resolve any possible questions regarding the relative charging tendencies of the two pipe types.

### 3. CHARGE RELAXATION

When charge is generated in a fuel, the charge creates an electrical field which causes the charge carriers to migrate to grounded walls and to recombine with charges of opposite polarity. In a flowing system, however, both charge generation and charge relaxation occur simultaneously so that in a long length of pipe, for example, an equilibrium is attained. Since the charge that can be generated by fuel flowing in a pipe is several orders of magnitude less than that generated in a filter-separator, the equilibrium charge level obtained in a pipe is usually very low relative to the charge leaving a filter.

Classically, the rate at which charge relaxes or decays is determined by the conductivity of the fuel (the reciprocal of resistivity). It is independent of the size, shape or geometry of the pipe, hose, filter case or tank except where the size controls the time available for the charge to relax (e.g., where pipe dimensions determine the residence time of flowing fuel).

The rate of charge decay is normally expressed as an exponential function based on Ohm's Law:

$$Q_t = Q_0 e^{-tk/\epsilon\epsilon_0} \quad (9)$$

where  $Q_t$  = charge after time,  $t$  (eg.,  $\mu\text{C}/\text{m}^3$ )

$Q_0$  = initial charge (eg.,  $\mu\text{C}/\text{m}^3$ )

$t$  = elapsed time (seconds)

$k$  = fuel conductivity (Siemens/meter)

$\epsilon$  = relative dielectric constant, a dimensionless quantity which varies only slightly for hydrocarbons and has a value of about 2

and  $\epsilon_0$  = the absolute dielectric constant of a vacuum ( $8.854 \times 10^{-12}$  ampere seconds/volt meter).

It is common practice to define relaxation time,  $T$ , as the time required for the original charge to decay to 36.8% of its original value:

$$\frac{Q_t}{Q_0} = 0.368 = e^{-1} \quad (10)$$

and  $T$  is related to  $k$  by the following relationship:

$$T = \frac{\epsilon \epsilon_0}{k} = \frac{17.7 \times 10^{-12}}{k} \approx \frac{18 \times 10^{-12}}{k} \quad (11)$$

On this basis, relaxation time would be expected to vary with conductivity as follows:

Conductivity		Relaxation Time,	
CU	k	Seconds	Minutes
0.01	$10^{-14}$	1800	30
0.1	$10^{-13}$	180	3
1.0	$10^{-12}$	18	0.3
10.0	$10^{-11}$	1.8	0.03
100.0	$10^{-10}$	0.18	0.003

(1 CU = 1 Picosiemen/meter =  $10^{-12}$  Siemens/meter)

Thus, highly refined jet fuels with low conductivities (0.1 to 2 CU) would be expected to require seconds to minutes to relax a significant amount of charge. Increasing the conductivity of fuel by an additive is a method used to insure rapid dissipation of charge although some of these additives are surfactants and reduce the efficiency of filter/separators.

However, it has been known for about 10 years that the conductivity of hydrocarbons which have been charged can be widely different from that of the uncharged hydrocarbon because of the change in ion concentration due to charge separation. This effect was first noted in the CRC Phase II work (5, pg. 139; 33), where glass wool filters gave half as much charging of the fuel as paper filters, but introduced about the same amount of charge into the receiving tank. The cause was traced to a greater loss in conductivity and therefore in relaxation rate in the glass wool-filtered fuel than in the paper-filtered fuel.

Since there is a change in conductivity on charging, the relaxation rate cannot be calculated from the conductivity as determined on the uncharged fuel, which is electrically neutral and has an equilibrium concentration of ions to conduct current. The conductivity under charged conditions is referred to as "effective" conductivity, to differentiate it from "rest" conductivity.

A more fundamental approach to charge relaxation has been proposed by Bustin et al (9) who pointed out that fuels which have very high resistivities (eg. a very small number of ionic particles) would behave differently in terms of charge relaxation when the number of charge carriers was suddenly increased (due to filter charging for example). In the extreme case of a fuel of infinite resistivity (no original charge carriers at all) the equation for charge relaxation turns out to be:

$$Q_t = \frac{Q_0}{1 + \frac{\mu Q_0 t}{\epsilon \epsilon_0 \times 10^6}} \quad (12)$$

where  $Q_0$  is the initial charge density and  $\mu$  is the ion mobility. Thus charge relaxation is controlled by the mobility of the ions produced in charging the fuel, not the conductivity of the fuel measured either as "rest" or "effective" conductivity. This equation describes a hyperbolic relationship; Bustin et al (9) confirmed that this relationship is realistic for fuels with very few charge carriers (as measured by rest conductivities below 1 CU).

The measurement of "rest" conductivity is of interest since it is important not only in the characterization of hydrocarbons as to charge relaxation rates, but also because it may provide some idea of whether or not a fuel will generate a charge. It has been stated (19) that a pure liquid of zero conductivity will not generate a charge. Addition of materials which increase fuel conductivity induce charge generation so that the generation rate appears to increase with increasing conductivity. At some conductivity, however, the rate of charge generation will reach a maximum and then decrease as increasing conductivity makes the relaxation time very short. This effect has been observed in several studies (1,2,5,50,67). However, Esso Research (1) has obtained data which show that a high molecular weight polymer can increase charge levels by 30-90 times with very little effect on the rest conductivity.

Douwes and van der Waarden (12) have reviewed the various methods and have developed an improved conductivity cell; they recommend extrapolation to zero time (see also 42) to overcome the effect of ion depletion. Recently, a method has been proposed as an ASTM method (57) for measuring the conductivity of low conductivity liquids, such as aviation fuels, which overcomes the problem of ion depletion by rapid measurement.

After charging, the effective conductivity generally changes too fast to allow for a good measurement in a conductivity cell. Effective conductivity generally can be obtained in two ways. One is by determining the decrease in charge with time at a fixed location in a fuel system after fuel flow is stopped. The second is by measuring the charge at two locations under flow conditions for which the residence time between the two measuring points is known. The effective conductivity,  $k_e$ , expressed as CU, can be determined by combining equations (9) and (11) in the form:

$$k_e = \frac{18 \log_e(Q_0/Q_t)}{t} \quad (13)$$

The effect of charging on conductivity has been observed many times since it was first noted in the CRC Phase II program. The effective conductivity,  $k_e$  of the charged hydrocarbon may be lower or higher than the equilibrium or rest conductivity,  $k_0$  as determined on the original uncharged hydrocarbon. Bruinzeel et al (4,6) report ratios as low as 0.1. In studies by Bulkley and Ginsburgh (7) the  $k_e/k_0$  ratios were always greater than 1. Carruthers and March found the ratio to be as low as 0.079 (10). Foster found that  $k_e$  varies with the extent of charging and may be time dependent (16). In 8 experiments reported by Gardner (18) the ratio varied between 0.07 and 0.19. In many measurements made by John (37) the ratio  $k_e/k_0$  was generally above 1 with  $k_0$  less than 2 CU, and less than 1 with  $k_0$  greater than 2 CU. According

to Masuda and Schon (54), the  $k_e/k_o$  ratio is larger than 1 when  $k_o$  is below 0.1 CU, but smaller than 1 when  $k_o$  is above 0.1 CU. In the CRC work (33), while there were pronounced differences in  $k_e/k_o$  between two types of filters, the average results indicated that the ratio of  $k_e/k_o$  would be greater than 1 below 1 CU and smaller than 1 above 1 CU. The change in conductivity on charging is the result of acquisition or depletion of ions of both signs (or of ionizable species) as the hydrocarbon passes through filters, pipes, etc. Such acquisition or depletion is observed in terms of charge density but affects conductivity in more complicated ways. After relaxation of the charge, the conductivity may return to the rest conductivity fairly rapidly, or very slowly. In some cases the conductivity will first decrease and then increase toward the rest conductivity, and in some cases it apparently never reaches it (37).

As indicated previously, an important advance in relaxation theory was made by Bustin, Koszman, and Tobby (9), who showed that, for liquids having resistivities above  $10^{14}$  ohm-cm (<1 CU), the relaxation rate follows a hyperbolic form. As a result, charge decay for these liquids can be far greater than that predicted by the ohmic theory. In this higher resistivity range, charge relaxation depends not on conductivity but only on charge density and on ion mobility. Liquids having resistivities below  $10^{14}$  ohm-cm (>1 CU) apparently follow the ohmic theory of exponential decay, which is primarily dependent on fuel conductivity.

Vellenga and Klinkenberg (66) have extended the relaxation theory based on Ohm's law, to take into account the effects of ion dissociation and state that it is more valid than either the exponential constant conductivity law or the hyperbolic law. Other developments include those by Gavis showing that in highly charged liquids relaxation is hyperbolic, but in weakly charged liquids it is exponential (22), and that ion mobility is related to polarity (23). A summary of developments through 1966 is given by Klinkenberg (43). More

recently, Gavis (24) analyzed the competing effects of ionic dissociation - recombination rates vs ion mobility and determined that the latter has a more important effect on the rate of relaxation in highly charged systems. If the mobility of the ion having the same polarity as the charge on the fuel is greater than that of the ions of opposite polarity, relaxation appears hyperbolic. If the opposite polarity ion has the greater mobility, relaxation tends to be ohmic.

From the above discussion, the difficulties involved in predicting relaxation rates even in highly conductive metal containers are apparent. Relaxation in containers or pipes of very low conductivity is much less clear and very little data are available. The reports which deal with this subject are discussed below:

Carruthers and March (10) studied relaxation in copper and Teflon tubes in the laboratory, measuring the relaxation current flowing from the tube to ground, and the remainder of the current flowing from the receiving tank to ground. Electrical connection to the Teflon tube was through brass nipples inserted into the ends of the tube; these were connected together and to the electrometer leading to ground. The results showed that charge relaxed slower in the Teflon than in the copper tube; relaxation time in the Teflon was about 2.25 times longer than in the copper.

Two dimensionless parameters were postulated; the first,  $\lambda$ , is the ratio of the residence time of the liquid in the pipe to the electrical relaxation time of the liquid; the second,  $B$ , is the ratio of the conductance per unit length of liquid to the conductance per unit length of liquid plus pipe wall. Equations for the relationship between  $\lambda$  and  $B$  were developed. The values of  $B$  vary with conductivity of the liquid and conductivity of the pipe. For copper or other metals,  $B = 0$ ; for Teflon,  $B = 1$ .



Good agreement between theory and experimental results was obtained with the copper tube up to about 3 electrical relaxation times. With the Teflon tube there was considerably more scatter, but in general the data points were grouped around the predicted curve for  $B = 1$ . These workers indicated that such measurements are very sensitive to minute amounts of impurities on the surfaces. Even blowing through the tube before an experiment could change the results by factors of 10 to 100 and films of moisture on the surfaces of insulating materials could allow currents to leak away which were a significant part of the currents to be measured.

In these tests, relaxation data were obtained in various lengths (60-175 feet) of 2-1/2 inch rubber hoses. Some of these were bonded with wire embedded in the hose and connected to the couplings at each end of the hose (the same situation that existed in the laboratory tests with Teflon). Other hoses were unbonded. The resistivity of the rubber in the hoses was  $4.5 \times 10^7$  ohm-meter; from this  $B$  was calculated to be nearly zero.

Data obtained with bonded hoses were in poor agreement with the values predicted for  $B = 0$ . However, the results could be brought into line with the theory by multiplying by the factor 0.079. The explanation given was that the effective conductivity, which was not measured, was equal to 0.079 times the rest conductivity. However, when the factor was used, data obtained with the unbonded hoses showed far less relaxation than predicted. Regardless of the theory, the results indicated that there was considerably less relaxation in unbonded hoses than in bonded hoses. This was observed even though the resistance of the unbonded hoses was found to be relatively low (eg.  $4.5 \times 10^7$  ohm meter), which would predict that the hose should act like a conductor. There is reason to believe that the data may not be correct, since this same type of hose was used to "insulate" the filter, the test hose sections and the receiving tank from each other in the test installation. Direct current measurements were made between the filter and test hose sec-

tions and ground, but the receiving tank was permanently grounded, so that the current carried into the tank with the fuel could not be measured. Further, based on the current measured between the filter and ground, the filter was only producing a charge density of about 10 to 11  $\mu\text{C}/\text{m}^3$ . It is possible that most of the charge was being grounded through the receiving tank because of low resistance connections between the filter, hose section and receiving tank, thus invalidating the results.

Shafer, Baker, and Benson (64) followed up the work of Carruthers and Marsh, using Teflon pipes, and Teflon pipes which had been manufactured with carbon liners to increase the surface conductivity. With plain, translucent Teflon pipes ( $R = \sim 10^{18}$  ohm-cm), electrical discharges could be observed running lengthwise inside with numerous lateral flashes branching off the path of the main discharge. (Similar results were obtained at Esso Research (58) in glass pipe.) After the initial discharge, the test pipe contained numerous pinhole punctures through which the fuel seeped. As flow continued a glow discharge and occasional small sparks were observed inside the pipe centered around one or more of the puncture points. A purple corona discharge could be observed streaming "into the punctured points from the air" which continued as long as fuel flowed and tended to erode or enlarge the pinholes.

When the Teflon pipe was cut open after the initial breakdown, wide and deep transverse and sometimes lateral paths were found to be centered around each pinhole, with lighter paths branching off from these and covering almost the entire inner surface with a rectangular-patterned network. It was indicated that the paths were proof that the discharges were occurring along the pipe surface and not in the body of the liquid. These tests were carried out with a fuel having a CU of 165 at a flow

rate of 15 GPM. Based on the measurements of pipe current, the charge density was about  $1500 \mu\text{C}/\text{m}^3$ . It was suggested that the potentials before breakdown may have been in the range of 50 to 100 KV. The experiment was repeatable.

With the Teflon pipes containing carbon liners, and having end-to-end resistances of about  $10^6$  and  $10^9$  ohms over a 3-foot length, the relaxation was essentially the same as that obtained with stainless steel pipe. Shafer et al (64) recommended that the resistance of hoses be not more than  $10^7$  ohms, which will give a maximum voltage on the hose of about 1000 volts under the usual charging conditions. They say that the maximum voltage can be calculated as follows:

$$V_{\text{max.}} = 0.1 R_T I_p \quad (14)$$

where  $R_T$  = length/conductance per unit length

and  $I_p$  = pipe current.

Again, the only data that have been obtained on charge relaxation in FRP were obtained at CLA-VAL Corporation (70) using 8-inch diameter Bondstrand 2000. One test was carried out in carbon steel pipe for comparison. A water white solvent of unknown conductivity was used and charge generated with a pair of 600 GPM filter-separators; the results are summarized below:

Pipe Type	Flow Rate, GPM	Temp., °F	Charge Density, $\mu\text{C}/\text{m}^3$ @		T, Sec.
			Pipe Inlet	Pipe Outlet	
FRP	600	76	152	12	23
	1200	76	152	22	15
	1200	76	250	30	14
Carbon Steel	1200	76	252	2	6

The relaxation times, T, calculated from the available data indicate that relaxation is about twice as fast in the steel pipe than in the FRP. These limited data suggest that a hazardous charge level (eg.

$>30 \mu\text{C}/\text{m}^3$ ) may occur at the outlet of an FRP pipe under certain conditions which would not result if a steel pipe of comparable dimensions were used. It was also noted that a potential was produced on the exterior of the pipe, which was highest near the inlet end and decreased in the direction of flow. Low intensity sparking was produced at the pipe surface when a grounding device was brought near the pipe. This was not considered to be a problem since plastic pipe is to be used underground.

The available data indicate that the rate of relaxation in plastic pipe is probably less than in comparable metal systems. The resistivity of the plastic appears to be a major factor in determining whether or not a hazardous situation can develop, since spark discharges and the production of voltages which were high enough to puncture the pipe wall were observed with Teflon which has a very high resistivity (eg.  $\sim 10^{18}$  ohm cm.), while these phenomena were not observed with Teflon having an inner coating of more conductive material or in FRP, a more typical commercial piping material which has a lower resistivity (eg.  $\sim 10^{13}$  to  $10^{14}$  ohm cm.).

Again because of the limited data available on full-scale studies and the fact that the fuel properties, which have a large effect on charge relaxation, were not clearly defined, a side-by-side comparison of FRP and metal pipe under closely matched conditions was considered necessary for developing recommendations regarding the use of such pipe in fueling systems.

#### 4. GROUNDING AND BONDING

Several workers have expressed concern over the high voltages that are built up on hoses, pipes, and tanks of high or even moderate resistivity. Bruinzeel (6) cites the case of an 83-foot length of 2-1/2 inch unbonded refueling hose, carrying fuel at 200 IGPM which was charged to  $270 \mu\text{C}/\text{m}^3$ . At the middle of the length of the hose the potential was 6000 volts and discharges of 0.1 to 0.2 microcoulombs were obtained by touching the outside of the hose with a probe.

Emekeev (15) states that non-conducting hoses are dangerous when used for the transfer of explosives.

Gibson and Lloyd (27) have shown that charged plastics generate discharges of 0.67 to 0.92 mJ which will ignite flammable vapor-air mixtures.

Gibson, in commenting on a paper by Tinson (65), states that "Incidents are known in which polyethylene pipes, electrostatically charged by the flow of fluids through them, have released electric sparks from their outer surfaces to the earthed metal collars supporting them". (J. Inst. Pet. 54 19 [1968]). He went on to say that "there is considerable evidence that the earthing of metal components on tanks made from very high resistivity materials will not make them identical, in terms of electrostatic hazard, with tanks made from conducting materials". Tinson replied "It is clear that proper electrical bonding in this case (eg. in the case of tanks made of materials having very high resistivities on the range  $10^{14}$  -  $10^{17}$  ohm-cm) includes not only the bonding of each metallic connection to the container, but also some additional precautions such as the incorporation in the container of a bonded liner or inner coating of moderate resistivity" (J. Inst. Pet. 54 140 [1968]).

Klinkenberg (40, pp. 93-94) states that the potential difference between earth and a charged liquid is much higher in a container made of an insulating material than in an earthed or grounded metal container; therefore sparks can occur between the liquid and, for instance, a grounded metal valve. Furthermore, the outside of the wall gradually collects a surface charge giving rise to electric discharges. Klinkenberg states that the situation can be made safer by partly earthing the liquid by means of an adequate area of earthed conductor in the liquid.

Klinkenberg (11, p. 190) has also stated that a highly charged hose is a hazard on an airfield in a possibly explosive atmosphere. With commonly occurring fuel conductivities and with insulating rubber hose, the maximum calculated voltage runs into the thousands of megavolts. He also has indicated (40, pg. 165) that a rubber hose is less effective than a steel pipe in relaxing charge and that the difference can be largely

eliminated by fitting an earthed metal wire inside the hose in addition to the one embedded in the rubber.

Carruthers, in discussing high voltages on refueling hoses (11, p. 194), states that bonding wires can get quite hot due to high currents flowing through them. Such currents can arise partly from nearby power generating equipment. In such cases, a bond wire is dangerous whether it is in the hose, on the outside of the hose, or embedded in the wall of the hose. A possible answer is a metallic sheath on the outside of the hose.

Shafer et al (64) recommend internal bonding wires in pipes of non-conducting materials, because of the possibility that sparks will puncture the wall if an outside bonding wire is used. The authors point out that an internal bonding wire would likely have little, if any, effect on the rate of charge relaxation from highly charged fuel.

Tinson (65) studied the hazards during the loading of fiber glass reinforced plastic tanks, concluding that if provision is made for proper electrical bonding, the hazards should be no greater than with metal tanks. Scholz (63) states that the surface resistance of such tanks should be under  $10^9$  ohms, or provisions made for grounding. Winter (67) states that tank linings are hazardous except where their conductivity is considerably greater than that of the hydrocarbon.

## 5. METHODS FOR MINIMIZING THE STATIC HAZARD

There are actually relatively few techniques or devices available for reducing or minimizing the static hazard in fuel transfer operations. The technique which is probably the most widely used is the relaxation principle, which calls for sufficient residence time following a filter/separator to permit charge to decay to a low level before delivery into a tank (7,8,9,13,14,59). It was Bustin et al (9) who first showed that the practice of using 30 seconds of relaxation was also valid for very low conductivity fuels although studies carried out by John (37) led him to conclude that there was no basis for considering 30 seconds an optimum relaxation time.

The use of antistatic additives which raise the fuel conductivity and provide for rapid charge relaxation has also seen wide application (6,7,14,39,59). However, there is some evidence that such materials may affect other fuel properties adversely, eg. by emulsifying water in fuel, or by decreasing storage and thermal stability (59).

As for devices, the Static Charge Reducer (SCR), which is based on Esso Research and Engineering Co. patents (56) and developed by American Oil Co. (28), is the one which has been used most widely in the field. The SCR which is manufactured by A. O. Smith, Erie, Penna., consists of a 3-foot long pipe section lined with a thick dielectric through which several pointed and grounded pins project. The potential developed across the dielectric by the flowing fuel induces charge to flow into or out of the fuel, reducing the overall charge on the fuel. Performance data have been obtained by Martel (53) at fuel conductivities generally ranging between 20 and 100 CU. The charge density at the outlet of the SCR was found to be below  $30 \mu\text{C}/\text{m}^3$  in all cases and was less than  $20 \mu\text{C}/\text{m}^3$  in all but 2 cases at charge densities up to  $494 \mu\text{C}/\text{m}^3$  at the SCR inlet. With high conductivity fuels, eg. 75 to 100 CU, the charge density delivered by the SCR tended to increase, but it was always well below  $30 \mu\text{C}/\text{m}^3$ .

Another approach to reduction of static charge which has been mentioned (14,59,69) involves the use of a radioactive source. Until quite recently, the technique was only considered for use in tanks where the source could ionize the vapor space and produce a conductive path through which the charge on the hydrocarbon surface could be dissipated. Quite recently, it was learned (Personal Communication from W. G. Dukek, Esso Research and Engineering Co., March 1972) that McDonnell-Douglas, Long Beach, California has tested a prototype device using  $\text{Sr}^{90}$  which reduced charge by 80 to 95 percent at flow rates between 400 and 1200 GPM. The device would probably require extensive development before it could be commercialized.

## 6. FIELD CONTACTS

A number of individuals who were either active in or whose interests could make them aware of research in this field were contacted to insure that no unpublished data or related programs were overlooked. Among the people contacted were W. Bustin, ERE (Esso Research & Engineering Co.); G. Chiotti, A. O. Smith; I. Kozman, ERE; J. Leonard, Naval Research Laboratory; C. Martel, Air Force Aero Propulsion Laboratory, Wright-Patterson AFB, Ohio, E. Sommer, ERE, who is a member of the American Petroleum Institute Static Electricity Committee, and J. Warren, Mobil Oil Co. None of them were aware of any information on this subject that had not been turned up in the literature search.

During this phase of the program, W. G. Dukek, ERE, attended a meeting of the International Air Transport Association at Geneva and reported that Mr. A. D. Radbone, Shell International Petroleum Co., London, had indicated his company was carrying out studies on charge generation and relaxation in FRP pipe. We wrote Mr. Radbone requesting any data that could be made available; we were informed that the work was not completed or published for distribution. Except for this work then, the background information is probably complete.



## B. ANNOTATED BIBLIOGRAPHY

1. Bachman, K. C. and Dukek, W. G., Static Electricity in Fueling of Superjets, Esso Research and Engineering Co. Brochure, January 1972.

A test program on static electrification of jet fuels carried out by Esso Research and Engineering Company has provided a high degree of assurance that high-speed fueling of superjet aircraft can be carried out safely. The program was conducted in a full-scale fueling rig which included the key section of an aircraft wing tank. A unique method was developed for measuring the energy in the spark discharges which occurred in the tank. The test results revealed that manifolding the tank inlet to distribute charged fuel is highly effective for minimizing the static hazard. With only normal aircraft components in the tank, no discharges could be produced under conditions simulating a manifold inlet. Under comparable conditions, discharges displaying energies of less than 0.06 millijoules, well below the minimum ignition energy of 0.26 millijoules for hydrocarbons in air at sea level, were detected when the tank was fueled through a single inlet. It was also demonstrated that incendiary sparks with energies as high as 0.8 millijoules could be produced when fueling through a single inlet if an unbonded charge collector were present in the tank; the maximum spark energy appeared to occur with fuel of about 3 picosiemens/meter rest conductivity. No incendiary sparks were detected with the unbonded charge collector present under conditions which represented filling through a manifold.

2. Bossi, H. G. (Convair), and Scheuermann (Esso Research), Electrostatic Discharges in Aircraft Fuel Systems - Phase I. Coordinating Research Council, Report No. 346, CRC Project No. CA-6-58, April 1960.

In the Coordinating Research Council's program to determine and define electrical discharge hazards, discharges were produced and detected at Wright Air Development Center by pumping JP-4 fuel at 250-900 gal/min through a 300 gal/min filter-separator into a 5000 gal rectangular tank containing a pointed probe. When 0.0001-0.0005% (1-5 ppm) asphalt was added to increase the charging rate, sparks occurred even at 250 gal/min flow rates. Sparks were also produced between grounded objects and either fixed or free electrically conductive objects inside the tank and in a glass wool filter through which JP-4 fuel, an additive, and entrained air were pumped. Techniques and equipment for detecting sparks and measuring their energy levels were developed. See Harris and Karel (33) for CRC Phase II.

3. Brown, R. N. (Army Engineer Research and Development Labs, Fort Belvoir, Va.), Electrostatic Charge Generation in Filter/Separator Vessels, AD-AD-473,807. AERDL 1827, August 1965.

This report covers an investigation of electrostatic charge generation in filter/separator vessels in individual filter/coalescer elements and the development and design of a filter/separator grounding device to dissipate electrostatic charge accumulating in military fuels. The report concludes that: (1) no hazardous charges develop on steel or aluminum

filter/separator vessels when supports and piping are well grounded. (2) no reliable information on the charging tendencies of individual filter/coalescer could be obtained; however, under certain optimum conditions, 9 to 10 KV were measured in the fuel leaving individual elements, (3) a short brass pipe nipple containing pointed metal probes extending radially inward, installed in the outlet piping and correctly grounded, will effectively dissipate electrostatic charges retained in the discharging fuel. (Author)

4. Bruinzeel, C. et al., Static Electricity in Aircraft Fueling, Report M. 206. Shell Research Ltd., April 1960.

Hydrocarbon products can become electrically charged during transfer; as a result, a charge can accumulate in a receiving tank, provided that the conductivity of the product is sufficiently low--as it generally is in the case of aviation fuels. In the past there has been no indication that this constituted a serious problem in the fueling of civil aircraft, but recent work has shown that the higher fueling rates now demanded may result in very high rates of charge generation during the passage of the fuel through modern types of filter and water separator. The accumulation of a large amount of charge in the fuel contained in an aircraft tank could result in an electric discharge between the fuel surface and the tank. Since the vapour mixture in a tank could be in the inflammable range at certain temperatures with present types of aviation turbine fuel, a discharge of sufficient energy could result in a fire or explosion.

The aim of the present work was to ascertain whether modern high speed fuelling procedures could give rise to an electrostatic hazard, and if possible to establish the degree of risk.

The results of this work indicated that electric discharges within an aircraft tank could result from the fuelling of aircraft at fuelling rates into a single tank of 200 Imp. gal/min. upwards, with fuel conductivity below 2 picomho/m. This level of conductivity is not unusual.

These discharges may be too weak to ignite an inflammable mixture, but the energy of some discharges was found to be of the order of ten times that established by other workers as being the absolute minimum energy for ignition of the most readily inflammable mixture. Increasing the flow rate into a single tank increases the possibility of incendiary discharges occurring. Since an inflammable vapour mixture is also possible in certain circumstances with either kerosine (Avtur) or wide range aviation fuel (Avtag), the risk of very high fuelling rates leading to a fire or an explosion cannot be dismissed.

5. Bruinzeel, C. (Shell Intern. Res. Mij. N.V.), Electric Discharges During Simulated Aircraft Fuelling, J. Inst. Petrol. 49, (No. 473), 125-39, 1963.

Photographic evidence showed that the critical periods for electrical discharges are the beginning and end of the fuelling operations, and that sparking during the early stage of filling is the more difficult to

suppress. The discharges lasted from a fraction of a microsecond to several microseconds, and their energy content ranged from below 0.2 mJoule (minimum for ignition) to several tens of millijoules. The results indicate that, in practice, the fuel conductivity must be at least 50 picomhos/m to prevent all possibility of explosion due to a discharge of static electricity. 20 references.

6. Bruinzeel, C., Luttik, C., Vellenga, S. J. and Gardner, L., A Study of Electrostatic Charge Generation During Low Temperature Refuelling of Aircraft, Nat. Res. Council of Canada, Aeronautical Report LR-387, Ottawa, Canada, Oct. 1, 1963.

During the period January to March, 1963, low temperature fuelling tests were carried out at R.C.A.F. Station, Winnipeg, Manitoba using R.C.A.F. aircraft and fuelling equipment. High electric field strengths were measured in the vapour space of a T-33 aircraft tip tank, a wing tank of a Yukon CC-106 aircraft and in a small experimental tank.

Discharges were observed at normal refuelling flow rates in the small test tank. Some of these discharges were sufficiently powerful to present a serious explosion hazard should the vapour be in the flammable region. This fact helps to confirm the theory that previous explosions in this type of aircraft could be attributed to electrostatic discharges.

It was found that, during low fuel and ambient temperature conditions, strong charging may persist up to a higher level of fuel rest-conductivity than would normally be found at higher refuelling temperatures. The main factor which caused this effect was that after transfer through the fuelling equipment, the conductivity of the fuel remained at a low level for a considerable period of time. The ratio of the effective conductivity  $k_e$  to the rest conductivity  $k_o$ , prior to transfer through the filtration equipment, was as low as 1/10.

It was demonstrated that even under the severest test conditions an effective anti-static additive gives complete protection against static generated in the fuel when added to give a fuel rest conductivity of 100 picomho/m ( $100 \times 10^{-12} \text{ ohm}^{-1} \text{ m}^{-1}$ ). It should be emphasized that the use of such additives does not eliminate the need for external bonding.

7. Bulkley, W. L. & Ginsburgh, I., (Am. Oil Co.) Safe Loading of Distillate Fuels as Affected by Their Electrical Characteristics, 33rd API Div. Refining Midyear Mtg. (Philadelphia 5/15-17/68) Preprint No. 08-68:13p.; cf. Hydrocarbon Process. 47, (No.5), 121-23, 1968.

A survey of available data on the effects of sparking potential, charge density, oil conductivity, relaxation times, charge generation, and temperature on internal sparking during the loading of intermediate vapour-pressure fuels, such as JP-4, or the switch loading of low vapour-pressure distillate fuels indicates that the long relaxation times of modern highly refined distillates and the use of filters that are prolific charge generators have increased in likelihood that the necessary

conditions for internal sparking and hence ignition will exist, compared with earlier years. Safe loading of such distillates requires, in addition to existing standard safety practices, the elimination of the flammable atmosphere by air eduction or by inerting, and/or the reduction of the charge density in the fuel by accelerating its relaxation rate with additives or by a static-charge neutralization device. The paper states that the effective conductivity of charged oil can be considerably different from the equilibrium conductivity measured on the uncharged oil, and that the relaxation time of charged oil is invariably shorter than the relaxation time measured on the uncharged oil.

8. Bustin, W. M., Culbertson, T. L., & Schleckser, Jr., C. E. (Esso Research) General Considerations of Static Electricity in Petroleum Products, API Proc., 37 (III), 24-43, 1957.

Experimental work has confirmed that electrical current generated in pipeline flow is given by:

$$I = (TKV^{1.75}) \left( I - E^{\frac{-L}{TV}} \right)$$

Where:

- I = current issuing from line with fuel.
- T = fuel time constant.
- K = factor determined by pipe diameter and fuel-pipe interface.
- V = velocity.
- E = base of Napierian logarithms.
- L = pipe length.

As suggested by this formula, an enlarged pipe section allowing low velocity for a short period of time will materially reduce the static charge. Filters of the type to be used in aircraft loading systems generate substantial charge in the fuel which can be reduced by a downstream relaxation tank of practical dimensions. Other safety measures include low pumping rates, avoidance of surface agitation and water, and use of floating-roof tanks to eliminate the vapor space. Tanker compartments are gas-freed when necessary. Carbon dioxide gas blanketing is planned for some barge operations.

9. Bustin, W. M., Koszman, I., & Tobye, I. T., (Esso Research), A New Theory For Static Relaxation From High-Resistivity Fuel, Am. Petrol. Inst. Proc., (III), 44, 548-61, 1964.

A new theory for static relaxation (in jet fuels) has been developed, based on different physical assumptions, which predicts much faster relaxation than the extrapolated ohmic theory for very high-resistivity fuels. Laboratory experiments and studies with full-scale loading equipment confirmed that the ohmic theory is invalid as a guide to charge relaxation when the fuel resistivity exceeds  $10^{14}$  ohm-cm. and that at least 60% charge removal occurs in 30 sec. under conditions where the ohmic theory would have predicted only a few percent. The development and testing of the new theory and its relationship to safety practices in tank-truck loading are discussed in detail.

10. Carruthers, J. A., & Marsh, K. J., (British Petroleum Co.), Charge Relaxation in Hydrocarbon Liquids Flowing Through Conducting and Non-conducting Pipes, J. Inst. Pet., 48, 169-179, 1962.

Charge relaxation in liquids flowing through pipes of any resistivity can be expressed as a "relaxation function" which depends on two dimensionless electrical parameters determined by the electrical conductivities of fuel and pipe and the flow conditions. Tests included laboratory experiments on iso-octane flowing through copper and PTFE tubes as well as full-scale experiments with an aircraft fueller and aviation kerosine using bonded and unbonded hoses. It is confirmed that breaking the bonding wire of a fuelling hose does not materially reduce the rate of relaxation of charge from the fuel.

11. Carruthers, J. A., & Wigley, K. J., (British Petroleum Co.), The Estimation of Electrostatic Potentials, Fields, and Energies in a Rectangular Metal Tank Containing Charged Fuel, J. Inst. Pet. 48, 180-195, 1962.

Electrostatic potentials and field patterns inside a rectangular metal tank partially filled with charged fuel are calculated and presented in the form of a double infinite Fourier series. This series may be summed to a high degree of accuracy by using a digital computer, but for practical applications single term approximations for fields, potentials, and energies are simpler and more convenient to use. Detailed comparison is drawn between field estimates using the approximate expression and field values measured in a simulated aircraft fuel tank during fuelling experiments. The agreement was satisfactory for most practical purposes. The calculations have been extended to include the important effects of surface charge on the electric fields in the vapour space of a tank. Fields produced by charged mists are also compared in magnitude with fields produced by charge distributed in liquid fuel.

12. Douwes, C., & van der Waarden, M., (Kkl./Shell-Lab.), Current Decay During Measurement of DC Electric Conductivity in Solutions in Hydrocarbons, J. Inst. Petrol. 53 (No. 523), 237-50 1967.

The conductivity of a number of compounds (e.g., chromium diisopropylmalicylate) which undergo current decay at concentrations of practical importance were studied by the homogeneous and inhomogeneous electric field, immersion cell, stainless steel cell, and ball methods at 10-10,000 picomhos/m and 200-100,000 v/m field strengths. These data were then used to derive equations for stirred and unstirred solutions for defined ideal conditions. After extrapolation to zero time, the results were found to be equal to one another and equal to a-c conductivity values determined at 1000 cps; the zero-time d-c conductivity was therefore an intrinsic property of solutions in hydrocarbons. The immersion cell method was found to be reliable enough to determine the d-c conductivity at 10-1000 picomhos/m and could be used in monitoring antistatic additives in petroleum products. 16 references.

13. Egorov, V. N., Preventing the Accumulation of Electrical Charges in Petroleum Products During Pumping into a Tank, Neftyanoe Khoz., 39, (No. 9), 50-55, 1961.

Formulas are derived for calculating the necessary dimensions of a chamber (enlarged pipe section) upstream from the tank for dissipating 95% of the accumulated static electricity, depending on the specific conductivity and natural charge-dissipation time of the product and the pumping velocity. The theoretical analysis is in good agreement with the results of laboratory experiments carried out by Bustin, Culbertson & Schleckser (8). Diagram, graph, and table. (in Russian)

14. Eichel, F. G., (Givaudan Corp.) Electrostatics, Chem. Eng. 74, (No. 6), 153-67, 1967.

A survey covers the origin and nature of electrostatic phenomena; electrostatic hazards in industrial plants; the basic relationships of electrostatics (force between charges, field strength, field and flux, electrostatic potential, field strength and voltage in filled containers, the capacitance of a body, relaxation time and half-value time, the energy of charged condensers, streaming current, and settling potential and field strength); 11 examples of the use of electrostatic calculations, including several on tank filling with benzene, a water-heptane mixture in a tank, crystals wet with heptane, and the pumping and filtration of aviation turbine fuel; and brief discussions of methods for controlling static electricity, with emphasis on the use of additives to increase the conductivity of hydrocarbons. Accepted electrostatic values for use in these calculations, including those of various hydrocarbons, are appended. 12 references.

15. Emekeev, V. I.; Shelekhov, P. Yu; Ganichev, G. A.; Abramov, V. F. (Severokavkaz. Gornomet. Inst., Ordzhonikidze, USSR) Electrical Phenomena During the Pneumatic Charging of Wells by Placer Explosives, Gorn. Zh., 145(3), 62-4, 1970.

Static elec. charges on the inner and outer surfaces of hoses depend on the particle size of the explosive, the velocity of the particles, temp., moisture, elec. cond. of the explosive and surrounding rocks, the quality and length of hoses, etc. A survey of mining accidents assocd. with this phenomenon and expts. under industrial and lab. conditions show that hoses made of nonconducting materials are dangerous.

16. Foster, M. D., (BP Research Center), The Dissipation of Electrostatic Charges in Purified Petroleum Products, London Conference on Static Electrification, Institute of Physics and Physical Society, 78-88, May 1967.

The full-scale studies of electrostatic charging during the refuelling of aircraft showed that the electrical conductivity of the fuel, when charged, could be different from that measured in the laboratory by direct-current methods; the conductivity could also be time dependent.

This paper suggests a simple model to account for such conductivity variation based on the comparative slowness of dissociation of the ionic materials responsible for the conductivity. The same model is applied to the observed time variation of current flowing through a petroleum liquid under the influence of an external electric field.

Preliminary experiments give consistent values for the ion-dissociation time constants measured in the two situations. The mobility of ions in the uncharged stressed liquid was  $2.5 \times 10^{-8} \text{ m}^2 \text{ v}^{-1} \text{ sec}^{-1}$  which is in good agreement with the value of  $4 \times 10^{-8} \text{ m}^2 \text{ v}^{-1} \text{ sec}^{-1}$  suggested by Klinkenberg.

17. Fridrikhsberg, D. A.; Shchiglovskii, K. B. (Leningrad. Gos. Univ. im. Zhdanova, Leningrad, USSR), Time-Dependence of Streaming Potential and Current in Nonpolar Liquids, Issled. Obl. Poverkh. Sil, Sb. Dokl, Konf., 3rd 1966 (Pub. 1967), 421-30 (Russ). Edited by Deryagin, B. V. Izd. "Nauka": Moscow, USSR.

The charging during flow through Cu and fluoroelast tubes of solns. of Nekal in petroleum ether with b.p.  $100-10^\circ$  was studied. Nekal was added to increase the cond. and capacity for charging of the petroleum ether, which were very low (the cond. was  $10^{-15} \text{ ohm}^{-1} \text{ cm}^{-1}$  without Nekal and  $2 \times 10^{-12}$  and  $2.6 \times 10^{-11} \text{ ohm}^{-1} \text{ cm}^{-1}$  with 5 and 50 mg. Nekal/l., resp.). The Nekal soln. was made to flow under the effect of air pressure from one 10-l. vessel into another through a tube with a length of 50 cm. and a diam. of 3 mm. The convection elec. current (streaming current)  $i_s$  and the resulting effective current  $i_r$  that charged the vessel receiving the liq. were detd. as a function of the time  $t$  of flow by means of a Faraday cage arrangement. As the charge in the receiver vessel changed with  $t$ , the potential  $V$  of an insulated metal screen surrounding this vessel passed through a max. and then decreased. On the basis of the changes in  $V$  that were measured,  $i_r(t)$  and  $i_s(t)$  were detd. ( $i_r = i_s - i_t$ , where  $i_t$  is the leakage current). The values of  $i_r$  and those of  $i_s$ , which followed from them increased with  $t$ , passed through a max., and then decreased. In prolonged expts. with flow of repeated portions of soln. through the Cu tube (pressure 1 mm. Hg, Nekal concn. 50 mg./l.),  $V$  initially had pos. values. These values decreased from expt. to expt. until  $V$  changed its sign and became neg. On cleaning of the tube, pos. values of  $V$  were restored. The tube surface was 1st charged neg. by adsorption of Nekal anions  $A^-$  according to the equation  $A^- + \text{Cu} \rightarrow \text{CuA} + e^-$ , while the  $\text{Na}^+$  ions derived from Nekal were transported into the receiver vessel with the result that  $i_r$  assumed a pos. value. In the 2nd stage,  $\text{Na}^+$  ions were adsorbed on the  $\text{CuA}$  layer and  $A^-$  ions were adsorbed on the wall of the fluoroelast tube, so that the values of  $V$  remained pos. and did not change from expt. to expt.

18. Gardner, L., (Nat'l Res. Council Can.), The Generation of Static Electricity During Aircraft Refuelling, Canadian Aeronautics and Space Journal, 10, (No. 7), 193-202, 1964.

One of the problems associated with refuelling turbine powered aircraft is the hazard created by the generation of electrostatic charge within the fuel. This hazard cannot be controlled by the normal grounding operations. A significant accumulation of electrostatic charge can occur within an aircraft fuel tank, as a result of this refuelling, such that localized fields in excess of 3,000 kV/m are formed. At these voltages electric discharges can take place within the vapour space of the fuel tank, which could produce an explosion. Investigations have shown that the use of microfiltration during fuelling has considerably increased this electrostatic hazard.

The electrical conductivity of the fuel is a property of prime importance. This conductivity to a certain extent regulates the quantity of charge generation and in addition controls the rate of charge relaxation. At higher conductivities the rate of charge relaxation becomes sufficiently rapid that any significant accumulation of potential within a fuel tank is avoided. Artificially increasing fuel conductivity by the use of fuel additives therefore offers an effective means of eliminating the electrostatic hazard due to the fuel.

Several investigations have been conducted to assess the extent of electrostatic charging during aircraft refuelling. One of the most recent was a low temperature investigation carried out at RCAF Station Winnipeg. A brief summary of the results of this investigation are given in this paper.

19. Gavis, J., & Koszman, I., (Johns Hopkins Univ.), Development of Charge in Low Conductivity Liquids Flowing Past Surfaces, J. Colloid Sci. 16 (4) 375-91, 1961.

A theory of the phenomenon in tubes was developed in connection with the generation of charge in pipes and pipelines carrying petroleum products, which may be responsible for explosions and fires in refineries and tankers. The equations were solved for the special case of uniform velocity profiles and the solution was shown to be the same as that for very low conductivity and to agree in form with reported experimental observations. Predictions made for higher conductivities on the basis of the equations also agreed with observation. 26 references.

20. Gavis, J., & Hoelscher, H. E., (Johns Hopkins Univ.), Phenomenological Aspects of Electrification, API Proc. 41 (VI) 18-25, 1961.

A theory for charge generation in hydrocarbons flowing past solid surfaces is proposed which explains the process in turbulent pipe flow and points up the most hazardous range of liquid conductivity, flow velocity, and pipe diameter and length. The theory is substantiated by experimental results obtained with n-heptane, doped to  $10^{-15}$ - $10^{-9}$  mho/cm conductivities with Shell ASA No. 1 additive, flowing at 2100-40,000 Re



in 4-40 cm long, 0.02-0.2 cm dia platinum, stainless steel, gold, silver, palladium, and glass tubes, as well as by data reported by other investigators. A final correlation is given in the form of an equation and also as a universal plot from which charge generation rates may be predicted accurately for a given system. It is applicable to turbulent pipe flow and may be used when the dimensions of the system and the conductivity and other physical properties of the hydrocarbon fluid are known. 10 references.

21. J. Gavis (Johns Hopkins Univ., Baltimore, Md.), Transport of Electric Charge in Low-Dielectric-Constant Fluids, Chem. Eng. Sci. 19 (3), 237-52 1964.

Electrokinetic phenomena are described in terms of the charge distribution within a fluid and at its surfaces. This takes the form of a linear partial differential equation for the transport of elec. charge by diffusion, conduction, and convection in the fluid. Applying the principle of similarity to the equation, the types of electrokinetic phenomena to be expected in a given system are characterized in terms of two ratios of characteristic lengths, the Reynolds no. and the Schmidt no. The solution of the charge transport equation is illustrated by application to a double layer at an infinite, plane, immersed surface; to a condition of relaxation of charge in a spherical container; and to a condition of steady flow in a tube. The theory developed may have applications to electrokinetic problems in atm. elec. 29 references.

22. Gavis, Jerome (Johns Hopkins Univ.), Relaxation of Electrically Charged Hydrocarbon Liquids, Chem. Eng. Sci. 22 (4), 633-5, 1967.

The rate at which an elec. charged, quiescent hydrocarbon liquid in a grounded container loses its charge is discussed. The expressions for the rate of relaxation of the elec. charged liquid are derived from the nonlinear partial differential equation for transport of charge in low dielec. const. fluids (ibid. 22(3), 359-64 (1967)). The limiting cases of highly charged and slightly charged liquids were studied; they relax hyperbolically and exponentially, respectively.

23. Gavis, J., & Wagner, J. P., (Johns Hopkins Univ.), Electric Charge Generation During Flow of Hydrocarbons Through Microporous Media, Chem. Eng. Sci. 23 (4), 381-91, 1968.

The liquid electrical conductivities, the volumetric flow rates, and the electric charge generation rates of solutions of ionizing additives in n-heptane flowing through 24 mm dia. cellulose acetate Millipore filters with porosities of 43-82% were measured in an electric charge generation apparatus at superficial velocities of 0.0149-37.9 cm/sec, which corresponded to  $Re\ 1.31 \times 10^{-5}$  to  $Re\ 0.532$  and to friction factors of  $8.75 \times 10^5$  to 22.7. The steady-state currents were found to vary from  $1.4 \times 10^{-12}$  to  $5.9 \times 10^{-7}$  amp. On the basis of the experimental data, an empirical correlation was developed for predicting the current flowing with a hydrocarbon liquid through any microporous (filter) medium as a function

of the liquid relaxation time, the liquid superficial velocity, and the nominal pore diameter and porosity of the medium. A physical description of the mechanism of charge generation is also presented.

24. Gavis, Jerome (Johns Hopkins Univ.), Effect of Ionic Dissociation and Recombination on the Relaxation of Charge in Low Dielectric Constant Fluids, Chem. Eng. Sci. 24 (3), 451-60, 1969.

The equation of charge transport in the absence of diffusion and convection, but with finite rates of ionic dissociation and recombination taken into account, is developed and solved for a system in which a uniformly charged low dielectric constant fluid is allowed to relax its charge at its boundaries. Solutions are given in analytic form for certain possible situations; but, in general, numerical solution of the highly nonlinear ordinary differential equations must be resorted to. When the positive and negative ions have similar diffusivities (or mobilities), the rates of relaxation are not very dependent on the dissociation and recombination rates unless the time for ion equilibration is large compared with the relaxation time of the uncharged fluid. If the fluid contains positive charge, the relaxation rate is but little affected by differences in ion diffusivities when the diffusivity of the positive ion is greater than that of the negative ion. If the negative ion diffusivity is greater, however, the rate of relaxation is much slowed when the charge density is large and the ion equilibration time is small compared with the relaxation time of the uncharged fluid.

25. Gibbings, J. C. (Univ. Liverpool), Electrostatic Charging in Laminar Flow in Pipes of Varying Length, J. Electroanal. Chem. Interfacial Electrochem. 25, 497-504, 1970.

The effect of the length of a stainless steel pipe containing a laminar flow upon the streaming current was investigated. It was found that a high charge developed in the entrance region, followed by a slow fall to the asymptotic value corresponding to a pipe of infinite length. Earlier papers dealt with turbulent flow, where the results were exactly the reverse.

26. Gibson, N. and Lloyd, F. C., (I.C.I. Ltd.), Electrification of Toluene in Pipeline Flow, London Conference on Static Electrification, Inst. of Physics and Physical Society, 89-99, 1967.

The electrification of toluene flowing in stainless-steel pipelines at velocities in the range 1-10 m/sec has been measured in a large-scale pipeline system (2275 liter capacity, pipelines 1.62, 2.88, 5.39, 8.35 and 10.90 cm diameter and 29 m long). The experimental data, which show the dependence of electric current on such parameters as flow velocity, pipe diameter and pipe length, are used to test the validity of the Koszman and Gavis, and Gibbings and Hignett equations relating these parameters.

27. Gibson, N., and Lloyd, F. C., (Imperial Chemical Industries, Ltd.), Incendivity of Discharges from Electrostatically Charged Plastics, Brit. J. Appl. Physics 16, 1619-1631, 1965.

Electrostatic charge densities of  $1.1\text{--}2.3\text{ nc cm}^{-2}$  can be generated over areas of polyethylene (polythene) sheet by rubbing. The nature and magnitude of electric discharges from the polyethylene sheet to an earthed electrode are a function of the relative humidity of the atmosphere and of the size of the electrode. The discharges change from corona to spark type if the radius of a hemispherical electrode is increased from 1 to 10 mm; with the latter-sized electrode the sparks can contain up to  $0.23\text{ }\mu\text{c}$  of charge. Such sparks, which have an equivalent electrical energy of  $0.67\text{--}0.92\text{ mJ}$ , can ignite flammable mixtures of coal gas, methane, acetone, methanol, toluene, cyclohexane and dioxane with air. For a fixed electrode system the incendivity of a spark is directly related to the electric charge in it. Similar results are obtained with Perspex (Lucite), polystyrene, polyvinyl chloride, nylon, and polypropylene.

28. Ginsburgh, I. (Am. Oil Co.), The Static Charge Reducer, J. Colloid Interface Science 32 (3), 424-32, 1970, also U.S. Patent 3,383,560.

A device is described which can neutralize much of the static electricity charge in hydrocarbon streams by injecting charge of the opposite sign through grounded pointed electrodes inserted through the wall of plastic insulating pipe. Marketed by the A. O. Smith Company.

29. Godwin, J. B., Jr., (Kelly Air Force Base), Static Electricity in Air Force Refuelling Systems, Lightning and Static Electricity Conference, AFAL-TR-68-290, Part II, 442-452, Dec. 1968.

The hazards of static electricity in aircraft refuelling and defuelling are discussed along with the Air Force's preventive procedures. Recent developments such as improved refining methods, cleaner systems, non-ferrous piping, and new coating systems (such as epoxy-coated fuel tanks) increase the hazards because they increase both static generation and relaxation time. Static charge protection based on sound engineering data rather than present state-of-the-art assumptions and individual theories is urgently needed. No data are given.

30. Goodfellow, H. D., May, Z. and Graydon, W. F., (Univ. of Toronto), Fluid Electrification Resulting from Constricted Flow, Can. J. Chem. Eng. 45, 17-21, 1967.

The electrification of fluids of low conductivity resulting from constricted flow has been studied. Currents and voltages have been measured using insulated test sections. For discussion purposes, the electrification process has been subdivided into two regions; an electrostatic region (high static voltages and low currents) and a streaming region (low voltages and high streaming currents produced by flow constriction).

Symmetrical negative and positive streaming current curves were obtained from the insulated metal tubes located upstream and downstream from the constriction. The magnitude of the streaming current was dependent on the constriction flow area, the polar solute, the conductivity of the solution, and the flow rate. Low voltages were measured in the streaming region because of the high conductivity of the fluid. Currents have been related to the measured voltage and the conductivity of the solution.

31. Goodfellow, H. D., and Graydon, W. F., Dependence of Electrostatic Charging Currents on Fluid Properties, Canadian Journal of Chem. Eng. 46, 342-348, 1968.

The dependence of the electrical charging of hydrocarbons on the chemical nature of non-hydrocarbon additives has been investigated. An improved apparatus and technique allowed the authors to obtain data for new fluid systems over a wide range of solution conductivities and flow velocities. Currents and voltages have been measured from insulated stainless steel tubes, for different concentrations of polar species in hydrocarbon solutions, for Reynolds numbers of 1800 to 35,000.

Recent electrification theories explain the charging process on the basis of a diffusion-controlled process. The magnitudes of the charging currents can be predicted using the usual mass transfer analogies. Experimental results, obtained for different polar additives studied, agreed with the theory. The sign of the measured current is not predicted theoretically. Potentials of both signs are observed. The particular sign obtained seems to be determined by the chemical nature of the polar additive. Different additives of similar chemical structure all give one sign.

32. Goodfellow, H. D., and Graydon, W. F., Electrostatic Charging Current Characteristics for Different Fluid Systems, Chem. Eng. Sci., 23, 1267-1281, 1968.

Electrostatic charging currents have been measured for the flow of several fluids (hydrocarbon solutions containing known concentrations of polar species) through small diameter stainless steel tubes. For tube diameters of 0.14 to 0.21 cm, solution conductivities of  $10^{-16}$  to  $10^{-9}$  ohm<sup>-1</sup> cm<sup>-1</sup> and flow velocities of 200 to 1100 cm/sec, the charging current magnitudes for the fluid systems cover the range of  $10^{-13}$  to  $10^{-8}$  amperes. In general, the flow of non-polar solvents of low conductivity containing alcohols, acids, nitrobenzene, and ASA-3 produces positive tube currents. The flow of non-polar solvents of low conductivity containing ketones, esters, and amines produces negative tube currents. The charging currents show some dependence on the chemical nature of the polar additives. The currents obtained indicate that using the conductivity as the only independent variable for the charging phenomena is misleading.

For low conductivity fluids, in which the elec. double layer thickness is equal to or greater than the diffusion layer thickness by a factor of 1.3, the measured charging currents increase as the conductivity increases.

The experimental data of this region have been compared with current magnitudes predicted from Koszman and Gavis modified form of Klinkenberg's diffusion equation. In this study, the experimental data show considerable scatter (approximately two-thirds of the data are within a factor of three of the predicted magnitude); but, the least squares line through all these data (approximately 3150 points) shows remarkably good agreement with the low-conductivity equation of Koszman and Gavis. A regression analysis gave a velocity and conductivity dependence which was slightly higher and lower respectively than the theoretically predicted dependencies. Charging current magnitudes exhibited no definite dependence on current polarity. For all fluid systems, measured/predicted current ratios show a relatively small variation with velocity changes and a greater variation with conductivity changes.

33. Harris, D. N., Karel, G., (Gen. Dynamics Convair Div.) and Ludwig, A. L., (Shell Oil Co.), Electrostatic Discharges in Aircraft Fuel Systems - Phase II, Coordinating Research Council, Report No. 355, July 1961. API Proc., 41, (VI), 26-35 1961.

In a Coordinating Research Council program, data on static generation were obtained during the fuelling of both a full-scale model of a typical jet aircraft wing tank and a 150 gal. single wing-tank compartment. High field strengths were attained over a wide range of operating conditions, resulting in discharges even at low flow rates. Filters were confirmed as prolific sources of charge generation; with one of the two types used, discharges occurred at fuel conductivities 5 picomhos/m. Spark energies were estimated at 0.5-1.5 millijoules. The conductivity effective in relaxing a charged fuel depended on the amount of charge carried, the nature of the charge separation surface, and the conductivity measured on an uncharged fuel. With effective conductivities measured under dynamic conditions, a simple linear relationship (as predicted by theory) was obtained between field strength in the vapor space and charge accumulation in the tank. Data obtained with the two models agreed closely enough to warrant further use of the small-scale rig. See Bossi and Scheuermann (2) for CRC Phase I.

34. Herzog, R. E., Hartung, H. A., (Atlantic Refining Co.) and Ballard, E. C., (Du Pont), Evaluating Electrostatic Hazard During The Loading of Tank Trucks, API Proc., 41 (VI), 36, 1961.

In addition to forming one side of a spark gap, grounded metallic objects above the oil surface can also create localized areas of high capacitance which tend to concentrate electrical energy for forming incendiary sparks. To assure safety, the combination of surface voltage and maximum capacitance should not develop energy levels above 0.2 millijoules. A floating probe is the most practical method for measuring surface voltage under actual tank truck loading conditions as long as a voltage measuring circuit is provided to draw a relatively small amount of electrical charge from the system. The maximum capacitance available for concentrating energy at possible spark gap locations can be estimated by measuring with a capacitance bridge the capacitance of various parts of the system.

35. Hignett, E. T., and Gibbings, J. C., (Univ. Liverpool, Engl.), The Entry Correction in the Electrostatic Charging of Fluids Flowing Through Pipes, J. Electroanal. Chem. 9 (4), 260-6, 1965.

The flow of liquids in circular pipes and the effect of the length of such a pipe upon the elec. charge generated was investigated. An electrokinetic entry effect was shown in that the so-called streaming-current developing in a pipe may be expressed as that which would develop in a pipe of infinite length. The correction length was 54.4 pipe diams., but this figure was not expected to be a universal const. nor to apply to laminar flow. The expt. was designed to demonstrate the existence of entry effects in electrokinetic phenomena and their possible expression by the general formula. The app. used in the expts. was constructed for use in general investigations of electrostatic effects of flowing hydrocarbon liquids. It consisted of a stainless steel reservoir from which the liquid was allowed to flow through a capillary tube, before discharging into an insulated stainless steel receiver. The reservoir and the stainless steel capillary tube were both elec. grounded. The streaming-current was detd. by measuring the current flowing from the receiver to ground.

36. E. T. Hignett and J. C. Gibbings (Univ. Liverpool, Engl.), Electrostatic Streaming Current Developed in the Turbulent Flow Through a Pipe, J. Electroanal. Chem. Interfacial Electrochem., 16 (2), 239-49, 1968, CA 68 14448.

The results of measurement of electrostatic streaming currents in turbulent flow through round pipes have been correlated in terms of dimensionless groups. One such group was proportional to the same power of the Reynolds no. as is the skin friction coeff. This same index was obtained for tubes of increased roughness and for results computed taking no account of the entry length correction. The velocity gradient at the wall is significant in an explanation of the large increase in streaming current through the transition region. The streaming current in the smooth tubes was independent of tube diam. suggesting that the charging phenomena was closely linked with the flow region very close to the wall and that these tubes were behaving as smooth tubes. A surface roughness that is too small to affect the skin friction coeff. is found to affect markedly the streaming current. 7 references.

37. John, A. W., (Socony Mobil Oil Co. Inc.), Some Effects of Refuelling Variables on Jet Fuel Electrification, API Proc. 45 (III), 247-278, 1965.

The effects of fuel flow rate and electrical conductivity, charge relaxation holdup, tank trailer inlet configuration, and filter element on the field strength, surface potential, charge density, streaming current, sparking tendency, and relaxation time were measured in a full-scale jet-fuel refueler test facility at Socony Mobil's Paulsboro laboratory. Correlations developed between the various parameters show that field strength, surface potential, and streaming current increase directly with flow rate and inversely with volume holdup, in exponential relationships.

The most important fuel variable is electrical conductivity and the most important equipment factor is the filter-separator fuel electrification. Inlet configuration affects the field strength, but not the current. A baffle over the bottom loading valve effectively reduces the field intensity and fuel volume holdup in a properly baffled chamber reduces fuel electrification. The only positively identified sparks in the refueller were induced by a grounded probe. The effect of changing filter elements on charge density was drastic; three different filter sets gave charge densities of 600, 1700, and 100 micro C/M<sup>3</sup>.

38. Keller, H. N., and Hoelscher, H. E., (Johns Hopkins U.), Development of Static Charges in a Nonconducting System, Ind. Eng. Chem., 49, 1433-38, 1957.

The generation of static charges was investigated by flowing n-heptane through polyvinyl chloride tubing into an insulated tank. Charging was dependent on plasticizer extracted from the tubing by the heptane. Charging with unplasticized Kel-F or polyethylene tubing was lower than with plasticized polyvinyl chloride tubing. However, if the unplasticized tubing were treated with plasticizer, or the plasticizer added to the heptane, the charging tendency increased considerably. Comparative data were not given.

39. Klinkenberg, A., Laboratory and Plant-Scale Experiments on the Generation and Prevention of Static Electricity, Presented to the Division of Refining, 37th Annual Meeting of the American Petroleum Inst., Chicago, November 12, 1957.

An analysis of case histories of explosions ascribed to static electricity indicated where research should start on this subject. This research provided information on the generation of electricity by hydrocarbon products in turbulent flow and on the extent to which the static electrification is increased by the presence of free water.

Full-scale experiments were undertaken in storage tanks and under conditions simulating fuelling of aircraft.

Strong electric fields, ranging up to 600 kv per m, have been measured in tanks. If the electric conductivity of the product was raised, the field strength was always ultimately reduced and became very small. A conductivity of  $10^{-11}$  ohm<sup>-1</sup> cm<sup>-1</sup> = 1,000 picomhos (micro-micromhos) per meter was found to safeguard even the case of strongest charging and still allow a comfortable safety margin. Research has been directed toward the development of suitable additives which would raise the conductivity of petroleum products to a safe level. It has been found that certain combinations of additives are far more active than the individual components, which makes it possible to keep the concentration of additive very low. A favorable combination has been found by Shell and is at present being employed to safeguard shipments of certain products. Only very small concentrations of this additive combination are required, viz., 0.7 lb of a concentrated solution per 1,000 bbl of product.

By antistatic doping of a product not only is the explosion hazard eliminated, but pumping rates can be increased above what was hitherto considered a safe maximum.

40. Klinkenberg, A., and van der Minne, J. L., Electrostatics in the Petroleum Industry, Elsevier Publishing Company, Amsterdam, 1958, 191 pp.

This book is a Royal Dutch/Shell Research and Development report relating to the subject of prevention of explosion hazards. The chapter headings in Part I include research and development on static electricity, explosions and fires, safeguarding operations. Reasons for the study, research and results are given. Part II, discussing theory and experiments, covers basic concepts, generation of electricity, electric conductivity and the electric field, ignition by electric charge, measuring methods, large scale tests in tanks and experiments with fuelling equipment. Plant-scale trials were made at two of the Group's refineries, Pernis in the Netherlands and Wilhelmshagen in Germany. The experiments are described and the principal findings presented.

41. Klinkenberg, A., Theoretical Aspects and Practical Implications of Static Electricity in the Petroleum Industry, Advances in Petroleum Chemistry and Refining (John J. McKetta, Jr., editor), Interscience, 8, 87-166, 1964.

Chapter 2 on static electricity includes basic mechanisms leading to ignition by static charge which cover contact by dissimilar materials, relative motion, insulation and collection of charges. The ensuing danger is the production of a high electrical potential, the static discharge and the ignition. The current and newer theories of the electrification of flowing media are presented. A discussion is given of the accumulation and relaxation of electrical charge and measuring techniques used in static electricity studies. A summary is given of experimental work in full-scale equipment. Antistatic additives are discussed and safety measures summarized. 95 references.

42. Klinkenberg, A., Electrical Conductivity of Low Dielectric Constant Liquids by D. C. Measurement, J. Inst. Petrol., 53, No. 417, 57-61, 1967.

In measuring electrical conductivity by the direct current method in solutions of very low ionic content, a kind of polarization is met, which is not normally observed in electrolytic cells, namely, polarization by depletion of ions. By measuring before a certain time has elapsed or by extrapolation to zero time, it can be ensured that this effect does not affect the results.

43. Klinkenberg, A., Static Electricity in Liquids, London Conference on Static Electrification, Inst. of Physics and Physical Society, 63-68, 1967.

In order to introduce some of the more recent developments in the knowledge of static electricity a survey is given in this paper of information on the properties and behaviour of the carriers of charge in a dielectric liquid, excluding the so-called high-field effects.



It is further indicated how the increased understanding of the behaviour of charge carriers has also been helping in the development of the differential equations, the equations of transport, and in the study of their solutions, the microscopic equations for charging and discharging.

44. Koszman, I., Development of Charge in Low Conductivity Liquids Flowing Past Solid Surfaces, D. Eng. Thesis, Johns Hopkins Univ., 1961, 155p.; Dissertation Abstr., 22 (8), 2732, Feb. 1962, Order No. 61-5689, Univ. Microfilms, Ann Arbor, Mich.

The development of electrical charge was determined in low conductivity liquids flowing past solid surfaces. A new theory of the phenomenon was presented and was applied to the rate of charge generation in turbulent flow in tubes. Two solutions of the equations were obtained with (1) low conductivity and high Reynolds number, and (2) high conductivity and low Reynolds number in the turbulent region. An experimental investigation was described of the dependence of the charging rate on the electrical conductivity of the liquid, the flow velocity, tube diameter, tube length, and the chemical and physical nature of the tube. The correlation developed was able to predict much of the previously published data, at least within the precision reported.

45. Koszman, I., & Gavis, J., (Johns Hopkins Univ.), Development of Charge in Low-Conductivity Liquids Flowing Past Surfaces . . . Engineering Predictions From The Theory Developed For Tube Flow, Chem. Eng. Sci. 17, 1013-22, 1962.

The theory is extended, by use of known correlations of turbulent mass transfer, in a form which may be experimentally tested. The charging current is described as a universal function of a dimensionless group  $G$  (four times the square of the tube radius divided by the product of the kinematic viscosity of the hydrocarbon, its relaxation time, and the seven-fourths power of the Reynolds number), which is related to the ratio of the laminar subzone thickness to the diffuse double-layer thickness in the liquid. The current can be predicted only for small enough values of  $G$ ; the prediction range must be determined by experiment. 22 references.

46. Koszman, I., & Gavis, J., (Johns Hopkins Univ.), Development of Charge in Low-Conductivity Liquids Flowing Past Surfaces . . . Experimental Verification and Application of the Theory Developed for Tube Flow, Chem. Eng. Sci. 17, 1023-40, 1962.

The theory was verified by measuring the steady-state currents developed in purified n-heptane (containing various additions of Shell Antistatic Additive #1) flowing turbulently at various rates through 0.0165-0.117 cm radius, 4.12-40.0 cm long tubes of various metals (stainless steel, gold, silver, palladium, platinum) or Pyrex glass. The data fell within the experimental scatter of the theoretical curve for smooth tubes over at least five orders of magnitude of the dimensionless group  $G$ , but the plot diverged from the theoretical curve where the ratio of laminar subzone thickness to

the double-layer thickness was  $\sim 2:1$ . The current was independent of tube material and was larger in rough than in smooth tubes, but no quantitative correlation with the friction factor could be established. Graphs, table, diagram, and 14 references.

47. Lauer, J. L., and Antal, P. G., (Sun Oil Co.), Electrostatic Charge Generation During Non-Uniform Flow of Hydrocarbons Through Porous Insulators, J. Colloid Interface Sci., 32 (3), 407-23, 1970.

The generation of charges in liquid hydrocarbons passing through a porous disc (of an electrical insulating material such as Teflon) located in the center of a non-metallic pipe was investigated by monitoring the current between two insulated metal electrodes, one upstream and one downstream. The early current was found to depend on the time elapsed since start of the flow and on the time of previous stationary contact between liquid and disc as well as on the parameters of liquid relaxation time, flow velocity, pore diameter, and porosity, in the general manner established by other investigators (Gavis, J. and Wagner, J. P., 23). While the transient current observed on starting and stopping the flow was similar to a polarization current, the time scale was much too long for it to be associated with the time constant of the circuit or the ordinary mechanism of dielectric polarization. Furthermore, the sign of the current depended on the nature of the solid and liquid and could sometimes be reversed by continued flow. It is possible to account for the experimental results on the basis of a model postulating convective diffusion of space charges out of the porous disc. The model is also consistent with the sign changes and magnitude variations of the currents observed when a hydrocarbon reactive at the porous surface was introduced ahead of the disc into a flowing inert hydrocarbon. Some deductions on the polarity and activity of the surface can then be made.

Particularly large transients were found to follow rapid changes of fluid composition. The results have implications on the percolation of liquid insulators (hydrocarbons) through beds of clay and similar materials.

48. Leonard, J. T., and Carhart, H. W., Electrical Discharges from a Fuel Surface, London Conference on Static Electrification, Institute of Physics and Physical Society, 100-111, 1967.

The nature of the electrical discharges taking place between a charged hydrocarbon-fuel surface and earthed probes of various configurations has been studied in a laboratory-scale apparatus. Fuel was circulated through a pump, bonded fiberglass filter and tank arrangement to produce electrical breakdown in the vapour space of the tank at gaps as large as 15 cm. Measurements were made of the total charge transferred and the duration of individual discharges as a function of gap width and earthed-probe geometry. True spark discharges occurred only at small gaps (up to 2.5 cm) with both pointed and small spherical electrodes. At larger gaps these electrodes gave corona discharges. However, with large spherical electrodes and larger gaps, a phenomenon was observed which has not been described in fuel studies. Discharge now occurred by means

of pre-breakdown streamers which never made the transition to filamentary sparks. The duration of individual discharges under these conditions was as much as seven times longer than for filamentary sparks for the same total charge. Hence the transfer of energy per unit time was much less. Photographic records showed that even at a 15 cm gap the streamers were highly luminous for only about 2 cm below the electrode before breaking up into a highly branched structure which faded out well above the surface of the fuel. The frequency of pre-breakdown streamers was found to vary with the charging tendency of the fuel, which, in turn, was related to the nature of the filter, the pumping rate and the conductivity of the fuel. As many as 100 streamers occurred per minute under optimum conditions. This mechanism of dissipation of field strength in a fuel system by repeated prebreakdown streamer discharges prevents the build-up of sufficient potential to allow filamentary sparks to occur. Because of the smaller concentration of energy in both space and time released by the pre-breakdown streamers, they are considerably less incendiary than spark discharges.

49. Leonard, J. T., and Carhart, H. W., (Naval Research Lab), Effect of a Static Dissipator Additive on the Charging Tendency of Jet Fuels, NRL Report 6952, Nov. 1969.

The effect of conductivity enhancing additives on the charging tendency of hydrocarbon fuels was examined in a laboratory-scale apparatus at various flow velocities. In these experiments, the term charging tendency refers to the current generated by a given quantity of fuel when passing through a fiberglass filter or an insulated section of piping rather than to the ability of a fuel to produce dangerously high potentials when loaded into a tank. It was found that the charging tendency increases with increasing conductivity, passes through a maximum and then decreases. At higher flow velocities, the charging tendency increases and the position of the maximum in the charging tendency vs conductivity curve shifts to a higher conductivity range. Thus, it can be shown that even high conductivity fuels ( $K \approx 100$  picomhos/m) can generate considerable electrostatic charge when passing through a fiberglass filter if the flow velocity is sufficiently high. However, as long as the ability of high conductivity fuels to generate charge is recognized and sufficient time is permitted for the charge to relax before the fuel enters a receiving tank, no increase in electrostatic hazard during fuel handling operations should occur.

50. Leonard, J. T., and Carhart, H. W., (Naval Res. Lab.), The Effect of Conductivity on Charge Generation in Hydrocarbon Fuels Flowing Over Fiberglass Filters, J. Colloid Interface Sci. 32 (3), 383-94, 1970.

Hydrocarbon-fuel electrostatic-charge generation, when flowing through a fiberglass filter element, was studied as a function of fuel cond. A modified version of the Shell fuel-charging tendency app. was used and the elec. cond. was detd. by the Shell Charged Ball method (A. Klinkenberg, et al., 1958). The static dissipator additives, used to adjust the cond.,

contained equal parts of: Cr salts of mono- and dialkylsalicylic acids, Ca aerosol didecyl sulfosuccinate, and a 50% conc. (in hydrocarbon solvent) of lauryl methacrylate-methylvinylpyridine copolymer. As the liq. cond. increased, the charging tendency (detd. by the filter current) increased, passed through a max., and then decreased. At higher flow velocities, the max. in the filter-current vs. cond. plot shifted to higher conds. The fuel-charge sign depended upon the surface of the filter material. With PhOH-HCHO resin-coated glass fiber, nylon, Dacron, and Kel-F filters, the streaming current was usually pos. With ordinary glass wool or fiber-glass filters without resin coating, the current was neg. By division of the fuel-flow from a storage tank into 2 streams each contg. different filter materials, 1 causing pos. fuel charge and the other neg. fuel charge, and by careful flow-control to each filter, fuel was delivered to the receiving tank with virtually no net charge. Hence, the fuel-charge level, in a practical system, can be reduced by using 2 types of filter elements in a filter/separator unit, each producing opposite-sign fuel charges. Also, the filter element can be made using alternate layers of filter materials which produce opposite-sign fuel charges.

51. Leonard, J. T. and Carhart, H. W., (Naval Research Lab.), Static Electricity Measurements During Refueler Loading, NRL Report 7203, Jan. 1971.

Measurements were made of the potentials developed on a fuel surface when loading refuelers at 300 and 500 gpm through 2-1/2-, 3-, and 4-in. hoses. The objectives in this study were to examine the effect of hose diameter and length on the level of charge on fuel entering a refueler and to provide an assessment of the electrostatic hazard that exists at a fill stand employing both a 30-second relaxation chamber and a bottom-loading capability. JP-5 fuel was used having a range of conductivities of  $1.8$  to  $4.6 \times 10^{-14}$  mhos/cm at  $78^\circ\text{F}$ . The results showed that at 500 gpm the maximum surface potential with the 2-1/2-in. hose was 32 kV whereas the values for the 3- and 4-in. hoses were in the range of 2 to 12kV. The 2-1/2-in. hose was the only one tested at 300 gpm, but since the maximum surface voltages obtained were 1.3 kV or less, it was concluded that the values for the other hoses would be below the limit of detection with the equipment available.

52. Luus, R., May, Z., & Graydon, W. F., (Univ. Toronto), The Electrification of Fluids in Turbulent Flow, Can. J. Chem. Eng., 41 (4), 165-69, 1963.

Static charges developed by flowing hydrocarbons (benzene, p- and o-xylene, kerosene) containing polar solutes ( $\text{C}_1$ - $\text{C}_{10}$  alcohols, phenol, or ketones) do not depend on the solvent, provided its pure state-conductivity is low. The magnitude and sign of charge is markedly affected by the chemical nature of the polar additive and of the conduit (glass, stainless steel, brass, copper, or teflon). Local charge production was highest near irregularities such as constrictions of the tube, sometimes resulting in reversal of the electric sign, in large voltages of opposite signs on a single tube, and in the production of sparks. The rate determining step could be diffusion of charged species from the interface across the boundary layer into the bulk of the fluid, once charge separation has occurred. Present theories oversimplify the process of charge formation. cf. (30).

53. Martel, C. R. (Air Force Aero Propulsion Lab Wright-Patterson AFB Ohio), An Evaluation of the Static Charge Reducer for Reducing Electrostatic Hazards in the Handling of Hydrocarbon Fuels, Report No. AFAPL-TR-70-22, July 1970.

The report describes the results of an experimental evaluation of the Static Charge Reducer. The Static Charge Reducer is a device which automatically neutralizes an electrically charged fuel as the fuel flows through it. The tests conducted confirmed the claims that the Static Charge Reducer would reduce the charge density of a flowing hydrocarbon fuel to below 30 microcoulombs per cubic meter. The tests also indicate the two corrosion inhibitor fuel additives significantly affect the electrical conductivity of fuel containing the ASA-3 antistatic additive.

54. Masuda, S., and Schon, G., Space Charge Distribution in Liquids After Passage Through a Filter, London Conference on Static Electrification, Inst. of Physics and Physical Society, 112-121, May 1967.

Measurement of space charge distribution downstream of a filter permits calculation of effective relaxation length and effective conductivity. With ASA 3 additive in n-heptane, the effective conductivity was larger than the rest conductivity in the lower rest conductivity range below about  $10^{-13}$  mho/cm, but smaller in the higher range.

55. Munday, J. C. Esso Research Charging Tendency Test, Esso Research and Engineering Co. Brochure, March 1959.

The Esso Research Charging Tendency Test measures the tendency of a liquid to produce static electricity when the liquid is moved over a charge-separating surface.

In the Esso Research test, the liquid is recirculated through a glass wool filter and a reservoir. Charge separation occurs at the surface of the glass wool, charges of one polarity being adsorbed on the glass wool. Charges of the opposite polarity are carried downstream into the reservoir and are measured with a micro-microammeter. This part of the test is essentially a "streaming current" test, but the currents are many times those obtained in classical test using capillaries for charge separation. The current, expressed in amperes, is recorded as the "ER-Charging Tendency."

During the recirculation of the liquid through the glass wool filter, electrostatic potentials may become so great that discharges occur within the liquid. These internal discharges take place in the filter or downstream of the filter and at times are clearly audible. The electricity discharged in this manner, which of course is not measured by the streaming current micro-microammeter, is detected in the ER test by radio equipment of special design. The frequency of the discharges is recorded as "Discharges in 10 Minutes." The time required for making a test is less than one hour.

56. Munday, J. C., and Wilson, J. A. (Esso Research), Neutralization of Static Charges, U.S. Patents 3,141,113 and 3,160,785.

Basic patents on the neutralization of static electricity in flowing liquids by means of grounded pointed electrodes inserted through the wall of insulating pipe. cf. (3)(28).

57. Proposed Method of Test for Electrical Conductivity of Aviation Fuels, ASTM Book of Standards, Vol. 17, 1170, November 1971.

This method applies to the laboratory determination of the "rest" electrical conductivity of aviation fuels and other similarly low-conductivity liquids in the range from 0.01 to 1000 pS/m. With suitable battery operated components, the method can be used in the field.

A sample of fuel is placed in the conductivity cell which is then connected in series with a d-c voltage source and a sensitive d-c ammeter. The conductivity is calculated by Ohm's law from the cell characteristics, the voltage across the cell, and the almost instantaneous peak current reading.

58. Rogers, D. T., McDermott, J. P., and Munday, J. C., Theoretical and Experimental Observations of Static Electricity in Petroleum Products, (Esso Research), API Proc., 37 (III), 44-64, 1957.

The more potent static-producing hydrocarbon fuels generally contain a larger amount of colloidal contaminants which are largely fuel degradation and oxidation products or residues from treating operations which can be removed by ultrafiltration and almost completely by adsorption on silica gel. The electrical potency of fuels is markedly increased by elevated temperatures, ultraviolet or  $\gamma$ -radiation, or contaminants, such as asphalt. The rate of charge production increases with flow rate and is accelerated by water, air, and dispersed solids. An increase in temperature from 50 to 105°F. reduced static production with some fuels. The discharge of static electricity as visible sparks from the surface of hydrocarbons occurs most readily at points of high curvature and at a potential which decreases with increasing conductivity. With some commercial fuels, discharges occur within the liquid phase at potentials close to those for air.

59. Rogers, D. T., and Schleckser, C. E., (Esso Research), Engineering and Theoretical Studies of Static Electricity in Fuels, Fifth World Petroleum Congress, Proc., 1959 G, 103-21, 1960.

This paper summarizes recent work which has been carried out on the problem of static electricity in hydrocarbon fuels. It is shown that static electricity is produced in liquid hydrocarbons when there is relative motion of the hydrocarbon and a second phase (solid, liquid or gas). The electrostatic charge thus produced may be carried in the bulk liquid or in hydrocarbon droplets. The conditions under which the electrostatic charge can reach hazardous levels are described.

The electrostatic charge in bulk liquid hydrocarbons can be reduced by at least four methods: (1) relaxation principle, (2) neutralization with electrodes, (3) antistatic additives, and (4) ionizing radiation. Methods (1) and (2) provide protection only at one point in a tank loading system, and method (1) requires relatively long holdup times for fuels having a combination of high charging tendency and low conductivity. Antistatic additives, which function primarily by increasing electrical conductivity, would provide rapid charge recombination or relaxation from time of manufacture to ultimate consumption. Several antistatic additives have been found which appear to be satisfactory as regards electrical properties, but considerable difficulty is being encountered in eliminating undesirable "side-effects", primarily the tendency to emulsify fuel and water. There appear to be several factors which will limit the use of ionizing radiation to special applications.

The possible hazard due to electrostatic charge carried by droplets can be reduced by minimizing misting (through low initial pumping rates and proper inlet configurations) or by inerting the vapor space in tanks.

Methods are also presented for measuring the charging tendency of liquid fuels in systems where the liquid hydrocarbon is the continuous phase and for calculating electrostatic potentials at the liquid surface in tanks being filled with hydrocarbons.

60. Rogers, D. T., and Munday, J. C., Static Electricity Studies in an Aircraft Fuel Tank, Esso Research & Engineering Co., Report No. RL-4M-60, Mar. 1960.

This report describes the measurement of the static electricity produced during the fueling of a tank from a Canadian CF-100 jet fighter with JP-4 and ASTM Type A-1 fuels. The tank was a No. 5 fuselage tank having a capacity of 300 U.S. gallons. Fueling rates of 140 gallons per minute through a 3" x 10' fueling hose were generally employed, using a 600 gpm filter having a 250-gallon liquid holdup. The large filter size resulted in a low flow rate through the filter and a long holdup time after passing through the filter elements. As a result the amount of static electricity reaching the tank was lower than would be expected with a smaller filter. Fuel temperatures varied from 66°F. to 102°F. On the basis of laboratory tests, the fuels appeared to be average with respect to static producing tendency and to electrical conductivity. Under these test conditions, the following observations were made:

In all tests, the field strengths in the vapor space of the tank were very low, and no spark discharges were recorded with radio discharge detection equipment.

Field strengths were highest during the first 20-40 seconds of filling when extensive splashing, spraying, and misting occurred. Presumably, this electrical field was produced by the entrainment of charged droplets. In some tests increasing the fuel conductivity by antistatic additives

increased the field strength during the period when misting was prevalent. This is in agreement with earlier work in which entrainment charging was not observed with low-conductivity liquids but became appreciable when the conductivity was  $3 \times 10^{-13}$  mho/cm. or higher.

In all cases, after the tank inlet nozzle was covered and misting subsided, antistatic additives reduced the field strength to a very low level.

Tank current was increased markedly by antistatic additives. In all cases, however, the higher conductivities of the additive blends would permit dissipation of the increased charge in less than 0.5 second.

Increasing the length of the fuel hose reduced significantly the amount of current entering the tank.

Temperature had a marked and variable effect on static production.

It is estimated that sufficient static electricity was produced in some tests to form incendiary spark discharges if insulated conductive objects had been present in the vapor space or if sharply pointed metal objects (at ground potential) had been located near the surface of the liquid.

Observed field strengths and surface potentials were considerably higher than values calculated for a simulated CF-100 tank on a theoretical basis.

61. Rutgers, A. J., DeSmet, M., and Rigole, W. (Univ. Ghent, Belgium), Streaming Currents with Nonaqueous Solutions, Journal of Colloid Science, 14, 330-337, 1959.

Streaming currents have been measured in benzene solutions of tetraisoamyl ammonium pierate between  $10^{-7}$  and  $10^{-3}$  mole/l. in long capillaries of various widths and wide capillaries of various lengths. A considerable influence of width and length was found. High  $\zeta$ -values (-280 mv.) were obtained at low concentrations. The corresponding theory is developed; over the length of a glass capillary an electrostatic potential  $V(x)$  develops, which shows resemblance to a catenary; measurements confirmed the theoretical expectation. The theory for the glass capillary is compared with the theory for a metal capillary developed by Klinkenberg and van der Minne.

62. Schaschl, Edward and Bernard, George G. (Pure Oil Co.), Glass Wool Treated with Polysiloxanes, U.S. 3,155,533 (Cl. 117-54), Nov. 3, 1964, Appl. Sept. 10, 1959; 6pp, C.A. 62 1429 (1965).

Glass wool is treated with polysiloxanes for generating and collecting static electricity thereby permitting evaluation of the static electricity dissipation characteristics of liquids. The static electricity generating characteristics of glass wool are enhanced by applying a coating of Me-substituted polysiloxanes, having the general formula



$\text{Me}_2\text{SiO} \{ \text{SiMe}_2\text{O} \}_n \text{SiMe}_3$ , where n is a no. from 10 to 1002, on the glass wool to make it oil-wettable, then circulating through the glass wool a fluid of low viscosity liquid  $\text{C}_{3-10}$  paraffin hydrocarbon and 0.5 to 2.0% by wt.  $\text{H}_2\text{O}$  until the capacity of glass wool to generate static electricity is reduced and thereafter washing glass wool with a solvent miscible with both oil and  $\text{H}_2\text{O}$ . Thus, glass wool was treated with General Electric silicone SC-87, (I), (Me-substituted polysiloxane contg. 16-27% unhydrolyzed chlorine) to make it oil wettable. A 5% soln. of I in hexane was prepd., the glass wool dipped in this soln., and then baked for 3 hrs. at  $200^\circ$ . The silicone-treated specimen was packed in the static electricity accumulation chamber. With this treatment alone, the charging rate again decreased compared with untreated glass wool, demonstrating the need for addnl. treatment. The oil-wettable specimen was further treated by flowing isooctane (1% by wt.  $\text{H}_2\text{O}$ ) through it until the charging rate dropped to zero, after which the treatment was completed by washing with  $\text{Me}_2\text{CO}$ . Then, a circulating liquid of 10% by wt.  $\text{Me}_2\text{CO}$  and 0.5%  $\text{H}_2\text{O}$  and the remainder isooctane was used. With this liquid the charging rate remained const. for an unlimited time with the rate greatly increased, only 0.31 sec. was required to completely charge the electroscope at 40 psig. pumping pressure. With untreated glass wool at a pumping pressure of 40 psig. an initial electroscope charge rate of 5.7 sec. which increased to 9.4 sec. after 1 hr. was obtained

63. Scholz, D. (Anwendungstech. Abt., Badische Anilin- and Soda-Fabrik A. G., Ludwigshafen/Rh., Ger.), Elimination of the Danger of Ignition on Electrostatically Charged GRP Surfaces, *Kunststoffe* 59(12), 838-42, 1969 (Ger).

The elimination of ignition caused by electrostatic charges on glass-reinforced plastic tanks is reviewed with 2 refs. Discussed are the redn. of the surface resistance under  $10^9$  ohms or enclosing conducting grids with nonconductors and grounding.

64. Shafer, M. R., Baker, D. W. & Benson, K. R., Electric Currents and Potentials Resulting from the Flow of Charged Liquid Hydrocarbons Through Short Pipes, *J. Res. Natl. Bur. Std. C* 69 #4:307-17, 1965.

In a study of the desirable electrical characteristics of hoses used to interconnect the various fuel handling components of aircraft and other internal combustion engines, measurements were made of the electric currents and potentials produced in pipes of intermediate and very high resistivities by the flow at 5-30 gal/min of electrically charged petroleum naphtha, with and without asphaltenes or a commercial antistatic compound as contaminants. Depending on electrical resistance in the pipes, pipe currents to the ground of  $10^{-8}$  to  $6 \times 10^{-6}$  amp produced potentials from essentially zero to >30,000 volts, sufficiently severe to cause breakdown and arcs in some of the pipes studied. Hazardous pipe potentials, resulting from static electricity, can probably be eliminated in practical applications if the electrical resistance from any portion of the interior surface of the pipe to the ground is not  $>10^7$  ohms.

65. Tinson, R., (Shell Res. Ltd.), The Electrostatic Hazard During Loading of Petroleum Products into Glass-Reinforced Plastic Tanks, J. Inst. Petrol. 53 #525:303-11 (1967).

Two glass-reinforced plastic tanks (one standing free on the ground and the other mounted on a road vehicle) were filled with aviation kerosine and gas oil at varying rates, and the fuel was filtered through either a basket strainer or a microfilter placed immediately upstream of the loading arm. Both tanks had metallic fittings insulated from the ground by the tank material. At rates up to 480 Imp gal/min. the charging current in the fuel was as high as 0.8  $\mu$ amp with the strainer and 22  $\mu$ amp with the microfilter. The gas oil became more highly charged than the kerosine during microfiltration. During fueling, potentials up to 11 kv built up on the insulated metal tank connections: when filtered through the strainer, potentials >1 kv built up only on connections well insulated from the ground, but when microfiltered, the potentials of connections were prevented from rising above 1 kv only by grounding them individually. If, in tanks constructed of highly resistive materials, provision is made for proper electrical bonding, the electrostatic hazards during the loading of petroleum products should not differ from those in similar tanks made from conducting materials.

66. Vellenga, S. J., and Klinkenberg, A., (Bataafsche Intern. Petrol. Maatschappij, The Hague, Neth.) Rate of Discharge of Electrically Charged Hydrocarbon Fluids, Chem. Eng. Sci., 20 (11), 923-30, 1965.

A mathematical analysis shows that the observed rate of loss by petroleum products of electrical charges acquired during handling can be correctly described by Ohm's law, which is more generally valid than either the exponential (constant conductivity) or hyperbolic law, and that conductivity depends on the charging conditions as well as the nature of the product. Moreover, the "ohmic theory", together with an association-dissociation mechanism, can account for the presence of a point of inflection in some observed charge decay curves.

67. Winter, E. F., (Shell Res. Ltd.), The Electrostatic Problem in Aircraft Fuelling, J. of the Royal Aeronaut Soc., 66, 429-446, 1962.

The results of investigations into the explosion hazard associated with fuelling aircraft lead to the following conclusions, which apply also basically to other stages of handling, such as the replenishment of fuelling vehicles and storage tanks.

In aircraft tanks being fuelled at high flow rates there is a possibility of electrostatic discharges occurring, of sufficient energy to ignite an inflammable hydrocarbon/air mixture.

Where there is little opportunity for the relaxation of charges between the fuelling equipment and the aircraft tank, such discharges may occur down to flow rates per tank of considerably less than 200 imp.gal./min.

Such discharges may result in an explosion if the fuel/air mixture in the tank is within the inflammable range. When kerosine fuel is used, such a mixture could only exist if the tank contents were above 38°C (100°F) or if a mist were generated. There is a much greater probability of inflammable conditions occurring in tanks containing wide-cut fuel (JP-4).

Attention to the design of the aircraft fuelling system, particularly with a view to reducing the rate of flow into individual tank compartments, can to some extent reduce the possibility of a hazard. So also can the provision of maximum relaxation space between the final microfilter and the tanks. Neither means, however, can eliminate the hazard; they can only reduce the chances of a mishap occurring.

Complete elimination of the hazard is possible by artificially raising the conductivity of all fuel supplied to some "safe" value. A safe value under the most critical practical conditions would be about 50 picomho/m. Fuel containing appreciably less than one p.p.m. of Anti-Static additive ASA-3 will fully meet this requirement.

68. Wright, L. & Ginsburgh, I., (Am. Oil Co.), Take a New Look at Static Electricity, Hydrocarbon Process. Petrol. Refiner 42 (10), 175-80, 1963.

Experiments at American Oil Co. showed: the ignition energy requirement for incendiary discharges between oil and a metal object is the same as for discharges between metal electrodes if the oil is negatively charged but is slightly higher if the oil is positively charged; the threshold oil surface potentials required to produce incendiary discharges from sample thieves and for other common geometries are of similar magnitude; potentials of the magnitude necessary for sparking actually exist in practical loading operations, so that various grounded internals in tanks must be suspect as static discharge promoters; small areas (1 ft. dia or less) of high surface potential can yield incendiary sparks to grounded objects; surface potentials inferred from field-strength meter readings should be viewed with caution, since the averaging process inherent in the use of the instrument may mask the true areas of danger; and the oil acts neither as a good conductor nor a good dielectric, but shares some properties of each.

69. Yamamoto, Kakuji (Metropol. Isotope Center Tokyo), The Effect of Radiation on Charged Glass Tubes, Oyo Butsuri 31, 357-9, 1962 (Japan).

Prevention of the electrostatic charge produced by liquid flowing in a glass tube was studied; 7.8-mm. diam. and 150-mm. long glass tubes made of 75 SiO<sub>2</sub>, 15.35 B<sub>2</sub>O<sub>3</sub>, 7.13 K<sub>2</sub>O, 2.5 Al<sub>2</sub>O<sub>3</sub>, and 0.03 wt. % Fe<sub>2</sub>O<sub>3</sub> were filled with 10 ml. of cyclohexane. The samples were irradiated with a 1-kc. <sup>60</sup>Co source at a rate of  $3.48 \times 10^2$  r./hr. to total doses of  $8.70 \times 10^2$ ,  $28.18 \times 10^2$ ,  $56.03 \times 10^2$ , and  $83.87 \times 10^2$  r. at 18°. Comparisons of electrostatic charge vs. vol., total dose, and irradiation induced charges showed that the charge decreased when the dose was sufficiently high.

70. Young, C. W., (HQ AFSC (SCOCM) Andrews AFB, Md.), Accumulation and Elimination of Static Electricity in Plastic and Metal Piping, Test conducted by CLA-VAL Corporation, Newport Beach, Calif., Jan. 20 - Feb. 11, 1969.

Static electricity measurements were conducted with fiberglass reinforced plastic and metal pipe and data were obtained with the static charge reducer. Tests were carried out at the Newport Beach facility of the CLA-VAL Company using 220 feet of 8-inch diameter fiberglass reinforced plastic pipe (Amercoat Corporation Bondstrand Series 2000 pipe) in a U-shaped run, 20 feet wide and 100 feet long, together with a Static Charge Reducer furnished by the A.O. Smith Corporation. Results were as follows:

Pearl white kerosene was charged to 235 micro C/M<sup>3</sup> by flowing it at 1200 gpm through a filter separator. Immediate passage through the SCR reduced the charge to 22; further passage through the 220 feet FRP pipe reduced the charge to 5.

In another test the kerosene, charged to 250 micro C/M<sup>3</sup> in the filter separator, was passed through the 220 feet of FRP pipe, which reduced the charge to 30. Further passage through the SCR reduced the charge to 16. In a comparable test with carbon steel pipe, the charge on the fuel was reduced from 252 to 2  $\mu\text{C}/\text{m}^3$ .

It was concluded that static charges were reduced when fuel is pumped through plastic pipe at linear velocities of 6-8 ft./sec. Low intensity sparks were produced at the surface of the plastic pipe when a grounding device was brought near the pipe surface (during pumping operations). This phenomena is not considered a problem since plastic pipe is to be used underground.

71. Zhukov, A. N.; Fridrikhsberg, D. A. (Shchiglovskii, K. B. (USSR)), Kinetics of the Electrification of Nonpolar Liquids, Vesin. Leningrad. Univ., Fiz., Khim. (2), 169-70, 1970.

The pos. current,  $I_{kp}$ , induced during the flow of petroleum ether contg. Nekal (Na dibutyl-naphthalenesulfonate) soln. through a nongrounded stainless-steel pipe after 0.5-1 min of flow reached a max. the highest of which was obsd. at a Nekal conc. of 2 mg/l., which corresponded to the optimum combination of charge d. and diffusivity. Neg. source current,  $I_{ki}$ , at Nekal concns.  $\leq 1$  mg/l. increased nearly linearly and at higher concns. passed through a max. after  $\sim 1$  min of flow. When the pipe was surrounded by a grounded metal shield, the corresponding values for  $I_{ki}$  dropped and those for  $I_{kp}$  increased because of the reduced potential of the pipe. Current in the pipe reached a max. after  $\sim 0.5-1$  min of flow which were highest at a Nekal concn. of 2 mg/l. and approached zero after 4 min of flow when the Nekal concn. was 6 mg/l.

## Appendix II

Table 16

### DIMENSIONS AND ELECTRICAL PROPERTIES OF FRP (BONDSTRAND 2000) PIPE

#### Pipe Dimensions

O.D. = 6.725 inches  
I.D. = 6.265 inches  
Wall Thickness = 0.23 inches

<u>Electrical Properties(a)</u>	<u>Test Data, Two Samples</u>	<u>Average</u>
Volume Resistivity, ohm-cm	$1.1 \times 10^{14}$ $8.8 \times 10^{14}$	$5.0 \times 10^{14}$
Surface Resistivity, ohms	$6.6 \times 10^{11}$ $8.1 \times 10^{11}$	$7.4 \times 10^{11}$
Dielectric Strength, Volts/mil	>230 >230	>230
Breakdown Voltage, KV (on 0.23 inch Thick Sample)	>53.4 >53.4	>53.4

(a) Data supplied by Ameron (Ref. 4)

Table 17  
INSPECTION DATA FOR TEST FUEL

	JP-8 Specifications MIL-T-83133	Test Fuel
Gravity, °API	39.0 Min. - 51.0 Max.	42.1
Distillation, °F		
Initial Boiling Point	Report	308
10% Evaporated	400 Max.	370
20%       "	Report	388
50%       "	450 Max.	418
90%       "	Report	458
Final Boiling Point	550 Max.	492
Residue, Vol. %	1.5 Max.	1.0
Loss, Vol. %	1.5 Max.	1.0
Flash Point, °F	105 Min.	122
Freezing Point, °F	-54 Max.	-58
Viscosity at -30°F, cSt	15 Max.	8.32
Aromatics, Vol. %	25.0 Max.	16.4
Olefins, Vol. %	5.0 Max.	2.8
Sulfur, Total, Wt. %	0.3 Max.	.07
Mercaptan Sulfur, Wt. %	0.001 Max.	.0008
Copper Strip Corrosion		
2 Hours at 212°F	No. 1b Max.	1
Existent Gum	7 Max.	0.4
Total Potential Residue - 16 Hr., mg/100 ml	14 Max.	0.8
Thermal Stability - 5 Hr. Test @ 6 lb/hr 300/400°F ΔP, In. Hg.	3.0 Max.	0.5
Preheater Tube Deposit Rating	<3	0
Aniline - Gravity Product	4800 Min.	5720
Luminometer Number	45 Min.	48.3
Water Separometer Index - Modified	70 Min.	97

Table 18

## MEASURED REST CONDUCTIVITIES FOR 0.2 CU FUEL

Test Date	Test Pipe		Initial Measurement		Second Measurement	
	Type	Length	CU	T, °F	CU	T, °F
2/14/72	FRP	Long	.32	52	.34	59.5
			.31	55	.43	69
2/16/72	"	"	.29	49	.39	66
			.32	54	--	--
			.28	46	.40	64
			.28	53	.39	70
2/17/72	Steel	Long	.30	49	.39	63
			.27	52	.32	66
			.27	52	.31	60
			.29	48	--	--
2/24/72	Steel	Short	.27	45	.42	62
			.27	47	--	--
			.25	49	.38	61
			.30	49	--	--
2/28/72	FRP	Short	.31	43	.35	58
			.28	51	.51	72
2/29/72	"	"	.28	51	.47	69

Table 19

## MEASURED REST CONDUCTIVITIES FOR 0.9 CU FUEL

Test Date	Test Pipe		Initial Measurement		Second Measurement	
	Type	Length	CU	T, °F	CU	T, °F
11/16/71	FRP	Long	.68	52	.89	61
			.83	57	--	--
			.83	58	1.16	67
			.99	59	--	--
			.89	65	--	--
			.92	63	--	--
11/17/71	Steel	Long	.92	60	--	--
			.99	63	--	--
			.86	63	--	--
			.89	64	--	--
			.89	65	--	--
11/18/71	Steel	Short	.99	63	--	--
			.89	62	--	--
			.96	66	--	--
			.96	66.5	--	--
11/19/71	FRP	Short	.99	59	--	--
			.94	61	--	--
			.94	64	--	--



Table 20

## MEASURED REST CONDUCTIVITIES FOR 3 CU FUEL

Test Date	Test Pipe		Initial Measurement		Second Measurement	
	Type	Length	CU	T, °F	CU	T, °F
12/20/71	Steel	Long	2.98	41	--	--
			2.98	42	3.5	53
			3.2	51	--	--
			3.3	47	--	--
			3.4	49	--	--
			3.4	50	--	--
12/21/71	FRP	Long	3.9	51	5.0	61
			3.6	50	--	--
			3.7	49	--	--
			3.8	48	--	--
			3.6	45	--	--
			3.6	49	--	--
12/27/71	FRP	Short	3.1	50	--	--
			3.3	51	--	--
			3.9	47	--	--
			3.4	47	--	--
			3.3	49	4.45	64
12/29/71	Steel	Short	3.1	50	--	--
			3.6	45	--	--
			3.7	45	4.9	58
			3.55	45	--	--
			3.55	48	--	--
			3.4	50		

Table 21

## MEASURED REST CONDUCTIVITIES FOR 5.5 CU FUEL

<u>Test Date</u>	<u>Test Pipe</u>		<u>Initial Measurement</u>		<u>Second Measurement</u>	
	<u>Type</u>	<u>Length</u>	<u>CU</u>	<u>T, °F</u>	<u>CU</u>	<u>T, °F</u>
1/17/72	Steel	Long	4.4	25	9.35	64
			4.7	33	--	--
			6.6	41	--	--
			5.8	42	8.3	58.5
			6.35	44	--	--
			5.8	42	8.3	59.5
			6.05	43	--	--
			5.8	42	--	--
1/18/72	FRP	Long	6.35	45	--	--
			5.8	46	--	--
			5.8	46	--	--
1/20/72	FRP	Short	6.05	43.5	8.0	64
			6.05	44	--	--
			5.8	45	7.7	65
			5.5	45	--	--
1/21/72	Steel	Short	6.6	45	--	--
			6.35	45	--	--
			5.8	45	--	--
			5.8	45	7.4	6.0

TABLE 22

EVALUATION OF CHARGE GENERATION  
USING FILTER BYPASS WITH 0.2 CU FUEL

Flow Rate, GPM	Test Pipe Code(a)	Charge Density, $\mu\text{C}/\text{m}^3$ , at			Fuel	
		Bypass Outlet	Pipe In	Pipe Out	Temp., °F	$k_o$ , CU
300	S-L	-0.1	-0.7	-0.9	37.1	.23
	P-L	0.0	-0.6	-0.9	42.1	.25
	S-S	-0.4	-0.7	-0.8	36.6	.22
	P-S	-0.4	-0.7	-0.7	36.1	.22
	Ave.	-0.2	-0.7			
600	S-L	-0.4	-0.9	-1.8	36.8	.23
	P-L	-0.4	-0.7	-1.2	40.2	.24
	S-S	-0.6	-0.9	-1.1	36.4	.22
	P-S	-0.5	-1.0	-1.1	34.8	.22
	Ave.	-0.5	-0.9			
1200	S-L	-0.8	-1.2	-2.5	36.8	.23
	P-L	-0.6	-1.1	-1.6	39.9	.24
	S-S	-0.7	-1.4	-1.6	37.4	.23
	P-S	-0.6	-1.2	-1.4	34.6	.22
	Ave.	-0.7	-1.2			
1500	S-L	-0.9	-1.3	-2.6	37.6	.23
	P-L	-0.7	-1.3	-1.7	40.4	.24
	S-S	-0.7	-1.3	-1.7	37.4	.23
	P-S	-0.7	-1.3	-1.5	35.2	.22
	Ave.	-0.8	-1.3			

(a) The code designates the pipe type - pipe length combination used, e.g., S-L is steel-long; P-L is FRP-long; S-S is steel-short, etc.

TABLE 23

EVALUATION OF CHARGE GENERATION  
USING FILTER BYPASS WITH 0.9 CU FUEL

Flow Rate, GPM	Test Pipe Code (a)	Charge Density, $\mu\text{C}/\text{m}^3$ , at			Fuel	
		Bypass Outlet	Pipe In	Pipe Out	Temp., °F	$k_o$ , CU
300	S-L	-0.9	-1.5	-1.2	62	.92
	P-L	-0.6	-1.2	-0.6	47	.67
	S-S	-0.8	-1.4	-1.4	62.5	.93
	P-S	-0.6	-1.5	-1.0	64.5	.97
	Ave.	-0.7	-1.4			
600	S-L	-1.3	-2.1	-2.5	62	.92
	P-L	-0.7	-1.4	-0.9	46.5	.66
	S-S	-1.3	-2.2	-2.6	62	.92
	P-S	-1.1	-2.3	-2.0	64	.96
	Ave.	-1.1	-2.0			
1200	S-L	-1.8	-2.6	-5.1	62	.92
	P-L	-0.8	-1.6	-1.3	47.5	.68
	S-S	-1.9	-2.8	-3.6	62	.92
	P-S	-1.4	-3.1	-2.8	64.5	.97
	Ave.	-1.5	-2.5			
1500	S-L	-2.8	-3.7	-6.2	62	.92
	P-L	-1.8	-2.6	-1.9	49.5	.71
	S-S	-2.9	-3.8	-4.7	63	.94
	P-S	-2.0	-4.4	-4.4	66	1.01
	Ave.	-2.4	-3.7			

(a) See Table 22.

TABLE 24

EVALUATION OF CHARGE GENERATION  
USING FILTER BYPASS WITH 3 CU FUEL

Flow Rate, GPM	Test Pipe Code(a)	Charge Density, $\mu\text{C}/\text{m}^3$ , at			Fuel	
		Bypass Outlet	Pipe		Temp., °F	$k_o$ , CU
300	S-L	+0.3	-0.5	0.0	36	2.8
	P-L	-0.2	-0.9	+0.3	39	3.0
	S-S	-0.2	-1.0	-0.2	41	3.1
	P-S	0.0	-0.9	+0.2	40.5	3.0
	Ave.	0.0	-0.8			
600	S-L	-0.2	-1.0	-0.5	35	2.7
	P-L	-0.8	-1.4	+0.3	38.5	2.9
	S-S	-1.0	-1.8	-1.2	39	3.0
	P-S	-0.6	-1.9	-0.4	38.5	2.9
	Ave.	-0.6	-1.5			
1200	S-L	-1.3	-1.9	-1.3	36	2.8
	P-L	-1.4	-2.4	+0.2	36.5	2.8
	S-S	-2.0	-3.1	-3.0	38.5	2.9
	P-S	-1.8	-3.1	-1.9	39	3.0
	Ave.	-1.6	-2.6			
1500	S-L	-1.5	-2.2	-2.0	37	2.8
	P-L	-2.0	-2.9	-0.2	38	2.9
	S-S	-2.5	-3.8	-4.0	39.5	3.0
	P-S	-2.5	-3.8	-2.7	40	3.0
	Ave.	-2.1	-3.2			

(a) See Table 22.

TABLE 25

EVALUATION OF CHARGE GENERATION  
USING FILTER BYPASS WITH 5.5 CU FUEL

Flow Rate, GPM	Test Pipe Code (a)	Charge Density, $\mu\text{C}/\text{m}^3$ , at			Fuel	
		Bypass Outlet	Pipe In	Pipe Out	Temp., °F	$k_o$ , CU
300	S-L	-0.1	-1.1	-0.3	37.5	5.4
	P-L	0.0	-1.4	-0.4	37.4	5.4
	S-S	0.0	-1.0	-0.5	40.3	5.7
	P-S	0.2	-1.3	0.0	40.6	5.7
	Ave.	0.0	-1.2			
600	S-L	-0.8	-2.4	-0.7	36.6	5.3
	P-L	-1.0	-2.5	0.0	36.3	5.3
	S-S	-0.8	-2.3	-1.1	39.1	5.5
	P-S	-1.0	-2.1	-0.2	38.4	5.5
	Ave.	-0.9	-2.3			
1200	S-L	-1.8	-3.6	-2.5	36.9	5.3
	P-L	-2.1	-3.8	+0.1	37.0	5.4
	S-S	-2.1	-3.7	-3.4	38.4	5.5
	P-S	-2.2	-3.4	-1.7	38.1	5.5
	Ave.	-2.0	-3.6			
1500	S-L	-2.2	-4.1	-3.7	37.7	5.4
	P-L	-2.5	-4.3	-0.1	37.6	5.4
	S-S	-2.6	-4.4	-4.4	38.4	5.5
	P-S	-2.5	-4.2	-2.3	37.8	5.4
	Ave.	-2.4	-4.2			

(a) See Table 22.

Table 26

EVALUATION OF CHARGE RELAXATION USING FRAM FILTER/SEPARATOR  
AS CHARGE GENERATOR WITH 0.2 CU FUEL

Flow Rate, GPM	Test Pipe Code(a)	Charge Density, $\mu\text{C}/\text{m}^3$ , at			T, Secs.	Temp., °F	Fuel		$k_e/k_o$
		Filter Out	Pipe In	Pipe Out			$k_o$ , CU	$k_e$ , CU	
300	S-L	- 74.	- 67.6	- 23.7	77	38.4	.23	.23	1.00
	P-L	- 75.	- 68.4	- 23.0	74	38.5	.23	.24	1.04
	S-S	- 77.	- 70.4	- 45.0	61	38.6	.23	.30	1.3
	P-S	- 72	- 66.1	- 40.6	56	39.1	.24	.32	1.3
		- 74							
600	S-L	- 125	- 115.	- 54.4	54	37.5	.23	.33	1.4
	P-L	- 125.	- 116.	- 54.1	53	37.5	.23	.34	1.5
	S-S	- 128.	- 120.	- 86.	41	37.9	.23	.44	1.9
	P-S	- 128.	- 119.	- 84.	39	38.0	.23	.46	2.0
		- 126							
900	S-L	- 148	- 138	- 75.5	44	37.4	.23	.41	1.8
	P-L	- 149.	- 140.	- 76.7	44	37.3	.23	.41	1.8
		- 151(b)	- 143.	- 78.6	45	36.5	.22	.40	1.8
	S-S	- 156	- 147.	- 115.	37	37.6	.23	.48	2.1
	P-S	- 149	- 141.	- 108.	34	37.5	.23	.53	2.3
		- 150							
1200	S-L	- 162.	- 154.	- 94.	41	37.5	.23	.44	1.9
	P-L	- 162.	- 155.	- 94.	40	37.3	.23	.45	2.0
	S-S	- 173.	- 167.	- 135.	32	37.8	.23	.56	2.4
		- 158.(b)	- 151.	- 123.	33	38.1	.23	.54	2.3
	P-S	- 167.	- 161	- 129.	31	37.8	.23	.58	2.5
		- 166							

(a) See Table 22.

(b) Not included in average.

Table 27

EVALUATION OF CHARGE RELAXATION USING FRAM FILTER/SEPARATOR  
AS CHARGE GENERATOR WITH 0.9 CU FUEL

Flow Rate GPM	Test Pipe Code (a)	Charge Density, $\mu\text{C}/\text{m}^3$ , at		T secs.	Temp., °F	Fuel		$k_e/k_o$
		Filter Out	Pipe In Pipe Out			$k_o$ , CU	$k_e$ , CU	
300	S-L	- 51.5	- 44.9	- 6.0	40	60	.88	.45
		- 47.5 (b)	- 41.9	- 5.6	40	57.5	.84	.45
	P-L	- 49.6	- 43.8	- 4.6	36	61	.90	.50
	S-S	- 49.0	- 42.6	- 20.0	36	60.5	.89	.50
	P-S	- 54.9	- 48.8	- 20.7	32	60.5	.89	.56
		- 51						.63
600	S-L	- 103	- 93	- 28.1	34	59.5	.88	.53
	P-L	- 94.	- 86.	- 22.6	30	59.5	.88	.60
	S-S	- 104.	- 93.	- 58.0	29	59.5	.88	.62
	P-S	- 108.	- 97.	- 57.6	26	59	.87	.69
		- 102						.79
910	S-L	- 149	- 137	- 51.6	27	60	.88	.67
		- 139 (b)	- 126	- 49.3	28	58.5	.86	.64
		- 143.	- 133.	- 45.0	24	61	.90	.75
	P-L	- 146.						.83
								.76
1200	S-L	- 153	- 142	- 64.5	26	58.	.85	.69
	P-L	- 145.	- 135	- 56.3	23	58.5	.86	.78
	S-S	- 147.	- 138.	- 100.	21	58	.85	.86
	P-S	- 149.	- 139.	- 98.	20	58	.85	.90
		- 148.						1.01
								1.06
Low Temperature Tests (c)								
300	P-S	- 35.6	- 32.6	- 17.6	44.	38.5	.65	.41
600 (d)	P-S	- 73.	- 67.7	- 46.5	36.	37.5	.63	.50
600 (e)	P-S	- 62.	- 59.5	- 40.8	36.	39.	.66	.50
1200	P-S	- 96.	- 93.	- 73.	28.	40.	.67	.64

(a) See Table 22

(b) Not included in average.

(c) Nominal Fuel CU had increased by  $\sim 0.15$  CU when these tests were run.

(d) Run in A.M.

(e) Run in P.M.



Table 28

EVALUATION OF CHARGE RELAXATION USING  
FRAM FILTER/SEPARATOR AS CHARGE GENERATOR WITH 3 CU FUEL

Flow Rate GPM	Test Pipe Code (a)	Charge Density, $\mu\text{C}/\text{m}^3$ , at		$\tau$ , secs.	Temp., °F	Fuel		
		Filter Out	Pipe In Pipe Out			$k_o$ , CU	$k_e$ , CU	$k_e/k_o$
300	S-L	8.9	4.1	0.0	41	3.1	--	--
	P-L	3.6	1.2	0.3	41.5	3.1	--	--
	S-S	2.0	0.2	0.0	40	3.0	--	--
	P-S	2.2(c)	0.2	0.0	41.5	3.1	--	--
600		1.7	0.0	0.0	41	3.1	--	--
		4.						
	S-L	6.6	5.9	0.2	40	3.0	--	--
	P-L	18.	15.1	0.1	40	3.0	--	--
910	S-S	22.	18.1	4.9	40	3.0	1.7	.57
	P-S	25.	20.1	5.2	40	3.0	1.8	.60
		18						
	S-L	27	23.5	2.5	39	3.0	1.5	.50
900	P-L	42.	36.6	2.8	40	3.0	1.7	.57
	S-S	55.	46.1	18.6	39.5	3.0	1.8	.60
		41						
	S-L	41	36.2	6.2	39.5	3.0	1.6	.53
1200	P-L	59.	52.2	6.9	39.5	3.0	1.8	.60
	P-S	72.	63.0	30.6	39.5	3.0	1.9	.63
	P-S	78.	68.0	31.6	40.	3.0	2.0	.67
		62						

(a) See Table 22.

(b) Indeterminable due to charge density value to &lt; 1.0. (c) Not included in average.

Table 29

EVALUATION OF CHARGE RELAXATION USING FRAM  
FILTER/SEPARATOR AS CHARGE GENERATOR WITH 5.5 CU FUEL

Flow Rate, GPM	Test Pipe Code (a)	Charge Density, $\mu\text{C}/\text{m}^3$ , at				T, secs.	Temp, °F	Fuel		
		Filter Out	Pipe In	Pipe Out				$k_o$ , CU	$k_e$ , CU	$k_e/k_o$
300	S-L	4.2	0.2	- 0.3		(b)	40.1	5.6	--	--
	P-L	5.0	0.6	0.7		(b)	40.8	5.7	--	--
	S-S	4.3	0.4	- 0.3		(b)	40.8	5.7	--	--
	P-S	4.8	0.3	0.1		(b)	41.5	5.8	--	--
		4.6								
600	S-L	- 9.1	- 7.2	- 0.8		(b)	39.2	5.5	--	--
	P-L	0.1	- 1.7	0.7		(b)	39.1	5.5	--	--
	S-S	0.	- 1.8	- 1.0		(b)	39.3	5.6	--	--
	P-S	1.1	- 1.2	0.0		(b)	40.3	5.7	--	--
		- 2.								
900	S-L	- 38	- 29.8	- 1.6		9.1	39.2	5.6	2.0	.36
		- 37(d)	- 28.9	- 1.5		9.2	39.1	5.5	2.0	.36
	P-L	- 18.	- 14.8	0.1		(b)	39.1	5.5	--	--
	S-S	- 17	- 13.5	- 3.8		7.2	39.0	5.5	2.5	.45
		- 14	- 12.4	- 2.7		5.9	39.0	5.5	3.1	.56
		- 22								
1200	S-L	- 70	- 56.5	- 3.9		7.5	39.6	5.6	2.4	.43
	P-L	- 38.	- 32.2	- 0.8		5.4(c)	40.0	5.6	(3.3)	(.59)
	S-S	- 34.	- 28.8	- 10.1		6.5	39.2	5.6	2.8	.50
	P-S	- 32	- 27.3	- 8.4		5.8	39.3	5.6	3.1	.55
		- 44								

(a) See Table 22

(b) Indeterminable due to charge density value  $< 1.0$ .(c) Charge density at pipe outlet only  $0.8 \mu\text{C}/\text{m}^3$ .

(d) Not included in average.

Table 30

EVALUATION OF CHARGE RELAXATION USING BENDIX GAGES  
AS CHARGE GENERATOR WITH 0.2 CU FUEL

Flow Rate, GPM	Test Pipe Code (a)	Charge Density, $\mu\text{C}/\text{m}^3$ , at		T, secs.	Temp., °F	Fuel		
		Gage Out	Pipe In Pipe Out			k <sub>o</sub> , CU	k <sub>e</sub> , CU	k <sub>e</sub> /k <sub>o</sub>
200	S-S	12.3	9.7	45	40.0	.24	.40	1.7
	P-S	20.1	16.8	55	40.5	.24	.33	1.4
300	S-L	9.6	8.1	52	39.6	.24	.35	1.5
	P-L	9.7	7.8	68	40.1	.24	.26	1.1
	S-S	10.8	8.9	44	39.6	.24	.41	1.7
	P-S	18.0	15.9	56	39.7	.24	.32	1.3
		20.9(b)	18.6	57	40.1	.24	.32	1.3
		<u>12</u>						
600	S-L	6.9	6.2	48	38.7	.23	.38	1.6
	P-L	6.9	5.9	73	38.8	.23	.25	1.1
	S-S	7.7	6.7	50	38.6	.23	.36	1.6
	P-S	15.5	14.4	60	38.8	.23	.30	1.3
		16.7(b)	15.7	58	39.3	.24	.31	1.3
		<u>9</u>						
1200	S-L	4.6	4.1	28	38.2	.23	.64	2.8
	P-L	4.8	4.2	60	38.6	.23	.30	1.3
	S-S	5.4	4.7	26	38.2	.23	.69	3.0
	P-S	11.0	10.3	67	38.3	.23	.27	1.2
		14.5(b)	13.9	56	39.3	.24	.32	1.3
		<u>6</u>						

(a) See Table 22.

(b) Not included in average.

Table 31

EVALUATION OF CHARGE RELAXATION USING BENDIX GAGES  
AS CHARGE GENERATOR WITH 0.9 CU FUEL

Flow Rate, GPM	Test Pipe Code (a)	Charge Density, $\mu\text{C}/\text{m}^3$ , at			T, secs.	Temp, °F	Fuel		
		Gage Outlet	Pipe In	Pipe Out			k <sub>o</sub> , CU	k <sub>e</sub> , CU	k <sub>e</sub> /k <sub>o</sub>
300	S-L	20.6	14.8	0.4	(b)	56.5	.82	--	---
	P-L	31.0	23.4	1.7	31	54	.78	.58	.74
	S-S	22.8	13.8	4.9	26	58.5	.86	.50	.58
	P-S	23.4 24.	17.1	6.4	28	58.5	.86	.56	.65
600	S-L	16.1	13.3	2.4	24	56	.81	.75	.93
	P-L	26.6	23.0	8.5	40	52	.74	.45	.61
	S-S	18.2	15.1	8.5	24	57	.83	.62	.75
	P-S	18.9 20.	15.5	10.1	26	57	.83	.69	.83
910	S-L	13.6	11.7	3.8	24	55	.79	.75	.95
	P-L	22.3	19.8	11.4	48	52	.74	.38	.51
1200	S-L	12.6	10.9	4.5	23	55	.79	.78	.99
	P-L	22.0	20.1	13.7	52	52	.74	.35	.47
	S-S	14.3	12.4	9.3	24	56.5	.82	.86	1.05
	P-S	15.2 16.	13.1	11.0	39	56.5	.82	.90	1.10
Low Temperature Tests (c)									
300	P-S	20.2	16.1	8.8	45	37	.62	.40	.64
600	P-S	16.1	13.9	10.1	43	36	.61	.42	.69

(a) See Table 22.

(b) Charge density at pipe outlet  $< 1.0 \mu\text{C}/\text{m}^3$ .(c) Nominal Fuel CU had increased by  $\sim 0.15$  CU when these tests were run.

Table 32

EVALUATION OF CHARGE RELAXATION USING BENDIX GAGES  
AS CHARGE GENERATOR WITH 3 CU FUEL

Flow Rate, GPM	Test Pipe Code (a)	Charge Density, $\mu\text{C}/\text{m}^3$ , at		T, secs.	Temp., °F	Fuel		$k_e$	$k_{e/k_o}$
		Gage Out	Pipe In Pipe Out			$k_o$	$k_e$		
300	S-L	150.	91.	0.0	44	3.2	--	--	--
	P-L	135.	79.	0.2	44.5	3.3	--	--	--
	S-S	120.	68.	0.4	44.5	3.3	--	--	--
	P-S	122.	70.	1.2	45	3.3	2.7	.81	
		<u>132</u>							
600	S-L	134.	106.	3.0	43	3.2	1.6	.50	
	P-L	123.	96.	5.4	43	3.2	1.3	.41	
	S-S	106.	82.	20.2	43	3.2	1.9	.59	
	P-S	109.	87.	27.5	43	3.2	1.5	.47	
		<u>118</u>							
900 910	S-S	93.	80.	36.2	42	3.1	1.6	.52	
	S-L	121.	104.	15.6	42	3.1	1.3	.42	
	P-L	110.	94.	21.2	42	3.1	1.0	.32	
		<u>116</u>							
1200	S-L	112.	101.	29.1	42	3.1	1.1	.35	
	P-L	102.	91.	34.8	42	3.1	.86	.28	
	S-S	86.	75.6	45.4	42	3.1	1.4	.45	
	P-S	89.	78.4	51.3	42	3.1	1.1	.35	
		<u>97</u>							

(a) See Table 22.

(b) Indeterminable due to charge density value  $< 1.0$ .

Table 33

EVALUATION OF CHARGE RELAXATION USING BENDIX GAGES  
AS CHARGE GENERATOR WITH 5.5 CU FUEL

Flow Rate, GPM	Test Pipe Code (a)	Charge Density, $\mu\text{C}/\text{m}^3$ @		T, secs.	Temp. °F		Fuel	
		Gage Outlet	Pipe In	Pipe Out			k <sub>o</sub> CU	k <sub>e</sub> CU
300	S-L	202.	100.	- 0.2	(b)	40.0	5.6	--
	P-L	181.	73.	0.2	(b)	40.4	5.7	--
	S-S	158.	63.3	- 0.3	(b)	39.9	5.6	--
	P-S	172.	68.9	0.1	(b)	40.4	5.7	--
		178.						
600	S-L	190.	136.	- 0.4	(b)	38.4	5.5	--
	P-L	187.	131.	1.8	9.4	38.5	5.5	1.9
	S-S	154.	104.	4.8	4.4	38.5	5.5	4.1
	P-S	166.	114.	20.	7.8	38.6	5.5	2.3
		174						
900	S-L	173.	137.	4.2	7.7	38.0	5.4	2.3
	P-L	164.	129.	8.4	9.8	38.6	5.5	1.8
	S-S	146.	114.	26.	6.2	38.3	5.5	2.9
	P-S	152.	119.	41.	8.5	38.2	5.5	2.1
		159						
1200	S-L	161.	134	16.7	9.6	38.6	5.5	1.9
	P-L	153.	125.	19.	10.7	39.3	5.5	1.6
	S-S	143.	119.	48.	7.5	39.1	5.5	2.4
	P-S	145.	121.	59.	9.4	39.5	5.6	1.9
		150						

(a) See Table 22.

(b) Indeterminable due to charge density value  $< 1.0$ .

Table 34

## SURFACE VOLTAGE DATA - USING BYPASS WITH 0.2 CU FUEL

Flow Rate, GPM	300		600		1200		1500	
Pipe Length	S	L(a)	S	L(a)	S	L(a)	S	L(a)
Pipe In, $\mu\text{C}/\text{m}^3$	-0.7	-0.6	-1.0	-0.7	-1.2	-1.1	-1.3	-1.3
Pipe Out, $\mu\text{C}/\text{m}^3$	-0.7	-0.8	-1.1	-1.2	-1.4	-1.6	-1.5	-1.7
Temp., °F	38.6	44.9	39	45.0	39	45	40.0	44.6
Rel. Hum., %	74	62	73(b)	63	72(b)	62(b)	70	60
Surf. V., kv, @ Ft. From Inlet								
1	.015	.110	-	.087	-	-	.010	.102
2	.024	.193	-	.135	-	-	.023	.205
4	.025	.290	-	.225	-	-	.028	.36
10	.33	.63	-	.42	-	-	.290	.40
20	.39	-1.01	-	.70	-	-	.92	2.2
30	.82	-.205	-	.70	-	1.2	.85	1.8
40	-5.8	-4.3	-	-3.8	-	-	-5.0	-
42	-	-	-	-	-	-	.33	-
44	-	-	-	-	-	-	2.0	-
50	3.0	1.58	2.5	.54	2.6	.78	2.6	1.26
60	2.0	-3.6	-	-2.0	-	-	1.71	-1.0
70	.28	-.32	-	.190	-	-	.250	.70
76	.32	-.47	-	.185	-	-	.33	.67
77	-	-.65	-	-	-	-	-	-
77.5	-	-.19	-	-	-	-	-	-
78	-	.24	-	-	-	-	-	-
79	.066	.39	-	.36	-	-	.060	.56
90	-	-2.6	-	-1.58	-	-1.06	-	-.63
110	-	-2.6	-	-1.29	-	-	-	-.090
120	-	-.30	-	-.185	-	-	-	.34
130	-	-3.15	-	-2.06	-	-	-	-.92
150	-	-3.6	-	-2.7	-	-2.35	-	2.0
170	-	-4.8	-	-2.0	-	-1.01	-	-.39
190	-	-3.6	-	-1.47	-	-	-	-.67
200	-	-.058	-	-.042	-	-	-	.238
210	-	-1.96	-	-1.03	-	-	-	-.39
230	-	.011	-	.020	-	-	-	.013
238	-	-.042	-	-.030	-	-	-	.024
239	-	.032	-	0.0	-	-	-	0.0

(a) Readings changed slowly; didn't stabilize during test.

(b) Estimated value.

Table 35

SURFACE VOLTAGE DATA - USING BYPASS WITH 0.9 CU FUEL

Flow Rate, GPM	300		600		1200		1500	
Pipe Length	S	L	S	L	S	L	S	L
Pipe In, $\mu\text{C}/\text{m}^3$	1.5	-1.2	2.3	-1.4	3.1	-1.6	3.4	-2.8
Pipe Out, $\mu\text{C}/\text{m}^3$	1.0	-0.6	2.0	-0.9	2.8	-1.3	4.4	-1.6
Temp., $^{\circ}\text{F}$	-	-	56.3	-	56.7	46.7	56.7	-
Rel. Hum., %	81	94	81	93	82	93	82	90
Surf. V., kv, @ Ft. From Inlet								
1	0.15	-.019	0.12	-.020	0.11	-.019	0.10	-.020
2	0.51	-.020	0.51	-.020	0.51	-.020	0.49	-.022
4	1.01	-.020	1.01	-.020	1.01	-.020	0.96	-.026
10	1.85	-.020	1.62	-.020	1.42	-.020	1.29	-.021
20	4.3	-	4.6	-	4.6	-	2.9	-
30	3.6	-.023	3.9	-.021	4.1	-.020	4.1	-.037
37	4.1	-	-	-	-	-	-	-
39	-2.7	-	-2.6	-	-2.2	-	-2.5	-
40	-6.3	-	-5.8	-	-5.3	-	-5.0	-
41	.78	-	.42	-	.83	-	0.30	-
43	1.45	-	1.37	-	1.26	-	1.01	-
50	1.62	-.024	1.53	-.023	1.5	-.027	1.31	-.071
60	1.26	-.024	1.20	-.024	1.15	-.029	.96	-.080
70	0.51	-.023	.47	-.023	.42	-.028	.34	-.071
76	0.30	-	.26	-	.24	-	.20	-
78	0.29	-.020	.25	-.021	.23	-.024	.17	-.037
79	0.22	-	.17	-	.15	-	.12	-
90	-	-.020	-	-.019	-	-.023	-	-.053
110	-	-.020	-	-.020	-	-.024	-	-.026
130	-	-.019	-	-.019	-	-.020	-	-.022
150	-	-.024	-	-.026	-	-.038	-	-.098
170	-	-.023	-	-.024	-	-.039	-	-.108
190	-	-.023	-	-.024	-	-.025	-	-.060
210	-	-.020	-	-.021	-	-.023	-	-.053
230	-	-.020	-	-.020	-	-.021	-	-.025
238	-	-.020	-	-.020	-	-.020	-	-.022
239	-	-.020	-	-.020	-	-.020	-	-.020



Table 36

## SURFACE VOLTAGE DATA - USING BYPASS WITH 3 CU FUEL

Flow Rate, GPM	300		600		1200	1500	
Pipe Length	S	L	S	L	S	S	L
Pipe In, $\mu\text{C}/\text{m}^3$	-0.9	-0.9	-1.9	-1.4	-3.1	-3.8	-2.9
Pipe Out, $\mu\text{C}/\text{m}^3$	+0.2	+0.3	-0.4	+0.3	-1.9	-2.7	-0.2
Temp., $^{\circ}\text{F}$	45.7	50.7	45.7	50.3	50.2(a)	46.9	50.2
Rel. Hum., %	66(a)	68	66	69	65(a)	64	74
Surf. V., kv, @							
Ft. From Inlet							
1	.22	-.017	.120	-.018	.080	.058	-.017
2	.70	-.013	.41	-	.31	.27	-
4	1.5	.013	1.10	-.014	.92	.87	-
10	3.6	.012	2.7	-.014	2.06	1.71	-.015
20	6.6	.042	6.6	-	6.3	6.0	-
30	7.1	.041	6.9	.012	6.6	6.0	-.010
37	6.6	-	4.3	-	3.4	3.05	-
40	-1.58	-4.3	-1.53	-	-1.85	-1.75	-.58
43	.47	-	.54	-	.068	.013	-
50	-.65	.23	-.67	.017	-.82	-.82	-.011
60	-.116	.20	-.19	.015	-.37	-.44	-
70	.018	.098	-.066	-.012	-.14	-.19	-
79	.014	.074	.083	-.018	.039	.020	-.018
90	-	.016	-	-.016	-	-	-.017
110	-	.018	-	-	-	-	-
120	-	-	-	-	-	-	-.022
130	-	.027	-	-.015	-	-	-.016
150	-	.045	-	-.017	-	-	-.017
170	-	.035	-	-.016	-	-	-.018
190	-	.042	-	-.015	-	-	-.018
210	-	.014	-	-.016	-	-	-
230	-	.030	-	-.017	-	-	-.018
238	-	.011	-	-	-	-	-
239	-	.012	-	-.018	-	-	-.018

(a) Estimated.

Table 37

## SURFACE VOLTAGE DATA - USING BYPASS WITH 5.5 CU FUEL

Flow Rate, GPM	300		600	1200		1500
Pipe Length	S	L	S	S	L	S
Pipe In, $\mu\text{C}/\text{m}^3$	-1.3	-1.4	-2.1	-3.4	-3.8	-4.2
Pipe Out, $\mu\text{C}/\text{m}^3$	0.0	-0.4	-0.2	-1.7	+0.1	-2.3
Temp., $^{\circ}\text{F}$	38.4	39.4	39.0	38.8	39.2	39
Rel. Hum., %	55	58	51	59	54	59
Surf. V., kv, @ Ft. From Inlet						
1	-.26	-.24	-.093	-.15	-.42	-.14
2	-.34	-.73	-.47	-.54	-1.12	-.51
4	-.58	-.33	-.76	-.85	-1.4	-.85
10	-.63	-1.01	-.92	-1.23	-4.8	-1.26
20	-1.10	-1.12	-1.53	-2.15	-7.1	-2.20
30	-1.29	-	-1.75	-2.35	-5.3	-2.40
40	-.24	-2.5	-.76	-1.20	-10.2	-1.33
50	-1.03	-1.31	-1.37	-1.96	-7.7	-2.06
60	-.51	-1.53	-.76	-1.10	-6.0	-1.20
70	-.20	-1.01	-.28	-.42	-3.9	-.47
76	-.22	-1.01	-.26	-.32	-3.6	-.33
79	-.095	-.44	-.12	-.15	-3.05	-.15
90	-	-1.12	-	-	-5.0	-
110	-	-	-	-	-3.3	-
120	-	-1.62	-	-	-8.4	-
130	-	-1.15	-	-	-6.3	-
150	-	-1.50	-	-	-7.7	-
170	-	-1.03	-	-	-5.8	-
190	-	-.63	-	-	-3.8	-
200	-	-.85	-	-	-4.6	-
210	-	-.28	-	-	-1.66	-
230	-	-.093	-	-	-.65	-
238	-	-.060	-	-	-.27	-
239	-	-.110	-	-	-.27	-

Table 38

SURFACE VOLTAGE DATA - USING FILTER/SEPARATOR WITH 0.2 CU FUEL

Flow Rate, GPM	300		600		900	1200	
Pipe Length	S(a)	L	S	L	S	S	L(b)
Pipe In, $\mu\text{C}/\text{m}^3$	-66.1	-68.4	-119	-116	-141	-161	-155
Pipe Out, $\mu\text{C}/\text{m}^3$	-40.6	-23.0	-84	-54.1	-108	-129	-94
Temp., $^{\circ}\text{F}$	43.9	40.1	42.3	40	41.9	41.7	40.3
Rel. Hum., %	65	57	68	56(c)	69	68	56
Surf. V., kv, @							
Ft. From Inlet							
1	.30	-1.66	-.016	-3.8	-.29	-.42	-4.3
2	.73	-4.3	-.222	-9.0	-.63	-.93	-9.3
4	.78	-2.25	-.112	-11.7	-.57	-.99	-13.8
10	2.8	-12	-4.1	-30.	-4.8	-7.1K	-43(b)
20	-4.3	-15.6	-15.6	-	-20.	-20.5K	-24(b)
30	-11.7	-26	-23.	-	-28.	-30.K	-43(c)
40	-30.	-43(c)	-38	-	-43.	-43.K	-43(c)
50	.27	-26	-13.8	-48(c)	-2.05	-21.5K	-48(c)
60	-6.0	-30	-15.6	-	-2.05	-23.K	-52(b)
70	-1.06	-30	-1.5	-34(c)	-2.7	-3.6K	-45(b)
76	-.49	-20.5	-1.75	-28	-2.06	-2.5K	-32(b)
79	.098	-24.5	-.32	-34	.54	-760.	-41(b)
90	-	-28	-	-34	-	-	-34(c)
110	-	-15.3	-	-	-	-	-26
120	-	-	-	-	-	-	-26
130	-	-23.	-	-	-	-	-28
150	-	-24.5	-	-28	-	-	-28
170	-	-20.5	-	-34	-	-	-38
190	-	-21.5	-	-	-	-	-38
200	-	-	-	-	-	-	-42
210	-	-12.	-	-	-	-	-28
230	-	-2.6	-	-5.5	-	-	-8.4
238	-	-1.2	-	-2.2	-	-	-3.15
239	-	-1.01	-	-1.75	-	-	-2.35

- (a) When flow rate was decreased from 600 to 300 GPM, surface voltage at 50 ft. decreased, went positive after 12 minutes and reached +270V after 14 minutes.
- (b) Readings made with Sweeney meter.
- (c) Estimated value.

Table 39

## SURFACE VOLTAGE DATA - USING FILTER/SEPARATOR WITH 0.9 CU FUEL

Flow Rate, GPM	300		600		1200	
Pipe Length	S	L	S	L	S	L
Pipe In, $\mu\text{C}/\text{m}^3$	-48.8	-43.8	-97	-86	-139	-135
Pipe Out, $\mu\text{C}/\text{m}^3$	-20.7	-4.6	-57.6	-22.6	-98	-56.3
Temp., $^{\circ}\text{F}$	-	-	-	-	-	-
Rel. Hum., %	84	62	89	64	91	65
Surf. V., kv, @						
Ft. From Inlet						
1	.098	0.0	-.21	-.34	-.42	-.96
2	.30	-.39	-.70	-1.29	-1.23	-2.06
4	.67	-1.03	-1.03	-2.35	-2.06	-3.4
10	1.01	-.92	-.54	-3.4	-1.40	-6.3
20	1.42	2.25	-4.6	-5.8	-7.1	-12.4
30	.78	-8.6	-5.8	-11.0	-6.6	-16.
37	1.26	-	-2.6	-	-4.6	-
37.75	-	-	-1.10	-	-	-
38	-	-	-.80	-	-2.20	-
40	-	-	-16.5	-	-11.0	-
42	.30	-	-	-	-	-
42.25	-	-	-1.47	-	-	-
42.5	.54	-	-	-	-	-
43	.76	-	-3.05	-	-	-
50	.85	-43(a)	-2.5	-14.9	-5.3	-30.
60	.36	-5.3	-2.35	-18.3	-5.3	-30.
70	.34	-13.4	-.51	-23.	-1.33	-34(a)
76	.087	-	-.60	-	-1.37	-
78	.087	-21.0	-.51	-34(a)	-1.23	-38(a)
79	.074	-20.5	-.37	-	-.85	-
90	-	-12.8	-	-16.	-	-2.5
100	-	-.85	-	-	-	-
110	-	-1.53	-	-6.3	-	-9.7
130	-	2.7	-	-1.1	-	-4.3
140	-	.033	-	-5.0	-	-
150	-	-11.7	-	-24.5	-	-24.5
170	-	-3.3	-	-24.5	-	-34(a)
180	-	-2.9	-	-	-	-9.7
190	-	2.8	-	-6.9	-	-
210	-	-2.9	-	-7.4	-	-10.2
220	-	-3.15	-	-7.4	-	-10.8
230	-	-.34	-	-.85	-	-1.18
238	-	-.34	-	-.76	-	-1.10
239	-	-.083	-	-.49	-	-.90

(a) Estimated value.

Table 40

## SURFACE VOLTAGE DATA - USING FILTER/SEPARATOR WITH 3 CU FUEL

Flow Rate, GPM	300	600		1200	
Pipe Length	S(a) (b)	S(a) (c)	L	S(a)	L
Pipe In, $\mu\text{C}/\text{m}^3$	0.0	-20.1	-15.1	-68.	-52.2
Pipe Out, $\mu\text{C}/\text{m}^3$	0.0	-5.2	-0.1	-31.6	-6.9
Temp., $^{\circ}\text{F}$	45.9	46.0	50.3	46.1	50.2
Rel. Hum., %	73	74	70	75	67
Surf. V., kv, @					
Ft. From Inlet					
1	.50	.2	-.017	2.	-.021
2	.60	.2	-.014	1.5	-.024/- .026
4	.80	.2	-.011	0.	-.033/- .040
10	1.2	.2	-.011	2.	-.19/- .021
20	2.9	.1	.015	2.	-.048
30	2.3	-.1	.014	1.	-.046
37	2.2	-	-	-	-
40	-4.	7.	-4.3	-3.	-2.06
43	.25	-	-	-	-
50	.30	-.1	.054	1.	-.080
60	.25	.1	.041	1.	-.074
70	.20	.2	.029	2.	-.045
79	.20	.1	.050	-1.	-.060
90	-	-	-.013	-	-.021
110	-	-	-.012	-	-.024
120	-	-	-	-	-.098
130	-	-	.010	-	-.025
150	-	-	.011	-	-.023
170	-	-	.013	-	-.029
190	-	-	.017	-	-.037
200	-	-	-	-	-.122
210	-	-	.010	-	-.025
230	-	-	.014	-	-.023
238	-	-	-	-	-
239	-	-	-.015	-	-.021

(a) Readings made with Sweeney meter.

(b) Pipe drying; top run  $\sim$ 50% wet on top; bottom run  $\sim$ 25% wet on top.

(c) Pipe  $\sim$ 50-75% wet on top, except at 40' where it was dry.

Table 41

## SURFACE VOLTAGE DATA - USING FILTER/SEPARATOR WITH 5.5 CU FUEL

Flow Rate, GPM	300	600		900		1200	
Pipe Length	S	S	L	S	L	S	L
Pipe In, $\mu\text{C}/\text{m}^3$	0.3	-1.2	-1.7	-12.4	-14.8	-27.3	-32.2
Pipe Out, $\mu\text{C}/\text{m}^3$	0.1	0.0	0.7	-2.7	0.1	-8.4	-0.8
Temp., $^{\circ}\text{F}$	41.3	41.2	43.8	41	42.9	40.8	41.8
Rel. Hum., %	47	47	46	49(a)	46	51	47
Surf. V., kv, @ Ft. From Inlet							
1	.027	.095	-.215	-.54	-1.96	-1.12	-4.6
2	-.36	-.42	-1.06	-1.12	-4.6	-2.25	-9.0
4	-.63	-.73	.068	-1.89	-7.7	-3.8	-17.7
10	-.23	-.51	-1.31	-3.15	-17.7	-8.1	-30.
20	-1.12	-1.33	4.3	-5.3	-13.4	-12.0	-34(a)
30	-1.29	-1.53	2.35	-5.5	-15.6	-12.4	-30.
40	-.25	-.78	-5.8	-4.3	-17.7	-12.0	-34.(a)
50	-1.20	-1.42	2.5	-4.3	-9.3	-9.7	-24.5
60	-.51	-.67	-3.4	-2.5	-13.8	-6.3	-23.
70	-.20	-.26	-2.5	-.76	-9.0	-1.58	-18.3
76	-.24	-.27	-2.35	-.47	-8.1	-.82	-16.5
79	-.11	-.12	-1.5	-.22	-7.1	-.41	-15.6
90	-	-	-2.6	-	-9.3	-	-17.7
110	-	-	1.53	-	-5.5	-	-15.6
120	-	-	-	-	-14.5	-	-24.5
130	-	-	-2.06	-	-10.5	-	-19.0
150	-	-	-3.6	-	-10.8	-	-18.3
170	-	-	-2.9	-	-2.4	-	-13.4
190	-	-	1.85	-	-2.06	-	-9.3
200	-	-	-	-	-5.5	-	-12.4
210	-	-	-.92	-	-2.35	-	-5.3
230	-	-	-.41	-	-.96	-	-1.96
238	-	-	-.17	-	-.34	-	-.70
239	-	-	-.18	-	-.33	-	-.58

(a) Estimated value.

Table 42

SURFACE VOLTAGE DATA - USING GAGES WITH 0.2 CU FUEL

Flow Rate, GPM	300	1200
Pipe Length	L	L
Pipe In, $\mu\text{C}/\text{m}^3$	7.8	4.2
Pipe Out, $\mu\text{C}/\text{m}^3$	2.4	3.0
Temp., $^{\circ}\text{F}$	43.0	43.1
Rel. Hum., %	39	41
Surf. V., kv, @		
Ft. From Inlet		
1	.87	.96
2	1.4	2.0
4	6.3	7.1
10	10.5	13.8
20	14.5	20.5
30	5.8	11.3
40	-23.	-20.5
50	5.0	7.1
60	3.8	5.5
70	-3.8	-4.6
76	5.3	4.1
79	1.96	1.03
90	-8.4	-6.3
110	-6.0	9.3
130	2.9	6.3
150	-8.6	-2.6
170	-1.37	2.8
190	3.8	7.4
210	-1.75	-.154/- .25
230	-.58	-.42
238	-.41	-.33
239	-.63	-.58

Table 43

## SURFACE VOLTAGE DATA - USING GAGES WITH 0.9 CU FUEL

Flow Rate, GPM Pipe Length	300		600		1200	
	S	L	S	L	S	L
Pipe In, $\mu\text{C}/\text{m}^3$	17.1	23.4	15.5	23.0	13.1	22.0
Pipe Out, $\mu\text{C}/\text{m}^3$	6.4	1.7	10.1	8.5	11.0	20.1
Temp., $^{\circ}\text{F}$						
Rel. Hum., %	94	80	93	83	93	83
Surf. V., kv @ Ft. From Inlet						
1	.012/ .014	.014/ .023	0/- .011	.018/	-.016(a)	-.016/ -.018
2	.037/ .067	.050	.019/ .022	.048	-.016(a)	.01/- .014
4	.056/ .066	.098	.033/ .048	.090	-.013/ -.018	-.017/ .011
10	.033/ .042	.135	.192	.147	-.014	-.023
20	.42	1.85	.138	1.75	.038(b)	1.10
30	.51	2.15	.250	1.96	.077	1.26
37	.24	--	.090	--	.023	--
50	.053	3.8	.045	3.6	-.039	2.5
60	.048	4.3	.046	3.8	-.024	2.5
70	--	3.6	.014	3.4	-.024	2.25
76	-.014	2.8	--		-.027	
78	-.015	1.2	-.010(b)	1.4	-.122(b)	.80
79	-.016	.73	-.013(b)		-.025(b)	
90		2.25		2.35		1.47
100						
110		1.06		1.8		1.31
130		.036		.70		3.55
140						
150		2.35		2.35		1.62
170		1.26		1.58		1.40
180						
190		1.40		2.40		2.25
210		.63		1.01		1.01
220		.34		.80		.80
230		.021		.060		.064
236						
238		-.028		.018		.017
239		-.030		-.016		-.015

(a) Pipe was wet.

(b) Some wet spots on pipe.



Table 44

SURFACE VOLTAGE DATA - USING GAGES WITH 3 CU FUEL

Flow Rate, GPM Pipe Length	300		600		1200	
	<u>S(a)</u>	<u>L</u>	<u>S(a)</u>	<u>L</u>	<u>S(a)</u>	<u>L</u>
Pipe In, $\mu\text{C}/\text{m}^3$	70	79	87	96	78.4	91
Pipe Out, $\mu\text{C}/\text{m}^3$	1.2	0.2	27.5	5.4	45.4	34.8
Temp., °F	46.6	50.1			46.1	50.3
Rel. Hum., %	78	69	76(b)	70(b)	75	70
Surf. V., kv, @ Ft. From Inlet						
1	.007	0	.2	.012	.2	-.007
2	.120	-.055	.8	.030	.8	.012
4	.30		1.7	.064	1.6	.032
10	.44	.110	3.1	.18	3.3	.050
20	3.8	.172	5.	1.01	6.	.31
30	3.6	.78	5.	2.15	5.	.34
37	.56				4.3	
40	12.4	17.	8.5	17.	8.	6.3
43	.96				3.7	
50	6.0		5.1			
60	3.9	2.9	5	5.5	4.9	4.3
70	.41	.87	1.4	2.2	1.8	2.0
79	-.020	.110	.3	.73	.2	.56
90		-.205		.26		.138
110		-.63		.185		.147
120				1.37		
130		-.51		.122		.095
150		.077		.199		.135
170		.016		.27		.24
190		-.63		.32		1.01
200				1.193		
210		-.90		-.147		.51
230		-.29		-.105		.190
239		-.25		-.029		.044

(a) Overcast, some drizzle; readings made with Sweeney Meter.

(b) Estimated value.

Table 45

## SURFACE VOLTAGE DATA - USING GAGES WITH 5.5 CU FUEL

Flow Rate, GPM Pipe Length	300		600		900		1200	
	S	L	S	L	S	L	S	L
Pipe In, $\mu\text{C}/\text{m}^3$	68.9	73.	114	131	119	129	121	125
Pipe Out, $\mu\text{C}/\text{m}^3$	0.1	0.2	20	1.8	41	8.4	59	19
Temp, °F.	43.8	50.1	42.8	49.8	42.5	51	42.6	52.2
Rel. Hum., %	63	47	60	40	58	44(b)	55	47
Surf. V., kv, @ Ft. From Inlet								
1	.67	3.6	3.3	5.5	3.8	6.0	3.4	6.6
2	2.7	9.3	7.4	11.3	7.4	14.5	6.3	15.6
4	.14	2.8	10.5	28	11.7	21.5	11.0	21.5
10	-.58	10.2	23	51(a)	24.5	36(a)	26	30
20	-2.4	5.5	38(a)	55(a)	42(a)	33(a)	42(a)	28
30	-13.1	-1.03	24.5	23	30		30	18.3
40	10.8	23	46(a)	55(a)		37(a)		26
50	2.9		28	38(a)	34(a)	20.5	38(a)	18.3
60	2.8	16.5	20.5	30	23	31(a)	24.5	26
70	.49	10.2	2.9	20	3.9		3.9	20
76	-.021	8.6	1.03	16.5	1.29	15.6	1.31	17.7
79	-.050	5.8	.51	16.5	.65	14.9	.67	14.9
90		7.4		15.6		18(a)		21.5
110		14.1		17		19(a)		17.7
120		2.4		23		26(a)		
130		-3.9		17.7		22(a)		23
150		6.0		11.3		20(a)		23
170		.32		11.0		16(a)		18.5
190		-3.15		7.7		16(a)		20
200						14(a)		
210		2.9		5.8		11(a)		17
220		9.3		2.5				
230		.87		.80		3(a)		
238		.33		.24		2(a)		1.45
239		.41		.14				1.37

(a) Readings made with Sweeney meter.

(b) Estimated value.

Table 46

TESTS WITH SCR IN COMBINATION WITH FRAM FILTER/SEPARATOR AT 0.2 CU

Flow Rate, GPM	Test Pipe Code(a)	Charge Density, $\mu\text{C}/\text{m}^3$ at			Fuel		SCR Efficiency, %(d)	
		Filter Out(b)	Pipe In(c)	Pipe Out	Temp. °F	Rest CU	Range	Aver.
300	S-L	-80.	0/-7	-2/-3	38.1	.23	91/100	96
	P-L	-78.	0/-9	-1/-3	38.1	.23	88/100	94
	S-S	-79.	0/-6	-2/-4	39.6	.24	92/100	96
	P-S	-84.	0/-8	0/-3	38.6	.23	91/100	96
600	S-L	-125.	6/-9	-2/-5	37.0	.23	93/100	98
	P-L	-126.	2/-17	-1/-9	37.6	.23	87/100	94
	S-S	-130.	2/-9	-2/-5	38.6	.23	93/100	96
	P-S	-130.	7/-13	2/-9	38.1	.23	90/100	98
900	S-L	-147.	-2/-15	-4/-8	36.8	.23	90/99	95
	P-L	-150.	-2/-14	-3/-7	37.2	.23	91/99	95
	S-S	-153.	1/-11	-2/-7	37.8	.23	93/100	96
	P-S	-157.	1/-20	0/-10	38.0	.23	87/100	94
1200	S-L	-164.	-4/-20	06/-14	37.6	.23	88/98	93
	P-L	-165.	1/-30	-8/-19	37.6	.23	82/100	91
	S-S	-168.	4/-20	-2/-15	37.8	.23	88/100	95
	P-S	-173.	-2/-25	-3/-7	38.2	.23	86/99	92

(a) See Table 22

(b) SCR Inlet

(c) SCR Outlet

(d) Efficiency, % =  $\left( \frac{|CD \text{ SCR In}| - |CD \text{ SCR Out}|}{|CD \text{ SCR In}|} \right) \times 100$

Table 47

SCR TESTS IN COMBINATION WITH THE FRAM FILTER/SEPARATOR AT 0.9 CU

Flow Rate, GPM	Test Pipe Code(a)	Charge Density, $\mu\text{C}/\text{m}^3$ at			Fuel		SCR Efficiency, %(d)
		Filter Out(b)	Pipe In(c,e)	Pipe Out	Temp. °F	Rest CU	
300	S-L	-52.9	-33. <u>+1</u>	-4.8	62	.92	38
	P-L	-48.0	-29.	-3.7	61.5	.92	40
	S-S	-51.0	-31.	-14.5	62	.92	39
	P-S	-57.	-32.	-13.0	63.5	.94	44
600	S-L	-113.	-60. <u>+2</u>	-20.	60.5	.90	47
	P-L	-102.	-58.	-16.5	61	.91	43
	S-S	-112	-59.	-37.7	61.5	.92	47
	P-S	-116	-59.	-35.5	62	.92	49
1200	S-L	-174.	-95. <u>+3</u>	-45.	60	.89	45
	P-L	-163.	-83.	-37.	60.5	.90	49
	S-S	-173.	-87.	-66.	60.5	.90	50
	P-S	-176.	-89.	-64.	60.5	.90	49

(a) See Table 22

(b,c,d) See Table 46

(e) ± Deviations apply to all runs at a given flow rate.

Table 48

TESTS WITH SCR IN COMBINATION WITH FRAM FILTER/SEPARATOR AT 3 CU

Flow Rate, GPM	Test Pipe Code(a)	Charge Density, $\mu\text{C}/\text{m}^3$ at			Fuel		SCR Efficiency, %(d)
		Filter Out(b)	Pipe In(c)	Pipe Out	Temp. °F	Rest CU	
300	S-L	+8.0	-0.2	-0.3	41.5	3.1	98
	P-L	+3.4	-0.4	+0.2	41.	3.1	88
	S-S	+2.3	-1.0	-0.2	41.5	3.1	56
	P-S	+1.5	-1.2	-0.1	41.5	3.1	20
600	S-L	-7.3	-5.0	-0.8	40.5	3.0	32
	P-L	-22.6	-6.5	+0.1	40.	3.0	71
	S-S	-26.	-7.3	-2.4	40.	3.0	72
	P-S	-28.	-6.5	-1.9	40.	3.0	77
900	S-S	-55.	-9.1 <sup>(e)</sup>	-4.5	41.5	3.1	83
1200	S-L	-45.2	-9.3	-3.1	41.5	3.1	79
	P-L	-69.	-10.3	-1.7	41.	3.1	85
	S-S	-82.	-10.(f)	-6.(g)	41.	3.1	88
	P-S	-86.	-13.(h)	-6.5	42.	3.1	85

(a) See Table 22

(b,c,d) See Table 46

(e)  $\pm 0.6$

(f) Wandering between 9 and 18

(g) Wandering between 6 and 7.5

(h)  $\pm 2$

Table 49

TESTS WITH SCR IN COMBINATION WITH  
FRAM FILTER/SEPARATOR AT 5.5 CU

Flow Rate, GPM	Test Pipe Code (a)	Charge Density $\mu\text{C}/\text{m}^3$ , at			Fuel		SCR Efficiency, % (d)
		Filter Out (b)	Pipe In (c)	Pipe Out	Temp, °F	Rest CU	
300	S-L	+ 5	- 0.9	- 0.1	40.5	5.7	82
	P-L	--	--	--	--	--	--
	S-S	--	--	--	--	--	--
	P-S	--	--	--	--	--	--
600	S-L	- 11.	- 5.6	- 0.6	38.8	5.5	49
	P-L	--	--	--	--	--	--
	S-S	--	--	--	--	--	--
	P-S	--	--	--	--	--	--
900	S-L	--	--	--	--	--	--
	P-L	- 18	- 8.1	+ 1.0	38.6	5.5	55
	S-S	- 17	- 8.2	- 2.8	38.8	5.5	52
	P-S	- 16	- 7.7	- 1.8	38.9	5.5	51
1200	S-L	- 69; - 70	- 10; - 10	- 0.8; - 0.8	38.2; 38.3	5.5; 5.5	86; 86
	P-L	- 37	- 9	+ 0.7	38.6	5.5	76
	S-S	- 36	- 11.0	- 5.0	38.7	5.5	69
	P-S	- 34	- 9.3	- 3.5	38.5	5.5	74

(a) See Table 22  
(b, c, d) See Table 46

Table 50

TESTS WITH SCR IN COMBINATION  
WITH BENDIX GAGES AT 0.9 CU

Flow Rate, GPM	Test Pipe Code (a)	Charge Density, $\mu\text{C}/\text{m}^3$ , at		Fuel		SCR Efficiency, % (d)
		Gages Out(b)	Pipe In(c)	Pipe Out	Temp., °F	Rest CU
300	P-L	+ 36.6	+ 15.5 ± .5	+ 1.6	54	.78
600	P-L	+ 26.7	+ 15.7 ± .3	+ 5.4	54	.78
1200	P-L	+ 18.6	+ 15.1 ± .2	+ 9.5	54	.78

(a) See Table 22.

(b, c, d) See Table 46.

Table 51

TESTS WITH SCR IN COMBINATION WITH BENDIX GAGES AT 3 CU

Flow Rate, GPM	Test Pipe Code(a)	Charge Density, $\mu\text{C}/\text{m}^3$ at			Fuel		SCR Efficiency, %(d)
		Gages Out(b)	Pipe In(c)	Pipe Out	Temp. °F	Rest CU	
300	S-L	149.	-3/-1	-0.2	44	3.2	98.5
	P-L	134.	-3.5/-.5	0.2	43.5	3.2	98.5
	S-S	126.	-3/-1	0.0	45	3.3	98.5
	P-S	122.	-2.5/1	0.2	44	3.2	99
600	S-L	134.	-7/-3	-0.2	43	3.2	96
	P-L	122.	-4/0	-0.9	43.5	3.2	98
	S-S	109.	-4/0	-0.4	43	3.2	98
	P-S	109.	-3/1	-0.1	43	3.2	99
900	S-S	97.	-6/0	-1.8	42.5	3.1	97
1200	S-L	113.	-5/1	-1.0	43	3.2	98
	P-L	102.	-4/0	0.5	43.5	3.2	98
	S-S	90.	-4/2	-1.0/0	43.5	3.2	99
	P-S	93.	-2/2	-0.7/0.3	44.5	3.3	100

(a) See Table 22

(b,c,d) See Table 46



Table 52

TESTS WITH SCR IN COMBINATION WITH THE BENDIX GAGES AT 5.5 CU

Flow Rate, GPM	Test Pipe Code(a)	Charge Density, $\mu\text{C}/\text{m}^3$ at			Fuel		SCR Efficiency, %(d)
		Gages Out (b)	Pipe In(c)	Pipe Out	Temp. °F	Rest CU	
300	S-L	205	-0.5/-1	-0.2	40.0	5.6	99.5
	P-L	179	-1.5/-6	0.2	40.1	5.6	96.6/99.2
	S-S	172	-1/-2	0.0	40.4	5.6	99.4/98.8
	P-S	177	-1/-2.5	0.2	40.7	5.7	98.6/99.4
600	S-L	190	0/-4.5	-0.5	38.8	5.5	97.6/100
	P-L	-	-	-	-	-	-
	S-S	164	-1.5/-4.5	-0.4	39.4	5.5	97.3/99.1
	P-S	172	-1.5/-6.	0.0	39.3	5.5	96.5/99.1
900	S-L	173	3.5/-4.5	-1.1	38.4	5.5	97.4
	P-L	-	-	-	-	-	-
	S-S	-	-	-	-	-	-
	P-S	-	-	-	-	-	-
1200	S-L	160	4.5/-3.	-1.7	38.7	5.5	97.2/100
	P-L	150	5./-.5	1.1	39.4	5.5	96.7/99.7
	S-S	138	7/-5	0/-2.5	39.3	5.5	94.9/100
	P-S	145	3/-3	0/-1.5	38.8	5.5	97.9/100

(a) See Table 22

(b,c,d) See Table 46

Table 53

SURFACE VOLTAGE DATA - USING SCR  
WITH FRAM FILTER/SEPARATOR AT 0.2 CU

Flow Rate, GPM	300		600		900	1200	
Pipe Length	S	L	S	L	S	S (a)	L
Pipe In, $\mu\text{C}/\text{m}^3$	0/-8	0/-9	7/-13	2/-17	1/-20	2/-25	1/-30
Pipe Out, $\mu\text{C}/\text{m}^3$	0/-3	-1/-3	2/-9	-1/-9	0/-10	-3/-7	-8/-19
Temp., °F	44.4	42.1	45.4	42.7	45.8	46.9	42.9
Rel. Hum., %	59	46	59	44	58	56	42
Surf. V., kv, @ Ft. From Inlet							
1	.67	.44	.22/.67	.140/.67	.012/.67	-.140/.67	0/-.67
2	1.47/ 1.58	.44/.80	.92/1.33	.140/.92	.30/1.33	-.021/ 1.33	.012/ -1.2
4	1.66/ 1.89	4.3	1.26/2.0	4.3	.30/1.33	0/1.89	1.33/3.9
10	8.1	5.5	6.3	5.01	3.9/5.3	2.20/3.9	1.33/2.6
20	6.6	6.3	6.0	4.6	3.6	.110/.67	-1.5/ -2.6
30	.76	-2.2	.193	-3.9	1.47	-5.5	-11
40	-23	-38(b)	-23	-38(b)	-23	-28	-38(b)
50	6.9	-10.2	6.0/7.1	-11.6/ -10.4	4.6/5.3	2.2/3.15	-16.5
60	.63	-9.0	.56/.80	-10.2	-.140/ .25	-1.66/ -2.6	-16.5
70	2.06	-19	1.85	-21.5	1.33/ 1.47	.80/1.2	-26
76	.25	-9.3	.014/ .250	-10.8	.042/ .110	-.30/ .130	-14.9
79	.34	-13.1	.34	-15.6	.25/.28	.193/.25	-18.3
90		-21.5					Stand
110		-4.8		-6.0			Off
130		-8.6		-9.0			Bolt
150		-16		-9.0			Broke
170		-8.6		-3.9			
190		-.41		.92			
210		-4.8		-4.6			
230		-1.12		-1.18			
238		-.67		.73			
239		-.80		.67			

(a) Bearing seized on electrostatic voltmeter following this run.

(b) Estimated value.

Table 54

SURFACE VOLTAGE DATA - USING SCR WITH  
FRAM FILTER/SEPARATOR AT 0.9 CU

Flow Rate, GPM Pipe Length	300		600		1200	
	S	L	S	L(a)	S	L(a)
Pipe In, $\mu\text{C}/\text{m}^3$	-32	-29	-59	-58	-89	-83
Pipe Out, $\mu\text{C}/\text{m}^3$	-13	- 3.7	-35.5	-16.5	-64	-37
Temp., $^{\circ}\text{F}$	-	-	-	-	-	-
Rel. Hum., %	80	62	80	61	80	60
Surf. V., kv, @ Ft. From Inlet						
1	.066/ .095	.012/ -.012	-.14/ -.25	-.34	-.36/ -.67	-.96
2	-.056/ .110	-.39	-.67/ -.92	-1.29	-1.2/ -1.66	-2.06
4	-.11/ .033	-1.03	-1.2/ -1.47	-2.35	-2.06/ -2.9	-3.4
10	1.15	-.92	-.56/ -.80	-3.4	-2.06/ -3.3	-6.3
20	-0.76	-2.25	-6.0	-5.8	-8.4	-12.4
30	-1.45	-8.6	-6.6	-11.0	-8.1	-16
37	--	--	-5.3	--	-8.4	--
39	-6.3		-9.3		-11.0	
40	-12.4	--	-17.7	--	-17.7	--
41	-0.85		-3.3		-6.3	
43	-.78	--	-3.6	--	-8.4	--
50	-.60	>-50(b)	-3.3	-14.9	-7.7	-30(-31)
60	-.73	-5.3	-3.05	-18.3(-21)	-6.3	-30(-30)
70	.25	-13.4	-.67	-23(-27)	-1.75	-34(-36)
76	-.13	--	-.76	--	-1.47	--
78	-.074	-20	-.67	-34(-32)	-1.33	-38
79	-.042	--	-.42	--	-.92	--
90	--	-12.8	--	-16	--	-2.5
100	--	-.85	--	--	--	
110	--	-1.53	--	-6.3	--	-9.7
130		2.7		-.87/-1.10		-4.3
140		.033		-5.0		--
150		-11.7		-24.5(-19)		-24.5
170		-3.3		-21.5(-15)		-34
180		-2.9				
190		2.8		-6.9		-9.7
210		-2.9		-7.4		-10.2
220		-3.15		-7.4		-10.8
230		-.34		-.85		-1.18
238		-.34		-.76		-1.10
239		-.083		-.49		-.90

(a) Sweeney Meter readings in parentheses.

(b) Estimated value.

Table 55

SURFACE VOLTAGE DATA - USING SCR  
WITH FRAM FILTER/SEPARATOR AT 3 CU

Flow Rate, GPM	300	600	1200	
Pipe Length	<u>S (a)</u>	<u>S (a)</u>	<u>S (a)</u>	<u>L</u>
Pipe In, $\mu\text{C}/\text{m}^3$	-2.5/1	-3/1	-2/2	-4/0
Pipe Out, $\mu\text{C}/\text{m}^3$	0.2	-0.1	-0.7/0.3	0.5
Temp., °F	45.8	46.2	-	50.3
Rel. Hum., %	75	76	76(b)	69
Surf. V., kv, @				
Ft. From Inlet				
1	.2	0.0	.1	-.014/.021
2	.3	.1	0.0	0/- .030
4	.8	.2	-.2	
10	1.7	.25	0.0	0/- .030
20	4.3	2.6	.8	0/- .037
30	4.1	2.4	.9	0/- .033
37	2.6	.8	.25	
40	-1.8	-3.2	-4.2	-1.8
43	.2	0.0	-.1	
50	.7	.3	-.3	.154/.25
60	.4	.3	-.1	-.095/- .140
70	.2	.1	.1	-.030/- .056
79	.1	0.0	.1	-.024/- .045
90				-.019/- .023
110				-.023
130				-.021
150				-.024
170				-.025/- .033
190				-.033/- .053
210				-.030/- .033
230				-.019/- .023
239				-.020

(a) Pipe drying; readings made with Sweeney Meter.

(b) Estimated.

Table 56

SURFACE VOLTAGE DATA - USING SCR  
WITH FRAM FILTER/SEPARATOR AT 5.5 CU

Flow Rate, GPM	<u>900</u>	<u>1200</u>
Pipe Length	<u>Short</u>	<u>Short</u>
Pipe In, $\mu\text{C}/\text{m}^3$	-7.7	-9.0
Pipe Out, $\mu\text{C}/\text{m}^3$	-1.8	0.7
Temp., °F	42.0	42.1
Rel. Hum., %	46	53
Surf. V., kv, @		
Ft. From Inlet		
1	-.28	-.39
2	-.85	-1.00
4	-1.33	-1.62
10	-1.89	-2.06
20	-3.6	-3.9
30	-3.4	-4.6
40	-2.5	-3.4
50	-2.9	-3.8
60	-1.62	-2.25
70	-.60	-.73
76	-.41	-.49
79	-.19	-.238

Table 57

SURFACE VOLTAGE DATA - USING SCR  
WITH BENDIX GAGES AT 0.9 CU

Flow Rate, GPM	600	1200
Pipe Length	<u>L</u>	<u>L</u>
Pipe In, $\mu\text{C}/\text{m}^3$	15.7	15.1
Pipe Out, $\mu\text{C}/\text{m}^3$	5.4	9.5
Temp., °F	-	-
Rel. Hum., %	71	69
Surf. V., kv, @		
Ft. From Inlet		
1	.037/.048	.012/.019
2	.058/.066	.021/.033
4	.074/.087	.012/.030
10	.27	.63/.73
20	2.35	2.25
30	2.40	2.60
50	5.0	5.5
60	5.0	5.3
70	5.0	5.3
78	3.9	4.1
90	3.8	4.6
110	3.05	3.6
130	2.00	1.96
150	3.4	4.1
170	2.6	3.9
190	2.2	2.4
210	1.26	1.89
220	1.12	1.58
230	.048	.066
238	.035	.050
239	.025	.034

Table 58

SURFACE VOLTAGE DATA - USING SCR  
WITH BENDIX GAGES AT 3 CU

Flow Rate, GPM	300	600	1200	
Pipe Length	<u>S</u>	<u>S</u>	<u>S</u>	<u>L</u>
Pipe In, $\mu\text{C}/\text{m}^3$	-2.5/1	-3/1	-2/2	-4/0
Pipe Out, $\mu\text{C}/\text{m}^3$	0.2	-0.1	-0.7/0.3	0.5
Temp., °F	46.2	46.1	45.8	49.6
Rel. Hum., %	77	76	78	62
Surf. V., kv, @				
Ft. From Inlet				
1	0	-.1	.2	-.066/-.25
2	-.7	-.2	0	-.47/-.80
4	-1.3	-.4	-.1	-1.29/-1.53
10	-3.4	-1.0	-.2	-2.4/-2.8
20	-5	5.	-4.8	-7.1
30	-6	-8	-5	-11.3
37	4.	-2.2	-1.6	--
40	-1.3	.7	.8	3.9
43	1.6	-.7	-.4	--
50	.4	0.	.2	4.8
60	.6	.1	.3	-3.05
70	0.	-.1	.1	-2.35
79	.2	0.	.2	-1.10
90				-1.15
110				-1.53
130				-1.29
150				-.82
170				-.76
190				-1.33
210				-1.12
230				-.37
239				-.077

Table 59

SURFACE VOLTAGE DATA - USING SCR  
WITH BENDIX GAGES AT 5.5 CU

Flow Rate, GPM	300		600	1200
Pipe Length	S	L	S	S
Pipe In, $\mu\text{C}/\text{m}^3$	-1/-2.5	-1.5/-6	-1.5/-6	+3/-3
Pipe Out, $\mu\text{C}/\text{m}^3$	0.2	0.2	0.0	0/-1.5
Temp., °F	43.5	49.1	43.1	43.1
Rel. Hum., %	52	62	57	57
Surf. V., kv, @				
Ft. From Inlet				
1	-.90	-.042/.23	-.85	-.47/- .67
2	-.42	2.06	-.80	-.36/- .67
4	-3.6	-13.1	-4.3	-3.9
10	-10.5	-17.7	-10.8	-9.3
20	-17.7	-19	-19	-17.7
30	-23	-24.5	-21.5	-18.3
40	-1.18	14.1	-2.7	-1.4
50	-4.1	-13.8	-5.5	-4.6
60	-2.5	7.1	-3.6	-2.7
70	-.18	--	-.30	-.22
76	-.28	5.8	-.33	-.30
79	-.16	2.5	-.20	-.181
90		3.8		
110		-15.6		
120		-3.6		
130		-9.7		
150		2.5		
170		-2.7		
190		-4.3		
200		6.6		
210		2.06		
230		.54		
238		.238		
239		.36		



Table 60  
OBSERVATIONS ON SPARK PRODUCTION USING SCR WITH FILTER/SEPARATOR

Nom. Fuel CU	Pipe Lgth.	Flow Rate, GPM	CD, $\mu\text{C}/\text{m}^3$ At Pipe In	Rel. Hum., %	Spark Characteristics Generated By											
					Foil Wrapping @ Feet From Inlet						Valve @					
					27			48			189			81 Feet		
					Lgth., Ins.	No./ Sec.		Lgth., Ins.	No./ Sec.		Lgth., Ins.	No./ Sec.		Lgth., Ins.	No./ Sec.	
0.2	Short	300	0/-8	59	<1/16	3-4		1/8	2-3		-	-		-	-	
		600	7/-13	59	~1/64	2		1/8	1		-	-		-	-	
		900	1/-20	58	~1/64	2		1/16	2-3		-	-		-	-	
		1200	2/-25	56	( a )			<1/16	2-3		-	-		-	-	
	Long	300	0/-9	46	-	-		1/8	2		-	-		3/8(b)	3-4	
		600	2/-17	44	-	-		1/8	1-2		-	-		1/4(c)	3	
		1200	1/-30	42	-	-		1/8	1-2		-	-		3/8(d)	3	
5.5	Short	900	-7.7	46	( a )			( a )			-	-		-	-	
		1200	-9.3	53	( a )			( a )			-	-		-	-	
	Long	900	-8.1	-	-	-		( a )			( a )			1/16	2	
		1200	-9.	-	-	-		( a )			( a )			~1/8	4	

- (a) Audible on radio only.  
 (b) 1/2 inch long to finger.  
 (c) 3/8 inch long to finger.  
 (d) 1/2 inch long to finger.

Table 61

## OBSERVATIONS ON SPARK PRODUCTION USING SCR WITH BENDIX GAGES

Nom. Fuel CU	Pipe Lgth.	Flow Rate, GPM	CD, $\mu\text{C}/\text{m}^3$ At Pipe In	Rel. Hum., %	Spark Characteristics Generated By									
					Foil Wrapping @ Feet From Inlet					Valve @ 81 Feet				
					27		48		189		81 Feet			
					Lgth., Ins.	No./ Sec.	Lgth., Ins.	No./ Sec.	Lgth., Ins.	No./ Sec.	Lgth., Ins.	No./ Sec.	Lgth., Ins.	No./ Sec.
5.5	Short	300	-1/-2.5	52	-	-	1/4	2	-	-	-	-	-	-
		600	-1.5/-6	57	-	-	1/4	2	-	-	-	-	-	-
		1200	3/-3	57	1/16- 1/8	1-2	1/16- 1/8	1-2	-	-	-	-	-	-
	Long	300	-1.5/6	57	-	-	1/8	2	( a )	( a )	( a )	( a )	( a )	( a )
		1200	5/-5	-	-	-	3/16	2	( a )	( a )	( a )	( a )	( a )	( a )

(a) Audible on radio only.

### APPENDIX III

#### A COMPARISON OF OHMIC AND HYPERBOLIC CHARGE RELAXATION

Data obtained in this program with the negatively charged fuel at 0.2 CU provide an opportunity to compare the conventional ohmic theory with the hyperbolic theory of charge relaxation developed by Bustin et al (as indicated in Appendix I, Section 3). The ohmic theory assumes that the number of charge carriers is constant and, because of this, that charge decays at a rate defined by their number as measured by the "rest" conductivity,  $k_o$ , which is a measure of the number of charge carriers in electrically neutral, or uncharged, fuel. However, the conductivity of charge fuel is not necessarily the same as uncharged fuel, and "effective" conductivity,  $k_e$ , which represents the conductivity of charged fuel, is often used to account for the relaxation rates that are observed in a flowing system. It is generally observed that the relaxation rates of fuels with rest conductivities above about 1 CU are more directly related to their rest conductivities than fuels with conductivities below 1 CU. The agreement for fuels above 1 CU has been explained by the fact that high conductivity fuels already contain a large number of charge carriers which would be little affected by charging of the fuel. It should be noted, however, that this study, as well as previous studies as described in Appendix I, show that fuels with  $k_o$ 's above 0.5 to 1.0 CU may actually behave as if they have conductivities lower than  $k_o$ , indicating

that the charged fuel has fewer effective charge carriers than the uncharged fuel. Since charge carriers are ion species which are normally in equilibrium with their parent molecules, the change in effective charge carriers is probably due to increased association of charges.

Fuels below 1 CU have so few charge carriers at rest that the total number may be increased significantly when the fuel is charged. In this study, as well as previous studies, this is reflected by  $k_e$  values which are greater than the  $k_o$  value of the fuel. Bustin et al have shown that the rate of relaxation for such fuels is controlled by the initial charge on the fuel,  $Q_o$ , and the mobility,  $\mu$ , of the charge carriers, rather than the conductivity. The charge decay rate appears hyperbolic rather than exponential and may be represented by the following relationship (Equation 12, Appendix I):

$$Q_t = \frac{Q_o}{1 + \frac{\mu Q_o t}{\epsilon \epsilon_o} \times 10^6} \quad (12)$$

This compares with the ohmic theory (Equation 9, Appendix I) where

$$Q_t = Q_o e^{-tk/\epsilon \epsilon_o} \quad (9)$$

A comparison of the two methods based on the data obtained in this study when the 0.2 CU fuel was charged negatively follows.

The calculated ion mobility,  $\mu$ , in  $m^2/volt \text{ sec.}$ , is shown in Table 62, along with the  $Q_o$ ,  $Q_t$  and  $t$  values for each test carried out with the 0.2 CU fuel when it was charged negatively (see Table 26).

Table 62

ION MOBILITY BASED ON TESTS CARRIED OUT  
WITH NEGATIVELY CHARGED 0.2 CU FUEL

Flow Rate, GPM	Test Pipe Code(a)	Charge Density, $\mu\text{C}/\text{m}^3$ , @		Residence Time, t, Seconds	Ion Mobility, $10^{-8} \text{ m}^2/\text{volt sec.}$
		Pipe In	Pipe Out		
300	S-L	-67.6	-23.7	80.5	.60
	P-L	-68.4	-23.0	80.3	.64
	S-S	-70.4	-45.0	27.2	.52
	P-S	-66.1	-40.6	27.2	.62
600	S-L	-115	-54.4	40.2	.42
	P-L	-116	-54.1	40.1	.43
	S-S	-120	-86	13.6	.42
	P-S	-119	-84	13.6	.46
900	S-L	-138	-75.5	26.8	.39
	P-L	-140	-76.7	26.8	.39
	P-L	-143	-68.6	26.8	.38
	S-S	-147	-115	9.06	.37
	P-S	-141	-108	9.06	.41
1200	S-L	-154	-94	20.1	.37
	P-L	-155	-94	20.1	.37
	S-S	-167	-135	6.80	.37
	S-S	-151	-123	6.80	.40
	P-S	-161	-129	6.80	.40

(a) See Table 22

(The charge densities obtained when the 0.2 fuel was charged positively were considered to be too low for generating meaningful data.)

The mobility  $\mu$  is given by a revised version of Equation 12:

$$\mu = ([Q_o/Q_t]-1)(\epsilon\epsilon_o \times 10^6/Q_o t) \quad (15)$$

As shown in Table 62, the highest ion mobilities eg. .52 to .64 m<sup>2</sup>/volt sec. were obtained at 300 GPM, which represents the lowest flow rate as well as the lowest inlet charge levels attained in this test series. The mobilities decreased with increasing flow rate. Over the highest two flow rates, which represent the highest inlet charge levels attained in this test series, the mobilities covered the rather narrow range of .37 to .41 x 10<sup>-8</sup> m<sup>2</sup>/volt sec. The reason for the change in mobility is not known although one might explain this trend in terms of rate of association of ions. However, these mobilities are in reasonably good agreement with the values reported previously by Bustin et al (eg. 0.52 to 0.97 x 10<sup>-8</sup> m<sup>2</sup>/volt sec. a fuel with a similar conductivity, eg. 0.25 CU).

Having established the ion mobility for this particular fuel it is possible to compare the hyperbolic relaxation theory with the ohmic theory. The charge level that would be expected after 30, 60, 90 and 120 seconds of relaxation for initial charges ranging from 100 up to 1000  $\mu\text{C}/\text{m}^3$  based on the hyperbolic relaxation theory are shown in Table 63. These values were calculated using Equation 12, assuming a mobility of  $0.38 \times 10^{-8}$  m<sup>2</sup>/volt sec., the average for the tests carried out in the steel pipe at 900 and 1200 GPM as shown in Table 62. This value was

TABLE 63

PREDICTED CHARGE DENSITIES FOR 0.2 CU FUEL  
 BASED ON HYPERBOLIC CHARGE RELAXATION

Initial Charge Level $\mu\text{C}/\text{m}^3$	Charge Density, $\mu\text{C}/\text{m}^3$ , Predicted By Hyperbolic Relaxation Theory <sup>(a)</sup> After Residence Times, in Seconds, of			
	<u>30</u>	<u>60</u>	<u>90</u>	<u>120</u>
100	61	44	35	28
300	104	63	45	35
500	120	68	48	37
1000	137	74	50	38

<sup>(a)</sup> With Ion Mobility,  $\mu = 0.38 \times 10^{-8} \text{ m}^2/\text{volt second}$ .

selected because it was based on the highest inlet charge levels attained in this test series and it provides the most conservative estimate of the time required for charge relaxation.

The data listed in Table 63 are shown graphically by the curved lines in Figure 22. The straight lines in this figure represent the charge levels that would be expected based on ohmic relaxation. The solid straight lines were obtained assuming that  $k$  had a value 0.38, the average  $k_e$  obtained for steel pipe with the negatively charged 0.2 CU fuel. The dashed straight lines were obtained using a value of 0.2 for  $k$ , representing the nominal rest conductivity of the fuel.

As shown, the hyperbolic theory generally predicts much faster relaxation of charge for short residence times than the ohmic theory does. This is shown in the following table, where the charge levels that would be expected after 30 seconds of relaxation based on both hyperbolic and ohmic charged decay are listed for initial charge levels ranging from 100 up to 1000  $\mu\text{C}/\text{m}^3$ .

Predicted Charge Levels After 30 Seconds Relaxation

Initial Charge Level, $Q_0$ , in $\mu\text{C}/\text{m}^3$	Charge Level After 30 Seconds, in $\mu\text{C}/\text{m}^3$ , Based On		
	Hyperbolic Theory	Ohmic Theory Using $k =$	
		$k_e = 0.38 \text{ CU}$	$k_o = 0.20 \text{ CU}$
1000	137	520	717
500	120	258	358
300	104	155	215
100	61	53	72



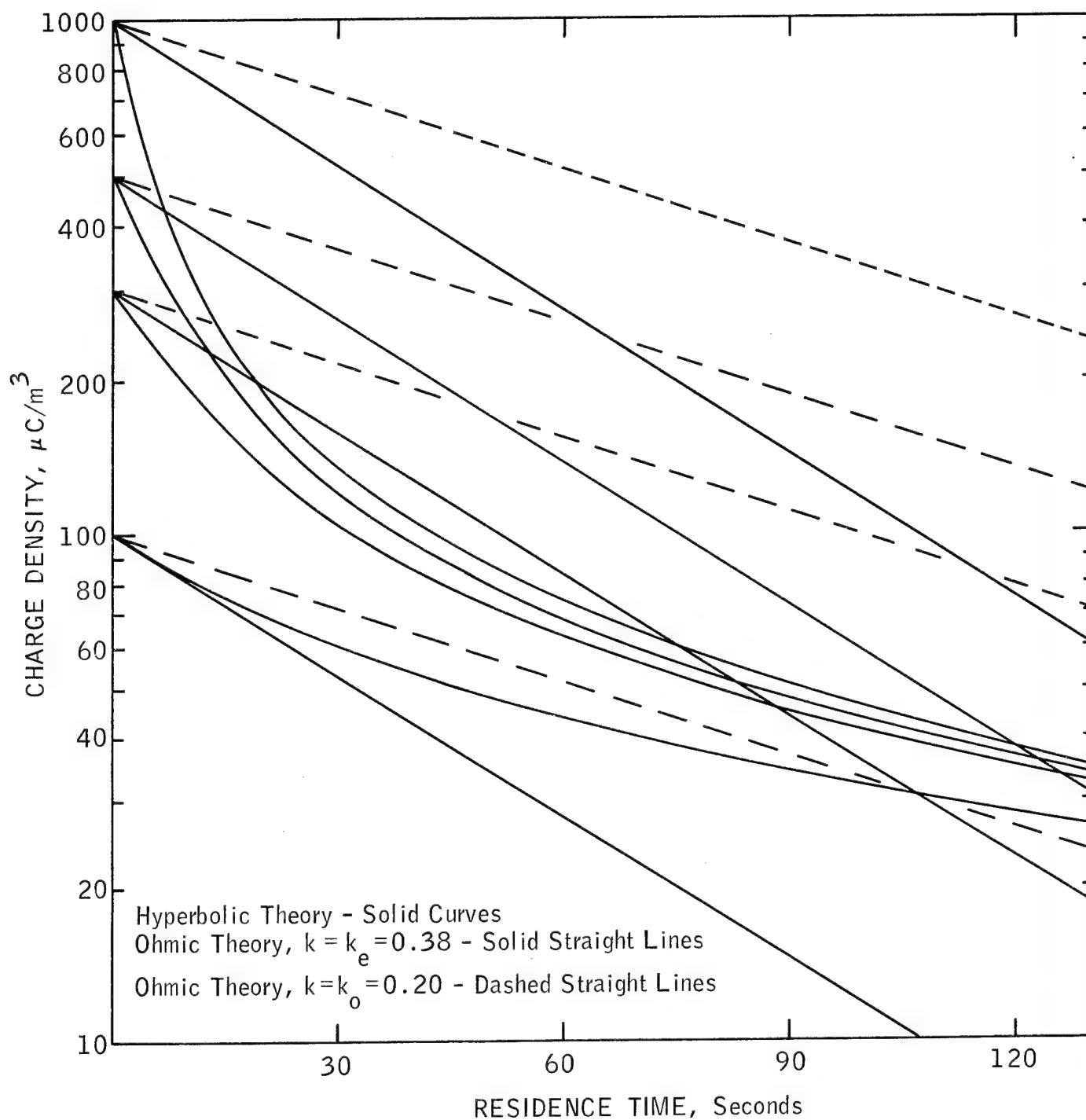


Figure 22. Predicted Charge Density Vs. Residence Time  
 By Hyperbolic and Ohmic Relaxation Theories

It should be noted that the charge predicted by the hyperbolic theory would be lower than that predicted by the ohmic theory in all cases except one. Since the hyperbolic theory predicts an increase in relaxation rate with increase in initial charge level, the differences between the charge levels predicted by ohmic and hyperbolic theories are substantial at the higher initial charge levels. However, it should also be noted that even with hyperbolic relaxation, the predicted charge level after 30 seconds does not reach  $30 \mu\text{C}/\text{m}^3$ , the charge level which has been used in this report to represent a "safe" charge level.

While the initial rate of relaxation predicted by the hyperbolic theory is generally faster than that predicted by the ohmic theory, even utilizing the effective conductivity, the time predicted for charge to decrease to  $30 \mu\text{C}/\text{m}^3$  would still be long as shown in Figure 22. The residence times required to reach  $30 \mu\text{C}/\text{m}^3$  from different initial charge levels, as predicted by the hyperbolic and ohmic theories, are shown in the following table for comparison.

PREDICTED RESIDENCE TIMES REQUIRED  
FOR CHARGE TO RELAX TO  $30 \mu\text{C}/\text{m}^3$

Initial Charge Level, Q, In $\mu\text{C}/\text{m}^3$	Residence Time, Seconds, Required For Charge to Relax to $30 \mu\text{C}/\text{m}^3$ By	
	<u>Hyperbolic Theory</u>	<u>Ohmic Theory, <math>k = k_e = 0.38 \text{ CU}</math></u>
1000	154	165
500	149	132
300	143	108
100	111	57

On the other hand the predicted charge level reached after 130 seconds of relaxation, the minimum amount of time that would be available in an Air Force hydrant system, would be close to  $30 \mu\text{C}/\text{m}^3$  under hyperbolic relaxation, regardless of the initial charge level, as shown in Figure 22.

#### REFERENCES

1. Keller, D. P. and Kleinmann, E. E., Aircraft Fueling System Study, Prepared under Corps. of Engineers Contract DACA-73-69-C-0013 by Phillips Scientific Corporation, Bartlesville, Oklahoma, Dec. 1969.
2. Personal Communication, C. W. Young, Headquarters AFSC/DEEE, Andrews AFB.
3. Ingram, H. I., Air Force Design Criteria for Aviation Fuel Systems, Industry-Military Jet Fuel Quality Symposium, San Antonio, Texas, October 1968.
4. Test Report on Bondstrand 2000-12 Pipe Prepared for Amercoat Corporation, Brea, Calif. by Delsen Corporation Testing Laboratories, Glendale, Calif., Oct. 11, 1968.
5. Personal Communication, H. J. Ingram, Directorate of Civil Engineering, Headquarters, U.S. Air Force, Washington, D. C.
6. Klinkenberg, A. and Van Der Minne, J. L., Electrostatics In The Petroleum Industry, Elsevier Publishing Co., New York, 1958, Page 116.
7. Generation, Measurement and Reduction of Static Electricity in the Handling of Petroleum Products, Revision II, Brochure Issued by A. O. Smith, Meter Systems Division, Erie, Penna., May 1969.
8. Special Service Bulletin on Possible Damage or Contamination of A. O. Smith - Static Charge Reducer, Issued by A. O. Smith, MSD, Erie, Pa., April 1, 1971.
9. Willig, Frank J. Method and Apparatus for Neutralizing Electrostatically Charged Fluids, U. S. Patent 3,629,656.

DISTRIBUTION

No. cys

HEADQUARTERS USAF

	Hq USAF, Wash, DC	20330
1	(SAMI)	
1	(OA)	
1	(PRE)	
5	(PREE)	
2	(PREER)	
1	(PRELA)	
2	(PRELB)	
1	(RDPQ, 1C370)	
1	Hq USAF, AFTAC (TD-3), Wash, DC	20333
1	USAF Dep, IG (AFIDI-AS2), Norton AFB, CA	92409
1	Dir Aerosp Safety (IGDS), Norton AFB, CA	92409
1	USAF Dir Nuc Safety (IGDN), Kirtland AFB, NM	87117
2	USAF Inspection and Safety Ctr (AFISC/SEOG), Norton AFB, CA	92409

MAJOR AIR COMMANDS

	AFSC, Andrews AFB, Wash, DC	20331
1	(DO)	
5	(DOB)	
1	(DLSP)	
5	TAC (DEE), Langley AFB, VA	23365
5	SAC (DEE), Offutt AFB, NE	68113
5	AFLC (DEE), Wright-Patterson AFB, OH	45433
5	ADC (DEE), Ent AFB, CO	80912
1	AUL (LDE), Maxwell AFB, AL	36112
2	AU (ED, Dir, Civ Eng), Maxwell AFB, AL	36112
5	AAC (DEE), APO Seattle	98742
	AFIT, Wright-Patterson AFB, OH	45433
2	(Tech Lib, Bldg 640, Area B)	
1	(DAPD)	
1	(CES)	

## DISTRIBUTION (cont'd)

No. cys

	CINCUSAFE, APO New York 09012
1	(DOA)
5	(DEE)
	CINCPACAF, APO San Francisco 96553
1	(DOA)
5	(DEE, Mr. Lau)
	USAF Academy, CO 80840
1	(DFSLB)
1	(FJSRL, CC)
2	(DFCE)

## NUMBERED AIR FORCES

5	5 AF, APO San Francisco 96525
5	7 AF, APO San Francisco 96307
5	13 AF, APO San Francisco 96274

## AFSC ORGANIZATIONS

1	ARL (STINFO Ofc), Wright-Patterson AFB, OH 45433
1	AFML (Tech Lib), Wright-Patterson AFB, OH 45433
2	ASD/ENVCC (Aerospace Fuels Laboratory), Wright-Patterson AFB, OH 45433
5	AFCEC (Air Force Civil Engineering Ctr), Tyndall AFB, FL 32401
	AFAPL, Wright-Patterson AFB, OH 45433
1	(Tech Lib)
5	(Charles Martel, SFF)
	ASD, Wright-Patterson AFB, OH 45433
1	(Tech Lib)
5	(DEE)
1	SAMSO (Tech Lib), AFUPO, Los Angeles, CA 90045
2	SAMSO (DEE), Norton AFB, CA 92409
5	ESD (DEE), L. G. Hanscom Fld, Bedford, MA 01730
	ADTC, Eglin AFB, FL 32542
1	(Tech Lib)
2	(DEE)

## DISTRIBUTION (cont'd)

No. cys

RADC, Griffiss AFB, NY 13440

1 (Doc Lib)

2 (DEE)

## KIRTLAND AFB ORGANIZATIONS

AFSWC, Kirtland AFB, NM 87117

1 (FTE)

AFWL, Kirtland AFB, NM 87117

5 (SUL)

5 (DEZ)

## OTHER AIR FORCE AGENCIES

1 USAF Eng LO, APO New York 09125

1 Hq Air Wea Svc (AWVAS), Scott AFB, IL 62225

2 TAWC (DEE), Eglin AFB, FL 32544

2 560 CES (HR) (CEFAC), Eglin Aux Fld II, FL 32544

2 USAF Reg Civ Eng, 526 Title Bldg, 30 Pryor St SW, Atlanta, GA 30303

2 USAF Reg Civ Eng, PO Box 1159, Cincinnati, OH 45201

2 USAF Reg Civ Eng, West Reg-Portland, OR 97209

2 USAF Reg Civ Eng, 630 Sansome St, Rm 1316, San Francisco, CA 94111

2 USAF Reg Civ Eng, Central Reg, 1114 Commerce St, Rm 226, Dallas, TX 75202

2 Hq SAAMA/SFQF, Kelly AFB, TX 78241

## ARMY ACTIVITIES

1 Comdg Off, (STINFO Ofc), Picatinny Arsenal, Dover, NJ 07801

1 Comdg Off, USAEC, Ft Monmouth, NJ 07703

1 Comdg Off, USAMC Fld Ofc, Kirtland AFB, NM 87115

1 Comdg Off, USA Rsch Ofc-Durham, Box CM, Duke Sta, Durham, NC 27705

1 Chief Of Eng (ENGMC-EM), Dept Army, Wash, DC 20315

1 Dir, USA Eng WW Exp Sta, PO Box 631, Vicksburg, MS 39181

## NAVY ACTIVITIES

1 Ofc Nav Rsch, Dept Navy (Code 418), Wash, DC 20360

1 Dir, NRL (Code 2027), Wash, DC 20390

2 OIC, Nav Civ Eng Corps Off School, USNCB Cen, Port Hueneme, CA 93041

1 Comdg Off, NWEF (Code ADS), Kirtland AFB, NM 87117

DISTRIBUTION (cont'd)

No. cys

OTHER DOD ACTIVITIES

2	Plastics Technical Evaluation Ctr, Picatinny Arsenal, Dover, NJ 07801
12	DDC (TCA), Cameron Sta, Alexandria, VA 22314

OTHER

2	Dept of Transportation, FAA/ARD-400 (Mr. C. L. Blake, Chief of Airport Division), Wash, DC 20590
5	Esso Research and Engineering Co., Products Rsch Div, PO Box 51, Linden, NJ 07036
1	Official Record Copy (DEZ, Mr. Frederick H. Peterson)



UNCLASSIFIED  
Security Classification

DOCUMENT CONTROL DATA - R & D		
(Security classification of title, body of abstract and indexing annotation must be entered when the overall report is classified)		
1. ORIGINATING ACTIVITY (Corporate author) Esso Research & Engineering Co., Products Rsch Div. PO Box 51 Linden, NJ 07036		2a. REPORT SECURITY CLASSIFICATION Unclassified
		2b. GROUP
3. REPORT TITLE EVALUATION OF THE HAZARD OF STATIC ELECTRICITY IN NONMETALLIC POL SYSTEMS--STATIC EFFECTS IN HANDLING JET FUEL IN FIBERGLASS REINFORCED PLASTIC PIPE		
4. DESCRIPTIVE NOTES (Type of report and inclusive dates) June 1971 through June 1972		
5. AUTHOR(S) (First name, middle initial, last name) Kenneth C. Bachman, J. C. Munday		
6. REPORT DATE June 1973	7a. TOTAL NO. OF PAGES 220	7b. NO. OF REFS 9
8a. CONTRACT OR GRANT NO. F29601-71-C-0071		9a. ORIGINATOR'S REPORT NUMBER(S) AFWL-TR-72-90
b. PROJECT NO. 683 M		
c. Task 2		9b. OTHER REPORT NO(S) (Any other numbers that may be assigned this report) Contractor Rpt No. RL.4PD.72
d.		
10. DISTRIBUTION STATEMENT Approved for public release, distribution unlimited.		
11. SUPPLEMENTARY NOTES		12. SPONSORING MILITARY ACTIVITY AFWL (DEZ) Kirtland AFB, NM 87117
13. ABSTRACT (Distribution Limitation Statement A) There is an increasing interest in fiberglass reinforced plastic (FRP) pipe for minimizing contamination in ground handling of aviation fuels. This report presents the results of a literature search and experimental study conducted to determine if static electricity hazards would be increased by substituting FRP for metal pipe in such systems. Experiments were conducted in 6 inch diameter, matched volume, carbon steel and Bondstrand 2000 pipes at four fuel conductivities between 0.2 and 5.5 CU and at flow rates between 200 and 1500 GPM at controlled temperatures. Charge generation in the pipes was low (2.5 $\mu\text{C}/\text{m}^3$ maximum with 0.9 CU fuel at 1200 GPM in steel); generation in FRP was generally less than in steel. Relaxation in FRP pipe depended on fuel polarity; on the average, relaxation was 8 percent faster, with negatively-charged fuel and 30 percent slower with positively-charged fuel than in steel. The slower relaxation should not prevent the use of FRP in Air Force hydrant systems handling JP-4 where a minimum of 2 minutes residence time is available downstream of filter-separators. Voltages up to 55 kv were measured on the FRP pipe and sparks up to 1/2 inch long could be discharged from ungrounded metal components on the FRP pipe. These effects should be of no concern in underground installations; methods for eliminating them in above-ground installations are recommended. An evaluation of the A. O. Smith Static Charge Reducer (SCR) showed that it was more efficient with positively- than negatively-charged fuel and that deposit-buildup could reduce its efficiency. Available data suggest that static electricity hazards might exist downstream of an SCR although the average charge level is below 30 $\mu\text{C}/\text{m}^3$ . An annotated bibliography covering 71 recent, relevant literature articles is included.		

DD FORM 1473  
1 NOV 65

UNCLASSIFIED  
Security Classification

14. KEY WORDS	LINK A		LINK B		LINK C	
	ROLE	WT	ROLE	WT	ROLE	WT
Fuel electrostatics Plastic fuel piping Fuel system hazards Fuel handling safety Fuel charging Refueling hazards						